LANDMARK PROCESSING BY HEAD DIRECTION CELLS

Yave Roberto Lozano Navarro

Thesis submitted to University College London for the degree of Doctor of Philosophy in Neuroscience

September 2015

Contents

DECLARATION

I, Yave Roberto Lozano Navarro, confirm that the work presented in this thesis is my own. Where information has been derived from other sources, I confirm that this has been indicated in the thesis.

ACKNOWLEDGEMENTS

Pursuing a doctoral degree in Neuroscience has been one of the great challenges in my life which would not have been possible without the encouragement of my parents Araceli and Roberto and my sister Heidi who have supported me unconditionally throughout my education. To my uncle Francisco, without whom I would not have been I able to cover the remaining tuition to enrol in UCL. To my supervisor, Kate Jeffery who has mentored, guided and supported me before and during the PhD, providing me with academic and personal advice, allowing me to persevere and succeed in the challenging field of behavioural electrophysiology. To my secondary supervisor, Frances Edwards for taking the time to review my upgrade report and guiding me on writing a thesis.

To the scholarship from the Mexican National Council of Science and Technology, CONACYT (313254) which enabled me to study at a world's leading research university in neuroscience. To the Medical Research Council grant G1100669, "A neuronal model of memory-integrative processing in the retrosplenial head direction system" which funded the work that I carried out.

To all the former and past member of the Institute of Behavioural Neuroscience (IBN) who have been both colleagues and friends during the arduous years of graduate school. Special thanks to Robin and Liz who trained me in single-unit recording and my lab brothers Amir, Giulio, Jonathan, Laurenz, Shaz and Pierre-Yves who have been a source of both friendship and continuous help during the long days at the IBN. To Meghan, who recorded the rats that are described in Chapter 7. Special thanks to Miguel, whose statistical expertise and programming experience helped me to tackle the difficult problem of analysing circular data. To Josh for reviewing several chapters of this thesis and being a source of continuous discussion. To Caswell, for taking the time to discuss and review my writing on continuous attractor networks. To all my relatives, teachers and friends who have encouraged me to pursue higher education. Your support has allowed me to come this far, both academically and geographically. Finally, to Kleo whose love has helped me in more ways that I can describe.

ABBREVIATIONS

ADN – Anterior Dorsal Thalamic Nucleus

AHV - Angular Head Velocity

AMN - Anterior Medial Thalamic Nucleus

ATN - Anterior Thalamic Nuclei

AVN - Anterior Ventral Thalamic Nucleus

CAN - Continuous Attractor Network

DG - Dentate Gyrus

dLGN - Dorsal Lateral Geniculate Nucleus

DTN - Dorsal Tegmental Nucleus

EC - Entorhinal Cortex

HD - Head Direction

HF - Hippocampal Formation

KDE - Kernel Density Estimate

LDN - Lateral Dorsal Thalamic Nucleus

LEC - Lateral Entorhinal Cortex

LMN - Lateral Mammillary Nucleus

MEC - Medial Entorhinal Cortex

MPC - Medial Parietal Cortex

MVN - Medial Vestibular Nucleus

nPH - Nucleus Prepositus Hypoglosi

PaS - Parasubiculum

PER - Perirhinal Cortex

PFD – Preferred Firing Direction

PHR - Parahippocampal Region

PMA - Posteromedial Visual Area

POR - Postrhinal Cortex

PoS - Postsubiculum

PPC - Posterior Parietal Cortex

PrS - Presubiculum

RSC – Retrosplenial Cortex

RSCd – Retrosplenial Dysgranular Area

RSCg – Retrosplenial Granular Area

Sub - Subiculum

ABSTRACT

Head direction (HD) cells are neurons that increase their firing rate whenever a rat faces within a range of heading directions, irrespective of its location within the environment. Their direction-specific firing is multisensory, where visual cues have a dominant role in controlling the preferred firing direction (PFD) to which an HD cell fires. Many studies have examined the role of visual cues in controlling the firing of HD and other spatially modulated cells, however, little is known about how visual information is integrated with a spatial navigation signal.

Therefore, the aim of this thesis is to investigate what properties of the visual environment are detected and used by the navigation system. To investigate this question, HD cells were recorded in the retrosplenial cortex (RSC) and the postsubiculum (PoS) of rats as they explored an arena with two oppositely positioned cards that varied in contrast, or the orientation, height and lateral position of a bar. The cue cards were rotated together to test the hypothesis that HD cells use differences in the visual properties of local cues to align their PFD. A second experiment tested the hypothesis that PoS HD cells process the configuration of landmarks, examining changes in the PFD when the spatial relation between multiple local cues was altered.

The main finding from these experiments is that contrast and orientation were reliably used as landmarks, while height and lateral position had a weaker effect in controlling the activity of HD cells. The second finding is that PoS HD cells were sensitive to changes in the spatial arrangement of familiar cues, selecting the cues that changed their position over those that remained stationary. Overall, these results show that HD cells process fine-grained visual form which might be used for complex image analysis and landmark processing.

I DESCRIPTION OF THE RESEARCH PROJECT

Spatial navigation and spatial orientation are complex behaviours that require the ability to estimate current position, heading direction, distance and speed travelled. For many foraging mammals such as rodents, it is fundamentally important to navigate efficiently as they must remember the location where food and predators were found. In humans, spatial navigation and memory represent two interlinked systems that integrate multimodal sensory information (visual, olfactory, vestibular among others) to create an internal representation of an environment or an event. The relationship between spatial navigation and memory is complex; however, it is likely that there are common neuronal mechanisms that evolved to compute spatial position and link this information with the features and location of landmarks to create a mental representation that can be used to encode events and objects (Buzsáki & Moser, 2013). To explore the role of landmarks in spatial orientation, the present thesis investigates how visual information is integrated with a spatial navigation signal.

In the last four decades, a large body of research has sought to characterise the brain regions and neural mechanisms involved in memory formation and spatial navigation in both humans and rodents. One line of research derived from studies of rodents has focused on investigating the sensory information and the neural computations that are necessary for determining spatial location and orientation. Most of this research has relied on electrophysiological methods that enabled the isolation and characterisation of the spiking activity of single neurons in freely moving animals. This approach has led to the discovery of several classes of spatially modulated cells whose spiking activity correlates with the animals' position within the environment and with head orientation.

From the various spatially modulated neurons that have been discovered, head direction (HD) cells encode the animal's perceived directional heading by increasing their firing rate whenever the rat faces within a restricted range of heading directions irrespective of its location within the environment (Taube, Muller, & Ranck, 1990). HD cells provide an animal with a sense of direction, integrating sensory information that is derived from internally generated inputs

such as self-motion cues with externally derived information from the environment such as visual landmarks, both of which provide signals that are used as potential cues during spatial orientation and navigation (Taube, 2007).

Amongst these cues, visual cues or landmarks play a dominant role in the representation of a spatial map, allowing a rat to compute its position and facing direction within an explored environment. Visual landmarks strongly influence the direction to which an HD cell will maximally respond, the region which is known as the preferred firing direction (PFD) (Taube, Muller, & Ranck, 1990b). The strong influence of landmarks on HD cell activity, a process that is referred to as "resetting", demonstrates that the HD signal incorporates visual information from the environment, encoding heading direction that is referenced to world-centred (allocentric) coordinates. These characteristics make the HD signal a good model system to investigate how sensory signals are transformed into a more complex, cognitive representation.

Since the discovery of HD cells, a large number of studies have characterised the circuit that generates the HD signal and examined the influence of self-motion and visual cues in controlling the activity of HD cells (Taube, 2007). Based on these results, it is well established that angular velocity signals derived from vestibular input are necessary for generating the HD signal, while self-motion cues are important for updating the activity of HD cells and visual cues reset the PFD to maintain an alignment with reference to landmarks (Stackman & Taube, 1997; Taube & Burton, 1995). The updating process of the HD signal has an important role in spatial navigation, providing a mechanism whereby heading errors are corrected while navigating based on self-motion information, a navigation strategy known as path integration (Valerio & Taube, 2012a). Functionally, the process of resetting heading estimates based on the relative position of landmarks is essential for encoding a spatial representation of an environment and navigating efficiently (McNaughton, Battaglia, Jensen, Moser, & Moser, 2006).

Although a large number of studies have examined the role of visual cues in controlling the spatial firing of HD and other spatially modulated cells (border, place and grid cells), little is known about the content of the visual input and what

visual properties of the environment are relevant for the HD system to use as orienting landmarks. In this regard, one hypothesis is that HD cells encode an allocentric referenced panoramic view of the visual scene, integrating specific information about the visual and spatial characteristics of the environment and the landmarks available to compute heading direction. Another hypothesis is that HD cells process landmarks as single, isolated cues serving as beacons without the need of extracting specific visual or spatial information from the objects or scene (Chan, Baumann, Bellgrove, & Mattingley, 2012).

Until now, no study has addressed what visual and spatial properties of landmarks are processed by HD cells and the content of the visual information that HD cells rely on to reset their directional firing. Therefore, to address these questions, the present thesis investigates whether simple local visual features of cue cards such as contrast, orientation, height and position are processed as landmarks and whether HD cells respond to changes in the spatial arrangement of a subset of these cues. To explore the relationship between landmark processing and HD cells, the recordings were conducted in the retrosplenial cortex (RSC) and the postsubiculum (PoS), two interconnected brain areas that receive direct projections from visual areas and are hypothesised to have an important role in linking the spatial representation derived from HD cells with landmark information (Yoder, Clark, & Taube, 2011).

This research is important as it seeks to understand the relationship between visual perception and spatial orientation, offering a potential model system with which to explore how visual signals are transformed from the visual cortex into the landmark representation used by spatially modulated cells. This would in part offer insight into how other spatially modulated cells process landmarks during the complex behaviour of spatial navigation.

To understand the background and the importance of these findings in the field of spatial navigation, the first three chapters present a literature review of selected topics relevant to the processing of landmarks by spatially modulated cells. The structure for the thesis and the topics that are discussed will be as follows:

Chapter 1 describes the behavioural aspects of navigation, introducing the different navigational strategies that are used by rodents, the information that is integrated during navigation and the role of landmarks in spatial orientation and navigation. This is followed by an introduction to the multiple spatially modulated neurons that have been discovered in the mammalian brain and a brief description of the general properties and functional significance of the different classes of spatially modulated neurons.

Chapter 2 describes the major anatomical connections amongst brain regions containing spatially modulated cells, focusing on the HD cell circuit. A description of the rodent visual system as it pertains to the landmark processing circuit and the anatomical connections of the PoS and the RSC are described in further detail.

Chapter 3 describes the firing properties of HD cells, how the signal is generated and the influence of self-motion and landmarks in controlling the PFD. Theoretical models of HD cells and the hypothesised functional role of the RSC and PoS in landmark processing are discussed.

Chapter 4 describes the surgical, behavioural and electrophysiological procedures that were used to examine landmark processing by HD cells. A description of the methods applied for isolating the activity of single neurons (spike sorting), the analysis to quantify the tuning curves of HD cells and a brief description of the analysis applied to examine the changes in the PFD as a result of the cue manipulations are presented.

Chapter 5 presents commonly used standard statistical methods for analysing HD cells, describing their advantages and limitations. A new method based on density estimates that was developed to visualise and analyse the population response of HD cells, examining changes in the PFD's are described and contrasted with standard methods. The chapter also describes the difficulties of null hypothesis testing applied to multimodal circular distributions, presenting a Bayesian analysis that can be used as an alternative method for drawing inferences from these distributions.

Chapter 6 describes the results of an experiment that investigated the landmark processing capabilities of PoS and RSC HD cells when rats were exposed to two cue cards that differed in contrast, orientation, height, lateral position and control stimuli comprising identical cues. The chapter also compares the general firing properties of PoS and RSC HD cells with those reported in previous studies.

Chapter 7 describes the results of an experiment that investigated whether PoS HD cells process the visuo-spatial configuration of multiple landmarks in a square environment with the aim of exploring what information is used for spatial orientation during the processing of a complex visual scene.

Chapter 8 provides a general discussion of the results, concluding remarks and suggestions for future experiments.

II REVIEW

Chapter 1 Behavioural and neural mechanisms of spatial navigation

1.1 Introduction

In order to survive and reproduce animals face the selection pressure of finding sources of food while avoiding predators. This requires traveling across a terrain which could be air, land or sea and navigating efficiently over both short and long distances. Small and large-scale navigation impose similar problems that need to be solved in order to obtain a good estimate of current location. Some of these problems include determining the starting position and the goal location, recalling the routes that have been travelled, and linking the locations that have been explored with the routes that have been traversed. The multiple challenges encountered during navigation had a selection pressure on a species' reproductive success, which through natural selection evolved adaptations that enabled animals to navigate efficiently. One of these adaptations was the development of neural circuits that were capable of processing incoming sensory signals, developing a representation of the external environment and selecting a navigation strategy to execute a motor response.

The topic of animal navigation is immense and has been studied by disciplines as diverse as ecology, ethology, psychology, neuroscience and robotics among others. The behavioural aspects of animal navigation have been extensively studied by both ethologists and psychologists who have characterised the sensory information and memory processes involved in navigation in species as diverse as insects, birds and mammals (Jacobs & Menzel, 2014). In the present thesis, the animal model that was the subject of study and which will be mainly discussed is the rodent, particularly the rat. However, other animal species are also discussed, providing a general framework showing that the behavioural and neural processes that underlie spatial navigation and memory have been conserved across the evolution of diverse species.

In this chapter, the topic of navigation and the neural representation of self-localisation is divided into three main sections. Section 1.2 presents the different navigation strategies that have been proposed, examining the information that is integrated during navigation, the role of landmarks in navigation and the spatial coordinate system or reference frame that is used by rodents to represent their location in the world. Section 1.3 provides a summary of the properties and anatomical location of several spatially modulated cell types that are responsible for the neural representation of self-location. Section 1.4 discusses the functional significance of these spatially modulated cells with an emphasis on the role of HD cells in spatial orientation.

1.2 Rodent navigation and memory

During navigation, multimodal information that is internally generated, also known as idiothetic, and information derived from the external environment known as allothetic, are integrated in the rodent brain to aid in spatial orientation. Idiothetic information is primarily though not solely derived from self-motion cues, while an important source of allothetic information is provided by visual landmarks, which play an important role in defining locations. The brain creates an internal representation of spatial location derived from idiothetic and allothetic cues to plan, select and execute a navigation strategy. Therefore, to accurately compute the present self-location and guide navigation, the spatial map needs to be aligned to features of the external world such as environmental landmarks that can be used reliably to compute position and facing direction. As will be discussed in the following sections, it is difficult to investigate the different sources of information that are processed during navigation as they are integrated in parallel, and rats often use multiple strategies to solve the same task.

1.2.1 Navigation strategies

As pointed out before, both the navigational strategies and the sources of information that contribute to the selection of these strategies are not mutually

exclusive and animals can flexibly use any available information to ensure their success in navigation (Figure 1.1). This fact makes it difficult to rule out that a rodent or any other animal is relying solely on one strategy when solving a particular task in a natural environment or in a laboratory set-up. Based on a large body of work from multiple disciplines, various taxonomies of navigational strategies have been proposed (O'Keefe & Nadel, 1978; Redish, 1999). As with any classification system, many terms have been introduced that describe the same navigational process. This section describes four navigational strategies that are commonly described in the rodent literature and the evidence for each (Figure 1.1).

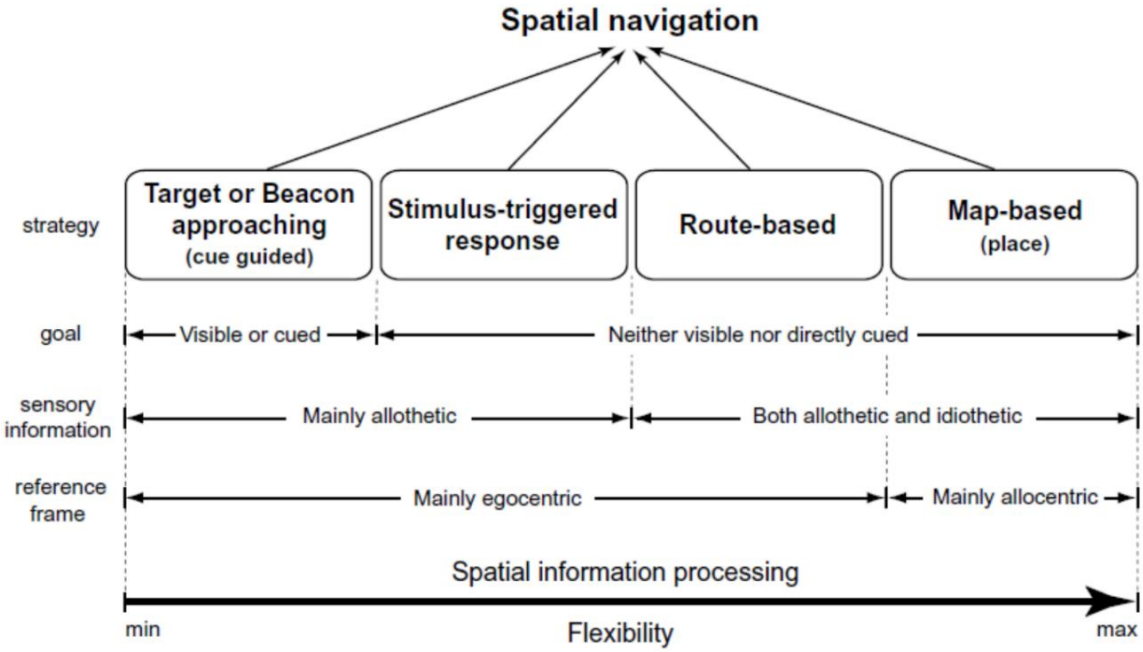

Figure 1.1 Schematic diagram of the classification of different spatial navigation strategies based on the availably of cues at the goal location, the integration of idiothetic and allothetic information and the reference frame used to encode self-position. Note that the different sources of information converge as a continuum rather than as discrete categories as shown in this image. Taken from (Arleo & Rondi-Reig, 2007).

One of the navigational strategies known as beaconing relies on sensory cues that can be perceived at a distance to aid animals in navigating towards a specific location. Studies conducted in wasps showed that they can identify the location of

the nest using nearby visual landmarks and that beaconing towards the nest is affected such that wasps will navigate towards the location of the landmarks disregarding the previously learned nest location (Tinbergen, 1951). Beaconing can be shown in rats that are trained to identify an escape or reward location based on the position of a cue that lies next to it in tasks such as the cued version of the water maze (Lozano, Serafín, Prado-Alcalá, Roozendaal, & Quirarte, 2013). A major limitation of a beaconing navigation strategy occurs when the relative position of the landmarks change or when the visual cues that define a specific location are ambiguous. An example of this was described by von Frisch (1974) who noted that birds find it difficult to build a nesting site in buildings that were highly repetitive.

Another navigational strategy called route following relies on the use of familiar paths to reach a goal location. This strategy constitutes a form of response strategy whereby the rat reaches the goal location by executing a learned motor sequence derived from body turns along a well-known path (Redish, 1999). Route navigation can be employed while travelling across well-known locations such as inside underground tunnels or in burrows where many interconnected passageways are available. However, as route following requires the use of well-known paths, it is inefficient when exploring a new environment and learning new paths that link different goal locations.

On the other hand, a different navigational strategy known as path integration can be used to compute the present location without external cues or learned routes. Path integration relies on estimating the current position from the past trajectory in relation to a known starting location such as the nest or the burrow. This is accomplished by integrating the animal's own movements such as the distance and direction travelled and using this information to compute a homing vector that is used for returning to the starting location or home site (McNaughton et al., 2006) (Figure 1.2).

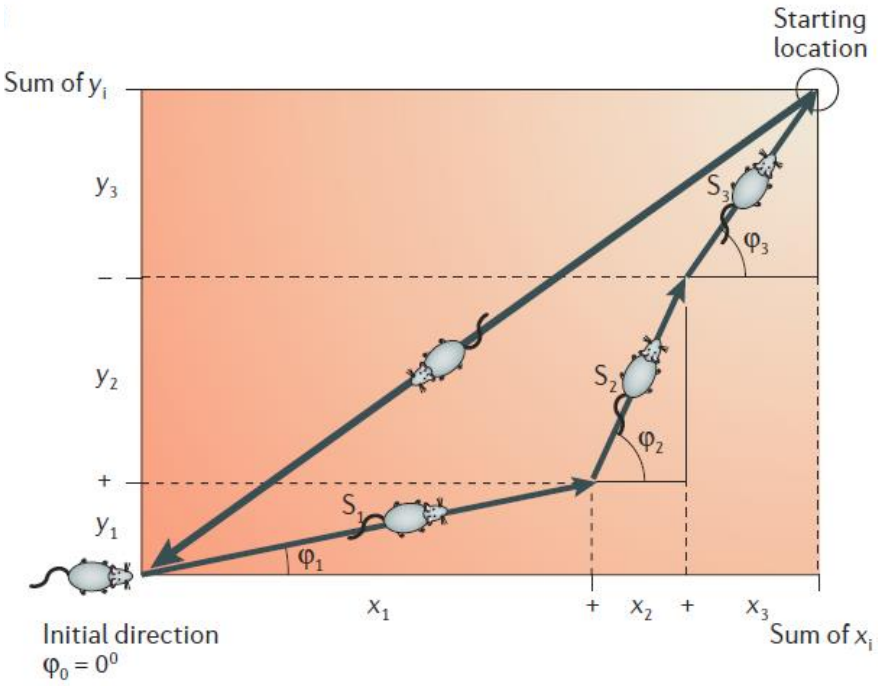

Figure 1.2 Path integration in rats. Vector addition derived from changes in distance and turning direction are used to compute a vector for the inbound path. Taken from (McNaughton et al., 2006).

A simple method for testing path integration is by letting an animal explore away from its home site in darkness and then either moving the animal to a new location or slightly rotating the animal before it returns to the home site. If the animal uses path integration, then it should move directly to where the home site should have been, traveling in a path that deviates from the correct direction by the amount that the animal was rotated. On the other hand, if it does not use path integration and instead relies on olfactory or other external cues, the animal should head back directly to the starting location. Evidence for path integration in mammals was first found in experiments which showed that gerbils can retrieve their pups in darkness within a circular arena and return to their nest (Mittelstaedt & Mittelstaedt, 1980). Furthermore, when the gerbils were slowly rotated below the vestibular threshold while picking up a pup, they returned in a direction that matched the amount that the gerbils were rotated as expected if the animal was using path integration to compute its homing vector. This experiment demonstrated that path integration

can support an internal sense of direction that does not depend on the availability of visual landmarks.

Path integration is a complex process that uses multimodal information derived from self-motion cues such as vestibular, proprioceptive and motor efference which can be used in parallel with other navigation strategies. As previously discussed, path integration can be useful for navigating in the absence of landmarks or over short distances, however, when navigating over large distances or unfamiliar terrain, it is prone to error accumulation that is reflected in heading errors (Etienne & Jeffery, 2004). Therefore, path integration is likely to exert control over navigation only when the animal can combine it with learned strategies such as those derived from route following and/or landmark cues from a familiar environment. Landmarks play a fundamental role in navigation and will be discussed further in Section 1.2.4, however it is important to point out that when an animal navigates in a familiar terrain, path integration can be used concurrently with landmark information. In this situation, familiar visual landmarks correct for heading errors by providing a stable reference point to which animals can reset their position and heading estimates to optimise large range navigational performance (Etienne, Maurer, Boulens, Levy, & Rowe, 2004).

Another navigational strategy which relies on idiothetic cues and landmarks for representing the environment is known as a cognitive map. The concept of a cognitive map was postulated by Edward Tolman to explain the results of experiments where 36% of rats (19 out of 53) chose a novel shortcut to reach a previously rewarded goal location that had been marked by a light when the familiar path was blocked and multiple arms became available (Tolman, 1948). At the time, the cognitive map theory posed a challenge to the behaviourist ideas which postulated that rats solved navigation tasks by relying on simple stimulus-response associations and not by creating an internal representation of the external world.

A defining characteristic of the use of a cognitive mapping strategy is the ability to guide navigation in situations where previously known paths to a goal are blocked and novel shortcuts need to be taken to reach a goal location. The cognitive map

strategy differs from the use of beacons or landmarks to reach a destination since these visual cues might not have been learned by the animal as it explores new paths to reach a goal location.

Questions remain about whether rats are capable of using a cognitive map, taking previously unavailable shortcuts to reach a goal location without relying on other navigational strategies such as beaconing, route following or path integration (Bennett, 1996; Jacobs & Menzel, 2014). A study that used a similar behavioural protocol as the one reported by Tolman (1948), eliminating the light above the goal location which probably acted as a beacon in the original study failed to find support for the hypothesis that rodents use a cognitive map (Muir & Taube, 2004). Consistent with this result, a recent study failed to find evidence for the use of a cognitive map, as rats did not take a novel shortcut to a goal location when the familiar path was blocked unless they had previously travelled the shortcut route, demonstrating that in rats the use of a shortcut path has to be learned (Grieves & Dudchenko, 2013). Altogether, these results strongly suggest that rodents do not rely on a cognitive map to flexibly navigate in changing conditions of the environment and instead rely on a combination of beaconing, path integration and available landmarks to update self-location and guide their behaviour during navigation.

1.2.2 Sources of information for navigation

During navigation, both proximal and distal senses are used to obtain short and long-range information about the environment. For rats, somatosensation (whisking and olfaction) are the primary proximal senses while vision is the primary distal sense (Geva-Sagiv, Las, Yovel, & Ulanovsky, 2015). This does not imply that these are the only sources of sensory information that rats employ during navigation. As described earlier, self-motion information plays a fundamental role in all navigational strategies, irrespective of the presence or absence of landmarks.

Regarding the sensory inputs that provide spatial information and are used as cues during navigation, a theoretical distinction has been made between internal

and external sources of information. In this framework, internal or idiothetic information refers to input that are derived from self-motion related signals through vestibular, optic flow, proprioceptive, and motor-efference signals, while allothetic information reflects the sensory perception of the environment and includes olfactory, auditory, somatosensory and visual signals (Arleo & Rondi-Reig, 2007). Idiothetic cues derived from the vestibular system provide information about linear displacement and turning direction through angular velocity signals from the semicircular canals (Cullen, 2012). In studies conducted in monkeys, optic flow (linear and radial) signals which change the retinal image during forward motion and head movements provide information about self-movement in relation to the visual information from the environment during locomotion, while proprioceptive feedback from the neck muscles and an efference copy of the motor command to turn the head, provide information about the neck's orientation in relation to the body axis (Crowell, Banks, Shenoy, & Andersen, 1998). The mechanisms and the projections by which vestibular information and optic flow are integrated by brainstem circuits, contributing to spatial orientation in rodents remain relatively unexplored.

However, solely relying on idiothetic cues leads to heading errors in path integration as the distance travelled increases: as a result, information that is derived from the environment, particularly from visual landmarks, can be used as an allothetic cue to update the animal's sense of position as it travels between locations, resetting the path integrator (Etienne et al., 2004). The contribution and weighing of idiothetic and allothetic cues in the selection of navigational strategies depends on the familiarity with the environment and contextual variables of the surroundings, such as the presence of landmarks and their relative importance to the animal. This multisensory integration of allothetic and idiothetic cues allows the brain to derive an estimate of self-position, enabling rats to adjust and flexibly switch between navigational strategies depending on the availability of landmarks and the demands of the environment (Figure 1.1).

In order for idiothetic and allothetic sources of information to be used as reliable cues during navigation and form the basis of a spatial map, they must be integrated

in relation to a coordinate system whose reference frame could either be body-centred or world-centred and anchored to a fixed location relative to the environment such as the positon of a landmark.

1.2.3 Reference frames

During navigation, spatial locations can be defined relative to the body or relative to the external environment. These coordinate systems for representing spatial locations are referred to as reference frames and vary depending on the origin to which they are centred. An egocentric reference frame is centred relative to the body axis or a part of the body (i.e., eyes, head, trunk), whereas an allocentric reference frame is centred relative to an object's or landmark's location, independent of the animal's position and orientation (Klatzky, 1998).

In the present discussion of reference frames, the origin for an egocentric reference frame will be defined relative to the orientation of the head while the origin for an allocentric reference frame has coordinates external to the animal and are defined relative to the environment or landmarks (Figure 1.3A). Both of these reference frames can be used to represent or encode the position of a visual cue in the environment and extract spatial information. However, as the rat moves about in the environment, computing self-location in relation to the position of a landmark changes in an egocentric reference frame while it remains unaffected in an allocentric reference frame (Figure 1.3B) (Wolbers & Wiener, 2014). The change between the self to landmark relation implies that the rat has to constantly update its spatial position in an egocentric representation which will be increasingly more complicated with a larger number of landmarks, leading to many heading errors (Figure 1.3B). In contrast, an allocentric representation can be used more flexibly to encode the spatial relationship between routes, places and goals without the need of continuously updating self-position and only periodically using landmarks to correct for path integration errors (O'Keefe & Nadel, 1978).

The use of reference frames provides a framework that explains how space is represented in the activity of spatially modulated cells, giving insight into how

idiothetic and allothetic information are integrated to update a rat's representation of self-location. As will be described in Section 1.3, several classes of spatially modulated cells found across the mammalian brain represent self-location in an allocentric reference frame using information derived from the environment such as visual landmarks to anchor the internally generated spatial map.

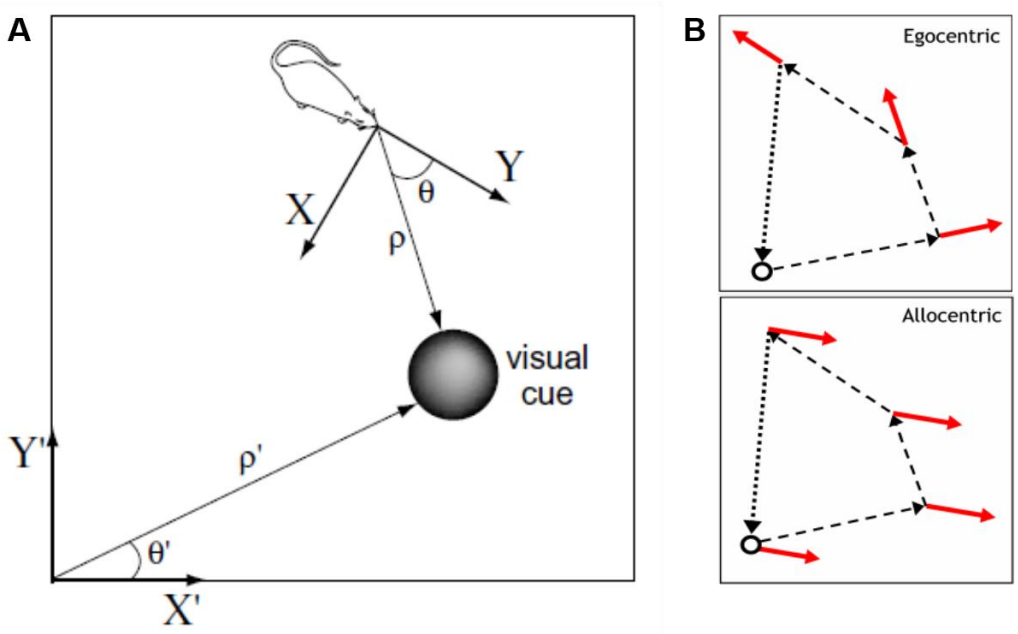

Figure 1.3 Allocentric and egocentric encoding in relation to a visual cue. **A.** An egocentric reference frame is centred on X-Y coordinates relative to the rat's head where θ is the angle between the rat's heading and the location of the cue, while ρ is the distance between the head and the cue. In contrast, in an allocentric reference frame the x-y coordinates are centred relative to the environment where θ' is the angle from the origin to the cue and ρ' is the distance to the cue. **B.** The vector for the egocentric encoding of the landmark location changes (red arrow) as the rat navigates in the environment while remaining in the same direction for an allocentric encoding. Taken from (Arleo & Rondi-Reig, 2007).

1.2.4 Role of landmarks in navigation

As animals navigate, it is important to adjust the travelled path across the journey to avoid getting lost as this can potentially risk its survival. To achieve this, animals

must identify features in the environment that can serve as cues to guide them as they travel while remembering important locations such as the home site or where food and predators were found. In rats, vision provides the most reliable source of information for long-range sensing and navigation, where objects or features in the environment are used as visual cues or landmarks to orient them towards a known location (Gallistel, 1990). Landmarks are therefore used for identifying behaviourally relevant locations, determining current position and heading direction and selecting a navigational strategy to reach a goal location by either taking a known path (beaconing, route following) or a novel path (cognitive map). Knowledge about both local and distant landmarks and the spatial relationship between them is essential for spatial orientation and the representation of a cognitive map, whereby estimates of distance and heading direction derived from path integration are combined with knowledge about landmarks to form a unified spatial map of the environment (Collett & Graham, 2004) (Figure 1.4).

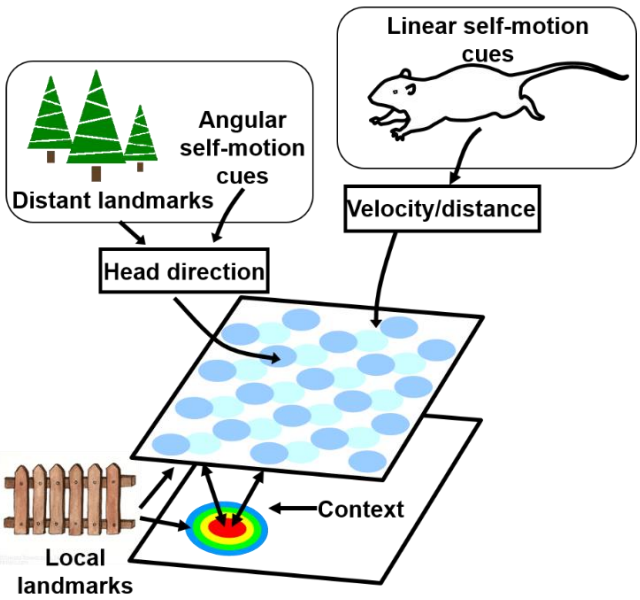

Figure 1.4 Schematic illustration of the integration of idiothetic and allothetic information such as landmarks (both proximal and distal) during navigation. Spatial orientation and the encoding of particular locations (signalled as context) is provided by determining current position and heading direction using available allothetic cues (i.e. relationship between landmarks, distance estimates to local landmarks) and idiothetic cues derived from self-motion information. Taken from (Jeffery, 2007b).

Behavioural evidence for the use of landmarks to guide navigation in rodents has been found in many spatial learning tasks such as the radial arm maze and the Morris water task where the animal has to learn to reach a specific location within the maze by relying on proximal and distal cues (Knierim & Hamilton, 2011). It is important to note that in much of the literature the term landmark has been broadly applied to any visual information derived from the environment that can potentially influence navigation. However, a categorical distinction has recently been made based on the relative distance of the landmark from the viewer and the function that the landmark might serve within a specific navigational context (Chan et al., 2012; Knierim & Hamilton, 2011). In the former, local or proximal landmarks are defined as intramaze cues such as the apparatus corners and boundaries, while global or distal landmarks are any extramaze features. In this view, spatial navigation towards a goal relies on both proximal and distal landmarks where distal landmarks provide directional information needed for orienting in an environment and proximal landmarks provide distance information needed to find a goal location (Knierim & Hamilton, 2011).

This model predicts that in laboratory tasks that are commonly used to study spatial learning in rodents, navigation is directed towards proximal, apparatus based landmarks rather than locations based on distal landmarks. Evidence for this was found in the Morris water task in which rats chose to navigate relative to the pool wall instead of the location relative to the distal cues (where they were previously trained) when the pool was shifted relative to room centred coordinates (Hamilton, Akers, Weisend, & Sutherland, 2007).

Little is known about how rodents select landmarks in the wild for navigation, however, studies conducted in a natural environment with the Columbian ground squirrel (*Spermophilus columbianus*) showed that they use both proximal (i.e. vegetation pattern, local relief and other burrows) and distal (i.e. forest edge, mountain outline) landmarks to locate the burrow with particular importance for orientation being placed to the upper portion of the horizon (Vlasak, 2006). It is interesting to note that in rodents there is a bias for processing moving overhead stimuli which can trigger an escape response (Wallace et al., 2013). To what

extent this overhead bias is mainly used for predator detection and avoidance or for learning the relationship of proximal-distal landmarks to a goal location remains an open question.

In relation to classifying landmarks based on their functional relevance within a specific navigational context, several properties have been suggested to be important for an object or feature in the environment to be perceived as a reliable indicator of position and hence act as a landmark. These properties include: 1) Uniqueness in physical appearance, 2) Stable spatial position within an environment, 3) Location within an environment, where landmarks located at decision points or at goal locations become more salient and memorable (Chan et al., 2012).

Self-localisation based on landmarks requires the extraction and recognition of visual features and patterns from the environment and one question that has been relatively unexplored is what visual features of these landmarks are extracted and selected to aid in spatial orientation. One hypothesis derived from experiments in insects suggests that animals use an image matching strategy whereby a visual snapshot of a panorama is used to identify the location of the nest site (Cartwright & Collett, 1983). This strategy consists of learning the different visual landmarks as a single panoramic view rather than as individual elements or snapshots which would require computing the spatial relationship between each landmark with respect to each other in order to find the location of the nest (a task that would require the use of a cognitive map). In the image matching strategy, learning the panoramic view of landmarks can be acquired by performing a scanning behaviour upon leaving the nest, creating a visual snapshot of the hive location which can then be compared with other panoramas as the honeybee returns to the hive (Cartwright & Collett, 1983). Whether rats use an image matching strategy during navigation is an open question, however, head scanning movements in rats which occur during exploratory behaviour and extend the region of visibility from different vantage points can provide information about self-position with respect to proximal and distal landmarks and might be used to obtain visual snapshots of the environment (Monaco, Rao, Roth, & Knierim, 2014).

To explore the role of landmarks in spatial orientation, experiments described in Chapter 6 investigated whether different visual features of landmarks influence the activity of HD cells, while Chapter 7 explored if the spatial configuration of multiple cues within an environment affect the likelihood that HD cells use the visuo-spatial features of landmarks for orientation.

1.3 Spatially Modulated Cells

The study of spatial representation in the brain began with the discovery of place cells in the rat hippocampus more than four decades ago. As the names suggests, these cells increase their firing rate whenever the animal visits a particular location of an environment, providing information about spatial position (O'Keefe & Dostrovsky, 1971). The discovery of place cells by John O'Keefe was made possible through both advances in electrophysiological methods for recording the activity of single neurons in freely behaving animals (described in Chapter 4) and his insight in adopting a neuroethological approach for studying neuronal activity in response to a natural behaviour. In this approach, as described by O'Keefe & Nadel (1978), a central theme was the focus on natural behaviour, that is behaviour that was generated through means of natural selection such as finding mates, navigation, locomotion and predator avoidance. The ethological approach was in striking contrast to the methods used in behavioural psychology which employed associative and reinforcement tasks that are particular to the laboratory and were used to characterise the brain areas that contribute to spatial learning and navigation.

The neuroethological approach proved to be a good method for investigating spatial representation in the rodent brain as other types of spatially modulated cells were subsequently discovered. Such neurons respond to the direction that the rat is facing (HD cells), in regularly spaced triangular locations (grid cells) and to edges or boundaries of an environment (border cells). It is important to note that all of these cell types provide a spatial representation of self-location in an allocentric reference frame and as a result their spatial firing properties are modulated by both proximal and distal features of the environment.

The following sections provide an overview of these classes of spatially modulated cells, briefly describing their general firing properties, neuroanatomical locations and response to sensory changes (primarily visual) in the environment. Details of the neural circuitry for these different cell types are described in Chapter 2 with a particular emphasis on the HD cell circuit as this cell type was the focus of study in the present thesis.

1.3.1 Place cells

Decades of research have shown the importance of the hippocampus in the encoding of long-term spatial and episodic memories in both rodents and humans (Bird & Burgess, 2008). In rodents a strong candidate for how this information can be encoded at the single-cell level was found in the activity of place cells, hippocampal neurons that fire whenever the rat enters a circumscribed area of the environment known as the place field (O'Keefe & Dostrovsky, 1971). Place cells are pyramidal neurons with complex spiking activity that are primarily found in the CA1 and CA3 subfields of the hippocampus (Henze et al., 2000; O'Keefe & Dostrovsky, 1971). The firing rate of the place cell increases as the rat passes through the centre of the place field and decreases as the rat is farther away from the place field (Muller, Kubie, & Ranck, 1987). The activity of a place cell can be visualised through both a spike plot which displays the path of the rat with superimposed spikes and a heat map which displays the firing rate of the cell (Figure 1.5).

The spatial characteristics of the rate map, such as the size, firing rate and x-y location of the place field relative to the enclosure or to external cues are used to quantify changes in place cells as a result of sensory manipulations in the environment. Studies have shown that the location where the place field originally fires when a rat enters a novel environment is random, however, the shape of the place field remains circular or slightly elliptical and its location remains stable when the rat is recorded in the same environment (Lever, Wills, Cacucci, Burgess, & O'Keefe, 2002; Muller & Kubie, 1987).

In response to sensory changes, such as when the rat is recorded in darkness, place cells generally preserve their spatial characteristics, however they gradually decrease their spatial information as the place field enlarges, suggesting that place cells can update their estimate of self-position by path integration and by integrating contextual information such as odour trails present in the environment (Jeffery, 2007a; Quirk, Muller, & Kubie, 1990).

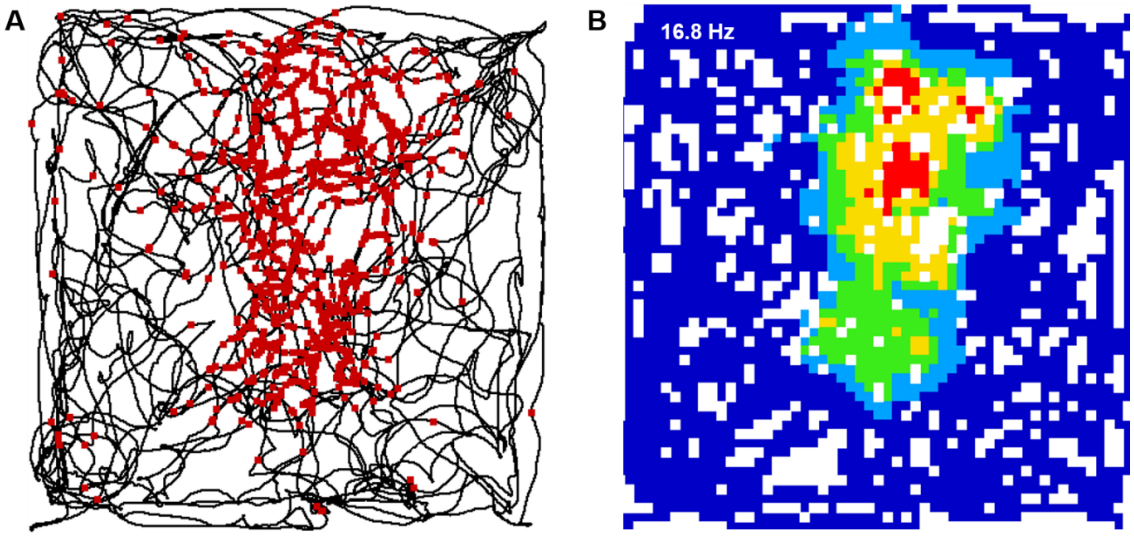

Figure 1.5 Place cell recorded in the hippocampus as the rat foraged for food inside a square environment. **A.** Spike plot of the rat's trajectory (black) with superimposed spikes (red) at locations along the rat's path. **B.** Spatial rate map, where redder colours indicate a high firing rate of the place field and the white pixels indicate unvisited locations. The peak firing rate of the place cell is shown on the top left. Image provided by Giulio Casali.

Place cells are strongly influenced by polarising visual cues located either inside or external (distal) to the environment such that when the cues are rotated, the place fields rotate by a similar amount (Muller & Kubie, 1987; O'Keefe & Conway, 1978). This phenomenon, called landmark control, occurs when the cue card is rotated before the rat is placed back inside the environment. If the cue card is rotated in the presence of the rat, landmark control over the place field is significantly impaired (Jeffery, 1998). These studies show that landmarks can reset the place cell representation provided that the rat perceives a stable relationship between idiothetic and allothetic cues. In instances when there is a

mismatch between idiothetic and allothetic cues, such as when visual cues are rotated in view of the rat, the information that is perceived to provide a better estimate of self-location exerts greater control over the spatial firing properties of places cells.

A more dynamic response is observed when place cells are recorded when the rat is placed in different environments or when sensory changes are made when the rat is recorded in a familiar environment. Studies have shown that when the rat is recorded in two different rooms or when two distinct environments are used within the same room, place cells that fire in one environment may not fire in the other environment, while other place cells randomly change the location of the place field, a phenomenon that has been called global remapping (Muller & Kubie, 1987; O'Keefe & Conway, 1978). In contrast, when a local change is made to a familiar environment such as when a white card is replaced by a black card of the same size and shape (Bostock, Muller, & Kubie, 1991), or when the shape of the environment is gradually morphed from a square to a circle or vice versa, place cells change their firing rate while maintaining their place field location, a phenomenon known as rate remapping (Leutgeb et al., 2005).

Place cells thus provide a continuously updated representation of the rat's position in relation to allocentric coordinates whose dynamic changes that occur during global and rate remapping are thought to reflect time-dependent modifications in the hippocampal memory trace that enable an animal to discriminate the experiences that occur in the same or in different environments (Moser, Kropff, & Moser, 2008; O'Keefe & Nadel, 1978). However, to have an accurate navigational system, the spatial map must link different locations, provide a representation of travelled direction, and provide a metric or scale which can be set in relation to borders or boundaries of the environment.

1.3.2 Head direction cells

In comparison to place cells, HD cells increase their firing rate whenever the rat is facing in a particular direction in the horizontal plane independently of its current

position (Figure 1.6). Originally discovered in the PoS by Ranck (1984) and characterised by Taube et al., (1990a), HD cells are found across many brain areas including the dorsal tegmental nucleus (DTN) (Bassett & Taube, 2001) lateral mammillary nuclei (LMN) (Stackman & Taube, 1998), anterior dorsal (ADN) (Taube, 1995), lateral dorsal (LDN) (Mizumori & Williams, 1993), anterior ventral thalamic nuclei (AVN) (Tsanov et al., 2011), hippocampus (Leutgeb, Ragozzino, & Mizumori, 2000), retrosplenial (RSC) (Cho & Sharp, 2001), parietal (Chen, Lin, Green, Barnes, & McNaughton, 1994) and entorhinal cortex (EC) (Sargolini et al., 2006), as well as in the dorsal striatum (Mizumori & Williams, 1993). A description of the HD cell circuit with an emphasis on the connectivity between the PoS and RSC are described in Chapter 2 while the firing characteristics of HD cells across these brain areas are described in Chapter 3.

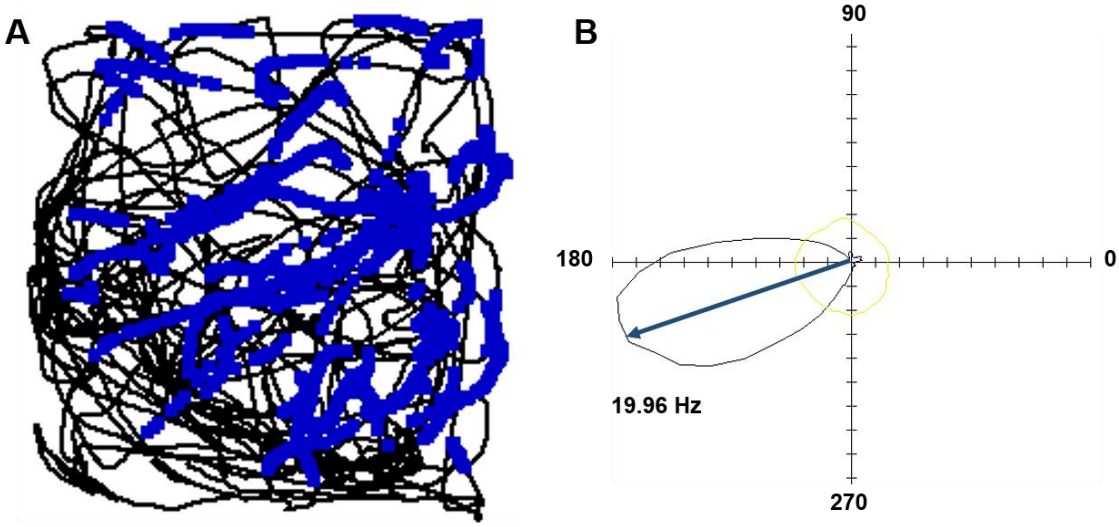

Figure 1.6 Head direction cell recorded in the postsubiculum. **A.** Spike plot of the rat's trajectory (black) showing a burst of spikes (blue) when the rat was facing within the HD cell's directional firing range. **B.** HD cell tuning curve in polar coordinates showing the PFD as a blue arrow at approximately 200° with a peak firing rate of 19.96 Hz. Image provided by the author.

The activity of a single HD cell can be visualised through both a spike plot and a rate map known as a head direction tuning curve (a plot of firing rate as a function

of head direction) where head direction can be displayed in linear or polar coordinates (Figure 1.6). Every HD cell can be characterised based on its tuning curve where the direction to which the cell fires the maximum number of spikes, known as the preferred firing direction (PFD) is the parameter most commonly used to analyse changes in the activity of HD cells. A detailed description of the analytical methods that are used to study the tuning curve characteristics of HD cells are described in Chapter 5.

When a large population of HD cells are recorded simultaneously, all 360° of allocentric space are encoded such that the activity of a single HD cell provides the momentary facing direction within the cell's directional firing range, while all the other HD cells remain inactive (Peyrache, Lacroix, Petersen, & Buzsáki, 2015). The activity of HD cells is tightly coupled to one another such that the angular distance, which is the angle between the PFD of pairs of HD cells remains constant (Peyrache et al., 2015). Similar to place cells, HD cells integrate multimodal information derived from allothetic and idiothetic cues, providing a spatial representation of heading direction (Wiener, Berthoz, & Zugaro, 2002). In this regard, allothetic cues, such as polarising cue cards play an important role in updating the PFD and correcting for accumulated errors derived from path integration (Blair & Sharp, 1996). The influence of idiothetic and allothetic cues in updating the HD signal and the role of landmarks in controlling the directional firing of HD cells are discussed in Chapter 3.

1.3.3 Grid Cells

Based on the discovery of place cells, it was hypothesised that there might be a spatial signal that could compute changes in the direction and distance travelled in a context-independent manner such that the representation for self-location would be invariant to modifications in the environments as occurs during place cell remapping (Redish, 1999). A likely candidate area in which to search for this spatially modulated cell type was the medial entorhinal cortex (MEC) as it provides strong projections to CA1 (Canto, Wouterlood, & Witter, 2008). The breakthrough

came with the discovery of spatially modulated cells recorded in layer II and III of the MEC which have multiple firing fields arranged in a grid of regularly spaced equilateral triangles that cover the entire environment that the rat has explored (Hafting, Fyhn, Molden, Moser, & Moser, 2005) (Figure 1.7A). These grid cells, as they were called, are characterised by several properties such as their orientation (angle between a grid axis relative to the environment or external landmarks), scale (distance between adjacent fields) and phase (offset between neighbouring grid cells) (Figure 1.7B).

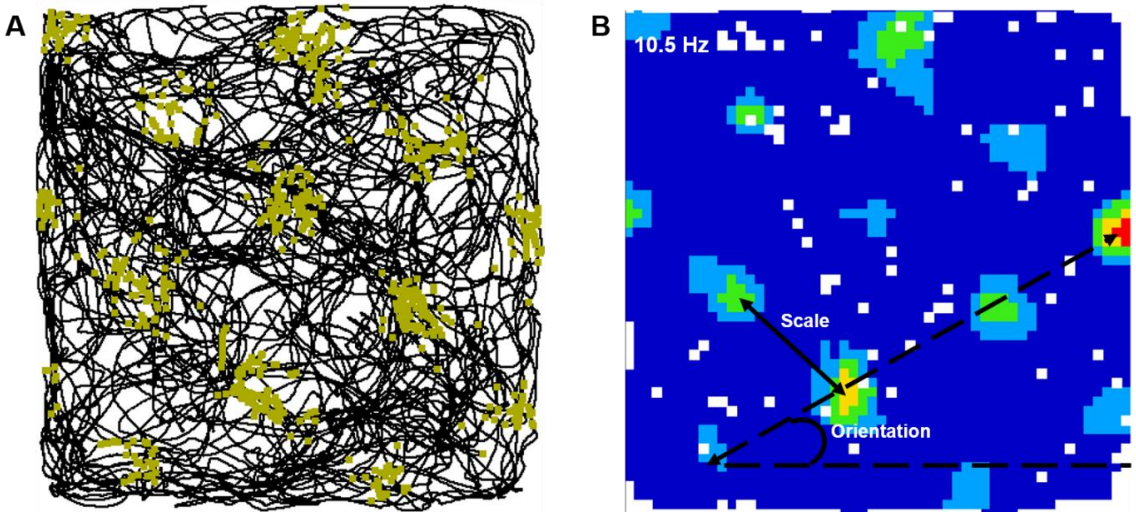

Figure 1.7 Grid cell recorded in the MEC. **A.** Spike plot of a grid cell showing regularly spaced firing fields. **B.** Rate map illustrating the orientation, scale and peak firing rate of the grid cell shown on the left. Image provided by Giulio Casali.

As with place and HD cells, their spatially modulated firing persists in darkness and is anchored to external landmarks, suggesting that they are involved in path integration, using idiothetic information to estimate distance and direction travelled and combining this signal with positional information from landmarks to correct for path integration errors (Hafting et al., 2005). Recently, a study found that the error accumulation from path integration and the observed drift in the regularly spaced grid pattern can be corrected when the animal encounters the wall of the environment, providing further evidence for the role of environmental boundaries

as landmarks that are used for updating self-position estimates (Hardcastle, Ganguli, & Giocomo, 2015).

An interesting characteristic of grid cells in the MEC is that they are topographically organised, such that the grid scale increases from dorsal to ventral layers and groups of grid cells with similar scale and orientation are clustered into discrete modules across the dorsal-ventral axis (Hafting et al., 2005; Stensola et al., 2012). The increasing dorsal-ventral grid scale is thought to be functionally important for multiscale spatial representations, providing maps of different spatial resolution that are needed for short and long-range navigation (Geva-Sagiv et al., 2015).

1.3.4 Boundary vector cells

Boundary vector cells were theorised based on studies which found that place cells stretch their place fields but maintain their allocentric firing location relative to the border of a box when the size and shape of a familiar environment was changed (O'Keefe & Burgess, 1996). Based on these results, the boundary vector cell model predicted the existence of spatially modulated cells that would provide input to place cells, firing at a specific distance and direction from an environmental boundary (Hartley, Burgess, Lever, Cacucci, & O'Keefe, 2000). Later such cells were found in the subiculum (Lever, Burton, Jeewajee, O'Keefe, & Burgess, 2009), the presubiculum (Boccara et al., 2010) and the MEC (Solstad, Boccara, Moser, & Moser, 2008). These cells, which were also called border cells, fire in relation to the distance of boundaries which can be either the wall, barriers or the edge of an environment when there are no walls present (Figure 1.8).

By firing along segments of the perimeter of the environment, border cells signal the distance to a boundary and might be important for providing an anchoring point, serving as proximal landmarks and calibrating path integration errors in the grid cell representation and possibly also in place cells (Hardcastle et al., 2015). Behaviourally, by representing the physical barriers of an environment, border cells might be useful in guiding animals to nearby goal locations when distal landmarks are unavailable.

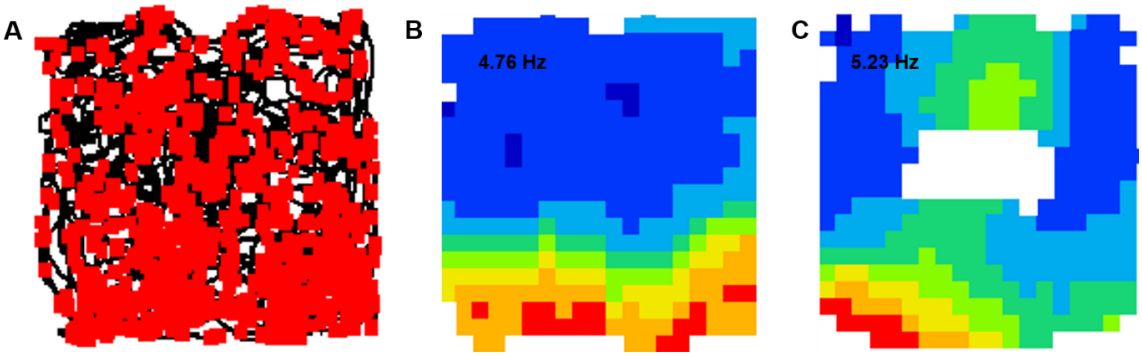

Figure 1.8 Border cell recorded in the subiculum as the rat foraged for food inside a square environment. **A.** Spike plot. **B.** Rate map showing a progressively lower firing rate as the rat moves farther away from the south wall. **C.** Introduction of a barrier creates a second firing field, consistent with the boundary vector cell model. Image provided by Shailendra Rathore.

1.4 Functional significance of spatially modulated cells

The neural representation of self-location which is embodied in the activity of several spatially modulated cells has been found across several species including mice (Yoder & Taube, 2009), rats (Taube et al., 1990a), bats (Finkelstein et al., 2015), monkeys (Robertson, Rolls, Georges-François, & Panzeri, 1999) and humans (Ekstrom et al., 2003), suggesting that it is a mechanism conserved across mammals. The intrinsic activity of these spatially modulated cells has allowed for a model system of how spatial orientation and navigation can be derived from the interaction of idiothetic and allothetic cues, allowing an animal to flexibly select among different navigation strategies depending on the conditions of the environment (navigating in the day or at night) and the availability of proximal and distal landmarks (Figure 1.4).

Though much remains to be known about how the spatial map is integrated by the convergent input of place, HD, grid and boundary vector cells, major advances have been made in characterising the properties and interactions of these cell types across a network of interconnected brain regions (Brandon, Koenig, & Leutgeb, 2014). An important question in the field which has not been fully addressed is how the activity of the different spatially modulated cells relates to

one another, for example how does the HD signal contribute to grid, border or place cell activity and what are the circuit mechanisms that give rise to each cell type (Figure 1.9).

One model system that has proved to be useful for studying the role of idiothetic and allothetic information is the HD system which provides strong input to the different types of spatially modulated cells and has been hypothesised to be important for maintaining their spatial properties. Furthermore, the importance of the HD signal can be seen in the multiple neuroanatomical regions where they are found (reviewed in Section 2.3) and the conjunctive codes found across various brain regions such as place by HD in the hippocampus (Cacucci, Lever, Wills, Burgess, & O'Keefe, 2004), grid by HD in the MEC (Sargolini et al., 2006) and HD by egocentric cue direction in the posterior parietal cortex (Wilber, Clark, Forster, Tatsuno, & McNaughton, 2014).

The current chapter reviewed the behavioural strategies, sensory information (idiothetic and allothetic) and the reference frames that rats use while navigating, integrating multimodal information to create an internal representation of space that is reflected in the activity of place, HD, grid and boundary vector cells which aid in self-localisation. These cells use allothetic information such as the apparatus boundaries, as well as local and distal cues of the environment as landmarks to anchor the location and orientation of their spatially modulated firing activity (Figure 1.9).

An important question that continues to be investigated relates to how a unified spatial map develops from the activity of multiple spatially modulated cells and the role of environmental cues in resetting these spatial representations (Figure 1.9). One view is that in order for a rodent to create an allocentric referenced spatial map, it must combine self-motion cues with information about landmarks to update its current position. In this model, landmarks provide a reference point to which rats orient as they navigate either in a familiar or a novel environment. However, a question that has remained relatively unexplored is what visual properties of the environment are combined during navigation and used as landmarks for spatial orientation.

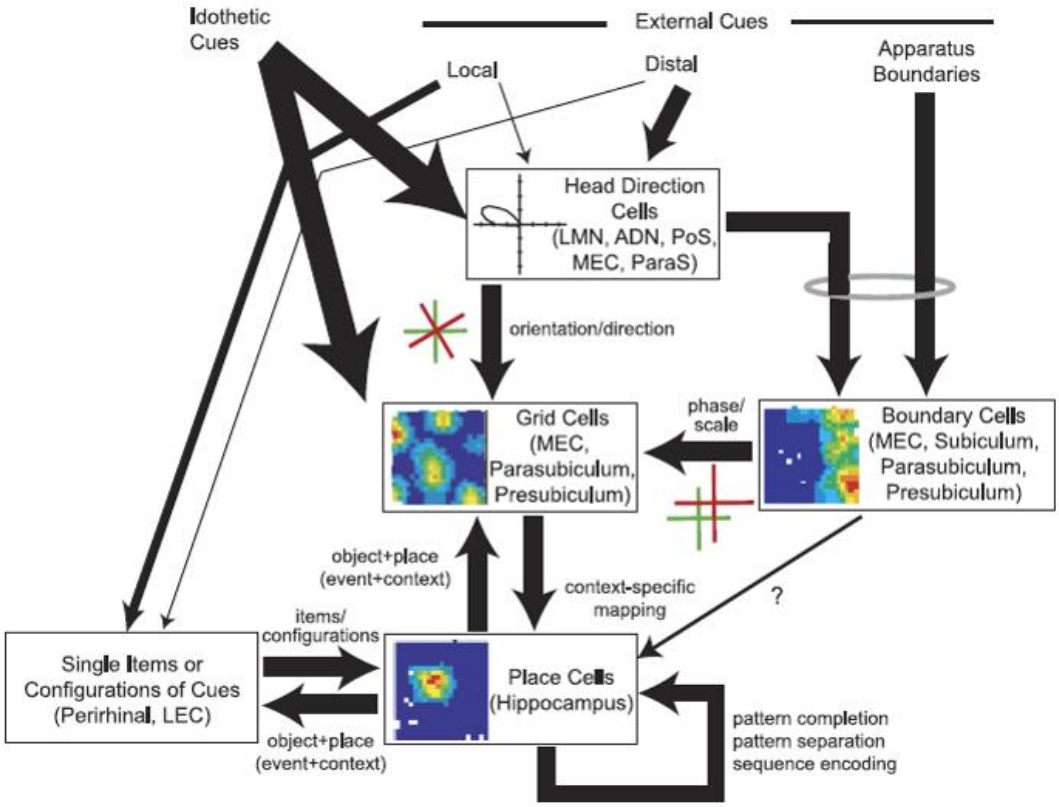

Figure 1.9 Schematic diagram of the allothetic cues that are integrated by the different types of spatially modulated cells. While HD cells integrate both local and distal landmarks to reset their orientation, boundary vector cells use the apparatus Taken from (Knierim & Hamilton, 2011).

To explore this question, Chapter 6 investigates whether different stimulus properties of static visual cues reset the activity of HD cells recorded in the RSC and the PoS of freely-foraging rats. As will be reviewed in Chapter 2, these two interconnected brain areas are part of the HD cell circuit, receiving direct visual input and combine this information with self-motion signal, linking landmark information with spatially modulated signals and relaying this information to other interconnected areas within the spatial navigation circuit such as the hippocampus and the MEC.

Furthermore, after identifying the visual cues that exert strong control over RSC and PoS HD cells, Chapter 7 investigates whether the 2-dimensional spatial relationship amongst different landmarks is used as a source of landmark

information, resetting the activity of HD cells or whether instead they rely on single, discriminable visual features for spatial orientation. The results obtained from these studies could provide insight into how spatially modulated cells encode visual stimuli from the environment, linking visual perception with self-localisation signals.

Chapter 2 Neuroanatomy and functional properties of head direction cell circuits

2.1 Introduction

To understand the relationship between HD, place, border and grid cells, the major anatomical connections between the areas where these spatially modulated cells have been found are described. Particular emphasis will be given to the connectivity of the HD cell circuit, describing the interconnections between the areas that are important for generating the HD signal and the visual information that resets the signal's preferred orientation. Since there are many interconnections in the HD cell circuit, to provide a better understanding of the functional properties of HD cells across brain areas, a two-stream processing model will be described. In this model, idiothetic and allothetic information streams are separated, providing a framework that aids in understanding the multisensory integration of the HD signal based on the results of combined lesion-recording experiments (Bassett & Taube, 2005; Taube & Bassett, 2003).

Since the current thesis investigates the role of visual cues on HD cell activity, particular emphasis will be given to the allothetic stream, describing the hypothesised landmark processing circuit and the visual inputs that are thought to be important for controlling the PFD (Yoder, Clark, & Taube, 2011). Therefore, a description of the rodent visual system and the various pathways that contribute to landmark processing and the anatomical connections of the PoS and the RSC, two brain areas in the HD cell circuit that are hypothesised to play an important role in the processing of landmarks, are described in further detail.

The level of neuroanatomical organization that will be primarily described in the present chapter is at the inter-regional circuit, describing the connectivity between anatomical areas with some emphasis on local circuits, providing details of the different connections between layers in a region of interest. The intrinsic projections within an area and the different neurochemical and morphological cell types are not discussed as little is known about their relationship to HD cell activity. However, as a general principal of neuroanatomy, it is important to mention that in

the cerebral cortex most of the long-range projections to, from and within a cortical area are excitatory, including those projections from and to the specific thalamic nuclei (Shepherd, 2004). Furthermore, in the cerebral cortex, most of the principal neurons which have long axons that send and receive information from other brain areas are primarily pyramidal cells, while the intrinsic cells or interneurons which communicate locally by relaying information between principal neurons are inhibitory (Shepherd, 2004).

Therefore, to understand the functional relationship between the multiple brain areas that contribute to the HD signal and how they integrate self-motion and landmark information, it is important to characterise and describe the main inter-regional connections. Furthermore, understanding the interconnections between microcircuits and the cell types that constitute the spatially modulated neurons is an important and ongoing challenge for understanding the structure-function relationship. New methods that combine juxtacellular recordings with labelling techniques in behaving rats will provide insight into how cell morphology is related to the electrophysiological properties of spatially modulated cells (Tang, Brecht, & Burgalossi, 2014). However, since little is known at the microcircuit level, the current review of the neuroanatomy of the HD cell circuit describes the connectivity at the inter-regional level since most of the studies that have investigated the functional role of the HD signal have used combined pharmacological lesion or inactivation techniques with single-unit recording methods. Consequently, the inter-regional neuroanatomical level of description will provide a framework to understand the relationship between anatomy and the processing of self-motion and landmark information that are integrated in the activity of HD cells to aid in spatial orientation.

2.2 Neuroanatomy of the spatial navigation circuit

To understand the anatomical relationship between HD cells and the other spatially modulated cells (place, grid and border cells), it is important to briefly describe the anatomy of the hippocampal formation (HF) and the surrounding parahippocampal region (PHR). A complete description of the cytoarchitecture

and the connectivity of the HF-PHR network in the rat brain is beyond the scope of this thesis and can be found in Cappaert, van Strien, & Witter (2015).

The HF consists of three distinct areas: 1) The dentate gyrus (DG), 2) the subiculum (Sub) and 3) the hippocampus which consists of sub-regions CA1, CA2 and CA3 (van Strien, Cappaert, & Witter, 2009) (Figure 2.1A). On the other hand, the PHR which has six layers and borders the HF is divided into five areas: 1) The presubiculum (PrS), 2) the parasubiculum (PaS), 3) the entorhinal cortex (EC) which is subdivided into the medial (MEC) and lateral (LEC) entorhinal cortex, 4) the perirhinal cortex (PER) and 5) the postrhinal cortex (POR) (Figure 2.1B). Some neuroanatomists suggest that based on differences in cytoarchitecture and connectivity in the rat brain, the PrS should be divided into a dorsal and a ventral region where the dorsal portion is referred to as the postsubiculum (PoS) and the ventral portion as the PrS (van Groen & Wyss, 1990). As both the dorsal and the ventral regions of the PrS contain HD cells (Giocomo et al., 2014a; Taube et al., 1990a), a distinction will not be made between the two sub-regions and the PrS will be referred to as the PoS.

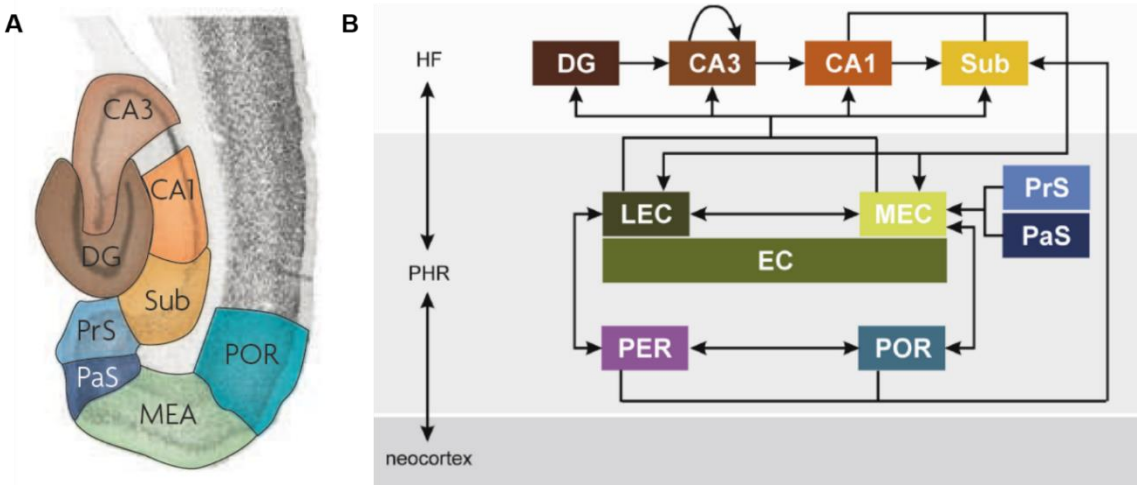

Figure 2.1 Illustration of the areas and the connectivity of the HF-PHR regions in the rat brain. **A.** Sagittal section of the rat brain showing the location of several areas in the HF and the surrounding PHR. **B.** Connectivity of the different sub-areas in the HF-PHR. Not shown are the areas of the neocortex that provide input to the PHR such as the RSC and the visual cortex. Taken from (van Strien et al., 2009).

In the current model of connectivity within the HF-PHR (Figure 2.1B), the MEC provides the major input to the HF, while CA1 and the Sub provide the main output to the PHR (Moser et al., 2014). From layers II and III of the MEC there is a strong input to the hippocampus which leads to the hypothesis that grid cells are important for the spatial firing of place cells (Canto et al., 2008). Consistent with this hypothesis, lesions of the MEC disrupt place field stability and spatial memory in the Morris water maze task (Hales et al., 2014). Interestingly, inactivation of the hippocampus led to a loss in the regular firing pattern of grid cells recorded in the MEC while at the same time increasing the tuning width of HD cells (Bonnevie et al., 2013). These results show a reciprocal influence of the hippocampus and the MEC, and further illustrate how the HD signal might compensate for the loss of spatial information provided by grid cells.

A direct link of the role of the HD signal in generating and maintaining grid cell activity was recently shown in a study where grid cells lost their triangular spatial firing pattern when the anterior thalamic nuclei (ATN) was either lesioned or inactivated, showing that HD cells are important for maintaining the metric properties of grid cells (Winter, Clark, & Taube, 2015). This study also provided evidence for the important role of the HD cell signal in providing information that is needed for path integration.

With regards to border cells, there have been no studies that have examined the contribution of the HD signal to the allocentric firing of these cells, however, based on the boundary vector cell model, one would predict a loss in the tuning properties of border cells and in the encoding of boundaries and barriers when the PoS is lesioned, as this region provides strong input to both the MEC and the Sub (Barry et al., 2006).

2.3 Neuroanatomy of the head direction cell circuit

The connectivity across all the brain areas where HD cells have been found is highly complex and its functional significance remains to be determined. Since the discovery of HD cells in the PoS, a large number of studies have sought to

identify the brain areas that play a role in generating and updating the HD signal. The ongoing research of combining lesion and recording studies across different brain areas has demonstrated the importance of idiothetic and allothetic inputs in generating and updating the activity of HD cells. These results have provided an anatomical-functional model where two pathways or streams of information have been described. In this model, the ascending pathway which originates at the peripheral vestibular organs provides information that is important for generating and updating the HD signal, while the descending stream which originates in the visual cortex provides information that is important for landmark processing and resetting the PFD (Bassett & Taube, 2005; Taube & Bassett, 2003). The two-pathway model thus separates the two major types of information that influence HD cell activity: self-motion and landmarks (Figure 2.2).

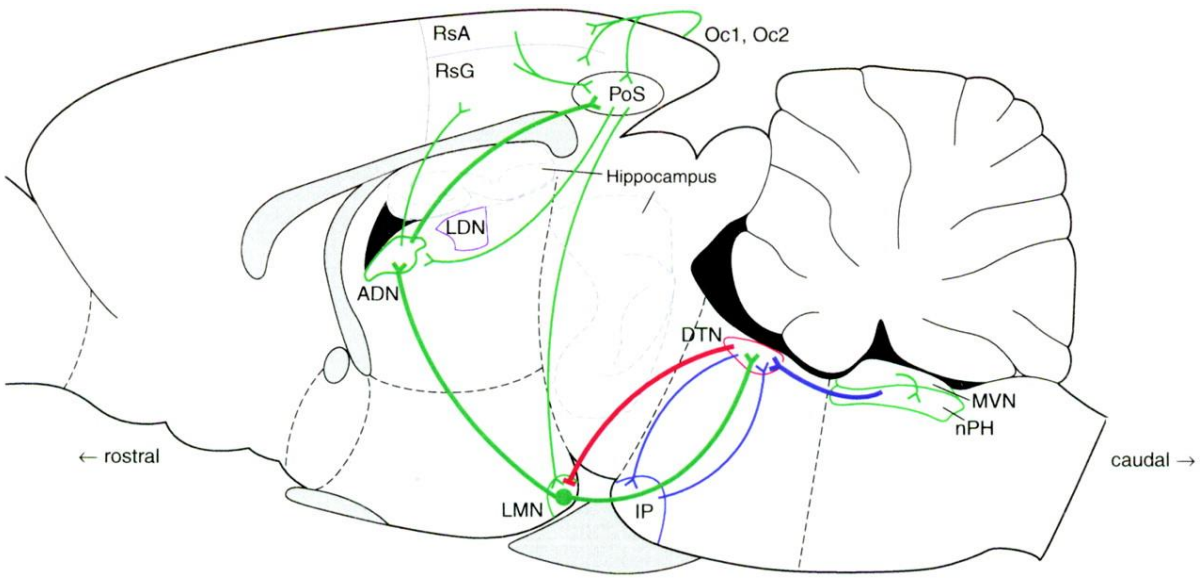

Figure 2.2 Sagittal section of the rat brain illustrating the ascending and descending pathways of the HD cell circuit. Note the reciprocal connections between the DTN-LMN and the ADN-PoS which have been hypothesised to play an important role in generating the HD signal and integrating idiothetic cues with landmark information. Abbreviations not previously defined: Oc1, primary visual cortex, Oc2, secondary visual cortex, RSCd, dysgranular retrosplenial cortex, RSCg, granular retrosplenial cortex. Taken from (Taube & Bassett, 2003).

The HD cell circuit is composed of highly interconnected cortical and subcortical regions that have many direct and indirect pathways as well as reciprocal connections. Most of the brain areas where HD cells have been found are part of the Papez circuit and include the lateral mammillary nucleus (LMN), the anterior dorsal thalamic nucleus (ADN), the anterior ventral thalamic nucleus (AVN), the RSC and the MEC, while other non-Papez circuit areas such as the dorsal tegmental nucleus (DTN) and the lateral dorsal thalamic nucleus (LDN) also constitute part of the HD cell circuit. Although the HD cell circuit receives multiple sources of information, vestibular and visual input play an important role in generating the HD signal and resetting the PFD respectively (Taube, 2007). These two sources of information respectively constitute the ascending and the descending pathways of the HD cell circuit.

The ascending pathway which is important for generating the HD signal starts at the semicircular canals which provide information about linear and angular head movement (Cullen, 2012) (Figure 2.2). This signal is then relayed to the medial vestibular nucleus (MVN), located in the brainstem which combines multisensory information such as neck proprioceptive signals, optic flow, and vestibular input to encode information about angular head velocity, postural control and balance (Vidal et al., 2015). From this convergence of signals, it is apparent that even at early stages of processing there is multimodal sensory integration, which becomes progressively higher in upstream cortical structures. From the MVN, the signal is relayed to the nearby nucleus prepositus hypoglosi (nPH) which is important for the control of eye movements and gaze stabilization during self-motion (Vidal et al., 2015). From the nPH, the signal projects to the DTN where approximately 75% of the cells are modulated by angular head velocity (AHV), increasing their firing rate linearly as a function of head velocity, while 11% are conjunctively modulated by both AHV and the direction where the rat turns its head, and 12% of the cells are allocentric encoding HD cells (Bassett & Taube, 2001; Sharp, Tinkelman, & Cho, 2001). From the DTN, the signal continues to the LMN, where approximately 50% of the cells are modulated by AHV and 25% by HD (Stackman & Taube, 1998).

The reciprocal connectivity between the DTN-LMN is interesting since the projections from the DTN → LMN are inhibitory while the connections from the LMN → DTN are excitatory (Hayakawa & Zyo, 1990). This type of reciprocal inhibitory-excitatory connectivity has been hypothesised to be functionally important for transforming the AHV signal into an allocentric HD signal according to attractor network models described in Section 3.5 (Sharp, Blair, & Cho, 2001). In one version of the attractor network model that has been postulated to explain HD cell firing properties, a layer of excitatory AHV cells activates conjunctive AHV-by-HD cells which in turn inhibit neighbouring excitatory HD cells that are interconnected in a ring, ensuring that only cells with similar directions fire simultaneously while all the other HD cells are inhibited (Taube & Bassett, 2003). This type of network architecture consisting of local excitation and inhibition has been hypothesized to be important for generating the HD signal and for shifting the activity of HD cells depending on vestibular, motor and visual landmark cues, although it has not been demonstrated in the rodent brain.

The signal from the LMN projects to the ADN where approximately 60% of the cells are tuned to HD (Taube, 1995). From the ADN, the HD signal is relayed to the PoS and the RSC (van Groen & Wyss, 1990; van Groen & Wyss, 2003). In the PoS approximately 25% of the cells are modulated by HD (Taube et al., 1990a) while in the RSC only about 10% are HD cells (Cho & Sharp, 2001). As one traces the HD signal across the ascending pathway, the percentage of HD cells becomes progressively lower. Whether this is the result of the strength of projections from the LMN and ADN to cortical areas such as the PoS and RSC or the distribution of a particular cell type that can integrate the inputs needed to encode HD remains to be characterised.

The PoS and the RSC, whose connectivity will be described in Section 2.6, provide input to the subiculum and the MEC where HD cells have been found (Cappaert et al., 2015; Sargolini et al., 2006). The specific functional role of these projections remains to be characterised, however due to their role in angular path integration (Section 3.3.2) and landmark based resetting (Section 3.3.1), it is likely that they provide important information about borders and geometric features of the

environment and visual landmarks that are integrated by border and grid cells. (Section 3.6).

One interesting feature of HD cells in the MEC which has not been observed in any other region where HD cells have been recorded is their topographic organization along the dorsal-ventral axis which only occurs in layer III and not layer V or VI which also contains HD cells (Sargolini et al., 2006). The topographic organization is such that HD cells with narrower tuning curves tend to be located along the dorsal region of layer III while HD cells with broader tuning curves are located in the ventral region of layer III (Giocomo et al., 2014a). The functional significance of this is unknown, however it might be possible that this is partly the result of differences in the population of HD cells in the PoS (estimated to be about 30%) that provide strong input into layer III of the MEC (Canto et al., 2008) compared to the sparser population of HD cells in the RSC (estimated to be about 10%) which project to layer V of the MEC (Czajkowski et al., 2013).

From the neuroanatomical connections, one can observe that vestibular signals propagate upstream across the brainstem and Papez areas, providing self-motion signals to brain regions where HD cells have been recorded. Evidence for the importance of vestibular signals in generating the HD signal is supported by studies which have found that lesions or inactivation of the vestibular input disrupts the activity of cells recorded in the ADN (Stackman & Taube, 1997) and the PoS (Stackman, Clark, & Taube, 2002) such that the directional firing characteristic of HD cells is no longer present. A similar result, in which direction specific discharge of cells was not found after lesions were made to the DTN (Bassett, Tullman, & Taube, 2007), or the LMN (Bassett et al., 2007; Blair, Cho, & Sharp, 1999) was found in recordings conducted in the ADN and in studies were the LMN (Sharp & Koester, 2008), or the ADN (Goodridge & Taube, 1997) was lesioned and single-units were recorded in the PoS. These results provide strong evidence for the role of ascending vestibular signals and self-motion information integrated in the brainstem and mammillary nuclei in generating the HD signal.

In contrast, when lesions are made to cortical structures such as the RSC (Clark, Bassett, Wang, & Taube, 2010), or the PoS (Goodridge & Taube, 1997) and

single-units are recorded in downstream areas such as the ADN, HD cells are present, conserving their characteristic Gaussian tuning curves, however they show an impairment in the ability of a visual landmarks to exert control over the PFD after rotation of a single polarising cue. Evidence for the important role of these cortical areas to landmark processing was found in a study in which bilateral lesions to the PoS with ibotenic acid led to a significant under rotation of the PFD in 31 HD cells recorded in the ADN when a single visual cue placed inside a cylindrical arena was rotated by 90° (Goodridge & Taube, 1997). In the study the authors reported a mean absolute deviation in the PFD (from an expected shift of 0° if there is complete cue control) of 76.3 ± 11.7° in PoS lesioned rats and 15.2 ± 2.9° in the control animals. A similar deficit in landmark control of HD cells recorded in the ADN was found after bilateral electrolytic or NMDA lesions to the RSC (Clark et al., 2010). In the study the authors reported a mean absolute deviation in the PFD of 40.5 ± 11.0° in the electrolytic lesioned animals (n=11 HD cells), 59.2 ± 12.2° for the neurotoxic and 15.2 ± 2.7° for the control animals

Altogether, these results provide evidence of a functional dissociation between the ascending vestibular driven pathway and the descending landmark processing pathway, highlighting the importance of the PoS and the RSC in the processing of landmark information and relaying this input to downstream structures.

2.4 Neuroanatomy of the landmark processing circuit

In the descending or landmark processing pathway, the PoS and the RSC have been hypothesised to play an important role in integrating idiothetic cues with landmark information and relaying this input to other brain regions across both the HD cell circuit and the HF-PHR (Yoder, Clark, & Taube, 2011). The PoS and the RSC are reciprocally connected and receive wide visual projections from multiple pathways which provide different signals that are important for landmark processing (Sugar, Witter, van Strien, & Cappaert, 2011; van Groen & Wyss, 1990a) (Figure 2.3). To understand the functional relationship between visual information and the processing of landmarks by HD cells in the RSC and the PoS, a description of the visual streams that converge on these areas will be described

followed by the connectivity of the PoS and the RSC with areas that provide spatial and non-spatial information. An overview of the rodent visual system will provide a general understanding of how primary and secondary visual areas extract visual information that is needed for object and landmark representation.

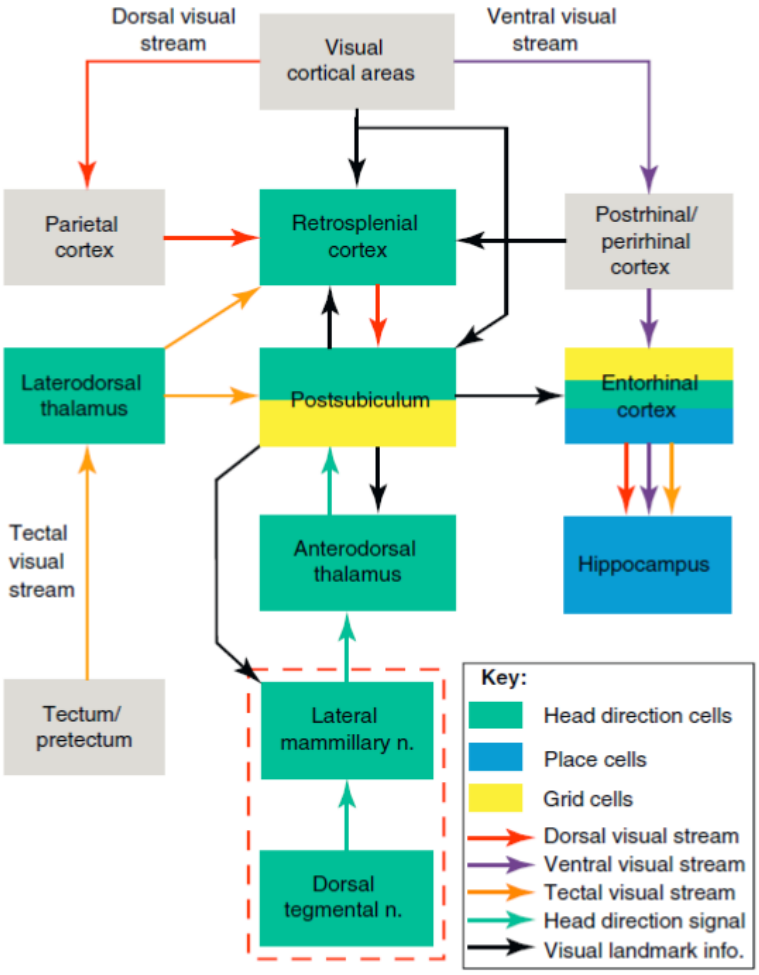

Figure 2.3 Schematic diagram of the landmark processing circuit where visual landmark information from the dorsal, ventral and tectal visual stream converges with the HD signal via the RSC, PoS and LDN. Taken from (Yoder, Clark, & Taube, 2011).

The visual system in the rodent and primate brain has a complex parallel organization where visual information is processed across multiple brain regions. In the primate visual system, two different anatomical and functional pathways have been characterised which separate visual information into a dorsal and a

ventral stream (Ungerleider & Mishkin, 1982). The dorsal stream is important for visuo-spatial processing while the ventral stream supports scene-object visual perception (Kravitz, Saleem, Baker, & Mishkin, 2011). The extent to which functional differences in the dorsal and the ventral visual stream are present in the rodent brain continues to be a matter of ongoing research and little is known about the visual pathways that contribute to scene-landmark processing in the rodent brain. Therefore, in the present discussion of the landmark processing circuit, the dorsal-ventral model from the primate literature will be used to present findings from experiments conducted in rats and mice, providing an anatomical and functional framework of how landmark information might be processed in the rodent brain.

In the landmark processing circuit, the dorsal visual stream follows a pathway from the visual cortex → parietal cortex → RSC → PoS, and direct projections from the visual cortex to the RSC and PoS, providing the necessary visual and spatial information required for identifying and retrieving the spatial location and features of known landmarks (Kravitz et al., 2011) (Figure 2.3). Support for the functional role of the dorsal visual stream in the processing of landmark location was found in a study where lesions of the visual cortex impaired landmark control by three-dimensional objects in hippocampal place fields (Paz-Villagràn, Lenck-Santini, Save, & Poucet, 2002). Until now, there have been no studies that have examined the effects of lesions to the visual cortex on HD cell activity in the RSC or the PoS, however one would expect a deficit in landmark control for both the single cue card protocol and for three-dimensional objects.

In contrast, lesions of the parietal cortex do not impair landmark control of a single cue card in ADN HD cells and lead to mild deficits in the dual-chamber task where HD cells rely on idiothetic cues to update their PFD as the rat walks from a familiar cylindrical environment to a novel rectangular environment via an unfamiliar path (Calton, Turner, Cyrenne, Lee, & Taube, 2008). These results are consistent with the role of the parietal cortex in egocentric, movement related encoding (Nitz, 2012) and do not rule out the functional role of the parietal cortex in landmark processing as information about the location of visual cues can arrive to the ADN

via downstream connections from visual areas to the PoS (Figure 2.3). Thus the PoS can extract visual features of landmarks and the environment and relay this information to downstream structures such as the ADN and LMN to aid in spatial orientation.

The functional role of the parietal cortex via the pathway from the PoS → RSC has been hypothesised to contribute to route planning by transforming the allocentric spatial representation of place, grid and HD cells into an egocentric representation of locomotor actions needed to plan movements in a navigational sequence (Calton & Taube, 2009; Whitlock, Sutherland, Witter, Moser, & Moser, 2008). This transformation is different from what occurs in the dorsal striatum where motor actions become linked to reward locations, as the parietal cortex representation is more flexible and can integrate multiple landmarks and reference frames to coordinate goal-directed navigation (Nitz, 2006; Penner & Mizumori, 2012).

Consistent with the hypothesised function of the parietal cortex in mediating egocentric-allocentric representations, early studies reported cells in the posterior parietal cortex (PPC) that were modulated by turning direction or forward motion or that shifted their firing direction in relation to a goal location marked by a light in an 8-arm maze (Chen, Lin, Barnes, & McNaughton, 1994). Recently, a study in which single-units were recorded in the PPC as rats continuously visited 32 reward locations marked by a blinking light in the perimeter of a circular arena reported classic allocentric encoding HD cells, neurons that fired in relation to the cue direction, which were called egocentric cue direction (ECD) cells, and conjunctive ECD by HD cells that were modulated by a combination of both (Wilber et al., 2014). Other studies found that PPC cells discharged when rats travelled a particular path to a goal when several routes were available, demonstrating that this activity is independent of place and HD (Nitz, 2006). Similarly, PPC cells have been shown to encode turning sequences and segments of a route as a rat moves in a maze with continuous passages (square spiral tracks), representing the rat's progression along a route independent of its allocentric position and direction of walking (Nitz, 2012).

On the other hand, lesions of the RSC disrupt landmark control of ADN HD cells (Clark, Bassett, et al., 2010) while PoS lesions disrupt landmark control of ADN (Goodridge & Taube, 1997) and LMN HD cells (Yoder, Peck, & Taube, 2015). These studies provide strong evidence that the pathway for landmark processing in the HD cell circuit is routed via the RSC and the PoS. Until now, no combined lesion-recording experiments have been conducted to examine the interaction between the RSC-PoS, however based on their strong interconnections and those with the ADN, one would expect a severe disruption in landmark processing after lesions to any of these two cortical structures.

In contrast to the dorsal visual pathway, the ventral visual stream follows a pathway from the visual cortex → POR/PER → RSC → PoS and can provide the input needed for landmark perception and recognition, helping to discriminate different environments by linking landmarks with contextual information via the POR and associating landmarks via the PER (Ranganath & Ritchey, 2012) (Figure 2.3). There have been no studies that have examined HD cell activity after lesions to the POR or the PER, however, single-unit recordings in the POR have found neurons that signal the conjunction of objects and locations, supporting the functional role of the POR in visual object discrimination (Furtak, Ahmed, & Burwell, 2012).

A separate source of visual information from the tecto-cortical pathway can reach the PoS and the RSC via the LDN (Figure 2.3). The LDN receives direct projections from the superior colliculus and projects to the RSC and the PoS (van Groen & Wyss, 1992). The pathway from the superior colliculus → tectum/pretectum → LDN → RSC-PoS might be involved in attention and orienting responses to visual and other salient sensory stimuli, guiding the direction and speed of eye movements during exploration and escape behaviours via its input from the superior colliculus (Sefton, Dreher, Harvey, & Martin, 2015). This information can aid in landmark processing and navigation by guiding current, visual attention and allowing the rat to monitor overhead stimuli for predator detection while accessing and encoding landmark information from the dorsal and ventral streams (Wallace et al., 2013).

Interestingly, unlike all other HD cells that have been recorded in the HD cell circuit, LDN HD cells require visual input to maintain their directional firing. This was found in a study where the directional firing of HD cells was lost when the rat was placed on the apparatus in darkness and was re-established when the lights were turned on (Mizumori & Williams, 1993). This study shows that the persistent directional firing of HD cells that is maintained by idiothetic cues is not present in the LDN as the main input for self-motion signals is routed via the ADN and not the LDN (Figure 2.3). Not surprisingly, lesions of the LDN do not impair landmark control in HD cells recorded in the PoS as landmark information arrives via direct and indirect visual pathways that do not include the tectal visual stream (Golob, Wolk, & Taube, 1998). A short description of the rodent visual system and the functional correlates of cortical visual areas in rats and mice will help to understand how visual stimuli are encoded in the brain and what visual features might be integrated in the RSC and the PoS for landmark representation and spatial orientation.

2.5 Rodent visual system

Rodents such as rats and mice have laterally placed eyes that provide them with a large panoramic field of vision of about 280° with a binocular overlap of approximately 40-60° (Artal, Herreros de Tejada, Muñoz-Tedo, & Green, 1998). Unlike primates, which have large eyes and about 99% of cones located in the fovea, rodents have relatively low visual acuity which is the result of having a much smaller eye and a retina that lacks a fovea (Jeon, Strettoi, & Masland, 1998). In the rodent retina, approximately 97% of the photoreceptors are rods which are specialised for vision under low light conditions (Jeon et al., 1998). Therefore, the lack of a fovea and the even distribution of rods across the retina provide rodents with a low-contrast and large peripheral vision at the expense of having low-acuity vision. To compensate for the low visual acuity, rodents rely on head movements rather than eye movements, obtaining a better sampling of the visual space (Huberman & Niell, 2011).

Neuroanatomically, the rodent visual system is hierarchically organised and divided into several distinct areas with multiple parallel pathways that extract visual information from the retina and transform sensory inputs into a representation of the environment in upstream cortical areas (Coogan & Burkhalter, 1993). The basic organization of the visual pathways is as follows: Retina → retinal ganglion cells → superior colliculus and dorsal lateral geniculate nucleus (dLGN) → primary visual cortex → extrastriate cortex.

In rats the majority of retinal ganglion cells project to the superior colliculus, where the major projection to the primary visual cortex is via the dLGN (Sefton et al., 2015). The functional significance of this segregation of pathways remains to be determined, however as discussed previously, it is likely that the tecto-cortical pathway has a role in attention and orienting to visual stimuli while the geniculo-cortical pathway relays visual information for image perception.

In contrast, the input from the dLGN reaches the primary visual cortex (also known as area 17 or V1) where neurons extract simple local image features with receptive fields that are tuned to orientation, spatial frequency and contrast (Girman, Sauvé, & Lund, 1999). In turn, V1 projects to a hierarchical series of extrastriate areas whose functional properties are beginning to be characterised and are likely related to processing global features of the environment (Katzner & Weigelt, 2013). Consistent with this hypothesis, the size of the receptive fields in extrastriate areas become progressively larger and less tuned to simple features like cells in V1, reflecting a higher level visual representation that might allow for the capacity to recognize an object independently of its size and position (Rousselet, Thorpe, & Fabre-Thorpe, 2004). Furthermore, as is the case in primates, visual information from V1 in rodents is likely segregated into a dorsal stream that carries information about object location and a ventral stream that carries information about object identity, though further studies are needed to confirm this.

In relation to the functional properties of extrastriate visual areas, a recent study examined brain activity in the mouse brain using in vivo two-photon calcium imaging in the posteromedial visual area (PMA), a region that receives visual input

from V1 and projects to the RSC. The authors found that cells in the PMA have a strong preference for cardinal orientations (horizontal and vertical) compared to oblique orientations (Roth, Helmchen, & Kampa, 2012). This result is interesting as natural scenes contain more horizontal and vertical edges than diagonals (Girshick, Landy, & Simoncelli, 2011) and the PMA is located in a region where it can extract this information from the environment and relay the input to the RSC for the processing of landmarks (Girshick et al., 2011; Switkes, Mayer, & Sloan, 1978). The study also found a subpopulation of neurons that were tuned to high spatial frequency and low speed of drifting gratings which might provide information that could aid to orient towards objects that move slowly as the rat locomotes, as is the case with distant landmarks. These findings suggest that the RSC could process high-level, object defining features such as the size and shape of visual stimuli by extracting low-level features such as orientation, spatial frequency and contrast from the primary and secondary visual cortex.

Furthermore, even though the receptive field model has proved fundamental to understanding the functional properties of cells in the striate cortex, the response of cells in V1 are not solely modulated by visual parameters. Recent studies have found that behavioural factors such as locomotion can influence the activity of neurons in V1 (Saleem, Ayaz, Jeffery, Harris, & Carandini, 2013). Therefore, future studies that seek to investigate the functional properties of extrastriate areas in both the dorsal and the ventral pathway would need to be conducted in alert, moving animals while they are presented with naturalistic visual scenes (Carandini & Churchland, 2013; Einhäuser & König, 2010).

In summary, based on anatomical and electrophysiological data, the visual system of rodents is capable of processing a vast amount of information needed for navigation. The integration of visual information with spatially modulated cells enables rodents to perform tasks where it is important to remember the features and the location of landmarks (Section 1.2). This is particularly important as the perception of a landmark will vary depending on the distance and the viewing angle, therefore it is fundamentally important for the visual system to extract features from the environment to create a spatial-contextual representation.

Consistent with this notion, studies have shown that rats are capable of invariant visual recognition, distinguishing the shape and other complex visual features when images are varied in size, position, viewpoint, rotation or a combination of these properties (Tafazoli, Di Filippo, & Zoccolan, 2012; Vermaercke & Op De Beeck, 2012).

2.6 Connectivity of the retrosplenial and postsubicular cortex

The RSC and the PoS are highly interconnected regions that have an important functional role in the integration of self-motion signals from the ascending stream and landmark information derived from various visual pathways. The interconnections of the RSC and the PoS with the ADN (van Groen & Wyss, 1990a; van Groen & Wyss, 2003), LDN (Thompson & Robertson, 1987; van Groen & Wyss, 1990a; van Groen & Wyss, 2003) and between one another (van Groen & Wyss, 1990a), place these structures at a key anatomical position to integrate and relay idiothetic and landmark information to other spatially modulated cells across the HF and PHR (Figure 2.4A).

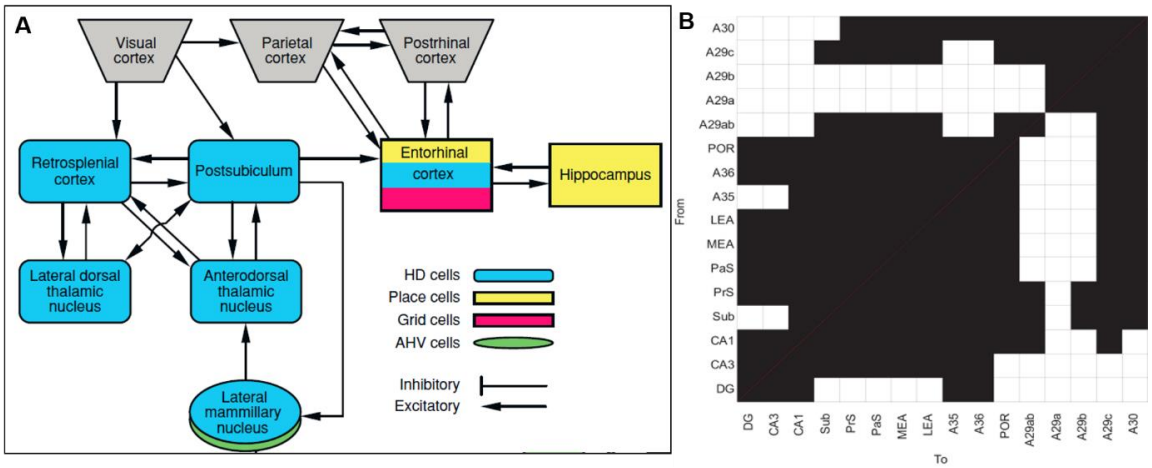

Figure 2.4 Main connections of the RSC and the PoS. **A.** Connections of the RSC and the PoS which contribute to landmark processing by HD cells. Note that most of the visual information is projected to the MEC and HCC via the PoS. **B.** Connectivity matrix of the PoS and sub-areas of the RSC with areas in the PHR and the HF. Abbreviations: Brodmann area A35 and A36, perirhinal cortex; PrS, dorsal presubiculum or PoS. Taken from (Taube, 2007) and (Sugar et al., 2011).

Before describing the afferent and efferent projections of the RSC and the PoS, it is important to describe the nomenclature that will be used throughout the text as different naming conventions have been used, making it difficult to compare the reported connections across different articles. Furthermore, in the anatomical literature the connections are often described in qualitative terms which do not specify the strength of the projections nor a detail connectivity between sub-regions. A recent effort to map and quantify at high-resolution the strength of connectivity across the mouse brain can be found in the Allen Brain Atlas (http://connectivity.brain-map.org/) which allows visualisation and reconstruction of projections across multiple regions of interest.

In the HD cell circuit and across the brain, the RSC represents one of the largest cortical areas in rats which receives wide projections from visual areas (Miller & Vogt, 1984), the thalamic nuclei (Vogt, 2015), the HF-PHR (Sugar et al., 2011) and the parietal cortex (Wilber et al., 2015) (Figure 2.4A). Based on these connections, it can be hypothesised that the RSC in involved in multisensory integration and the processing of both spatial and non-spatial signals that are required for navigation.

The RSC has been divided into two main areas: 1) A dysgranular area (RSCd), also known as area 30 or A30, located in the dorsal region, and 2) a granular area (RSCg), known as A29 and located in the ventral region of the RSC (Sugar et al., 2011). The term granular refers to the densely packed pyramidal cells that are most densely concentrated in layer II and layer III. The RSCg has been further divided into areas a, b, c and ab, where the area ab is located at the most ventral region of the RSC (Sugar et al., 2011). The PoS and the sub-areas of the RSC have diverse connections with regions of the HF and the PHR where HD signals and landmark information converge with different types of spatially modulated cells.

The connectivity of the RSC and the PoS with the PHR and HF can be visualised in a matrix diagram which provides valuable information about differences in the connections at the inter-regional circuit level. The diagram can be used to identify afferent, efferent and reciprocal connections of the RSC and the PoS with regions

in the PHR and the HF, as well as intrinsic projections within sub-areas of the RSC (Figure 2.4B). A summary of the main connections of the PoS and the RSC are described in this section. A detailed description of the intrinsic connections between the layers of the RSC and its sub-areas and between the HF-PHR and the RSC sub-areas are described in Sugar et al., 2011.

Visual information to the RSC projects from V1 and targets A30 and to a lesser extent A29b, while substantial projections from the visual association cortex (area 18b) target A30, A29b and A29a (van Groen & Wyss, 2003). There are also strong back projections from A30 to V1 and to 18b (Miller & Vogt, 1984). In the PoS, visual input comes directly from V1 and indirectly via the RSC (Vogt & Miller, 1983).

The RSC receives most of its afferent thalamic input from the ADN, LDN, AVN and anterior medial (AMN) thalamic nucleus (van Groen & Wyss, 1992). The direct connection from the ADN → RSC is sparse, as most of the ADN input is indirectly projected to A30 and A29c via the PoS (van Groen & Wyss, 1995). The LDN provides strong input to A30, A29c and A29ab (van Groen & Wyss, 2003). In comparison, the AMN only projects to A30 and the AVN to A29c (van Groen & Wyss, 1990a, 1995).

The efferent projections from the RSC to the thalamic nuclei are less selective as they arise from both the dysgranular and granular areas and connect strongly to the LDN, AMN and AVN (van Groen & Wyss, 1990a; van Groen & Wyss, 2003). The PoS on the other hand has strong reciprocal connections with the ADN and LDN, and a direct projection from the PoS to the LMN (van Groen & Wyss, 1990b) (Figure 2.4A).

The RSC is strongly connected with the PoS, as all sub-regions of the RSC project to the PoS and the PoS projects to A30, A29b and A29ab (van Groen & Wyss, 1992a; van Groen & Wyss, 2003). The RSC also has wide connections with the PHR and the HF (Figure 2.4B). Particularly noteworthy are the projections from all the sub-areas of the RSC to CA1 and the inhibitory input from CA1 to A30, A29a, and A29b (Cenquizca & Swanson, 2007; Miyashita & Rockland, 2007). Another

important anatomical connection is between the RSC and the MEC, where the MEC sends modest inputs to the RSC (Wyss & van Groen, 1992) and caudal portions of A30 project strongly to layer V of the MEC (Czajkowski et al., 2013). The PoS also provides input to layers III and V of the MEC (Dolorfo & Amaral, 1998) where HD cells have been recorded (Sargolini et al., 2006). The projection from the RSC and the PoS to the MEC could provide self-motion signals needed for the emergence of grid cell firing and landmark information needed to anchor the orientation of grid cells.

In relation to the connections with the parietal cortex, a recent study found that most of the inputs to the medial parietal cortex (MPC) come from the RSCd (A30) while only a minor projection comes from the PoS (Wilber et al., 2015). Additionally, the connections between the parietal cortex and the MEC are generally weak and most of the input from the MPC to the PHR is relayed via the RSC → PoS pathway (Wilber et al., 2015). Given the strong reciprocal connections between the RSCd and the MPC, this suggests that the function of these two areas is tightly coupled. As previously described and based on electrophysiological data, it is likely that the RSC-MPC play a role in allocentric-egocentric coordinate transformations where allocentric signals from place, grid and HD cells are converted into an egocentric reference frame needed for route planning and the execution of locomotor actions (Calton & Taube, 2009; Whitlock et al., 2008).

The current chapter described the general neuroanatomy of the spatial navigation circuit with an emphasis on the connectivity of the HD cell circuit. A two-stream processing model of idiothetic-allothetic signals was introduced to understand the role of self-motion in generating the HD signal and visual landmarks in providing an allocentric reference point to which HD and other spatially modulated cells anchor their activity. The two-stream model provides a neuroanatomical framework that will aid in understanding the functional role of the RSC and the PoS in landmark processing and the results of many experiments that have investigated the influence of idiothetic and allothetic cues in the HD system which are discussed in Chapter 3.

The projections and functional correlates of visual areas that provide input to the PoS and the RSC in the rodent brain were described in this chapter to understand the hypothesised role of these two brain areas in linking visual input with spatial navigation signals. Furthermore, knowing the neuroanatomical connections of the RSC and the PoS is important to understand how landmarks are processed, that is, which visual and spatial features of visual cues in the environment are effective for anchoring the activity of HD cells and how the HD system selects amongst different allothetic cues to reset their PFD, a topic that is investigated in Chapter 6 and Chapter 7 respectively.

Chapter 3 Multisensory processing by head direction cells

3.1 Introduction

The encoding of head direction in allocentric space has been found in species as diverse as flies (Seelig & Jayaraman, 2015), mice (Yoder & Taube, 2009), rats (Taube et al., 1990a), bats (Finkelstein et al., 2015) and macaques (Robertson et al., 1999) providing evidence of a neural computation that has been conserved across the animal kingdom. The functional role of the HD signal is hypothesised to be related to spatial orientation, navigation and memory, where multiple sensory and motor signals converge to provide the ongoing perceived directional heading as the animal moves about in the world (Taube, 2007).

In rats, HD cells are found in a wide number of interconnected brain areas that are responsible for generating, updating and resetting the HD signal (Section 2.3). In this circuit, ascending vestibular input relayed through subcortical regions are important for generating the HD signal, while descending input from visual cortical areas relayed through the PoS and the RSC provide visual information that is important for the processing of landmark cues and resetting the PFD of HD cells (Section 2.4).

The aim of the current chapter is to describe the multiple sources of sensory information that influence the activity of HD cells, emphasizing the role of visual stimuli in controlling the PFD in order to understand how landmark cues are processed by HD cells. To understand the influence of landmarks on HD cell activity and other spatially modulated cells, it is important to first describe the firing characteristics of HD cells and the general properties of the HD signal (Section 3.2). The quantitative description of the tuning curve characteristics and the analysis that are commonly applied to study cue control experiments in HD cells are discussed in detail in Chapter 5. A summary of the studies that have investigated the influence of allothetic and idiothetic cues are presented in Section 3.3, seeking to dissect the contribution of multisensory cues in the activity of HD cells. The factors that influence the likelihood that visual cues are used as

landmarks to control the activity of spatially modulated cells are discussed in Section 3.4, presenting studies that have investigated the role of the geometrical properties of the environment and the influence of the features and proximal-distal location of visual cues in controlling the spatial firing properties of HD cells.

A theoretical model that seeks to explain how the HD signal is generated and updated by self-motion and visual cues is described in Section 3.5, discussing attractor network models and the role of angular velocity signals and external landmarks. Finally, the chapter concludes with a discussion of the hypothesised role of the HD signal in path integration and the role of the PoS and the RSC in the integration of visual landmark information with self-motion signals (Section 3.6). As the activity of HD cells is tightly coupled with that of place and grid cells, examples from cue control studies in which these spatially modulated cells where recorded are discussed throughout the chapter.

3.2 Properties of the head direction signal

A typical HD cell has a Gaussian shaped unimodal tuning curve where the cell's firing rate decreases as the rat moves its head in the horizontal plane away from the cell's PFD (Section 1.3.2 and 5.3). Each HD cell has a single PFD whose directional firing range represents a particular range of head orientations in allocentric coordinates such that a population of HD cells maps all 360° of azimuth space (Taube et al., 1990a). In adult rats, the directional firing range varies from 60-150° and the peak firing rate can vary from 5-120 Hz across brain regions (Taube & Bassett, 2003). With the exception of HD cells in layer III of the MEC where the directional firing range increases along the dorsal-ventral axis, no topographic organization in the tuning curve properties of HD cells has been observed in any other brain region (Giocomo et al., 2014).

Even though there is large variability in the peak firing rate of HD cells within a brain area, the range of the peak firing rate does not differ between interconnected areas as for example between the PoS and the ADN (Taube & Muller, 1998). Interestingly, in recordings of neural ensembles of HD cells in the PoS and the

ADN, pairs of cells that had a smaller angular distances with respect to their PFD's were strongly correlated in terms of their firing rate, particularly in the ADN compared to the PoS (Peyrache et al., 2015). In terms of the directional firing range, a general trend has been observed such that HD cells recorded in subcortical areas as for example the LMN (Stackman & Taube, 1998) and the ADN (Stackman & Taube, 1997) tend to be more broadly tuned compared to those recorded in cortical areas such as the PoS (Taube et al., 1990a) and the RSC (Cho & Sharp, 2001). However, no study to date has made a quantitative analysis comparing the tuning curve properties across brain areas and no experiment has addressed whether there is a functional significance of HD cells having different peak firing rates and directional firing range as is the case of neurons in V1 where narrower tuning curves are more likely to represent cardinal orientations (Li, Peterson, & Freeman, 2003).

When multiple HD cells are simultaneously recorded and visual cues in the environment are rotated without the rat being present, the activity of HD cells is tightly coupled such that their tuning curves shift together by a similar magnitude and direction (Taube et al., 1990b), suggesting that the population activity maintains an internal consistency that is referred to as the coherency of the ensemble (Johnson, Seeland, & Redish, 2005). Recent studies have shown that the internal coherency of neuronal ensembles is stronger in the ADN compared to the PoS, perhaps due to differences in the strength of connections with areas that provide angular head velocity signals such as the DTN and the LMN (Section 2.3) (Peyrache et al., 2015).

Several properties of the HD signal found across different studies conducted in rats and mice suggest that it has an important role in spatial orientation and navigation. These include maintaining an internal coherency during cue manipulations (Taube et al., 1990b), having a persisting directional selectivity when the animal is recorded in darkness (Blair & Sharp, 1996) or before eye opening in the rat pup (Bjerknes, Langston, Kruge, Moser, & Moser, 2014; Tan, Bassett, O'Keefe, Cacucci, & Wills, 2015) and not requiring external sensory input to maintain its internal network activity during sleep (Peyrache et al., 2015).

Additionally, the HD signal is supramodal, meaning that it does not depend on a single sensory modality to maintain its directional firing as demonstrated in studies where the rat is recorded in the absence of polarising cues (Goodridge & Taube, 1995; Taube et al., 1990b), blindfolded (Goodridge, Dudchenko, Worboys, Golob, & Taube, 1998) or in path integration tasks (Taube & Burton, 1995; Valerio & Taube, 2012).

3.3 Integration of sensory cues by head direction cells

Multiple sources of information are integrated during navigation, influencing the activity of spatially modulated cells such as place and HD cells (Wiener et al., 2002). These multisensory signals coming from idiothetic input provided by the vestibular system, optic flow, proprioceptive and motor-efference signals, as well as allothetic input derived from the sensory features of the environment, influence the location, direction and orientation of place, HD and grid cells (Section 1.2.2 and Section 1.3).

A large number of studies have sought to dissect the contribution of idiothetic and allothetic inputs in the activity of place and HD cells by manipulating visual, vestibular and motor cues. In the context of spatial navigation, the term cue refers to any signal that bears information which the animal can potentially use for self-localization. The studies that have addressed multisensory integration in place or HD cells are primarily carried out by either modifying a single cue across a specific dimension, such as distance, location or feature in the case of visual cues, or by co-manipulating visual, vestibular and motor cues, creating a mismatch between the different sources of allothetic-idiothetic inputs. To understand how multiple sensory cues are combined in spatially modulated cells, representative studies will be discussed in this section to illustrate the influence of allothetic and idiothetic cues on the activity of HD cells, while a detailed description of the role of visual cues is discussed in the following section.

The overarching idea from these studies is that the brain improves the computation of self-location by combining sensory information within and across modalities,

weighing the different cue information and selecting amongst the most reliable cues in order to derive a unified representation of perceived directional heading. Although a discussion of the different models that seek to explain cue integration is beyond the scope of this this thesis, Fetsch, DeAngelis, & Angelaki (2013) provide a model of optimal visual-vestibular cue integration based on Bayesian probability theory. Their model seeks to explain how multiple sensory cues that arise from different sensory modalities are combined in an optimal manner, where optimality is defined as the estimate that gives the lowest degree of uncertainty or variance (Fetsch et al., 2013). Adapted to multisensory integration by HD cells, the model implies that when estimating the current directional firing from multiple sensory cues such as visual, vestibular and motor, a weighted average of the estimates obtained from the individual cues is performed, such that the cues are weighted in proportion to their relative reliability, that is to how precise they measure a specific sensory cue. This implies that there is an optimal range of values for each sensory cue such that the probability of a given cue controlling the PFD will depend on: 1) How close the stimulus properties matches the optimal processing of a given cue and 2) which cues have a higher relative reliability when multiple cues are present. This model will be used throughout this chapter to explain the results of cue control experiments, idiothetic-allothetic cue conflict experiments, and to elucidate how visual cues are selected as landmarks, exerting a consistent and reliable control over HD cell activity.

3.3.1 Influence of allothetic cues

In the first study that characterised the effects of environmental manipulations on PoS HD cells, Taube et al., (1990b) recorded rats as they foraged for food inside a 76 cm cylindrical enclosure with a prominent white card attached to the inner wall. Surrounding the arena, a black circular curtain was used to visually isolate the cylinder and ensure that the white card was the only strong visual asymmetry in the environment (Muller, Ranck, & Taube, 1996). The authors found that when the cue card was rotated in steps of 90° in the presence of the rat, there was a consistent under-shift in the PFD. In contrast, if the cue card was rotated by the

same magnitude when the rat was outside of the arena and the rat was disoriented (being transported inside an opaque box and rotated slowly) prior to being placed back into the arena, the majority of HD cells rotated in direct proportion to the cue card rotation, showing a mean absolute deviation in the PFD shift of 18.9°, where 0°would indicate perfect cue-following, demonstrating strong landmark control over PoS HD cells (Taube et al., 1990b). A similar mean PFD shift deviation of 13.2° was observed in single cue control experiments of HD cells recorded in the ADN (Taube, 1995).

It is important to note that for these experiments, the minimum absolute mean deviation that can be obtained if there is perfect cue control is 0° where larger values indicate weaker or no landmark control. However, even when there are no changes in the position of the cue card and the rat is familiar with the environment, removing the rat across trials leads to an average shift in the PFD of about 5°, which has been interpreted to be the result of self-motion cues interacting with landmark information in the process of resetting the firing of HD cells (Taube et al., 1990b; Taube, 1995). It is important to note that the average shift of 5° is within the range of the 6° bin size that is commonly used to create a histogram of the firing rate as a function of heading direction. Therefore, it is possible that such changes are the result of the analysis applied to estimate the tuning curve parameters of an HD cell rather than an actual mechanism of error correction by the HD system. A detailed discussion of the methods that are applied to analyse HD cells are presented in Chapter 5.

No study to date has examined landmark control of RSC HD cells using the single cue card protocol in the cylindrical arena. However, a similar study landmark control study was conducted by recording single-units in the RSC in rats that were trained on a spatial working memory task in an 8 arm radial maze with four cue cards arranged in the recording room at the level of the maze (Chen, Lin, Barnes, et al., 1994). The authors found a highly variable response in RSC HD cells to the cue control experiments in which the four distal cues were rotated together by either 90° or 180°. In about 24% of RSC HD cells, the PFD maintained an angular distance relative to the cue cards within ±45° showing good landmark control,

while 61% of HD cells remained relatively unchanged after the cue rotations and 15% of the total recorded HD cells did not have any relationship between the PFD and the cue rotation. The lack of strong landmark control by RSC HD cells might have been the result of the experimental protocol since the rats remained in the maze while the light was turned off and the cue cards were rotated, leading to a conflict between idiothetic and allothetic cues such that idiothetic cues had a higher reliability as the cue cards were perceived to be unstable. It is also possible that the rats left scent trails that might have contributed to the lack of shift in the PFD. These results highlight some of the difficulties of conducting cue control studies, where uncontrolled cues can contribute to the variability in the PFD shifts during the processing of landmarks, where idiothetic and allothetic cues are weighted by HD cells to reset their PFD.

In the cue control experiment of Taube et al., (1990b), the observed under-shift in the PFD when the cue card is rotated in the rat's presence is the result of a cue conflict between self-motion and visual cues, where these two sources of information provide a different estimate of self-position. In terms of the multisensory integration model, one could interpret this effect as being the result of a decrease in the relative reliability of the visual cue and an increase in the relative reliability of the self-motion cues, such that when both are weighted, HD cells shift by a magnitude less to what is expected if there is complete stimulus control by the cue card. This assumes that HD cells are primarily controlled by self-motion and visual cues, however, olfactory cues such as urine spots and scent trails left by the rat or auditory cues coming from the recording equipment or from other location could potentially exert some control over the directional firing. Although it is possible that these uncontrolled stimuli influence the activity of HD cells, cue control experiments using olfactory or auditory stimuli do not reliably control the PFD. This was shown in a study conducted in blindfolded rats where the rotation of an olfactory cue (a peppermint extract) exerted weak landmark control over the PFD as demonstrated by a mean PFD shift of 55.2° when the olfactory cues were rotated by 90° (Goodridge et al., 1998). Similarly, 1 Hz auditory clicks presented as auditory cues with speakers located inside the recording arena exerted weak landmark control over the PFD, resulting in a mean PFD shift of

37.8° (Goodridge et al., 1998). These results suggest that although olfactory and auditory cues can weakly influence HD cell firing, they do not exert the same magnitude of stimulus control over the PFD as is observed with visual cues.

On the other hand, when the rat is disoriented prior to being exposed to the rotated cue card, the polarising white card exerts strong landmark control over PoS and ADN HD cells (Taube et al., 1990b; Taube, 1995). In this situation, the relative reliability of the cue card is high, while that of self-motion cues is lower. As a result, the weighted average of these two cues will favour the estimate derived from the location of the cue card. Strong landmark control in these studies is favoured by the rats being recorded in a familiar environment such that when the rat is exposed to a novel landmark and disoriented before being placed into the recording arena, it takes between 3-8 minutes for a cue card to reliably control the PFD (Goodridge et al., 1998).

It is important to note that the neural effects of disorientation on idiothetic input remain to be determined; however, it is likely that linear and angular head velocity signals are impaired, affecting heading direction estimates since the rat's internal sense of orientation obtained from self-generated movements are disrupted. This would occur as a result of interfering with continuous vestibular cues that provide the rat with an estimate of the speed at which it is moving or accelerating (Redish, 1999). Thus, when the animal is disoriented, the computation of self-location derived from path integration provides low relative reliability, and as a result visual cues become predominant above idiothetic cues in the estimation of directional heading.

Furthermore, the effect of disorientation on cue control by HD and place cells is highly variable, with some studies finding poor landmark control after disorientation (Knierim, Kudrimoti, & McNaughton, 1995, 1998), while others reporting a minimal effect (Dudchenko, Goodridge, & Taube, 1997). It is likely that one of the reasons for the variable results is the lack of a systematic protocol that controls vestibular stimulation, as the disorientation protocol is often conducted manually by the experimenter. This is particularly important as studies have shown that slow rotations of the rat and the environment below vestibular threshold gain control

over place cells (Jeffery, Donnett, Burgess, & O'Keefe, 1997) and over both ADN HD cells and CA1 place cells (Hargreaves, Yoganarasimha, & Knierim, 2007).

In summary, the results of the above studies indicate that in the absence of visual cues, idiothetic information can control the location or directional firing of place and HD cells. In contrast, when salient visual cues are available and have a high relative reliability, they are perceived as stable and the spatial information derived from the visual landmarks predominates over idiothetic cues in controlling place field or PFD orientation. This is probably accomplished by a weighted average obtained from the spatial and non-spatial information derived from the cues available such that the probability that an HD cell would be controlled by a specific cue depends on the relative reliability of the allothetic and idiothetic cues, where a greater weight is given to visual cues compared to self-motion cues when both are not in conflict with one another (Stein & Stanford, 2008).

3.3.2 Influence of idiothetic cues

A question that has been explored since the discovery of place and HD cells pertains to the contribution of self-motion cues such as vestibular, proprioceptive, motor efference and optic flow to the directional firing of these cells when visual landmarks are either available or absent. Studies have shown that HD cell activity is maintained, albeit with some drift in the PFD when rats are recorded blindfolded (Valerio & Taube, 2012), in darkness (Blair & Sharp, 1996) or in the absence of polarising cues in the environment (Goodridge & Taube, 1995; Taube et al., 1990b), suggesting that visual cues are not necessary for maintaining the firing of HD cells and that idiothetic cues can maintain the firing of HD cells when visual landmarks are not available.

The information derived from the vestibular system such as angular velocity signals are important for the spatially modulated activity of HD and place cells as demonstrated in a study where temporary inactivation of vestibular input disrupted the directional firing of PoS HD cells and the location-specific firing of hippocampal neurons (Stackman et al., 2002). Other studies have investigated the role of self-

motion cues by recording HD cells in tasks that rely on path integration. In one of these tasks, the rat walked across a dual-chamber apparatus starting from a familiar cylindrical arena and moved to a novel rectangular environment that was out of view across a 40.5 cm U shaped elongated passageway (Stackman, Golob, Bassett, & Taube, 2003; Taube & Burton, 1995; Yoder, Clark, Brown, et al., 2011). Since the environment was unfamiliar, the location of potential landmarks had not been learned and as a result the rat had to rely on self-motion information which progressively accumulates error as the distance between the familiar and the novel environment increases.

Consistent with this hypothesis, when the passageway (40.5 cm long) that connected the two environments was located in the same room, there was an average PFD shift of 18° (Stackman et al., 2003; Taube & Burton, 1995), and when the passageway was 11.4 m long and the two environments were located in different rooms, the average PFD shift was about 30° (Yoder, Clark, Brown, et al., 2011). If the rats were recorded in darkness as they walked across the 40.5 cm passageway, the average PFD shift was about 30° (Stackman et al., 2003) which was larger compared to when the rat walked the same distance with the lights on. In comparison, when rats travel along a complex route in a 14-unit T-maze which they previously explored, HD cells shift by an average of 18° as the rat has access to all of the familiar visual cues (Yoder, Clark, Brown, et al., 2011). The large PFD shift when rats travel the passageway in darkness is due to a lack of idiothetic signals derived from optic flow and the absence of allothetic cues that can calibrate the path integrator.

The influence of self-generated movements, proprioceptive and motor efference on HD cells has been studied primarily through two approaches: 1) Recording before, during and after the rat is tightly restrained by being wrapped in a towel and rotated slowly in the horizontal plane through the cell's directional firing range (Knierim et al., 1995; Taube, 1995), or 2) recording while the rat remains stationary as it drinks water from a tray located in the centre of a rotatable platform that is surrounded by a black cylinder with a white cue card attached to the inner wall (Zugaro, Tabuchi, Fouquier, Berthoz, & Wiener, 2001). When the rat is restrained,

there is a significant reduction in the firing rate and the directional tuning of ADN HD cells that is recovered once the rat is unrestrained and moves freely, suggesting that proprioceptive and motor efference signals are needed to maintain HD cell activity (Knierim et al., 1995). A limitation of this study is that it cannot dissociate whether the effects on HD cell activity are due to the lack of self-initiated movements or to other factors related to the stress that arise from the tight restraint. To investigate this question, Zugaro et al., (2001), trained rats to remain immobile while recording ADN HD cells. The authors found that the mean peak firing rate decreased by 27% and that there was no significant change in the PFD and the directional firing range compared to when the rat was freely foraging. These results highlight the importance of self-initiated movements and proprioceptive feedback in the persistent firing activity of HD cells.

A study that examined if HD cell activity was maintained while rats remained head fixed and loosely restrained was conducted by Shinder & Taube (2011). The author's recorded ADN HD cells as the rat was passively rotated in a platform while being head fixed to an apparatus frame with its body loosely restrained. The main finding was a lack of change in the tuning curve properties compared to when the rat was freely foraging. It is likely that these results differ from those previously reported due to differences in the magnitude of the body restraint which affected proprioceptive and motor efference signals. Furthermore, the linear and angular velocity input was better controlled for in this study compared to when the rat was manually rotated while being tightly restrained, showing that the vestibular input needed to sustain HD cell activity does do not need to be self-generated. Future studies would have to examine the extent to which head and body restraint affects the activity of DTN-LMN cells that are modulated by angular head velocity which is hypothesised to be important for the generation of the HD signal (Sharp et al., 2001). The results of the Shinder & Taube (2011) study also show that HD cell activity can be generated in head-fixed animals as long as they have access to linear and angular velocity signals. These results are consistent with previous findings were HD cells have been recorded in head-fixed primates (Robertson et al., 1999) and head-fixed flies (Seelig & Jayaraman, 2015) that had access to self-motion signals.

Studies that have investigated the influence of motor efference on ADN and PoS HD cells have been conducted by passively transporting rats aboard a wheeled cart from a familiar to a novel environment in the dual-chamber apparatus with the aim of disrupting the continuous information derived from self-locomotion (Stackman et al., 2003). The results showed that passively transporting the rat to the unfamiliar environment leads to an average shift in the PFD of 70° (Stackman et al., 2003). Based on these findings, the authors concluded that motor efference and proprioception cues are important for maintaining a stable PFD in conditions that require path integration. However, strong evidence for the role of HD cells in path integration was found almost a decade later in a study conducted by Valerio & Taube (2012), who recorded HD cells in the ADN of blindfolded rats that had been trained in a food-carrying task where they had to search for a pellet in a walled circular arena and return to a familiar refuge. In this study the authors found a strong correlation between the PFD shift and the heading error that matched the direction that the rat travelled after collecting the pellet.

Lastly, the influence of optic field flow on ADN HD cells was investigated in a study in which a moving dot array was projected over the surface of a curtain as rats foraged for food on a circular platform (Arleo et al., 2013). The authors found that optic flow information updated the PFD, albeit at drift speeds that were threefold lower than expected if one assumes complete control of the directional firing by optic flow signals. These results show that optic flow signals contribute to updating the PFD and suggest that other idiothetic cues are weighing on the activity of HD cells to provide an estimate of directional heading.

In summary, idiothetic cues and particularly vestibular input are essential for the location-specific and directional firing of place and HD cells. The vestibular input that is needed to sustain spatially modulated activity can come from either the animal's self-motion or it can be induced externally by rotating the rat. Furthermore, motor, proprioceptive and optic flow signals control the directional firing of HD cells, showing the multisensory integration of idiothetic cues during navigation.

3.4 Factors that influence landmark control

The previously described cue control experiments are often conducted using a single polarising card subtending the inner wall of an environment that is highly familiar to the rat. As a result, the studies do not address which sensory features of the environment are effective for anchoring the activity of HD cells and how the HD system selects amongst different allothetic cues to update the PFD.

To address these questions, the following sub-sections briefly summarise the results of studies that explore the time course needed to learn about the location of landmarks, the time that it takes to update the PFD, the role of proximal and distal visual cues and the influence of geometric features of the environment in controlling the activity of HD cells. The influence of allothetic and idiothetic cues on HD cells was discussed in Section 3.3, along with studies that explored cue conflict between these two sources of information. Therefore, the present section focuses only on the influence of visual cues with studies that investigate visual-visual cue conflicts.

3.4.1 Learning of visual landmark cues

As previously discussed, place and HD cells are controlled by a complex interaction between idiothetic cues and external landmarks. The reliance on visual or self-motion cues on HD cells is variable and depends on many factors such as the degree of disorientation (Knierim et al., 1995), the location of the cue (Zugaro et al., 2004), the prior experience with the cue (Taube & Burton, 1995) and the magnitude of the cue conflict (Knierim et al., 1998; Knight et al., 2014). In instances when there is a conflict between idiothetic and familiar landmarks, the visuo-spatial information derived from the learned visual cues dominates over idiothetic information, controlling the PFD of HD cells recorded in the ADN (Goodridge & Taube, 1995) and the PoS (Zugaro, Tabuchi, & Wiener, 2000). These studies have shown that when there is a mismatch between the two sources of information, familiar visual cues generally tend to exert a greater weight in the activity of HD cells with significant under-rotation compared to when allothetic and idiothetic cues

are in agreement with one another. A detail summary of the studies that have examined the effects of cue conflict on HD cell activity employing different manipulations are described by Knight et al., (2014).

Experience can also influence the spatial firing of place, HD and grid cells depending on whether the rat is familiar or unfamiliar with the environment as would occur when the rat explores it for the first time (Barry, Hayman, Burgess, & Jeffery, 2007; O'Keefe & Burgess, 1996; Taube & Burton, 1995). Depending on the familiarity with the environment, the activity of HD cells is likely to undergo two different processes referred to as resetting and remapping. When the rat is placed into a familiar environment and the position of the cues are changed, resetting is more likely to occur, whereby HD cells update their PFD in relation to familiar visual cues (Taube et al., 1990b). The resetting process is thought to provide a mechanism for reorientation relative to familiar landmarks. In contrast, when the rat is placed by the experimenter into a new environment, remapping is more likely to occur, whereby HD cells change their PFD to an arbitrary direction and subsequently remain stable (reset) as the rat becomes familiar with the features of the environment including the position of salient landmarks (Taube et al., 1990b). It is important to note that HD cell remapping does not occur when the rat locomotes from a familiar to a novel environment as path integration can maintain the bearing of the PFD, albeit with some deviation (Stackman et al., 2003; Taube & Burton, 1995; Yoder et al., 2011).

In studies where rats are taken from a familiar to a novel environment, the PFD becomes stable once the rat learns about the stability of the cues, presumably by a weighted cue average of idiothetic and allothetic inputs. Interestingly, the process of updating the PFD in relation to visual cues does not require the hippocampus as lesions to this structure do not impair cue control or the tuning curve properties of HD cells in the PoS and the ADN when the rat is recorded in a novel environment across days (Golob & Taube, 1997). This suggests that the process of updating the PFD in relation to visual cues might be driven by the current sensory and spatial information derived from the environment through a process similar to perceptual learning. Further studies need to explore whether

other structures that are connected to the HD cell circuit such as the RSC encode long-term information about landmarks or whether they act as a working memory system, allowing for the short term recognition and use of landmarks for spatial orientation.

The learning of landmarks can occur very fast, as demonstrated by a study where a single 1 minute exposure to a novel cue was sufficient for PoS and ADN HD cells to exert reliable cue control in 5 out of 8 HD cells recorded (Goodridge et al., 1998). Furthermore, the transitioning period for an HD cell to change its PFD to a new orientation occurs very fast as shown in a study in which ADN HD cells were recorded as rats remained still by drinking water while a single cue card was rapidly rotated by 90° in between a short period of light and darkness (Zugaro, Arleo, Berthoz, & Wiener, 2003). The authors found that the PFD transitions to a new orientation within 80 ± 10 ms after the visual cue is rotated. These results show that rats can use familiar landmarks to rapidly reorient in an environment and provide evidence that the updating process of the PFD relative to static landmarks is dynamic and undergoes abrupt transitions between different HD bearings, consistent with continuous attractor network models (Section 3.5).

3.4.2 Learning of foreground and background cues

The single cue experiments do not strictly address if there is a preference for foreground compared to background cues since the black curtain that surrounds the dimly lit recording environment does not constitute a controlled distal cue. To dissociate the influence of proximal and distal cues in landmark control, a cue conflict experiment is commonly carried out where salient proximal and distal cues are rotated in opposite directions relative to one another.

In a study that sought to characterise the type of visual cues that control HD cell activity, three different objects arranged at equal angles with respect to each other were placed at the edge of a standard 76 cm cylindrical arena surrounded by a black curtain (Zugaro, Berthoz, & Wiener, 2001). The authors found that when the objects were rotated by 120° across trials, ADN HD cells shifted by the same

magnitude and direction as the objects in all of the recorded sessions, demonstrating strong landmark control. In contrast, when the cylinder was removed and the same protocol was repeated, the PFD did not shift and remained fixed relative to the room coordinates in all the HD cells recorded. These results suggest, although they do not conclusively show that visual motion signals, such as parallax, influences the landmarks that are selected by HD cells to anchor their directional firing, favouring distal background cues over proximal cues. An alternative explanation is that after removing the cylindrical enclosure, rats had access to distal cues such as the surrounding black curtain which was arranged as a square enclosure and had remained out of view before. In order to rule out this explanation, the curtain should have been rotated across trials to examine whether rats are using the curtain drapes as a cue to control the firing of HD cells.

A study that explicitly tested if ADN HD cells select background cues on the basis of dynamic visual information such as motion parallax and optic field flow was conducted by Zugaro et al., (2004). In the experiment, the rat was placed on an elevated platform 22 cm in diameter surrounded by a 3 m diameter cylindrical curtain. Inside the arena, two freely standing white cue cards with a black vertical stripe were placed at 90° of each other. The size of the cue cards and the distance relative to the platform were in a 1:4 ratio in order to make the relative distance of the cards the distinguishing feature rather than their salience or apparent size. When the cue cards were rotated by 90° in opposite directions, thus creating a conflict between the proximal and the distal cue, the authors found that the PFD followed the background cue in 57% of the trials, the foreground cue in 9%, the configuration of the two cards in 25% and in 9% of the trials the PFD did not shift.

These results provide support that background cues are more effective at controlling the PFD compared to foreground cues. This might be due partly to the effect of motion parallax in the processing of landmarks, such that background cues are perceived to shift less rapidly compared to foreground cues as an animal moves around the environment, providing depth information and allowing a reliable reconstruction of the spatial relation among landmarks (Wiener et al., 2002). Therefore, distance parallax in conjunction with idiothetic cues derived from optic

flow signals during movements contribute to the updating process of HD cell activity (Arleo et al., 2013).

3.4.3 Processing of geometric cues

The shape of the environment can also be used as a landmark for orientation influencing the activity of HD cells. An early study that tested this hypothesis found that PoS HD cells shift their PFD by an average of 78° when the shape of the environment is changed from a cylinder to a rectangle (Taube et al., 1990b). Further support for the influence of the environment's geometric features on HD cells was found in a study in which rats that were trained to perform a working memory task by retrieving water from cups placed in the corner of a square box were subsequently tested in a rectangular box with a similar cue card located in the same position (Golob, Stackman, Wong, & Taube, 2001). The authors found that during the training session when the rat was exposed only to the square arena, in about 23% of the trials ADN HD cells shifted their PFD by a magnitude that was a multiple of 90°, with 88% of the shifts being either 90° or 270°. A similar result was found in the testing session when the rat was placed inside the rectangular arena where the PFD shifted in 12/13 trials in multiples of 90 ± 18° with 10/12 shifts of 270°. Another study found that the geometrical features of the environment exert a greater influence when the rats are disoriented prior to being placed in the environment compared to when they are not disoriented (Knight, Hayman, Ginzberg, & Jeffery, 2011).

These results suggest that HD cells are sensitive to the geometric properties of the arena, however they do not reliably control the PFD and are overridden by the visuo-spatial information of a salient familiar visual cue. When the rat is disoriented, the geometry of the enclosure can be used as a landmark, however under normal circumstances when there is no conflict between self-motion and allothetic cues, the rat relies on both visual cues and path integration to reset the PFD. In addition, the 90° remapping observed in HD cells is consistent with the observed changes in the orientation of grid cells when the rat is taken from a

circular arena to a polarised geometrical environment such as a square arena (Stensola, Stensola, Moser, & Moser, 2015). This change is consistent with the hypothesis that distal cues set the orientation of the rat's internal coordinate system by the activity of HD cells, and local cues such as boundaries and geometrical properties of the environment set the translation and scale of the metric system computed by grid cells (Knierim & Hamilton, 2011).

The activity of HD cells is also strongly coupled with that of place cells. For instance when distal landmarks are rotated or when the environment is displaced to different locations relative to the distal room cues, the location and directional firing of place and HD cells tends to be maintained (Yoganarasimha & Knierim, 2005). At the population level, however, the encoding of self-location based on local and distal cues is more dynamic in place cells compared to HD cells. While simultaneously recorded HD cells coherently represent either the local cues such as the geometric features of the environment or the distal landmarks, CA1 place cells can either be coupled to the activity of HD cells (Yoganarasimha & Knierim, 2005) or decouple (Yoganarasimha, Yu, & Knierim, 2006) where place fields remap and are controlled by local, distal or a complex combination of both cues.

3.5 Theoretical models of head direction cell activity

One of the most widely applied models used to explain the population coding of HD cells is that of a continuous attractor network (CAN) model (McNaughton et al., 2006). There are many different variants of these models and what they have in common is that they are comprised of a network of interconnected excitatory and inhibitory neurons that are capable of reaching a stable pattern of firing and maintain a representation for a particular time interval (Rolls, 2010).

A CAN is composed of units or neurons that are embedded in a chart with a particular geometric arrangement or manifold in which neural activity can be focalized within a restricted region of the chart known as the activity pocket. Neural activity in the chart can be in a high or a low energy state which can be represented by changes relative to the background firing rate. In a high energy state, the activity

pocket has the capacity to propagate across the active chart as it receives dynamic input from other layers of the network, whereas in a low energy or stable state the activity pocket does not propagate (Samsonovich & McNaughton, 1997). The low energy state can be offset by coordinated excitatory input, leading to a directional shift in the activity pocket that is dependent on the source of the incoming information (Rolls, 2010).

One of the early models visualized the HD system as a one-dimensional ring attractor with HD cells representing all 360° of heading directions (Skaggs, Knierim, Kudrimoti, & McNaughton, 1995). In this ring model, each HD cell has a different PFD and neighbouring HD cells have strong excitatory connections, whereas those that represent distant PFD's have strong inhibitory connections. The activity pocket which represents the Gaussian shaped tuning curve that codes for the rat's current HD propagates across the ring driven by a hidden layer of excitatory rotation cells that provide an angular velocity signal that is integrated with the current HD. The layer of rotation cells in turn receives excitatory input from cells in the vestibular nucleus that signal information about linear and angular head movement. Rotation cells were predicted to be turn modulated, that is to respond in relation to both angular velocity and the turning direction of the head in the horizontal plane (Skaggs et al., 1995). Such angular head velocity cells which linearly increase their firing rate as a function of angular speed for both clockwise and counter-clockwise head movements were subsequently found in the DTN and the LMN (Bassett & Taube, 2001; Stackman & Taube, 1998).

In the ring model, left rotation cells enable the propagation of the activity pocket counter-clockwise by exciting HD cells that code counter-clockwise head movements while a layer of interneurons provides global inhibition to all other HD cells in the ring preventing the HD system from representing two different heading directions at the same time. This type of architecture is supported by the reciprocal inhibitory connections between the DTN and the LMN (Sharp et al., 2001). An interesting property of turn modulated HD cells is that of anticipatory time interval coding where the activity of an HD cell predicts future heading movement by approximately 38 ms in the LMN (Stackman & Taube, 1998), and 25 ms in the

ADN (Blair, Lipscomb, & Sharp, 1997). In the PoS the anticipatory time interval is close to zero, implying that HD cells in this region code for the instantaneous heading direction (Taube & Muller, 1998). While this property was not predicted by the Skaggs et al., (1995) model, recent CAN models have sought to account for these results by postulating that rotation cells are inhibitory rather than excitatory, however until now the model has not been successful in explaining differences in anticipatory time interval and directional firing range across interconnected brain areas of the HD circuit (Song & Wang, 2005). A summary of the experimental evidence that support the ring attractor model of HD cell activity can be found in (Knierim & Zhang, 2012; Taube & Bassett, 2003).

In addition to rotation cells, Skaggs et al., (1995) introduced a layer that provides visual input and updates the PFD in relation to landmarks. These visual feature detectors were predicted to respond to the location of visual cues in relation to egocentric coordinates and to strengthen their connection weights as they become associated with a particular heading direction. Feature detector cells thus modify their firing rate as a function of egocentric direction in such a way that only those visual cells that have been strongly linked with a particular PFD will become active while all other visual cells will be inhibited for that particular PFD. Recently, a study found what might be a candidate visual feature detector cell according to the Skaggs et al., (1995) model in single units recorded in the PPC that fired in relation to the cue direction in egocentric coordinates and conjunctive egocentric by allocentric HD cells (Wilber et al., 2014). Although continuous attractor network models have postulated visual feature detectors that could shift the activity pocket, it remains to be determined what neurophysiological processes enable landmarks to reset the orientation of HD cells.

3.6 Role of the RSC and the PoS in landmark processing

Landmarks correct for path integration errors by minimising the drift that would occur if the animal was solely relying on idiothetic cues. The strong influence of landmarks has been shown in studies where rotation of a single salient cue card located inside a cylindrical arena leads to a corresponding shift in the location,

direction and orientation of place, HD and grid cells (Hafting et al., 2005; Muller & Kubie, 1987; Taube et al., 1990b). These studies demonstrate the importance of landmarks in providing a spatial reference point to which spatially modulated cells anchor their firing activity. They also support the hypothesis that the activity of spatially modulated cells across the HF-PHR and the interconnected HD cell circuit is closely interrelated. Furthermore, based on studies that have found a strong coupling in the activity of simultaneously recorded HD cells with both place (Knierim et al., 1995) and grid cells (Sargolini et al., 2006) during cue rotation experiments, it has been hypothesized that HD cells provide the reference direction to which place and grid cells anchor their spatially modulated firing. Additional support for the important role of the HD cell signal to grid cell firing was found in a study where lesions or inactivation of the ATN disrupted grid cell activity, where the cells lost their characteristic regular triangular firing pattern (Winter et al., 2015).

An important question that remains to be fully explored is how the activity of neurons in visual areas contribute to the processing of landmarks by spatially modulated cells and what pathways bring this information into the HD cell circuit and the HF-PHR. Currently there are few studies that have explored these questions, though the results of combined lesion and recording studies suggest that the PoS and the RSC play an important role in the processing of landmark information, integrating visual input from primary and secondary visual areas (Section 2.6) with self-motion signals from the LMN and ADN and relaying this visuo-spatial information to other areas of the HD cell circuit (Section 2.4) and across the HF-PHR (Section 2.2).

The important role of the PoS in landmark processing has been shown by studies where lesions to this brain area lead to a disruption of landmark control in HD cells recorded in the ADN (Goodridge & Taube, 1997), LMN (Yoder et al., 2015), and CA1 place fields (Calton et al., 2003). The magnitude of disruption in the HD cell signal, landmark control and path integration after lesions to the PoS and single-unit recordings in the ADN and the LMN varies, with more severe impairments in HD cells activity occurring in the ADN. This was shown by a significant increase in

the directional firing range and a uniform distribution in the PFD shifts of ADN HD cells recorded in both the single cue rotation protocol and the dual-chamber task (Goodridge & Taube, 1997). In comparison, LMN HD cells which also showed an increase in the directional firing range, had a unimodal distribution of PFD shifts with a mean direction of 0° albeit with a different variance compared to the control group in both the single cue rotation protocol and the dual-chamber task, showing that there was a mild disruption in landmark control and path integration in LMN HD cells. These results might have been due to the feedback connections between the ADN and the PoS, leading to a larger deficit in landmark control and path integration compared to the downstream connection from the PoS to the LMN. Although the results of these studies were not directly compared, a detail discussion of the analysis commonly applied to the study of HD cells are presented in Chapter 5, providing examples of how the reported results might under-sample the variability that could capture small differences between a control and lesion-recording group.

Similarly, lesions to the RSC lead to a widening in the directional firing range of ADN HD cells, a drift in the PFD during cue control experiments conducted with the lights on and in darkness, a mild impairment in landmark control and no disruption to path integration in the dual-chamber test when the experiment is conducted with the lights on (Clark, Bassett, et al., 2010). Other studies have shown that temporary inactivation of the RSC leads to deficits in the performance of rats tested in darkness on a spatial working memory task in an 8 arm radial maze and also disrupt the stability of place fields recorded in the same task (Cooper & Mizumori, 2001). The behavioural impairments are consistent with similar findings from a study that found that RSC-lesioned rats displayed deficits in a path integration task when conducted in the dark (Elduayen & Save, 2014) and also with a large body of work that has found spatial working memory deficits and heading direction errors in RSC lesioned rats (Vann & Aggleton, 2004).

In summary, the literature review chapters provided evidence that the PoS and the RSC are involved in spatial orientation and navigation, linking visual landmark information with self-motion signals and relaying this information across the HD

cell circuit and the HF-PHR. However, the specific role of the PoS and the RSC in landmark processing remains to be characterised, as few single-unit recording studies have been conducted in the RSC and little is known about the visual and spatial properties of landmarks that are selected by HD cells to reset their orientation. Therefore, to address this question, Chapter 6 presents experiments that investigated whether local visual features of static cue cards such as contrast, orientation and position are processed as landmarks by RSC and PoS HD cells, while Chapter 7 investigated whether PoS HD cells respond to changes in the spatial configuration of a subset of these cues. For the experiments described in Chapter 6, it was hypothesised that if HD cells distinguish the visual features of the cue cards, the PFD should maintain a consistent angular distance with respect to the location of the cue stimuli. If, on the other hand, the angular distance of the PFD with respect to the cue cards clusters at two radial positions 180º apart, this would indicate that HD cells do not distinguish the cue cards and are unable to reliably use the visual features as landmarks to aid in spatial orientation. Thus, the distributions of the PFD's that deviate from circular uniformity can be used as a measure of visual discrimination by HD cells.

After determining the visual features that reliably control the PFD, a subset of these cues were selected to examine whether PoS HD cells process the spatial relationship between the positions of familiar landmarks. For these experiments, which are described in Chapter 7, it was hypothesised that if PoS HD cells process multiple cues as an array, that is, as a configural landmark representation, the PFD should remap to a random direction when the spatial arrangement of the familiar cues are modified, indicating that the new cue array is treated as a different landmark configuration. On the other hand, if the distribution of PFD's is unimodal with a mean direction at 0º, this indicates that a subset of the cues control the PFD. The general methods for these experiments are described in Chapter 4 and a statistical method that was developed to visualise and analyse changes in the PFD as a result of the cue manipulations are described in Chapter 5 which are compared to commonly applied methods.

III EXPERIMENTAL CONTRIBUTIONS

Chapter 4 General methods

4.1 Subjects

Adult male Lister Hooded rats (*n*=20), weighing between 314-440 g at the time of surgery were housed individually in a colony room on an 11:11 h light-dark cycle with 1 hour simulated dawn and 1 hour simulated dusk. The simulated dusk period was from 11:30 AM-12:30 PM and the dark cycle was between 12:30 PM-11:30 PM. All rats were provided with ad libitum access to food and water prior to surgery and were food restricted to maintain 90% of their weight one week after surgery, the day on which they were first recorded. All experiments were licensed by the UK Home Office and were conducted in accordance to the restrictions and provisions contained in the Animals (Scientific Procedures) Act of 1986.

4.2 Electrodes and microdrives

Custom-made 16 or 32-channel microdrives (Axona Ltd., UK) were configured with tetrodes and implanted in either the RSC or the PoS. The tetrode configuration was selected as it provides an effective method for separating extra-cellular spikes recorded from multiple cells (McNaughton, O'Keefe, & Barnes, 1983). A list of the microdrive configurations and the brain area where the electrodes were implanted for each rat in which HD cells were recorded is listed in Table 4.1. The tetrodes or single wires were constructed from individual 17 or 25 µm diameter, 90:10 platinum-iridium wire (California Fine Wire, USA).

A day prior to surgery, the tetrodes were cut to a desired length depending on the brain area where they were to be implanted. The initial impedance of each electrode in a saline solution was measured, providing an initial value to which subsequent plating sessions were compared. The electrode tips were subsequently plated in a 1:9 0.5% gelatine:Kohlrausch platinum plating solution using a pulse generator (Thurlby Thandar TGP-110, UK) and a current source

(A.M.P.I. ISO-FLEX, Israel) that delivered 2 μA for 550 ms to each channel. The tetrodes were plated to a minimum impedance of 250 kΩ to optimise signal: noise levels in every channel.

Rat number	Electrode implant brain area	Microdrive configuration
646	Right PoS	16 channels; 4 tetrodes
645	Left PoS	16 channels; 4 tetrodes
638	Left PoS	16 channels; 4 tetrodes
637	Left PoS	16 channels; 4 tetrodes
630	Right PoS	16 channels; 4 tetrodes
602	Left RSC	32 channels; 8 tetrodes
599	Left RSC	32 channels; 8 tetrodes
593	Left PoS	16 channels; 4 tetrodes
592	Left PoS	16 channels; 4 tetrodes
572	Right RSC	16 channels; single electrodes
567	Left RSC	16 channels; 4 tetrodes
551	Right RSC	16 channels; 4 tetrodes
537	Right RSC	16 channels; 4 tetrodes
536	Left RSC	16 channels; 4 tetrodes
525	Right RSC	16 channels; 4 tetrodes
524	Right RSC	16 channels; 4 tetrodes
519	Right RSC	16 channels; 4 tetrodes
511	Left RSC	16 channels; 4 tetrodes
507	Left PoS	16 channels; 4 tetrodes
502	Left RSC	16 channels; 4 tetrodes

Table 4.1 Brain area and hemisphere where microdrives with different electrode configuration were implanted. The table only includes the rats in which HD cells were recorded, n=20 out of 28 implanted rats. Rats 599 and 602 were implanted by Pierre-Yves.

4.3 Surgery

The procedures described below follow standard stereotaxic surgery techniques used for the chronic recording of extracellular neuronal activity in freely behaving

rats (Szymusiak & Nitz, 2003). To describe briefly, rats were anaesthetised with 3% isoflurane (Abbott, Maidenhead, UK) and O2 (3 L/min) that was lowered to 2-2.5% half way through the surgery. Prior to placing the rat on the stereotaxic apparatus (Kopf, Germany), the analgesic (Caprieve, UK) was administered (0.1 ml/100g of rat weight diluted in 1:10 ratio with injectable water). Breathing, reflexes and body temperature were monitored by the experimenter throughout the surgery.

Once the rat was placed over a heated pad in the stereotaxic apparatus, the eyes were protected with a carbomer (Viscotears, UK) which was added whenever necessary throughout the surgery. Iodine (Betadine, UK) was placed as an antiseptic over the shaved head where an incision was made along the midline of the rat's head exposing bregma and lambda. Dorsal-ventral coordinates of bregma and lambda were then taken, ensuring that the skull was flat within a range of 0.2 mm. Subsequently, the location of the implant site was labelled with a surgical marker, using bregma as a cranial landmark and seven holes were drilled into the skull using a 1.0 mm drill bit, inserting jeweller screws (1.6 x 3 mm, Small Parts, USA) at each hole positioned at different locations of the cranial bones. One of the screws made contact with the frontal cortex which had a wire attached to it that was later connected to the microdrive and used as a ground wire. A craniotomy was then made at the desired implant coordinates using a 2.7 mm trephine bit and after removing the dura, the electrodes were lowered at the target coordinates. The implant coordinates for both the RSC and the PoS were taken from previous studies that characterised the spatially modulated firing characteristics of HD cells in these brain areas (Cho & Sharp, 2001; Taube, Muller, & Ranck, 1990) (Table 4.2).

The metallic guide cannula that covered the electrodes was lowered and sterile Vaseline was placed at the perimeter of the cannula. The microdrive's feet and guide cannula was then fastened to the skull with dental acrylic (Simplex rapid, Associated Dental Products Ltd, UK). After the dental acrylic had solidified, the ground wire was soldered to the microdrive and surgical tape (Finepore, UK) was placed around it to protect it. After the surgery, the rat was monitored until it awoke

and meloxicam (Metacam, UK) was given in jelly as a pain relief for three days. For one week after surgery the rat was given ad libitum access to food and water and was weighted daily.

Brain area	Anterior-posterior	Medial-lateral	Dorsal-ventral
RSC	-5.4 - -5.5	0.6 - 0.8	0.2 - 0.9
PoS	-6.7, -7.5, -8.0	2.8 , 3.2, 3.2	1.6 , 1.9, 1.8

Table 4.2 Electrode implant coordinates in mm for the RSC and the PoS taken from bregma. The values for the RSC represent a range of coordinates that were used for the placement of the electrodes, whereas those of the PoS denote three different sets of implant coordinates that were used. Dorsal-ventral coordinates were taken from the brain surface (Paxinos & Watson, 2007).

4.4 Signal processing and tracking

A week after surgery, the rats were screened for spatially modulated spiking activity, particularly for single-units that were tuned to head direction. All of the screening sessions took place inside a white walled 76 x 76 x 50 cm box. Alternating black stripes attached to one wall of the box were used as a polarising cue. The room cues remained unchanged across the screening sessions. The recording system consisted of a headstage amplifier attached to an Axona DacqUSB data acquisition system (Axona Ltd., UK) via a flexible lightweight tether. The headstage served as a buffered impedance amplifier that minimised noise from environmental sources and was connected to the preamplifier and system unit. The system unit filtered the signal from each channel and had audio-video input-output to record and visualise the rat's position while enabling the experimenter to listen to the threshold-triggered spikes.

The threshold-triggered spikes from individual channels in a tetrode were collected at a sampling rate of 50 Hz, amplified 6,000-20,000 times, band-pass filtered to 360 Hz high pass and 7 kHz low pass in order to reduce movement artefacts and subsequently stored for 200 μs pre-threshold and 800 μs post-threshold. The waveforms from all four channels within a tetrode were stored when the amplitude of a spike crossed a user defined threshold for any of the individual channels. The

EEG was recorded at a sampling rate of 250 Hz and was band-pass filtered between 0.34-125 Hz.

To track the rat's head location and orientation in the horizontal plane, two light-emitting diodes (LEDs) separated by 8 cm were attached to a stalk that was connected to the headstage. The stalk that held the LEDs was fixed relative to the centre of the rat's head along the transverse axis. The LED positions were distinguished based on differences in their brightness (pixel intensity) as they were sampled at a rate of 50 Hz by a camera attached to the ceiling above the recording arena. Spike times (the time during the trial when a cell fired a spike above threshold) and the sampled positions of the rat's head in x and y coordinates were saved for offline analysis. See Figure 4.3 for a diagram of the signal recording and tracking set-up.

4.5 Screening procedure

The screening for HD cells consisted of identifying channels with low spiking activity from one tetrode and referencing them against a channel with high spiking activity from a different tetrode. After a suitable signal-to-noise ratio was determined for each channel, a 5 or 10 minute trial was recorded. This was followed by the isolation of single units (Section 4.7.1) and examination of rate maps (Section 4.7.2) using the software TINT (Axona Ltd., UK). If spatially modulated cells were not found after a screening session, the tetrodes were lowered 50 µm and the rat was screened again 4 hours or a day later. A record of the date and the tetrode depth at which HD cells or other spatially modulated cells were isolated, was kept to provide an estimate of the region within the RSC or PoS in which those spatially modulated cells were recorded.

In the screening sessions where a candidate HD cell was found, independent 5 or 10 minute trials were recorded to examine the stability of the clusters and the HD cell tuning properties such as the firing rate and PFD ensuring that the putative HD cell was not an artefact. All of the screening trials were conducted in a separate room from where the cue control experiments took place (Section 4.6.3).

4.6 Recording procedure

The experiments consisted of exposing adult rats to a variety of cue cards placed inside a cylindrical or square arena as they foraged for food. The cue cards differed in their visual properties and were designed to examine if rats use specific visual features (Chapter 6) and their spatial relationship or configuration (Chapter 7) as orientating landmarks. The hypothesis were tested by recording RSC and PoS HD cells, examining landmark control as a result of the different cue manipulations.

4.6.1 Recording arenas

The recording environment consisted of a cylindrical arena 51 cm high x 74 cm in diameter or a square arena 1 x 1 m wide, 60 cm high located in the centre of a circular black curtained enclosure 260 cm in diameter. The recoding arenas were made of plywood and the inner wall was painted with light grey acrylic matt (Johnstone's Trade, UK), a paint that is washable and stain resistant. The size of the cylinder and the colour of the wall was selected as it has been the standard apparatus used on a large number of cue control studies that have characterised the firing properties of HD cells and to minimise the potential use of the geometric properties of the arena such as corners for orientation (Taube, 2007).

The recording arena rested over a black vinyl sheet laid on tinfoil that was grounded to the preamplifier. The floor was labelled at 45° intervals for the cylinder and at 90° intervals for the square arena, marking the location of the arena and the cue cards throughout the recording session. The base of the arena was movable and could be cleaned and rotated between the recording trials. The arena was lit from above by six light fixtures attached to the ceiling. A radio attached to the ceiling provided a source of white noise that masked sounds that could potentially serve as auditory cues. Previous studies have shown that auditory cues do not exert strong stimulus control over the PFD of PoS HD cells (Goodridge et al., 1998), however, it is not known the extent to which RSC HD cells use auditory cues for landmark processing given the important role of this brain area in forming multimodal associations between environmental stimuli (Robinson, Keene,

Iaccarino, Duan, & Bucci, 2011; Vann, Aggleton, & Maguire, 2009). Therefore, to control for potential auditory cues, white noise was used throughout all the experimental sessions.

4.6.2 Cue cards

Attached to the inner wall of the arena, polypropylene sheets were used as cue cards. The cue cards were held in place with Velcro tape in order to facilitate their removal, wiping and placement across trials. Each cue card was 51 cm in height and 50 cm wide and covered approximately 80° of arc of the cylinder's wall. For the two cue experiments, both the black and the white card had a bar which differed in its position and orientation and covered the card from side to side or top to bottom (Figure 4.1).

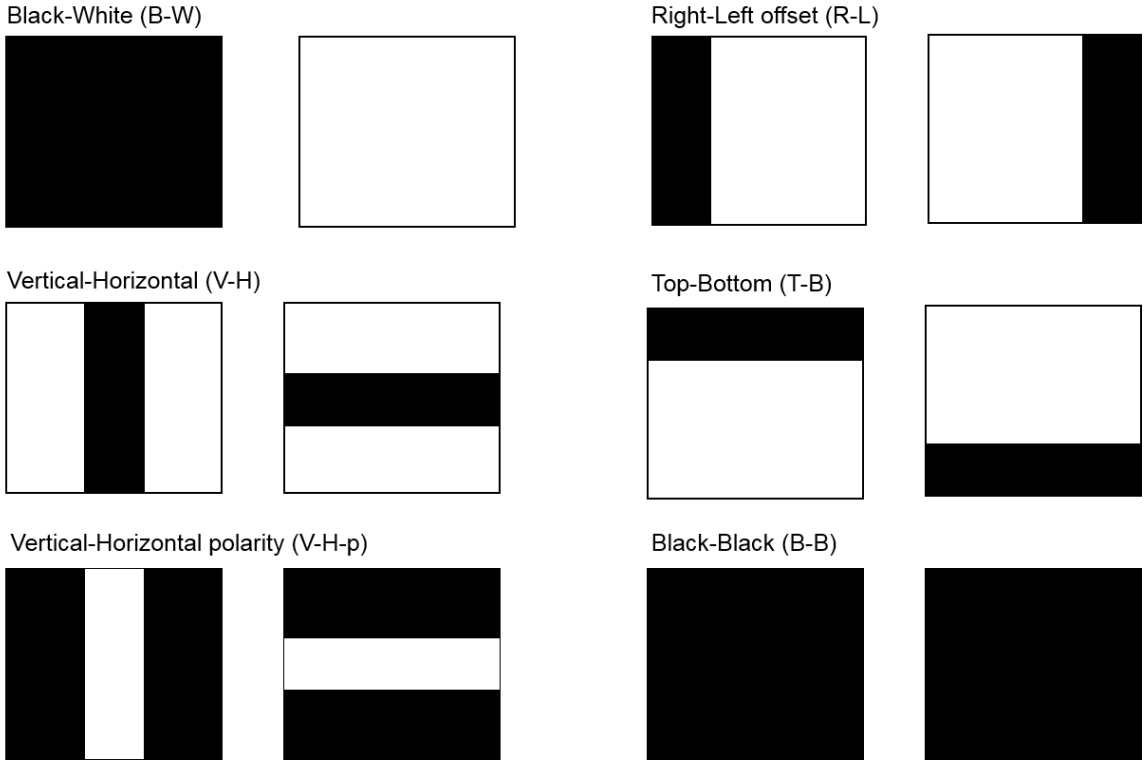

Figure 4.1 Schematic diagram of the cue cards that were used to investigate the visual processing abilities of HD cells. Each cue pair is displayed as seen from the point of view of the rat. Abbreviations denote the name given to each cue card pair.

The bars were 14 x 50 cm and each bar covered approximately 28% of the background card. The contrasting bars were made from the same material as the card and were attached to the cue card with Velcro tape. In the cylindrical arena, the adjacent edges of the cue cards were evenly separated from each other by 100° of arc and were located at 180° with respect to the midline segment of the cue cards. In the square arena, the cue cards were attached to the centre of each wall.

4.6.3 Cue control protocol

After isolating an HD cell during the screening trials, the rat was taken to the experiment room inside a closed opaque box. Afterwards, the rat was connected to the headstage, carried back to the box and passively rotated inside the curtained enclosure before being placed into the recording arena. This manipulation was done to disorient the rat and disrupt idiothetic information, preventing the rat from relying on self-motion cues to reset it orientation and instead use the available visual cues located within the arena (Etienne & Jeffery, 2004).

In the cue control experiments, each session consisted of a series of baseline and rotation trials. The baseline trials ranged from 1-4 trials during which the cue cards were not rotated. The baseline trials were followed by a series of rotation trials which ranged from 4-8 trials per session. For the recording sessions with the two cue cards, the starting location of the cues, the magnitude (45°, 90°, 135° or 180°) and the direction of the cue rotations (clockwise or counter-clockwise) were pseudo-randomly assigned. The same protocol was followed for the three cue experiments with the exception that the cue cards were rotated by ±90° and 180°. The location of the cue cards for each trial were drawn on a sheet of paper based on room centred coordinates using the door of the room as a reference point. This was done in order to aid the experimenter in the placement of the cue cards across the experimental session. The length of each trial was 5 minutes for the

experiments conducted in the cylinder and 10 minutes for the experiments conducted in the square arena.

The start of every trial was initiated via remote control after having placed the rat inside the cylinder facing a random direction. Throughout the trial, the experimenter remained outside of the curtained enclosure while moving around the perimeter and periodically throwing rice into the arena to increase the rat's sampling of locations and facing directions. At the end of each trial, the rat was taken out of the arena and was placed in a holding box outside the curtained area where it remained while the experimenter cleaned the recording arena, the base and the cue cards with 75% ethanol. To control for olfactory cues, the base of the recording arena was rotated by a pseudo-random amount and both of the cue cards were inverted and swapped in the location where they were attached to the inner wall of the arena. All of these manipulations were conducted across trials to scramble olfactory cues, preventing the rat from using scent trails and increasing the likelihood of landmark control by the different cue cards that the rats were exposed to.

The inter-trial interval was approximately 5 minutes, the time that it took the experimenter to set up the environment and disorient the rat prior to the start of a new trial. The order in which the two cue cards were presented between sessions was pseudorandomly selected, as HD cells were sometimes not present across consecutive days.

4.7 Data analysis

All data was analysed using Tint (Axona, UK) and Matlab R2013a (MathWorks, USA) using custom written functions as well as functions taken from the GitHub UCL/mTint repository (https://github.com/UCL/mTint). Circular statistics and kernel density estimates were carried out with functions from the CircStat toolbox (Berens, 2009) and functions written in the statistical software R (R Core Team, 2014) with the help of Miguel Angel Valencia using the package circular (Lund & Agostinelli, 2013).

4.7.1 Spike sorting

Cluster-cutting was used as a method of spike sorting to isolate the spikes that belonged to different cells using the software TINT (Axona, UK). Single units were isolated by plotting the peak-to-peak amplitude of one electrode against a different electrode within the same tetrode. This yielded six different scatter plots of the waveform amplitude of one electrode against the waveform amplitude of a different electrode (Fig 4.2).

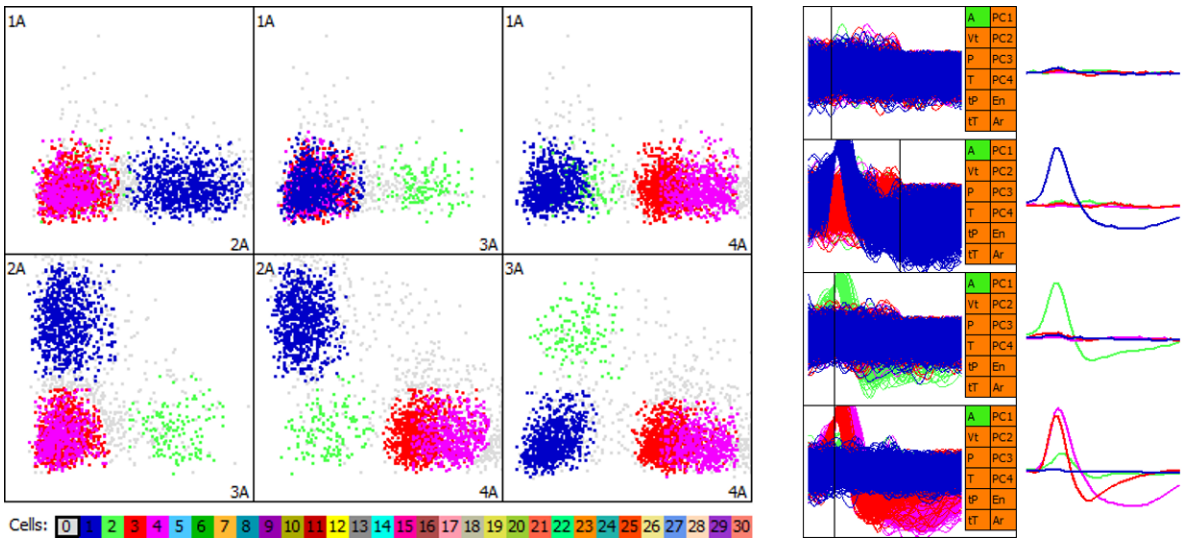

Figure 4.2 Illustration of spike-sorting procedure from Tint (Axona, UK). The image shows the spike separation based on amplitude differences between electrodes in a given tetrode. Spikes that have similar waveform characteristics, such as amplitude, group together, permitting the sorting of spikes into different clusters.

The scatter plots form clusters that are grouped and separated by identifying waveforms with similar characteristics, thus separating spikes that belong to different cells. Clusters for each recorded trial were isolated and sorted based on amplitude differences by both visual inspection and KlustaKwik (Axona, UK), a spike sorting algorithm that separates clusters based on amplitude differences using the statistical method of principal component analysis.

Spike sorting oftentimes requires subjective criteria when splitting, grouping or eliminating clusters, particularly when the clusters are not separated easily as is

the case for the red and magenta clusters shown in Figure 4.2. Therefore, to minimise spike sorting errors a systematic approach was followed by implementing the following steps: 1) Spike sort only clusters that have clearly distinguishable boundaries, 2) eliminate the clusters that do not have a 2 ms refractory period as determined by the inter-spike interval histogram, 3) use the first baseline trial as a template for cluster-cutting all the subsequent trials within a session, comparing the inter-trial cluster stability by template matching, 4) assign the same cell number for a given cluster within a session and between sessions when there is no cluster drift. The last step is carried out to ensure that cells that are recorded across days are given the same identifier.

4.7.2 Head direction cell rate map

A firing rate map was generated by taking the timestamp data of the spike times and head position samples that were recorded while the rat foraged for food in an open environment. An image of the screening arena and the procedure used to construct a HD tuning curve is shown in Figure 4.3. The position samples and the spike times were sorted into a circular histogram of 60 bins of 6° of head orientation. The mean firing rate of each angular head direction bin was calculated by,

$$Mean\ firing\ rate\ of\ bin_i\ (Hz) = \frac{\sum spikes\ in\ bin_i}{\sum dwell\ time\ in\ bin_i\ (s)}$$

where the firing rate of the $_{i^{th}}$ angular bin is equal to the total number of spikes in the angular bin_i divided by the dwell time, or the total amount of time that the rat's head was located at bin_i. An angular bin size of 6° was used to estimate the mean firing rate in each bin since it is within the resolution range of HD as derived from the pixel separation between the two LED's mounted on the headstage and is consistent with the conventions used in the analysis of HD cells (Taube et al., 1990).

Based on the firing rate of all the angular bins, a histogram was constructed for each candidate cell and a smoothing kernel of 5° was applied to minimise random

influences to the firing rate histogram with minimal loss of information (Abeles, 1982). The resulting smoothed histogram constitutes the HD tuning curve.

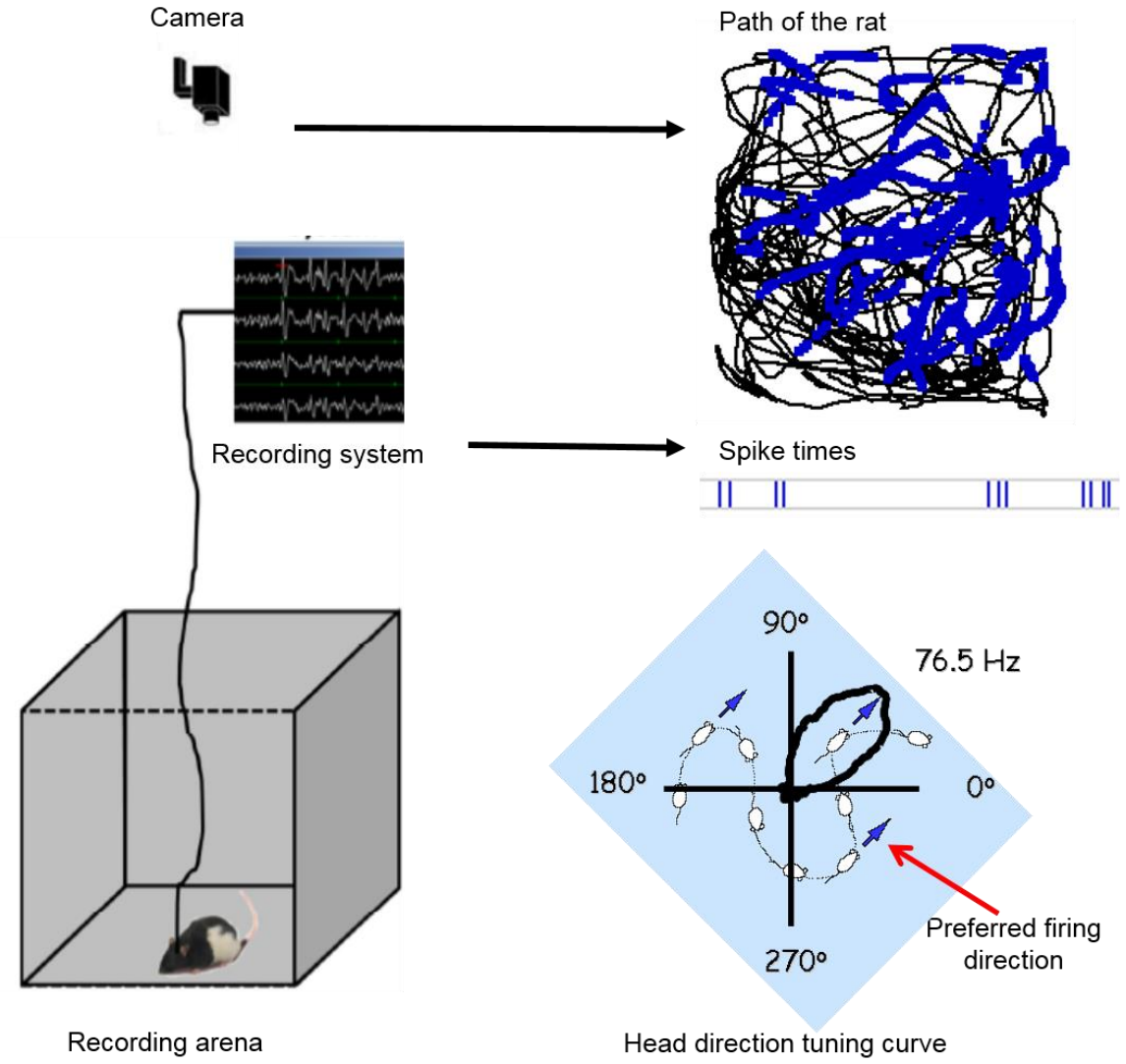

Figure 4.3 Schematic diagram of the recording setup and construction of an HD cell firing rate map. The figure shows the recording arena that the animal explored as the spiking activity of neurons was recorded and the position of the head tracked with a camera. The path of the rat (black) with superimposed spikes (blue dots) is shown above the tuning curve. The HD tuning curve was constructed by plotting in polar coordinates the firing rate in each angular bin using the spike times and the head position samples. The blue arrow shows the PFD and the peak firing rate (Hz) of the HD cell.

4.7.3 Head direction turning curve parameters

The parameters of the HD rate map that were used to characterise the properties of each candidate HD cell were derived from the smoothed firing rate across all the angular bins and were calculated using the MATLAB circular statistics toolbox CircStat (Berens, 2009). All of the CircStat functions take their input in radians, however for an easier interpretation of the results, all angles are reported in degrees. The parameters that were used to quantify the tuning curve characteristics for each HD cell were: 1) The firing rate, 2) the PFD, 3) the tuning width, and 4) the mean vector length (R).

Section 5.3.1 explains in detail how these parameters were calculated. The firing rate was defined as the bin with the maximum firing rate and constitutes the peak firing rate that is estimated from the mode of the circular histogram. The PFD is the directional bin where the maximum firing rate is found. The tuning width is the directional firing range of the cell and was computed by taking two standard circular deviations of the firing rate by HD function. The mean vector length was used as a measure of the strength of the directional tuning between the firing rate and HD. The values of the resultant vector length range from (0,1) where a value of 1 indicates that all of the spikes fired within the same HD bin while a value close to 0 indicates that the spikes were randomly distributed across all heading directions. A correction factor for binned data was applied to calculate the mean vector length.

4.7.4 Head direction cell inclusion criteria

For a candidate cell to be classified as an HD cell, a two part criterion had to be met. The cell inclusion criterion was the following: 1) The peak firing rate had to be greater than 1 Hz, and 2) the mean vector length had to be statistically significant as determined by the Rayleigh test ($p < 0.05$), corresponding to a mean vector length of 0.3. Trials that did not meet the two part criteria were not included in the analysis. The Rayleigh test was used to evaluate whether the firing rate of

a cell had a significant directional preference compared to being randomly distributed around all the head directions.

The Rayleigh test is a statistical method that can be applied to detect unimodal deviations from circular uniformity, assuming that the data was drawn from a von Mises distribution, which is the equivalent of a normal distribution for circular data (Section 5.3.2), whose Gaussian shaped function is similar to the tuning curve of HD cells since the firing rate peaks at a particular direction and drops off with increasing distance from the PFD. The Rayleigh test determines if there is statistical evidence that the spikes are not are not randomly (uniformly) distributed across the sampled head directions and are instead clustered at one direction. This is carried out by calculating the probability (*p*-value) that the mean vector length is larger than 0 and comparing the *p*-value to a pre-assigned level of significance, $\alpha = 0.05$ under the null hypothesis that the data is uniformly distributed (Fisher, 1995).

4.7.5 Head direction cell shift analysis

To evaluate the response of RSC and PoS HD cells as a result of the cue manipulations, several standard and non-standard analyses were conducted. A general description is given in the sections below while a detail description and the rationale for a new method that was developed for visualising and analysing changes in the PFD for a population of HD cells is presented in Chapter 5. The specific inferential statistical tests that were applied to each experiment are described in the analysis section of Chapter 6 and Chapter 7.

4.7.5.1 Head direction rate maps per session

To visualise the behaviour of each candidate HD cell across a recording session, an exploratory analysis was conducted prior to applying inferential statistics. The exploratory analysis consisted of a composite image that included a spike plot to visualise the spike distribution in relation to the path coverage, a 500 ms autocorrelogram histogram with a bin width of 1 ms to identify rhythmic firing

patterns, and a polar plot of the HD cell tuning curve. The polar plot displayed the HD cell tuning curve with arrows pointing to: 1) The PFD (green arrow), 2) the midpoint location for each of the cue cards (Cue1 with a solid arrow and Cue2 with a dashed arrow), and 3) the door location of the experimental room (red arrow) which was used as a reference point for room centred coordinates (Figure 4.4).

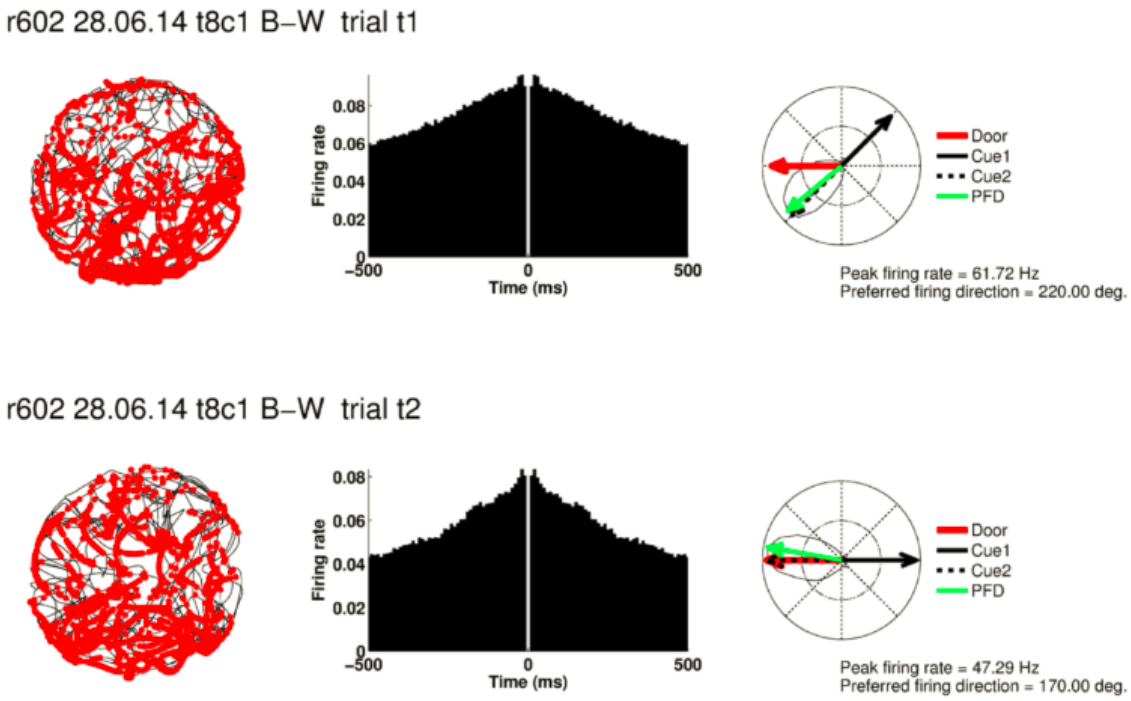

Figure 4.4 Example of a composite image of a single HD cell recorded with the Black-White (B-W) cue cards in the cylindrical arena displaying the first two cue rotation trials (t1 and t2). Cue1 corresponds to the card with the first letter of the cue card pair, in this case the black card (B), while Cue2 correspond to the white card (W). The vectors are displayed in polar coordinates where 0° is at east and 180° is at west. The peak firing rate and the PFD are displayed below the polar plot.

Every HD cell within a session was identified with a heading that included the rat number, the date of the experiment, the tetrode and cell number, the cue card pair, and the trial number. For each session the trials during which the cue cards were not rotated are referred to as baseline trials and are abbreviated with the letter ‘b’, while the trials during which the cues were rotated are abbreviated with the letter

‘t’. The relation between the PFD and the location of one cue card was used to quantify the response of each HD cell across a session as a result of the cue manipulations.

4.7.5.2 Quantification of changes in the PFD

To measure the changes in the PFD of individual and simultaneously recorded HD cells as a result of the cue manipulations, the angular distance between the PFD and the location of Cue1 was calculated. The angular distance denoted as θ_i, represents the smallest angle between the midpoint location of Cue1 and the PFD in a given trial. As the two cue cards were always kept at the same angular distance with respect to each other in the two cue experiments (Chapter 6) and the standard sessions of the three cue experiments (Chapter 7), the location of any of the cue cards can be used as a reference point to calculate θ_i.

To quantify the change in the PFD of each HD cell within a session, the change in the angular distance θ_i was calculated independently for each HD cell across trials. Specifically, the change in θ_i for a given HD cell in each trial, denoted as θ_s was calculated by determining the angular distance between θ_i with respect to the circular median direction of θ_i’s for a given HD cell across a session (Section 6.3.1) with the formula,

$$\theta_s = (\theta_i, d(\psi))$$

Where θ_i is the angular distance between the PFD and the location of one cue card and $d(\psi)$ is the median direction for a sample of θ_i. The angular distance shift, θ_s represents the change in the PFD of a single HD cell in one trial centred at the median and can have values that are positive or negative and range from 0±180° which reflect the direction to which the PFD shifted (see Figure 6.4 for an illustration of how θ_s was calculated).

4.7.5.3 Kernel density estimates and population analysis

In order to visualise the changes in the PFD due to the cue manipulations in a population of HD cells and obtain an estimate of the underlying distribution and concentration of the data, a circular kernel density estimate (KDE) was used using a von Mises distribution as the smoothing kernel function. A description of KDE's and the advantages of this statistical method compared to commonly applied methods reported in the analysis of HD cells is presented in Section 5.5.1 with a description of the implementation of this method applied to the experiments presented in Chapter 6 and 7.

4.8 Histology

After completion of electrophysiological recordings, the rats were anaesthetised and killed with an overdose of sodium pentobarbital (150 mg/kg) (Euthatal, UK) and perfused transcardially with saline followed by 4% formalin solution. The brains were kept in 4% formalin until a day prior to being sectioned. 24 hours before sectioning the brains, they were placed in 4% formalin and 20% sucrose solution for cryoprotection. Coronal or sagittal sections of the brains were cut in 40 µm sections with a Cryostat (Model OTF, Bright Instruments, UK) at -20° C and mounted on microscopic slides (Superfrost BDH, UK). The brain sections were Nissl stained with 0.1% Cresyl violet (Sigma-Aldrich, UK) or 0.5% Thionin (Sigma-Aldrich, UK) and covered slipped with DPX (Sigma-Aldrich, UK). The slides were examined under a light microscope (Leica, UK) and imaged with a digital camera mounted on the microscope. Images with visible electrode tracks were saved for histological analysis. The electrode location was verified by examining the brain region where the final electrode track was located using the rat brain Atlas of Paxinos & Watson (2007).

Chapter 5 Population analysis of head direction cells

5.1 Background and rationale

With the development of multi-electrode arrays and silicon probes that enable the recording of a large number of neurons simultaneously in awake behaving animals and sophisticated virtual reality methods that allow the recording of many trials during a session, it is becoming increasingly important to analyse very large datasets (Buzsáki, 2004; Carandini & Churchland, 2013). In the field of research where experiments examine the changes of spatially modulated cells as a result of sensory manipulations, multiple datasets are often collected from many animals and combined to examine the population coding of a spatial representation.

In the analysis of HD cells, different criteria are often employed by different research groups to define a putative cell as being tuned to HD and different methods are used to analyse the population activity of these cells as a result of an experimental manipulation. Although this is not unique to the field of research that investigates spatially modulated cells, the present chapter will focus on HD cell analysis.

The chapter begins with a description of widely used statistical methods that have been applied to classify a single cell as being tuned to HD, followed by a description of the three main parameters that are used to characterise the tuning curve of an HD cell and the factors that can affect the estimates of these parameters (Section 5.3). This is followed by a description of commonly used or standard methods that have been applied to analyse changes in the firing of HD cells in both single-unit and combined lesion-recording experiments employing different behavioural tasks (Section 5.4). Afterwards, a description of non-standard methods for visualising and analysing changes in the PFD for a population of HD cells is presented (Section 5.5), with special emphasis on kernel density estimation (KDE) methods which were applied to analyse the results of the present experiments. The chapter ends with concluding remarks and a discussion of future directions for the analysis of HD cells.

The aim of this chapter is not to review every method that has been reported in the analysis of HD cell activity. Rather, by describing commonly used analysis with examples from published research, it seeks to explain the advantages and limitations of particular methods and how they may or may not be well suited to characterise and analyse the firing properties and behaviour of single HD cells or the population activity of multiple HD cells.

5.2 Methods

To illustrate the different methods for analysing HD cells, whenever relevant, data collected from the two cue experiments described in Chapter 6 will be used. The analysis and the plots presented in this chapter were generated with MATLAB R2013a (MathWorks, USA) and R statistical software (R Core Team, 2014) using functions taken from the CircStat toolbox (Berens, 2009) and the R packages circular (Lund & Agostinelli, 2013) and sm (Bowman & Azzalini, 2014). The formulas and descriptions of the different circular statistical tests are based primarily on the following references (Berens, 2009; Fisher, 1995; Pewsey, Neuhäuser, & Ruxton, 2013; Zar, 2010).

5.3 Head direction cell tuning curve parameters

Classifying an individual neuron as tuned to head direction is commonly the first step that is carried out after spike sorting and prior to conducting a formal analysis of the data. Although the rationale for selecting a particular statistical method for assessing the directional preference of a cell and for analysing the response of a population of HD cells is often omitted in research articles, it is of the utmost important as the statistical model that is chosen will in large part determine the inferences that are derived from the data. This section describes commonly used methods for displaying and analysing HD cell tuning curves, presenting the three most commonly studied parameters: 1) The firing rate, 2) the directional firing range or tuning width, and 3) the PFD (Figure 5.1A).

HD cells are typically visualised by plotting the firing rate as a function of the rat's directional heading in either linear or polar coordinates (Figure 5.1). HD is measured by tracking the position of two LEDs as the rat moves its head in the horizontal plane while the firing rate is calculated by dividing the 360° range of heading directions into equally size bins of a predefined bin width and calculating the mean firing rate of every angular bin_i by,

$$Mean\ firing\ rate\ of\ bin_i\ (Hz) = \frac{\sum spikes\ in\ bin_i}{\sum dwell\ time\ in\ bin_i\ (s)}$$

where the dwell time is the total amount of time that the rat sampled a heading direction in the angular bin_i.

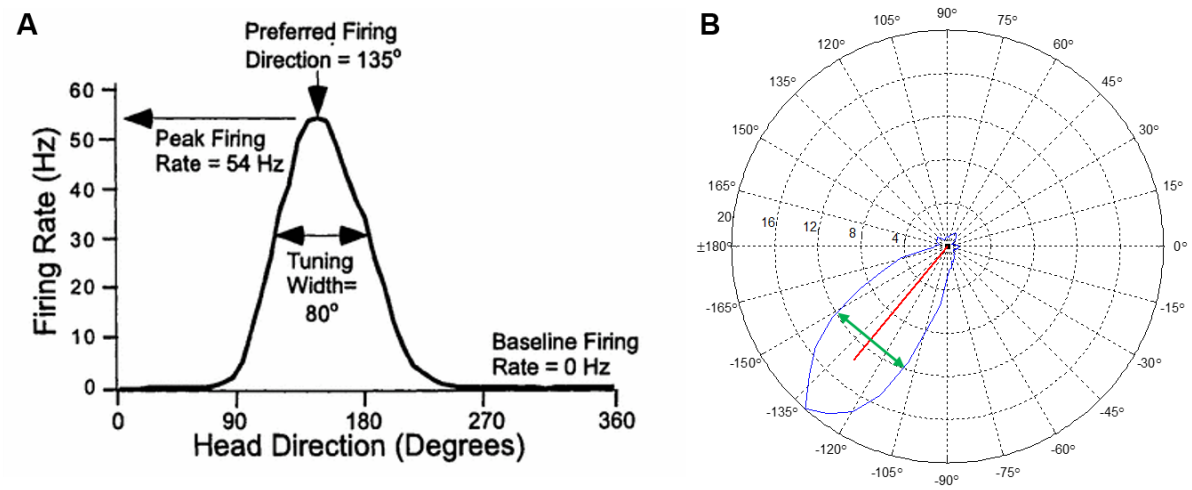

Figure 5.1 Tuning curve of an HD cell displayed in linear and polar coordinates. **A.** The three most commonly used values that are used to parametrise a HD cell tuning curve are shown. **B.** HD tuning curve (shown in blue) displayed in polar coordinates where concentric circles indicate the firing rate, the red arrow points to the circular mean direction or PFD at approximately 130°, and the green arrow is the directional firing range or tuning width.

The selection of the bin width affects the values of the parameters that are estimated from the HD firing rate histogram since the probability of finding a spike at a particular HD interval increases as the bin width becomes larger (Abeles, 1982). Because HD cell tuning curves are constructed from binned data, another

factor that can potentially affect the firing rate in an angular bin is the time that the rat spends sampling a particular heading direction. If the rat has a preference for facing a particular direction, or if it stands still facing in a specific direction, this can result in a biased estimate of the firing rate since the probability that a cell will fire a spike at the sampled angular bin will be higher compared to when the rat uniformly samples all the heading directions. For this reason it is important to include a selection criteria for an HD cell based on a minimum peak firing rate. To avoid this potential sampling bias, the experimenter randomly tosses food inside the recording arena, encouraging the rat to sample all locations and heading directions. Therefore, to minimise these random influences to the HD cell's tuning curve with minimal loss of directional information conveyed by a spike train, a smoothing kernel is commonly applied to the firing rate histogram (Abeles, 1982). In the present thesis the peak firing rate and the PFD of all the recorded HD cells were estimated from the smoothed HD firing rate histogram.

The factors that were previously mentioned may not have a considerable impact on the tuning curve of HD cells that have a high signal inside the cell's directional firing field and a low background firing rate outside the firing field, such as those that are commonly recorded in adult rats across most brain areas. However, for putative HD cells that have a sparse directional firing field, such as those reported in layer III of the MEC in adult rats (Giocomo et al., 2014) or in the ADN, PoS, PrS and MEC of rat pups before eye opening (Bjerknes et al., 2014; Tan et al., 2015), a biased classification of single units as HD cells and inaccurate estimates of the cell's tuning curve parameters might be obtained if conducting a standard analysis.

These factors are important to consider when analysing spatially modulated cells, where the extent to which the firing rate histogram is unimodal and the peak firing rate is above a pre-defined threshold are the two most commonly used parameters to select neurons that are tuned to HD. After filtering cells based on an inclusion criterion, the tuning curve parameters such as the PFD, tuning width and firing rate are calculated, where changes in the PFD are used to measure the effects of sensory manipulations in the activity of HD cells. The estimation of tuning curve parameters and the statistical analyses that are commonly applied for identifying

HD cells and analysing changes in the PFD as a result of cue control experiments are discussed in the following sections. This will provide background information to understand the advantages and limitations of standard methods before presenting an alternative method that was developed to analyse the population activity of RSC and PoS HD cells as a result of the cue control experiments described in Chapter 6 and Chapter 7.

5.3.1 Estimation of tuning curve parameters

For most HD cells recorded in adults, the firing rate versus HD histogram has a Gaussian shape tuning curve, for which a standard circular analysis can be applied to estimate the firing properties of these cells, such as the firing rate, PFD and the tuning width. The first method used to estimate the tuning curve parameters for an HD cell applied a triangular fitting model to the firing rate versus HD histogram (Taube et al., 1990a). In this method, a best-fit line is drawn from the mean background firing rate to the maximum firing rate of the cell (Figure 5.2).

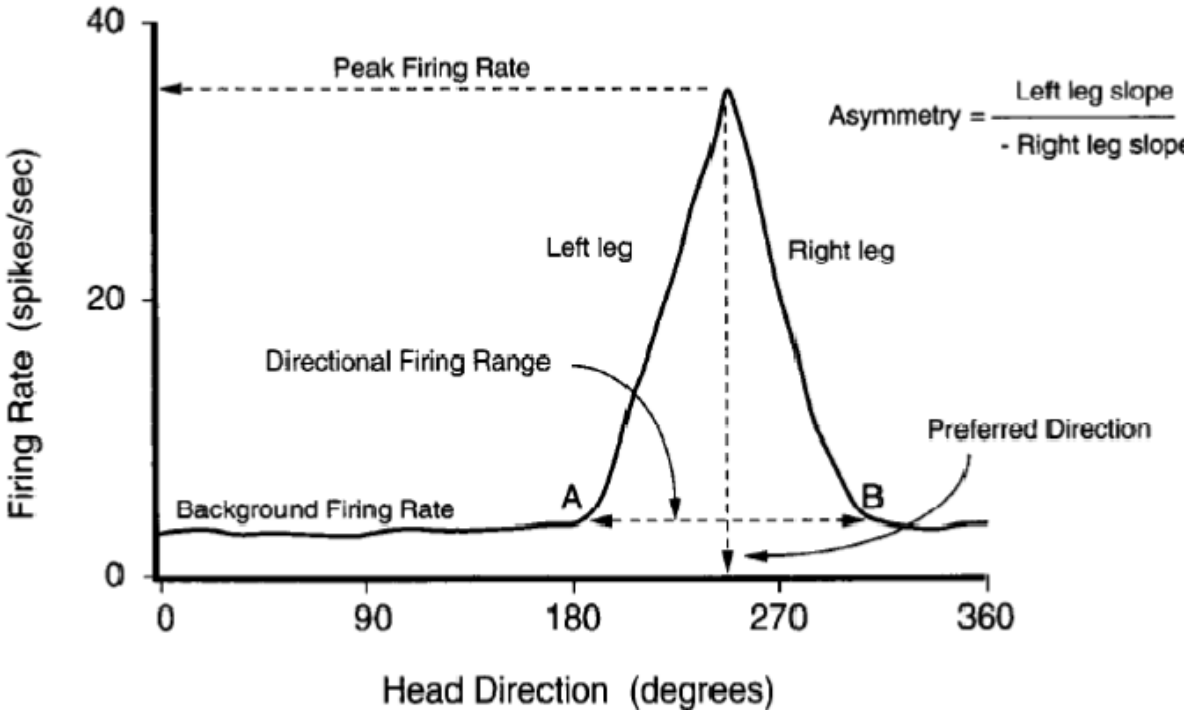

Figure 5.2 Triangular fitting method applied to estimate HD cell tuning curve parameters. Taken from (Taube, 1995).

Based on the triangular model, the point at which the two fitted lines intersect is taken as the peak firing rate of the cell and its value is used to parametrise the PFD, while the directional firing range or the tuning width is calculated as the range from the local minimum A to the local minimum B (Figure 5.2). The triangular fitting method provided a good early approach for approximating the tuning curve parameters of HD cells, however, this method assumes a linear relationship between firing rate and HD, where the firing rate decreases at a constant rate as it gets farther away from the direction where the cell reaches its maximum firing rate. This linear rate coding assumption may not reflect how neurons encode multisensory information since it is likely that a Gaussian function provide a better model to describe the tuning curves and the average response of a neuron as a function of HD (Fetsch et al., 2013; Johnson, Jackson, & Redish, 2008).

An alternative method for plotting and analysing HD cells is to display the tuning curve in polar coordinates and estimate the tuning curve parameters using circular statistics. The use of a circular representation enables one to calculate a single vector that can be used as a parameter to describe the discharge pattern of a single-cell in relation to HD. To do so, the mean firing rate in every angular bin_i is treated as a point on a unit circle with corresponding X_j and Y_j coordinates (Figure 5.3A);

$$X_j = \frac{\sum_{i=1}^{n} n_i \cos \emptyset_i}{\sum_{i=1}^{n} n_i} = \frac{\text{Sum ((number of spike in bin }_i)*\cos(\text{bin}_i \text{ direction}))}{\text{Total number of spikes}}$$

$$Y_j = \frac{\sum_{i=1}^{n} n_i \sin \emptyset_i}{\sum_{i=1}^{n} n_i} = \frac{\text{Sum ((number of spike in bin}_i)*\sin(\text{bin}_i \text{ direction}))}{\text{Total number of spikes}}$$

where the data in each angular bin_i constitutes one vector pointing to a particular direction (Figure 5.3). The sum of all the individual vectors divided by the total number of vectors *N* yields the mean resultant vector ($\bar{r}$),

$$\bar{r} = \frac{1}{N}\sqrt{(\sum_{i=1}^{n} x_j)^2 + (\sum_{i=1}^{n} y_j)^2}$$

with a corresponding mean direction ($\bar{\theta}$). The absolute value is taken to obtain the mean resultant vector length (*R*), also known as the Rayleigh vector,

$$R = |\bar{r}|$$

whose magnitude lies in the range (0,1). The mean direction, $\bar{\theta}$, is a measure of the circular mean of the individual mean firing rate in all the angular bins and can be used to estimate the PFD (Figure 5.3B).

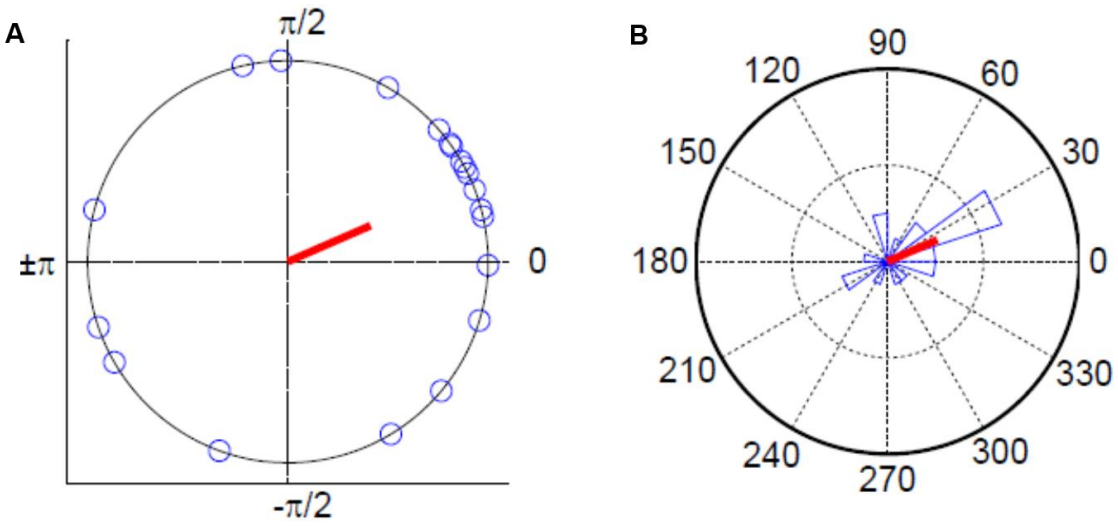

Figure 5.3 Illustration of the direction and magnitude of the mean resultant vector length for a sample of data consisting of *N* = 20 observations. **A.** Scatter circular plot. **B.** Angular histogram showing the mean vector direction (red line), $\bar{\theta}$ = 23.5° with a Rayleigh vector, *R* = 0.45. Taken from (Berens, 2009).

The magnitude of the mean vector length *R*, provides a measure of the vector strength and is the most commonly used measure of concentration for unimodal circular data that is applied to classify an individual cell as being tuned to HD and to test for unimodal departures from uniformity in a sample of changes in the PFD (Section 5.4). Values of the mean vector length closer to 1 indicate that the data is clustered at a particular location while those closer to 0 indicate that the data is close to being uniform. Related to the mean vector length is the sample circular variance defined as,

$$V = 1 - R$$

whose range is (0,1) where values closer to 0 indicate that the data is less spread out around the circle and more concentrated around the mean direction (Fisher, 1995).

5.3.2 Statistical test for identifying head direction cells

The classification of single cells as being tuned to head orientation is assessed by examining the extent to which spike trains are not uniformly distributed around the sampled heading directions and are instead concentrated at a specific directional range. Formally, this is determined with a Rayleigh test, a statistical method that evaluates the probability that the firing of a cell is uniformly distributed in all heading directions against an alternative unimodal model (a von Mises distribution) with a single peak or mean firing direction, denoted as $\bar{\theta}$ (Fisher, 1995).

The Rayleigh test is carried out as a null hypothesis test, using the mean vector length as the test statistic and calculating the probability (*p* value) that the mean vector length was sampled from a uniform random distribution. If the computed *p* value is less than the pre-assigned level of significance, α, the null hypothesis that the data is uniformly distributed is rejected (Batschelet, 1981). It is important to note that the value of the Rayleigh vector is a biased estimator of concentration if there are a small number of observations in the sample ($N < 10$) distributed around the circle. Furthermore, since *R* is calculated using a binned dataset (firing rate per angular bin), a biased estimate of the mean vector length can be obtained. Therefore, to correct for this bias, the bin spacing d is multiplied to the *R* value;

$$c = \frac{d}{2 * \sin(d/2)}$$

setting $R_C = c*R$ (Berens, 2009; Zar, 2010). Furthermore, prior to applying the Rayleigh test to the binned data in order to identify candidate HD cells, it is common practice to exclude cells based on a threshold peak firing rate which is usually a firing rate < 1 Hz, as these cells often have a low signal-noise ratio and very few spikes that have low directional information content which may not constitute allocentric encoding HD cells. As an inclusion criterion to select neurons recorded in the PoS and the RSC that were tuned to HD in the experiments described in Chapter 6 and Chapter 7, the cell needed to have a firing rate > 1 Hz and yield a statistically significant ($p < 0.05$) mean vector length as determined by the Rayleigh test.

The Rayleigh test can be used to detect deviations from uniformity assuming that HD tuning curves follow a Gaussian function, also known as a von Mises distribution. The von Mises distribution can be thought of as the analogue of the normal distribution as it is symmetric and its density decreases with increasing distance from the centre (Fisher, 1995). However, in contrast to the normal distribution where the standard deviation (σ) characterises the dispersion of the probability density function, in the von Mises distribution the dispersion is controlled by the concentration parameter kappa (κ). The von Mises distribution is thus a symmetric and unimodal distribution composed of angular data θ, whose probability density function is given by;

$$f(\theta; \mu, \kappa) = \frac{1}{2\pi I_0(\kappa)} \exp(\kappa \cos(\theta - \mu))$$

where μ is the mean direction, $\mu \in [0, 2\pi)$, κ is the concentration parameter, $\kappa \geq 0$, such that when κ=0, the distribution is uniform and when $\kappa \to \infty$ all points stack at μ and $I_0(\cdot)$ is the modified Bessel function of order zero which serves as a normalising constant. In the von Mises distribution, the larger the value of κ, the lower the dispersion of the angular data and the more peaked the distribution (greater concentration of data at a particular direction), whereas if κ is equal to zero, the distribution is uniform without any peaks (Fisher, 1995).

Although the sample mean direction, $\bar{\theta}$, can be used to estimate the PFD (Figure 5.4A), its value can vary depending on how well the data is concentrated at a particular direction, that is on how well the tuning curve fits a von Mises distribution. In instances when the tuning curve deviates from a von Mises distribution (Figure 5.4B), the angular bin with the highest firing rate (the mode) can be used instead, providing a robust estimator of the PFD. For tuning curves that are unimodal and close to symmetric, the mean direction, $\bar{\theta}$, provides a good measure of central location and a good estimate of the PFD (Figure 5.4A). On the other hand, for tuning curves that are not symmetric, such as those that have a higher dispersion and skewness, the mode provides a more robust measure of the PFD compared to the mean direction (Figure 5.4B).

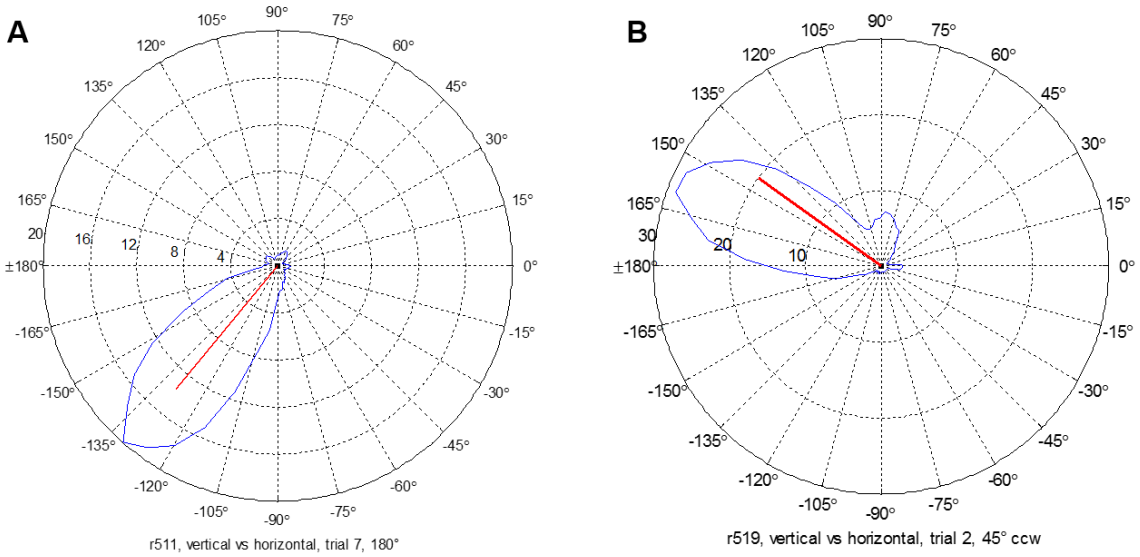

Figure 5.4 Estimates of the PFD based on the mean direction. **A.** For unimodal and symmetric tuning curves, the mean direction, $\bar{\theta}$, shown in red provides the same estimate of the PFD as the mode. **B.** For non-unimodal and skewed tuning curves, the mean direction provides a biased estimate of the PFD compared to the direction where the maximum firing rate occurred, at approximately 155-160°. The polar plots were constructed using 60 bins of 6°.

An example of how the dispersion and skewness of the tuning curve can affect the estimates of the PFD based on the mean direction or the mode is illustrated in Figure 5.4A which provides an example of HD cells recorded from two rats with electrodes implanted in the RSC. Figure 5.4A shows a highly symmetric tuning curve where the mean direction and the mode fall within the same bin, providing a similar estimate of the PFD. In contrast, Figure 5.4B shows an HD cell tuning curve that is not symmetric due to a second smaller peak at about 60°-105°. For skewed tuning curves, the estimate of the PFD derived from the mean direction provides a different estimate of the PFD compared to the mode which does not reflect the local maximum of the firing rate versus HD circular histogram.

Although most of the HD cells that have been recorded in different brain areas are characterised as having a unimodal firing rate distribution with a single PFD, HD cells with bimodal tuning curves have been reported. For these non-classical HD cells, the second peak, which has a smaller peak firing rate compared to the local

maxima, it has been generally attributed to be due to noise in poorly isolated units. However, a recent study has questioned this assumption showing that for well isolated cells, 12% of ADN HD cells and 32% of PoS HD cells were not unimodal, where the tuning curves showed a second peak that was 50% or more of the maximal peak firing rate (Peyrache et al., 2015). This study suggests that the second peak outside the directional firing range where the maximum peak firing rate is found constitutes spikes that carry HD information. Future studies would have to determine the firing properties of these non-classical HD cells and the effects in the PFD of the two peaks after idiothetic and allothetic cue manipulations. For such cells with two PFD's, the local peaks can be determined from the firing rate histogram, however, the Rayleigh test would be an inappropriate statistical test to classify a neuron as being tuned to HD since the circular distribution of the firing as function of HD deviates from a unimodal von Mises distribution. For such cases, a different statistical test described in Section 5.5.2 can applied to detect multimodal departures from uniformity.

5.4 Standard methods for analysing a population of HD cells

After classifying a single-cell as being tuned to HD, the next step in the analysis consists of quantifying the changes in the PFD as a result of an experimental manipulation and determining if these shifts are randomly distributed or are concentrated at a particular mean direction. The most frequently studied manipulations in HD cell studies involves combined lesion-recording experiments or single-unit recordings where the variable of interest are changes in the tuning curve parameters, more commonly changes in the PFD of the recorded HD cells across different experimental conditions such as the control vs the lesioned group or the different sensory manipulations that were conducted (Chapter 3).

When analysing the population response of HD cells and applying inferential statistics, it is important to note that HD tuning curve parameters such as the PFD constitute angular data and can only be analysed with circular statistics and not with linear models as a biased estimate is obtained (Zar, 2010). Secondly, when selecting a circular statistical test and applying a null hypothesis test, the statistical

power derived from the test affects the *p*-value and thus the inferences that are drawn from the data (Halsey, Curran-Everett, Vowler, & Drummond, 2015). Therefore, it is important to adhere to the distributional assumptions of a statistical test whenever possible as the *p*-value is only as reliable as the sample from which it has been calculated (Krzywinski & Altman, 2013). Considering that these factors are relevant for selecting and interpreting a statistical test, it is important that the distributional assumptions are followed as much as possible.

From a statistical point of view, the analysis of HD cells thus requires a display of the distribution of PFD's with corresponding descriptive statistics such as the mean direction, Rayleigh vector and angular variance, which provide a quantitative summary of the distributions. The collected data are then subjected to inferential hypotheses tests that examine the probability that the distribution of shifts in the PFD differs significantly from uniformity with an alternative hypothesis of unimodality, assuming a von Mises distribution. If there are a priori reasons for expecting that the distribution of PFD shifts will be concentrated at a specific direction of the unit circle, a *V*-test with a specified mean direction is applied, otherwise, a Rayleigh test with an unspecified mean direction is conducted (Pewsey et al., 2013). From these tests, the magnitude of the mean vector is the most commonly used measure to assess whether changes in the PFD after a certain experimental manipulation are clustered around a particular direction or are instead randomly distributed around all the heading directions.

Although these parametric circular tests are robust to deviations from unimodality, the mean resultant vector, *R*, which is calculated from the data is not a useful indicator of the spread of the data unless the changes in the PFD are clustered at particular interval around the circle (Fisher, 1995). Furthermore, *R* is a biased estimator of concentration if there is a small number of observations ($N < 10$) and they deviate from unimodality as would be the case with bimodal or multimodal distributions.

As the mean resultant vector, *R*, is the most widely used test statistic applied to the analysis of HD cells in studies that investigate if there is an effect in HD cell activity as a result of lesioning a particular brain area (Clark, Bassett, et al., 2010;

Yoder et al., 2015) or in studies that examine the magnitude of cue control in HD cells as a result of manipulations to the environment (Clark, Harris, & Taube, 2010; Knight et al., 2011), the value of *R* and its corresponding *p*-value determine in large part the statistical inference and interpretations that are derived from the data. Therefore, biased *R* values can be obtained if there is a small number of observations which may or may not be clustered at a particular direction (Figure 5.5).

To examine the distribution of PFD shifts as a result of cue control experiments, it is common practice to combine all the recorded trials of single or multiple HD cells recorded per session independently for each animal, obtaining a single estimate (commonly the mean direction of a small number of observations) of the HD cell(s) behaviour for each session. This method of analysing changes in the activity of HD cells by pooling all the trials per session undersamples the variance that occurs across trials which could be the result of the experimental manipulation. This can potentially have the effect of decreasing the likelihood of observing differences both within and between groups since there is a considerable reduction in the number of observations that are used to calculate the final *R* value per group condition.

Furthermore, since the number of HD cells that are typically recorded per animal tends to be relatively low, all the HD cells recorded across animals are combined into a single distribution in order to examine the population activity in each experimental condition. In this situation, if animals contributed a large proportion of the data, the population analysis is subsampled, reducing the data points and testing if the effect or lack of an effect is still present.

As an illustrative example of how sample size can affect *R* values which provides a measure of concentration at a given direction, the results of a study that examined the influence of the environment's geometry on HD cells will be discussed. The results of this experiment are shown as a circular scatterplot of the PFD shifts of all the HD cells that were recorded in rats that were exposed to an environment shaped as a teardrop (*n*=12) and an environment shaped as an

isosceles triangle with a white cue card attached to the shortest wall (*n*=15) (Figure 5.5).

As can be seen from Figure 5.5, the number of data points within each condition (teardrop and isosceles triangle) tended to be small (N < 15) and the data for each condition was further subdivided by the magnitude of the rotation in the environment (90° or 180°) relative to room coordinates, reducing the sample size.

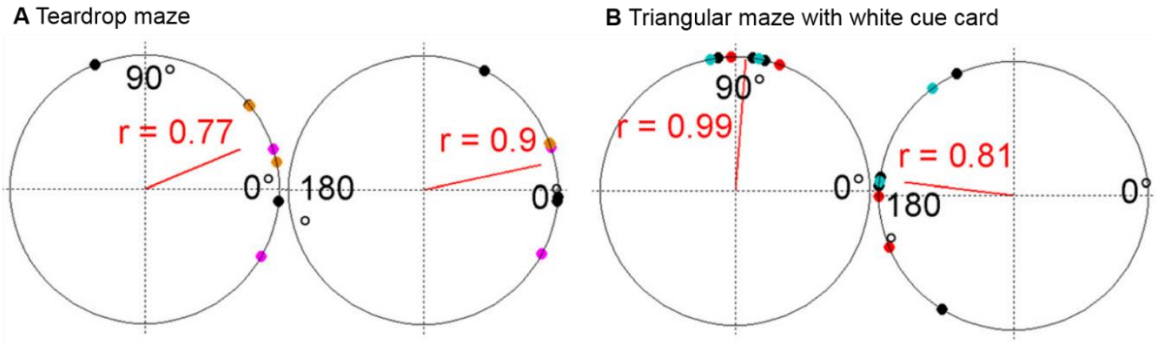

Figure 5.5 Circular scatter plots of the PFD shifts as a result of rotating **A.** the teardrop maze and **B.** the isosceles triangular maze by 90° or 180° as shown on the left and right circular scatter plot per condition. The red line shows the mean resultant vector. All Rayleigh tests had a $p < 0.01$. Taken from (Knight et al., 2011).

In this analysis it is important to note that although there were *a priori* reasons for splitting the data by the magnitude of the cue rotation to examine if the mismatch between local and background cues had an effect on the PFD, the data could have been normalised to 0° and combined if no differences had been found between the two distributions of PFD shifts. A Rayleigh or a *V*-test with an expected mean direction could then have been conducted with the combined data, yielding a better estimate of the *R* value. In the study, the authors correctly concluded that the geometry of the teardrop maze did not influence the PFD of HD cells, while the salient polarising cue card exerted strong control over the PFD. If the two cue rotation magnitudes for each condition had been combined and normalised to 0°, the outcome of the statistical test and the conclusion would likely have been the same since the HD cells showed a similar behaviour regardless of the cue rotation.

Overall this example was described to illustrate how the sample size and the captured variance per HD cell can influence the value of the mean resultant vector *R* which is the most commonly used statistic to test whether a sample of PFD shifts or PFD deviations are clustered at a particular direction.

It is important to mention that when comparing the distribution of PFD's between two or more groups, conducting independent Rayleigh or *V*-tests is not a valid method of assessing differences between groups as these tests only examine departures from uniformity for one sample. Therefore, for comparing the distributions of two or more samples of circular data, Watson's two-sample U^2 test (Zugaro et al., 2004), or the Watson-Williams F test (Taube, Wang, Kim, & Frohardt, 2013) can be applied to test for a common mean direction. Watson's two-sample U^2 test is a non-parametric test that does not assume an underlying von Mises distribution as other parametric circular tests and can be applied to compare samples that were drawn from either unimodal or multimodal distributions (Zar, 2010). For a comparison of more than two samples, the Watson-Williams high concentration F-test can be conducted as a one-way ANOVA, examining whether the mean direction of the samples are equal (Pewsey et al., 2013). This parametric test assumes that the samples were drawn from a von Mises distribution with a common concentration parameter, $\kappa > 1$, however it is fairly robust against deviations from this assumptions (Zar, 2010).

5.5 Non-standard methods for analysing a population of HD cells

A different situation can arise from circular distributions that have a similar mean direction, albeit with a different variance. In such cases, examining departures from uniformity with a Rayleigh or a *V*-test within each group will likely yield a significant *p*-value.

In cases where the experimenter wants to determine whether two or more unimodal distributions that have a similar mean direction differ from each other, testing for a common mean direction will not reject the null hypothesis and it will be concluded that that there are no differences between the groups. This occurs

because the mean vector *R* is not a measure that is robust for detecting changes in the variance as it only examines departures from uniformity against a von Mises alternative and does not test if two or more distributions have a similar variance. Therefore, testing for a common mean direction for samples whose PFD's are concentrated at a similar direction is not a sensitive measure for detecting changes that are reflected in the variance and which might be the result of the experimental manipulation, albeit with a smaller effect.

An example of this situation is taken from a study that examined path integration and landmark control of LMN HD cells after lesions to the PoS (Yoder et al., 2015). In the study the authors reported that PoS lesions disrupt landmark control and the stability of the PFD when rats are recorded in darkness or as they walk from a familiar to a novel environment in a dual-chamber task where rats have to rely on path integration to maintain update the PFD as they travel between the two environments connected by a passageway. Independent *V*-tests showed that as the rat walked from the familiar to the novel environment, the PFD shifts for both the control and the PoS lesioned rats were significantly clustered at a mean direction of 0°, at a $p < 0.01$ (Figure 5.6).

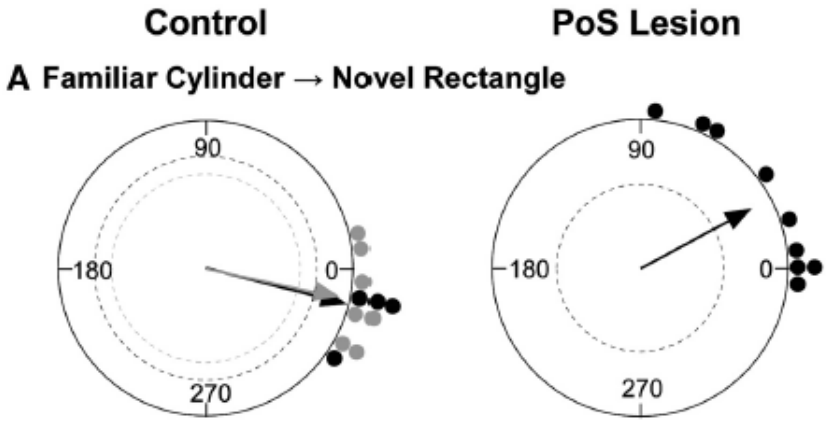

Figure 5.6 Distribution of the PFD shifts in the control and the PoS lesion group in the dual chamber task. A. PFD shifts as the rat walked from the familiar cylindrical arena to the novel rectangular arena. Each black dot is the mean directional shift of one LMN HD cell in a session. The grey dots correspond to data from a previously published paper by the same research group where ADN HD cells were recorded in the same task. Taken from (Yoder et al., 2015).

If the researchers had only tested for uniformity against a unimodal alternative with a specified mean direction they would have concluded that lesions of the PoS do not impair the activity of LMN HD cells during a path integration dependent task. This conclusion would have been incorrect since the control and the lesion group need to be compared with each other in order to draw such inference. Furthermore, a test for a common mean direction between the two groups would likely have yielded a non-significant result as both group have a mean direction close to 0°. However, as can be observed from the samples of circular data in Figure 5.6, the PFD shifts are more spread out (less concentrated at 0°) in the lesion group compared to the control group. Therefore, to determine if there were differences between the two groups, a test for a common concentration would be better suited as it captures the features of the distributions, in this case the variance better than a comparison of the mean direction. This is precisely what Yoder et al., 2015 carried out, comparing the parameter, κ, which measures the concentration around the mean direction of each group. In the paper, Yoder et al., 2015 reported that the control group (κ = 12.68) differed significantly from the PoS lesion group (κ = 2.61) at a $p < 0.05$ and concluded that lesions to the PoS produce a mild disruption of path integration in LMN HD cells.

This example illustrates that examining the variance of the sample and not solely relying on the *R* value as a measure of concentration is an important analysis that captures the features of the distribution and can be used to compare two samples of circular data such as a control and a lesion-recording group.

5.5.1 Kernel density estimates

In instances when a large number of trials and HD cells have been recorded, it is important to obtain an estimate of the underlying population density in the distribution of PFD's. A conventional method for estimating and displaying the probability density function is through a linear histogram. However, linear histograms have several limitations that impact the estimate of the underlying probability density function and hence the inferences that are derived from the data (Fisher, 1995). Such limitations include having a fixed number of bins whose

bin size affects the shape of the distribution, influencing the data that lies at the bin edges. As a result, the linear histogram can generate discontinuities that affect the distribution of the data. Furthermore, linear histograms are not appropriate for displaying or analysing angular data as there is no true zero in a circular scale and hence the designation of high and low values is arbitrary and measures of central tendency calculated on a linear scale yield biased estimates for circular data (Zar, 2010).

In terms of visualisation, linearizing a circular histogram by unwrapping it, leads to misleading results as the location of the mode(s) depends on the starting value of the histogram (Mardia & Jupp, 2000). An example of this situation is illustrated in Figure 5.7A, where angular data plotted as a linear histogram shows a bimodal distribution, while plotting the same set of data in a circular scale shows that the distribution is unimodal. A better approach for graphically representing angular data is to use a scatter diagram where each data point is displayed on the circumference of the circle. If there are many data points, the dots can be stacked on top of each other or superimposed. The scatter diagram can provide a good graphical representation of the density when the data is clustered at a particular direction(s).

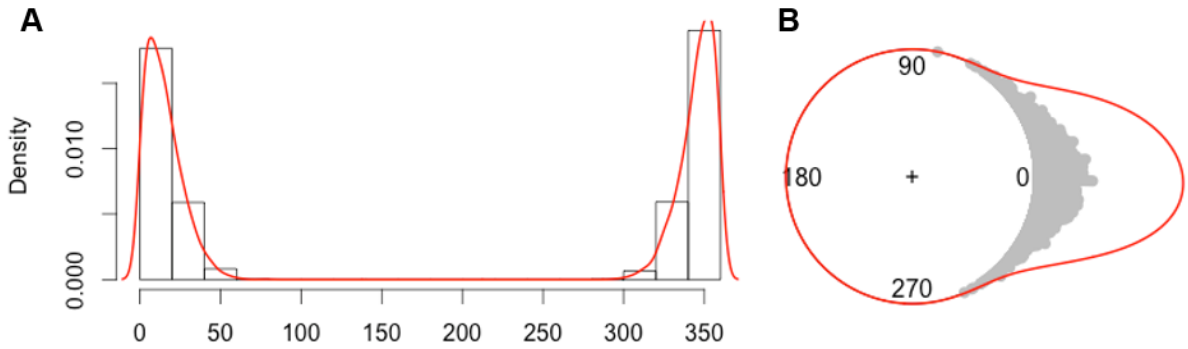

Figure 5.7 Simulated density estimates for a sample of PFD angular shifts. **A.** Linearized circular histogram with smoothed density estimate showing a bimodal distribution. **B.** KDE of the same dataset applying a von Mises kernel drawn as a contour red line over the circular scatter plot.

However, both circular scatter plots and histograms suffer from the same drawbacks as their linear counterparts as they do not provide a smooth estimate of the underlying population density. To overcome these limitations and obtain a better estimate of the underlying density for a distribution of angular shifts in a population of HD cells, a nonparametric density estimation method can applied. One nonparametric method that can be used to approximate the underlying probability density function of a data sample is known as the kernel density estimation (KDE) method. The major advantage of the KDE method compared to the circular histogram is that it does not depend on the starting position of the bins and spreads the influence of data points that are close to each other, providing a smooth density estimate and minimising the effects of data that lies at the bin edges. The KDE thus provides a better estimate of the underlying distribution, removing discontinuities that are artefacts of the bin locations (Figure 5.7B) (Fisher, 1995).

Although the KDE method has not been applied to analyse changes in the firing of HD cells, a density estimation method was recently applied to examine the distribution of directional tuning in HD cells recorded in layer III and V of the MEC across the dorsal-ventral axis (Giocomo et al., 2014b) and to estimate the angular offset of grid cell orientation relative to the borders of the environment (Stensola et al., 2015). Another study that applied a KDE method characterised in great detail the distribution of PFD's of single-units recorded in the motor cortex of rhesus monkeys during arm reaching movements (Naselaris, Merchant, Amirikian, & Georgopoulos, 2006). As these examples illustrate, KDE's have been applied in different areas of neuroscience to estimate the probability density function in a variable of interest and are good procedures for visualising and drawing inferences from a dataset. Applied to the population analysis of HD cells, circular KDE's allow for the visualisation of the distribution of changes in the PFD, where the shape of the density estimate (uniform, unimodal or multimodal) can be used to assess the fit of a statistical model and thereby evaluate the adequacy of a statistical test prior to conducting a hypothesis test, thus helping to draw a valid statistical inference and reaching a conclusion from the data.

The nonparametric KDE's that were applied to visualise the changes in the PFD of RSC and PoS HD cells which are reported in Chapter 6 and Chapter 7 use the von Mises distribution (Section 5.3.2) as the smoothing kernel where the spread of the data is controlled by the parameter kappa (κ),

$$f(\theta; \mu, \kappa) = \frac{1}{2\pi I_0(\kappa)} \exp(\kappa \cos(\theta - \mu))$$

where the value of κ**,** affect the underlying density function such that large bandwidth values of κ produce spiky density estimates with many modes, capturing the variation associated with individual observations rather than the structure of the population, while small κ values produce very smooth density estimates that capture little of the variation associated with individual observations (Mardia & Jupp, 2000).

Formally the circular KDE can be thought of as a moving average of a random sample of angles $\Theta_1, \ldots, \Theta_n$ covering the range [0, 2π) where the contribution (1/*n*) of each data point is spread out over a small arc containing that data point. The overall density estimate $\hat{f}(\theta)$ in a given direction θ is the sum of all the individual contributions,

$$\hat{f}(\theta; v) = \frac{1}{n} \sum_{i=1}^{n} K_v(\theta - \Theta_i)$$

where K_V is the circular kernel function (von Mises distribution) with concentration $v > 0$, which controls the amount of smoothing referred to as the bandwidth. Therefore, the nonparametric circular kernel density estimator for a population of *n* HD cells with von Mises distribution centred in the sample points Θ_i and with a given bandwidth v, was computed with the formula,

$$\hat{f}(\theta; v) = \frac{1}{2n\pi I_0(v)} \sum_{i=1}^{n} \exp(v \cos(\theta - \Theta_i))$$

Given that the smoothing parameter v controls the concentration of the data, an important issue when applying KDE's to circular data is choosing a bandwidth that best describes the features of the population density without oversmoothing

leading to a loss of important information and allowing subtle features of the distribution to emerge (Fisher, 1995). One method for choosing the smoothing parameter consists of a plug-in-rule selecting different bandwidth values using one von Mises or a mixture of von Mises distributions and comparing the different density estimates based on an information content criterion. Another method and the one used for selecting the bandwidth value for the KDE's reported in Chapter 6 and Chapter 7 relies on likelihood cross-validation rules (Hall, Watson, & Cabrera, 1987). In this method the smoothing parameter is obtained as the value of v that maximises the logarithm of the likelihood cross validation function,

$$\mathrm{LCV}(v) = \prod_{i=1}^{n} \hat{f}_{-i}\,(\Theta_i; v)$$

where $\hat{f}_{-i}$ is the circular kernel density estimator function shown at the bottom of page 122 leaving out the ith observation. This method is a data driven approach that computes the KDE using *n*-1 observations with a determined bandwidth. This is done *n* times (2,000) selecting the value that maximises the equation above.

5.5.2 Statistical analysis of multimodal distributions

Circular KDE's have many advantages for displaying data compared to circular scatter plots and histograms, providing a better estimate of the density function. However, a difficult problem arises when conducting inferential statistics with circular distributions that are not unimodal and hence cannot be strictly analysed with parametric circular statistics.

For example, Watson's U^2 test can be used as an omnibus test to detect multimodal departures from uniformity and the *V*-test can examine unimodal departures from uniformity at a predicted mean direction; however they are both unable to determine whether the underlying distribution is bimodal or multimodal. This is the case for all the parametric circular statistical tests, as they assume that the sampled data was drawn from a von Mises distribution. As a result, these tests examine if the sampled data deviates from a uniform distribution or from a

unimodal distribution against any alternative without explicitly testing the different multimodal alternatives (i.e. bimodal, trimodal, etc.). These limitations make it difficult to conduct hypothesis tests for non-unimodal data using standard circular analysis, as the underlying von Mises model is not flexible enough to capture the underlying structure of multimodal, highly peaked or skewed distributions (Oliveira, Crujeiras, & Rodriguez-Casal, 2014). This raises a difficult problem which has not been fully addressed in the analysis of HD cells, as it is often assumed (sometimes erroneously or with limited data) that the sampled data fits a von Mises distribution.

An alternative non-parametric method that can be applied for analysing circular data that is not unimodal is known as a bootstrap analysis where the collected data is randomly sampled and a distribution is generated from the data, creating confidence intervals that can be used to identify local peaks in the circular distribution. Although the bootstrap analysis is a powerful approach for analysing large datasets, treating a variable such as head orientation or PFD shift as continuous, it underperforms in small dataset as it is very sensitive in detecting small local peaks that might not constitute a true effect if the sample had been larger.

A different approach is to divide the continuous circular data based on *a priori* categories and compare the expected frequencies against the observed frequencies between categories with a relative frequency test. Although this a simple non-parametric test, little can be inferred about the true value of the distribution. A more powerful analysis can be conducted by using a Bayesian approach which is a statistical method that allows the use of prior information to evaluate the posterior probabilities of different hypotheses. In this regard, Bayesian statistics provide a flexible method for describing and quantifying data using probability to model uncertainty and obtain estimates of unknown quantities. Using Bayesian statistics, an estimate of the underlying population parameter can be obtained, helping to draw inferences about the probabilistic likelihood of different outcomes (Kruschke, 2015). Bayesian statistics were applied to evaluate the different hypotheses of the two cue experiments and are described in Section 6.3.5.1.

Hypothesis testing with Bayesian statistics differs from classical hypotheses testing as both the null and the alternative hypotheses are evaluated, where the probability of obtaining data that falls into each model or category can be estimated (Kruschke, 2015). In contrast, in classical hypotheses testing only the probability of obtaining data under the null hypothesis is examined without testing the likelihood of the alternative hypothesis. In this respect, Bayesian statistics can weight competing models and estimate the probabilistic likelihoods of the data under each model without relying on how unlikely they are under only one model.

Bayesian methods rely on the laws of probability, applying Bayes' theorem to generate a posterior distribution with a parameter value that ranges from [0, 1] representing the probabilistic likelihood of obtaining data under a given model, thus assessing the probability that a certain hypothesis is true. The conclusions from Bayesian analysis are thus based on posterior distributions arising from combining observations conditioned on a particular outcome with prior information derived from the actual data. For multinomial models, Bayesian analysis can be applied to estimate the probabilistic likelihood of observations belonging to different categories based on the *a priori* hypotheses.

In this regard Bayesian analysis using multinomial variables are similar to applying a Chi-square test as it examines the probability of data falling in a particular fixed category. However, unlike null hypothesis testing using relative frequency tests, Bayesian analysis provides a continuous probabilistic likelihood of the different models instead of a point estimate (*p*-value) of obtaining data under the null hypothesis. Furthermore, Bayesian estimation methods are more powerful than relative frequency tests when drawing inferences from small dataset as the posterior distribution is generated by randomly sampling the data.

5.6 Discussion and future directions

The current chapter reviewed the standard statistical methods that have been applied for classifying neurons as HD cells and estimating their tuning curve parameters such as the directional firing range and the PFD. The mode of the

firing rate histogram which corresponds to the peak firing rate was selected as the parameter of choice for defining an HD cell's PFD as it is less variable compared to the circular mean direction and provides a precise measure of the directional firing of an HD cell when the tuning curve is not symmetric. A disadvantage of using the mode compared to the circular mean direction as a measure of the PFD is that its accuracy lies in a range that is dependent on the size of the bin and therefore its value will be discrete, for the case of the current analysis a multiple of 6°.

The estimate of the PFD is important since this parameter is the most commonly used measure of the directional firing of an HD cell. Thus the question of how to extract the maximum information from tuning curves is an important topic that was not discussed at great length in this chapter and which has been previously addressed in the context of defining the orientation selectivity of cells in the visual cortex (Grabska-Barwińska, Ng, & Jancke, 2012).

Once the tuning curve parameters of single HD cells have been calculated, it is important to examine the changes in the directional firing of a population of HD cells recorded from several animals as a result of an experimental manipulation (lesion, behavioural or both). The commonly applied population analysis consists of calculating the mean direction of multiple recorded trials/sessions for each HD cell and obtain a single estimate of that cell's behaviour. These point estimates are then pooled into a single distribution corresponding to all the HD cells recorded in a particular experimental condition.

The disadvantage of such an approach is that the variance of the population distribution of HD cells is significantly reduced, thus decreasing the variability that reflects changes in HD cell activity that are the result of the experimental manipulation. This is reflected in a population distribution that commonly has a relatively small number of observations and a high mean vector length value that is clustered at a particular direction affecting the inferences that are drawn from a single sample when testing for uniformity against a unimodal alternative (von Mises distribution) with a specified mean direction. Furthermore, the reduction in the variance will impact the final *R* value that is obtained, decreasing the likelihood

of detecting differences between groups as the most commonly used circular statistical tests rely on comparisons of the mean vector length and the mean direction.

To overcome these limitations, a circular KDE method was applied to analyse the population response of HD cells, specifically changes in the PFD as a result of cue control manipulations. The advantage of KDE's over standard methods such as circular histograms is that they provide a nonparametric estimate of the underlying population density, capturing the variability of individual HD cells that occurs within a session, for instance when the PFD switches relative to the two cue cards. This is achieved by pooling all the individual trials recorded across the HD cell population without the need of computing a mean direction for each individual HD cell separately. The power of the KDE is the ability to provide a reliable statistical method that can be applied to visualise and estimate the underlying distribution of a large population of HD cells without relying on an arbitrarily chosen bin size to construct the circular histogram which creates discontinuities that strongly influence how the graph is interpreted. Instead, the smoothing parameter of the KDE which controls the global appearance of the distribution can be chosen using a variety of data-driven methods such as cross-validation rules, which perform well when the underlying density follows a von Mises distribution.

The disadvantages of the circular KDE method is that the density estimate heavily depends on the sample size and only simple inferences can be drawn with a small sample ($n > 30$), inferring for example that the sample was probably drawn from a unimodal distribution (Fisher, 1995). In contrast, with a large sample size there is more information about the true underlying density, from which inferences can be drawn about deviations from unimodality. Furthermore, if a von Mises kernel is chosen, the performance of the KDE may not provide an accurate representation of the underlying density for distributions that are multimodal, highly peaked or skewed. This is particularly important as the selection of an unsuitable bandwidth for a von Mises kernel can provide a misleading estimate of the density and compromise the evaluation of the statistical significance of the observed features of the distribution (Oliviera, Crujeiras, & Rodriguez-Casal, 2014). Therefore,

selecting the appropriate statistical model to draw probabilistic inferences from the data is a critical step in the population analysis of neuronal data (Kass, 2005). Furthermore, from a statistical point of view, it is important to explain why a particular statistical test was chosen, if the assumptions of the test were examined and if any departures were observed in order to make the process of statistical inference clear to others who might want to apply a similar analysis to address a related question.

In summary, advances in recording methods can shift the field of single-unit experiments from single-neuron and multiple-trials to multiple-neuron and single-trial methodologies yielding information about how neuronal ensembles encode features of the environment and the underlying attractor network properties that update and reset the activity bump in HD cell ensembles. At the same time, advances in data analysis can aid to extract the maximum information from neuronal populations, employing decoding methods that can predict which stimulus or behaviour are most likely to elicit a particular neural response, and information theory methods that can be used to quantify the amount of information about a given stimulus or behaviour that is encoded by the response of multiple spike trains (Quian-Quiroga & Panzeri, 2009). Overall, these advances will provide insight into how the brain computes self-location by combining sensory information from different modalities which might be reflected in both the rate and temporal spiking activity of both spatial and non-spatially modulated cells.

Chapter 6 Landmark feature processing by head direction cells

6.1 Background and rationale

Based on a vast literature that has examined the effects of visual cue manipulations on the activity of HD cells across many interconnected brain areas (see Taube, 2007; Yoder, Clark, & Taube, 2011 for a review) and studies that have investigated the behavioural deficits in spatial navigation as a result of lesions to the RSC and the PoS (Stackman, Lora, & Williams, 2012; Vann & Aggleton, 2004), there is strong support for the role of these brain areas in spatial orientation and allocentric referenced memory. Regarding the role of HD cells in the RSC and the PoS, it has been hypothesised that they play an important role in the integration of self-motion signals with visual information, resetting the rat's internal sense of direction relative to cues in the environment (Yoder, Clark, & Taube, 2011).

These visual landmarks anchor the firing direction to the external world, where objects (Zugaro, Berthoz, et al., 2001) and salient visual features of the environment act as positional and directional cues that aid animals in forming an allocentric referenced map (Yoder, Clark, & Taube, 2011). In this context, landmarks constitute any visual information derived from the environment that aids in creating a spatial representation and identifying the current facing direction which includes both local and distal features of the environment such as objects, borders, edges, or any other information derived from the surrounding panorama (Knierim & Hamilton, 2011). For the present experiments, the term "landmark" will be used to denote the local, static cue cards attached to the inside wall of the recording apparatus.

Many studies have characterised the pathways that are important for generating and updating the HD signal (see Section 2.3 for a review); however an area of research that remains relatively unexplored in the study of spatially modulated cells relates to the brain regions and the pathways that are involved in the processing of landmark information (see Section 2.4 for a review). An important question, and one addressed in the present study, is how visual information is

transformed into a landmark representation and what sensory features of the environment such as contrast, orientation or position make for a static visual cue to be processed as a landmark.

To address these questions, the aim of the experiments described in the present chapter was to examine what visual properties of landmarks are sufficient to reset the spatial firing of HD cells. In other words, how fine-grained is the visual discrimination ability of the HD system? The answer to this question will provide an important step towards understanding the transformation between retinal input and the HD signal. This question was addressed by conducting cue control experiments and recording HD cells in the PoS and the RSC as rats foraged for food inside a cylindrical arena with distinct polarising cue cards attached to the inner wall. The recordings were conducted in these two brain areas because they play an important role in landmark processing, linking spatial information derived from HD cells (Cho & Sharp, 2001; Taube et al., 1990a) with visual information from the primary visual cortex (van Groen & Wyss, 2003; Vogt & Miller, 1983). Furthermore, as both the PoS and the RSC project to the hippocampus and the MEC, examining cue control of HD cells in these brain areas can provide insight into how visual and spatial information that is relevant for the processing of landmarks is integrated by other spatially modulated cells in the PHR-HF (Sugar et al., 2011).

Therefore, the current study seeks to investigate for the first time the visual properties that HD cells in rodents use to align their directional firing in reference to landmarks. Specifically, the aim of the study is to determine whether HD cells can distinguish contrast, orientation, and position and use these visual features as landmarks to reliably reset their PFD. Addressing this question is important since the cell types and function of neurons that are involved in visual processing and the representation of self-location in the mammalian brain are beginning to be well characterised. However, there is a substantial gap in understanding the relationship between visual perception and spatial orientation at the single-cell level.

As will be described below, the main finding is that HD cells in both the RSC and the PoS discriminate the visual features of the cue cards, as shown by the cells adopting a consistent firing direction within the arena relative to the cue pair. However, the likelihood of landmark control varied between the visual stimuli, where contrast and orientation had a high probability of discrimination and landmark control, while vertical and lateral position showed a lower probability of discrimination and landmark control. Furthermore, landmark control for the different cue types did not differ between brain areas, suggesting that the activity is tightly coupled in the HD cell circuit, consistent with attractor network models. These results show that HD cells can reliably use different visual features to aid in spatial orientation, and offer a potential model system with which to explore how visual signals are transformed from the visual cortex into the landmark representation used by spatially modulated cells.

6.2 Methods and hypothesis

This section provides a brief description of the experimental protocol, the hypotheses and a classification system based on the predicted response profile of RSC and PoS HD cells as a result of the cue card manipulations.

6.2.1 Experimental procedure

In order to investigate the visual features that rats use for spatial orientation and thereby process as landmarks, a pair of contrasting cue cards were placed inside a cylindrical arena. A detailed description of the experimental set-up and the behavioural protocol is provided in Section 4.6. To briefly summarise, an experimental session consisted of recording HD cells as the rat foraged for food inside a light-grey cylindrical arena with two opposing cue cards attached to the inner wall, 180° apart. The cue card pair varied in contrast (black-white), orientation (vertical-horizontal) and position of a bar in the y-axis (top or bottom of the card) or lateral position (left or right of the car) with control stimuli comprising identical black cards (Figure 6.1).

The cue control session consisted of a series of trials 5 minutes each starting with trials where both cue cards were not rotated (baseline trials) followed by trials were the two cue cards were rotated together (rotation trials) by a different magnitude and direction (±45°, ±90°, ±135° or ±180°). All of the cue rotations were carried out before the start of each trial. The order of presentation for the different cue card pairs and the cue rotations were pseudorandomly assigned between rats, to prevent temporal effects due to the changing experience of the rat across days.

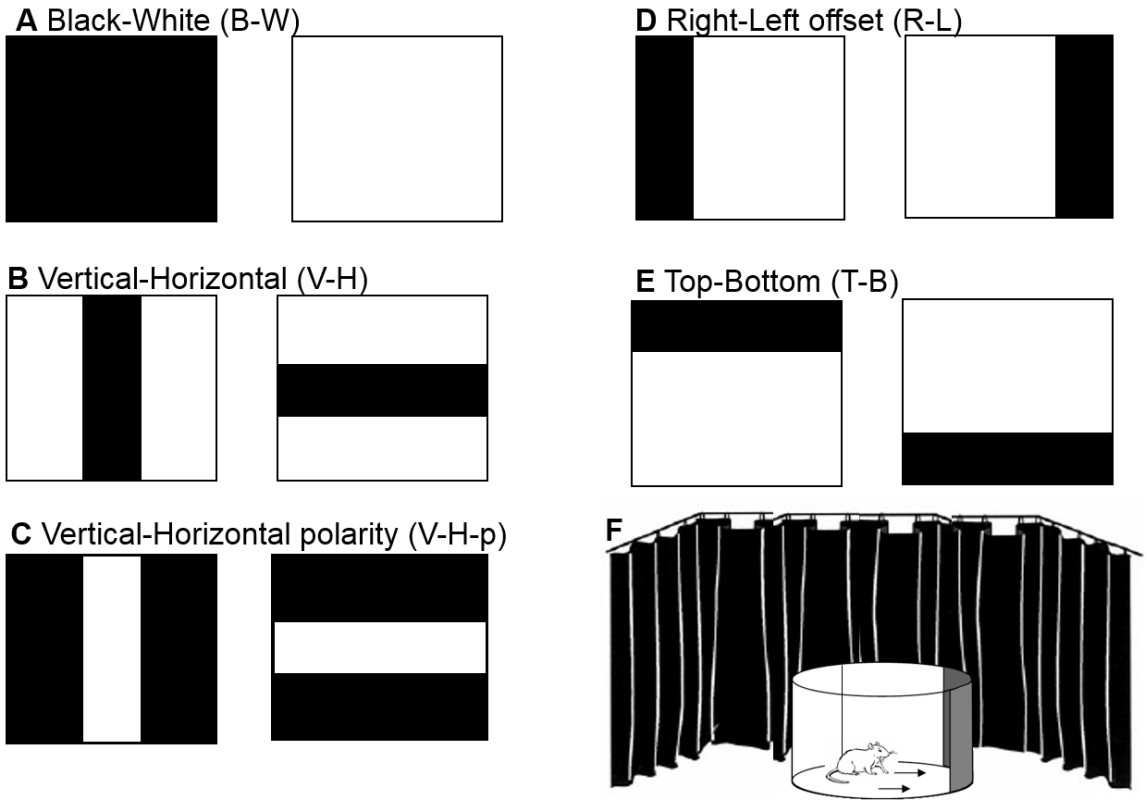

Figure 6.1 Illustration of the stimuli and recording arena that were used to investigate the landmark processing capabilities of HD cells to: **A.** Contrast (black-white), **B.** orientation with white background display (vertical-horizontal), **C.** orientation with black background display (vertical-horizontal-polarity), **D.** lateral position (right-left offset) and **E.** vertical position (top-bottom). The control cue cards (not shown) consisted of identical black cards (B-B). The abbreviations that are used throughout this chapter for the cue cards are shown above the image of every cue card pair. **F.** The size of the cylindrical arena was 51 cm high x 74 cm in diameter, surrounded by a 260 cm diameter circular curtained enclosure. Diagram in **F** adapted from (Zugaro et al., 2001).

6.2.2 Hypothesis

To determine if HD cells can use the different visual features of the cue cards (contrast, orientation, and position) as landmarks, the hypotheses made predictions about the changes in the PFD in relation to the cue card pair (Figure 6.2). It was predicted that if HD cells discriminate and use the visual features of the cue cards as landmarks, RSC and PoS HD cells are expected to maintain a consistent PFD within the arena relative to a given cue card pair across a session (Figure 6.2B). This finding would indicate that HD cells can distinguish or discriminate the features of the cue cards and reliably use the information derived from the cues for spatial orientation.

Alternatively, if HD cells do not discriminate the visual features of the cue cards, the PFD should change randomly by 180° across trials within a session (Figure 6.2C). This finding would indicate that although HD cells respond to the cue cards, showing some degree of landmark control to either of the two cue cards, they do not discriminate a given visual feature of a cue card pair and hence are unable to reliably use this information for spatial orientation. Another two possible outcomes are that HD cells disregard both cue cards and the PFD changes its orientation randomly across a session or that instead HD cells lock to external, room referenced cues whereby the PFD does not change as the cue cards are rotated (Figure 6.2D).

Based on these hypotheses, three schematic models were made to illustrate the potential outcomes for a population of HD cells. In these models, the changes in the PFD of a population of HD cells are predicted to follow, within the reference frame of the cue pair, either a uniform, unimodal or a bimodal circular distribution (Figure 6.3). If there is no landmark control, the circular distribution of PFD deviations are predicted to be uniform, lacking a local maximum (Figure 6.3A). In contrast, if there is landmark control and discrimination, the distribution of PFD deviations are predicted to be unimodal with one local maximum at approximately 0° with a concentration density that decreases with increasing distance from the local maximum (Figure 6.3B).

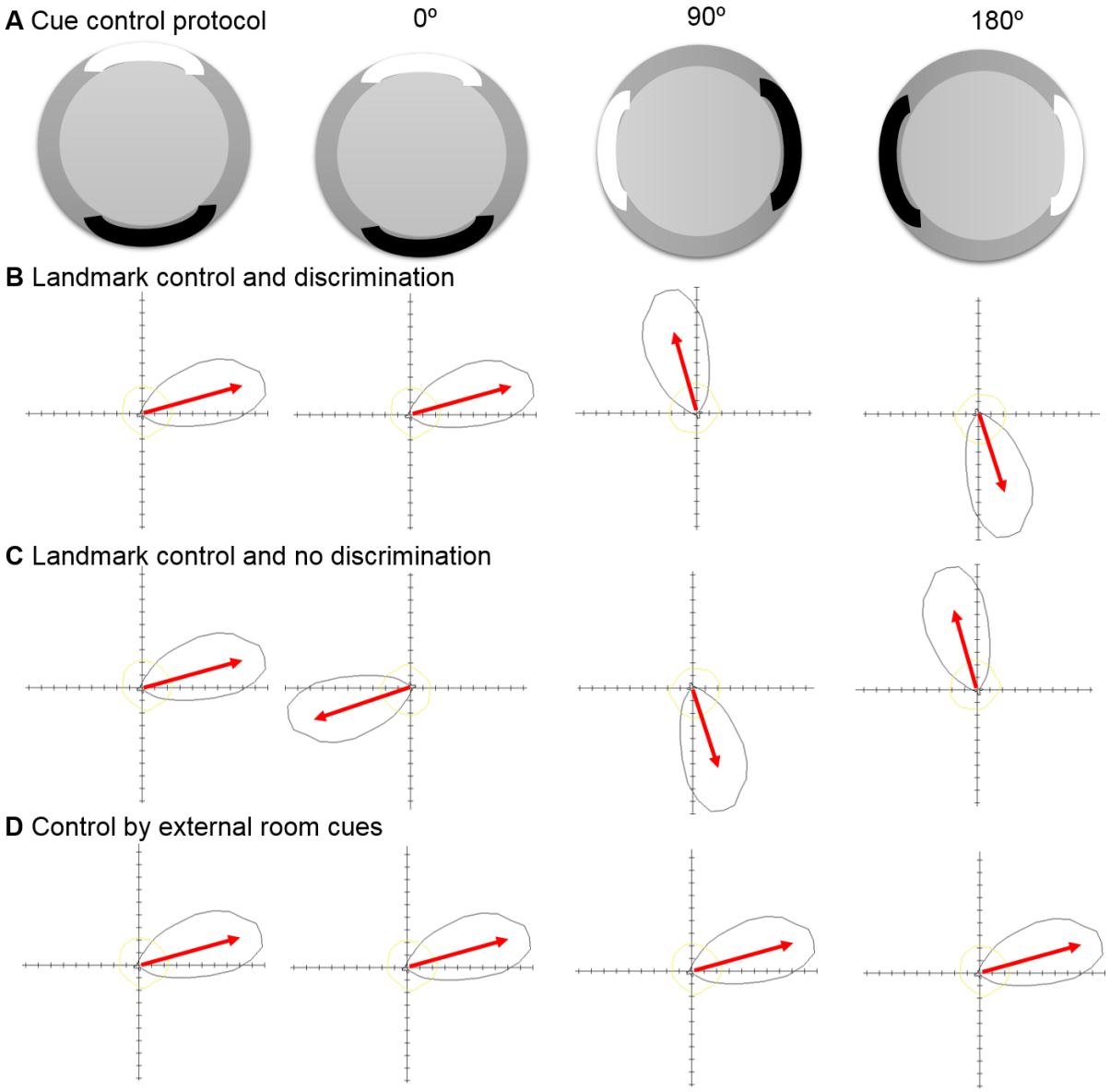

Figure 6.2 Schematic diagram of the predicted outcomes of a single HD cell recorded in the two cue protocol. **A.** Illustrative example of the recording set up showing the location of the black and the white cards across a session consisting of two baseline (0° rotation) and two cue rotation trials (90°and 180°). **B.** Landmark control and discrimination, where the red arrow represents the PFD of the tuning curve. **C.** Landmark control and no discrimination. Note how the PFD changes by 180° from what is predicted if HD cells discriminate contrast and use this feature as a landmark. **D.** HD cells locked to external, uncontrolled cues. The directions in all of the plots, are reported according to polar coordinates where 0° is east and 90° is north.

On the other hand, if there is landmark control and no discrimination, the distribution of PFD deviations is predicted to be bimodal with two local maxima at approximately 0° and 180° (Figure 6.3C).

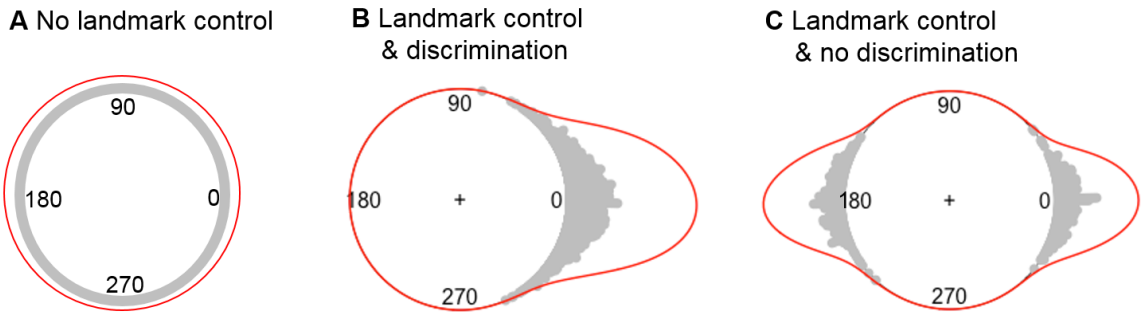

Figure 6.3 Models that illustrates three competing hypothesis. The circular kernel density estimate shown in red illustrates the expected response for a population of HD cells that showed: **A.** No landmark control, **B.** landmark control and discrimination, or **C.** landmark control and no discrimination.

The unimodal outcome would follow a von Mises distribution where the mean resultant vector length R and the mean direction $\bar{\theta}$ can be used as a measure of concentration and central tendency to examine departures from uniformity or from unimodality against a predicted mean direction (Section 6.3.3). In contrast, for bimodal distributions, the use of a single measure of central tendency that characterises the circular distribution will yield a biased estimate of the population parameter (Section 5.5.2). Therefore, to overcome this limitation and analyse this outcome, the distribution of PFD deviations was sorted into three nominally predicted cell response categories (Section 6.3.5) and a Bayesian analysis was conducted to examine the probability that data would fall in each category (Section 6.3.5.1).

Due to lack of prior data, no predictions were made regarding the effect of brain area. Similarly, no predictions were made regarding the magnitude of landmark control for the different cue card pairs, although it was expected that HD cells would be able to distinguish contrast (a black from a white cue card) as previously reported in cue control experiments with place cells (Fenton, Csizmadia, & Muller,

2000). Finally, it was expected that the magnitude of cue rotation would have no effect on landmark control, yielding a similar mean direction relative to the landmark array for all the PFD distributions irrespective of cue type.

6.3 Data analysis

The data were analysed with MATLAB R2013a (MathWorks, USA) and R statistical software (R Core Team, 2014) with functions taken from the CircStat toolbox (Berens, 2009) and the R packages circular (Lund & Agostinelli, 2013), sm (Bowman & Azzalini, 2014) and NPCirc (Oliviera et al., 2014).

To examine the behaviour of HD cells in response to the cue manipulations and address the hypotheses previously described (Section 6.2.2), all of the cells that passed the inclusion criteria for being directionally tuned were analysed (Section 4.7.4). Since simultaneously recorded HD cells maintain a regular angular offset with respect to one another and shift coherently (Johnson et al., 2005; Peyrache et al., 2015), the data from these sessions cannot be treated as independent. Therefore, to weigh all the sessions equally irrespective of the number of HD cells recorded, the sample median direction was calculated for each HD cell ensemble, obtaining one estimate of the change in the PFD per trial (Section 6.3.1). The use of the median direction as a measure of the change in the PFD for an HD cell ensemble likely affected the sampled variance within a session, contributing to values in the distribution of PFD deviations that are closer to 0° and 180° corresponding to cue discrimination and no cue discrimination respectively (Figure 6.3).

For all of the analysis reported, the unit of measure constitutes the PFD deviation of a single HD cell or an ensemble of HD cells recorded in one trial for a given cue card pair. For logistical reasons, the same HD cell or rat was not exposed to all of the cue card combinations. Therefore, because the data constitutes several rats implanted in two brain areas (RSC and PoS), where the number of sessions and HD cells recorded per cue type and rat differs across the groups, the assumption of independent observations does not hold strictly. The rationale for combining the

data across animals was to increase the sample size per experimental condition and obtain a better estimate of the underlying density using the KDE method described in Section 5.5.1.

The data from all the baseline trials was analysed irrespective of brain area and cue type to determine whether the PFD was stable in relation to the proximal cue cards. The data from the rotation trials was then analysed to determine whether HD cells were controlled by the proximal cue cards or by uncontrolled distal cues. After determining that the changes in the PFD are relative to the proximal cue cards in both the baseline and the rotation trials, the data was combined for all subsequent analysis.

After merging the baseline with the rotation trials, the effect of brain area was subsequently analysed to determine whether HD cells recorded in the PoS could be combined with those recorded in the RSC (Section 6.3.4). Subsequently, the effect in the magnitude of cue rotation (0°, 45°, 90°, 135° and 180°) was analysed followed by an analysis of the PFD deviations in each cell response category (Section 6.3.5.1). For all the null hypothesis tests, a $p < 0.05$ was considered as statistically significant.

6.3.1 Preferred firing direction shift analysis

For every session the minimum angular distance between the PFD and the midpoint location of Cue1, the angle that is referred to as θ_i, was calculated. Afterwards, the sample median direction, denoted by $d(\psi)$ was calculated independently for each HD cell in a session by identifying the angle ψ that minimises the spread of all θ_i values of every HD cell recorded within a session, using the following formula taken from Pewsey, Neuhäuser, & Ruxton, 2013.

$$d(\psi) = \frac{1}{n}\sum_{i=1}^{n}\{\pi - |\pi - |\theta_i - \psi||\}$$

A diagram that illustrates the median direction for a simulated sample of θ_i values is shown in Figure 6.4B. Subsequently, the PFD deviation of each HD cell across

trials with respect to the median, denoted by θ_s, was calculated by obtaining the minimum angular distance between every θ_i and the corresponding median direction of the session, $d(\psi)$.

$$\theta_s = (\theta_i, d(\psi))$$

The reason for selecting the median direction instead of the mean direction is because the median provides a robust measure of central tendency when the sample is skewed and the data is not clustered at a particular location as illustrated in Figure 6.4B (Pewsey et al., 2013). The skewness comes from the variability in the changes of the PFD relative to the cues, where θ_i could vary by as much as ±180° if the PFD changes between the two cue cards. At first glance the PFD deviations of 180° might be thought of as outliers; however they cannot be excluded from the sample as they represent the expected behaviour of HD cells that do not discriminate the cue cards, albeit show landmark control (Section 6.2.2).

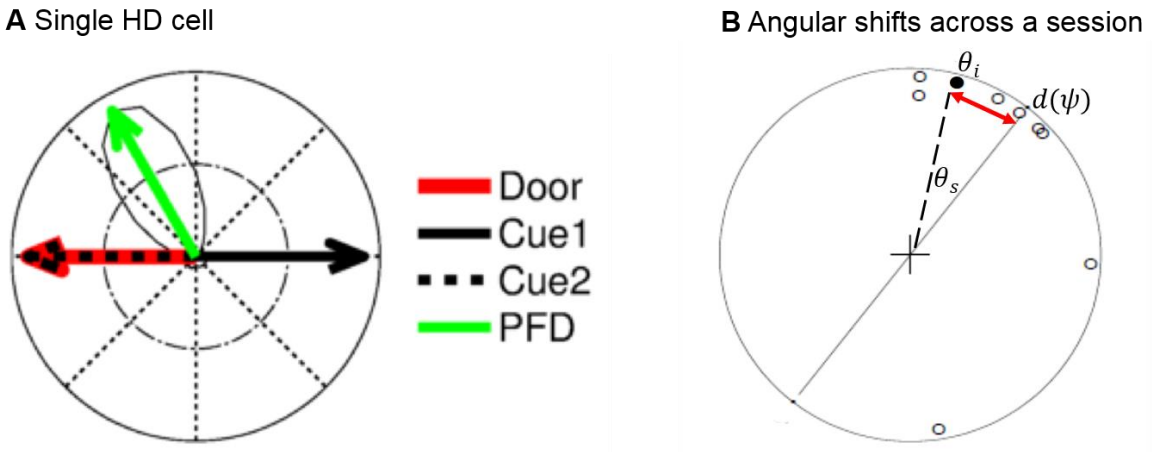

Figure 6.4 Calculating the change in the PFD of an HD cell across a session. **A.** Polar plot of one HD cell showing arrows pointing to the PFD (green arrow), the location of Cue1 (black solid arrow), Cue2 (black dashed arrow) and the door of the recording room (red arrow). The minimum angular distance between the PFD and Cue1 was used to calculate θ_i. **B.** Illustration of a distribution of θ_i values (open dots) for one session showing the sample median direction at $d(\psi)$. The PFD deviation, θ_s (marked as a red arrow) for one HD cell in a single trial is denoted as the angular distance between $d(\psi)$ and θ_i (black dot).

6.3.2 Nonparametric density estimation

After calculating the PFD deviation of individual HD cells and ensembles, a graphical representation of the estimated probability density function was used to capture the variability of individual HD cells at the population level. This was achieved by using a circular nonparametric kernel density estimation (KDE) method (Section 5.5.1).

The nonparametric KDE uses a smoothing kernel derived from the von Mises distribution whose concentration is controlled by the parameter kappa (κ). The KDE for the population of PFD deviations (θ_s) was computed by considering θ equally spaced points that covered the range [0**,** 2π), given the samples $\theta_i \ldots \theta_n$ with the formula,

$$\hat{f}(\theta; v) = \frac{1}{n} \sum_{i=1}^{n} K_v(\theta - \Theta_i)$$

where K_V is the von Mises distribution,

$$f(\theta; \mu, \kappa) = \frac{1}{2\pi I_0(\kappa)} \exp(\kappa \cos(\theta - \mu))$$

where μ is the mean direction, κ is a measure of concentration (when κ=0, the distribution is uniform and when $\kappa \to \infty$ all points stack at μ), and $I_0(\cdot)$ is the modified Bessel function of order 0.

The value for the bandwidth was selected using a cross-validation method described in Section 5.5.1.

6.3.3 Circular summary statistics

The summary statistics that were used to describe the main features of the distribution of PFD deviations included: 1) The mean direction ($\bar{\theta}$), 2) the mean vector length (*R*), and 3) the sample circular variance (*V*). A *V*-test was used to examine if the distribution of PFD deviations were clustered at a mean direction of 0°, as predicted from the hypotheses (Section 6.2.2). The *V*-test is a modified

Rayleigh test of uniformity with alternative hypothesis of unimodal distribution at a given mean direction.

6.3.4 Inferential statistics

To examine whether the baseline and the rotation trials could be merged and treated as equal, a randomisation version of Watson's two-sample U^2 test compared the randomised sample of baseline trials with the randomised sample of rotation trials for all the trials irrespective of cue type and brain area. The randomised samples are obtained by randomly permuting the combined sample of size $n_1 + n_2$ formed from the two samples and using the first n_1 observations as the first sample and the remaining n_2 as the second sample. For the original data and each of the 1,000 random permutations, N_R, the test statistic and the p-value are calculated from the proportion of $N_R + 1$ values that are greater than or equal to the value of the test statistic for the original sample (Pewsey et al., 2013).

To examine whether there was an effect of cue type and brain area, a Harrison-Kanji two-way ANOVA was applied (Berens, 2009). The Harrison–Kanji test is a circular version of a two-way ANOVA that evaluates whether the mean direction of two or more groups are equal. If a main effect of cue type and no effect of brain area and no interaction between brain area and cue type are found, the data were merged and treated equally for subsequent analysis. Otherwise, separate analysis would have to be conducted by splitting the data based on brain area and cue type. Subsequently, to determine whether there was an effect in the magnitude of the cue rotation, a Watson-Williams high concentration F-test was conducted as a one-way ANOVA, examining whether the mean direction of the samples were equal (Pewsey et al., 2013).

To test the hypothesis of no landmark control for each cue type (Section 6.2.2), individual V-tests were applied to determine whether there is enough evidence to suggest that the PFD deviations are not uniformly distributed and are instead clustered at a mean direction of 0°. If the hypothesis of no landmark control is rejected, the remaining two hypotheses were evaluated applying a Bayesian

analysis in order to determine the probability that the PFD deviations would fall into one of the pre-determined cells response categories.

6.3.5 Cell response classification

If the directional shifts of RSC and PoS HD cells as a result of the different cue manipulations are not uniformly distributed and are instead clustered at a particular mean direction, the PFD deviations were sorted into three categories in order to evaluate if HD cells could discriminate and use as a landmark a given visual feature (Figure 6.5). The interval size for each category was 90° and divided the distribution of PFD deviations into four equally sized angular bins. The bin interval was chosen based on previously reported cue control studies which have shown that the PFD of PoS HD cells can shift by as much as ±45º between trials when a single cue card of a similar angular size as the one presented in the current experiments is rotated (Taube et al., 1990b).

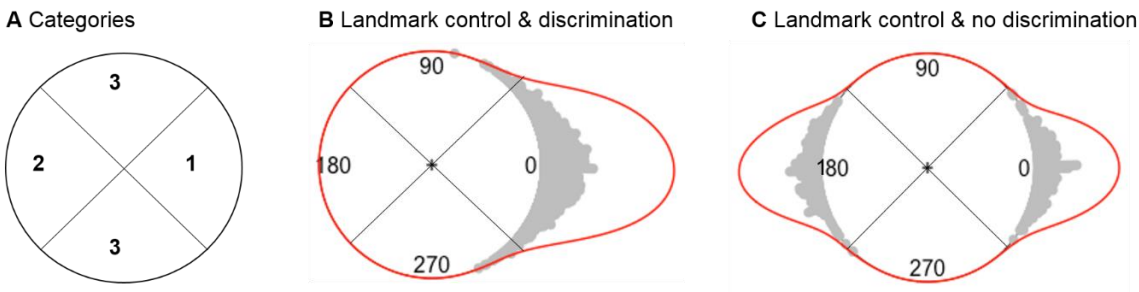

Figure 6.5 HD cell response categories of nominally predicted variables. **A.** Circular distribution divided into the three cell response categories of the distribution of PFD deviations. **B.** Simulated distribution of PFD deviations that primarily fell in category 1, corresponding to landmark control and discrimination. **C.** Simulated distribution of PFD deviations that fell equally in both category 1 and category 2, corresponding to HD cells that showed landmark and no discrimination.

Accordingly, the relative frequency of PFD deviations that fell within the range of one of the following three categories was determined for each cue card pair: Category 1, [315º, 45º], landmark control and discrimination; category 2, [135º,

225º], landmark control and no discrimination; category 3, [45º, 135º] and [225º, 315º], no landmark control and no discrimination (Figure 6.5).

6.3.5.1 Bayesian analysis

The aim of the Bayesian analysis was to draw inferences from the observed distributions of PFD deviations in each cue card pair with the goal of evaluating the evidence for the competing models, where each hypothesis represents one of the cell response categories (Figure 6.5). This can achieved by estimating the parameter values of the multinomial distribution, corresponding to the probability that a PFD deviation θ_s, would fall into one of the three categories. Formally, this is calculated using the conditional probability derived from Bayes rule,

$$p(\mu|y = category_i) = p(y = category_i|\mu) \times \frac{p(\mu)}{p(y)}$$

where $p(\mu|y = category_i)$ is the posterior distribution or the probability of obtaining a parameter value μ conditional upon a PFD deviation falling in y, where y corresponds to the $category_i$, $p(y = category_i|\mu)$ is the likelihood or the estimate of observing data given a model, $p(\mu)$ is the prior or the probability of μ before y is observed and represents the initial beliefs about the parameter estimate which was chosen to be uniformly distributed with no preference between categories, and $p(y)$ is the marginal likelihood, or the total probability of y that is the same for all the hypotheses and serves as a normalising constant, maintaining the range of the probability between [0,1].

To draw inferences from the posterior probability distribution within each cue card pair, the median and the 95% credible interval were used to estimate the parameter μ for each category. The evidence for the competing hypothesis was examined by comparing the difference in the parameter μ, such that $\Delta\mu = \mu_1 - \mu_2$ where μ_1 is the probability that a PFD deviation falls in category 1 and μ_2 is the probability that a PFD deviation falls in category 2. If $\Delta\mu > 0$, the majority of the PFD deviations are located in category 1, indicating that HD cells showed landmark control and discrimination of a given cue card feature (Figure 6.5B). In

contrast, if $\Delta\mu < 0$, the majority of the PFD deviations are located in category 2, indicating that HD cells showed landmark control and no discrimination. Alternatively, if $\Delta\mu = 0$, the PFD deviations are evenly distributed between category 1 and category 2, indicating that the two cue cards exerted the same degree of landmark control, a situation that is predicted to occur if HD cells are recorded when rats are presented with two identical cue cards.

Markov chain Monte Carlo simulations were conducted by random sampling 10,000 times the parameter values μ from the posterior distribution in order to ensure that the estimates generated from the posterior distribution such as the median and the 95% credible interval were stable and provided an accurate estimate of the distribution. Three parallel Markov chains with a different random number generator were plotted as posterior distribution.

6.3.6 Co-rotation analysis

The aim of the co-rotation analysis was to examine if simultaneously recorded HD cells exhibit a coherent PFD shift in their activity, consistent with attractor network models and previous studies were HD cell ensembles have been recorded (Bjerknes et al., 2014; Peyrache et al., 2015). The analysis included cells that passed the HD cell inclusion criteria in sessions for which *n* > 1 HD cells were simultaneously recorded. As the co-rotation analysis made pairwise comparisons between all the HD cells recorded across a session, only those sessions in which HD cells were recorded across all trials were included in the analysis.

To quantify the PFD shift of individual HD cells across a session, the PFD of $cell_i$ in trial $t_n$was subtracted to the PFD of the same $cell_i$ with respect to the previous trial t_{n-1} according to the formula,

$$PFD\ shift_{cell_i} = PFD_{cell_i,t_n} - PFD_{cell_i,t_{n-1}}$$

where the first trial in a session corresponds to the first baseline trial. After determining the PFD shifts for each HD cell across a session, the angular offset between pairs of simultaneously recorded HD cells, θ_{trial} was calculated independently for each trial by,

$$\theta_{trial_n} = \min(PFD\ shift_{cell_i}, PFD\ shift_{cell_i})$$

where θ_{trial_n} is the minimum angular distance (angular offset) of the PFD shift between pairs of HD cells recorded in the same trial such that the same HD cell was not compared with each other. To avoid having repeats of θ_{trial_n} for the same pair of HD cells, only one pairwise comparison was included. The angular offset from all θ_{trials} across all sessions irrespective of cue type was combined to obtain a KDE of the ensemble rotation for each brain area. The ensemble activity was analysed by comparing the distribution of θ_{trials} of the RSC and the PoS using a *V*-test with a predicted mean direction of 0°. The *V*-test was applied since the ensemble activity of HD cells is hypothesised to be strongly coupled, where the distribution of θ_{trials} for each brain area predicted to be concentrated at a mean direction of 0°. To examine if there were differences in the co-rotation shifts between HD cells recorded in the PoS compared to those recorded in the RSC, the angular dispersion around the mean angle of each sample was compared using Wallraff's nonparametric test. Wallraff's test computes the angular distance between each observation and the mean direction for that sample and subsequently compares the angular distances between the two samples with a Kruskal-Wallis rank sum test (Pewsey et al., 2013).

6.3.7 Tuning curve characteristics

To compare the peak firing rate and the tuning width of all the HD cells recorded in the PoS with those recorded in the RSC, the tuning curve parameters of the first baseline trial from every session were used. The first baseline trial was selected as a representative sample of the HD cell's peak firing rate and tuning width for a session as it is assumed that there are no significant changes in these tuning curve parameters across a session. A univariate density estimation method was applied to test for equality of densities between the distribution of the peak firing rate and the tuning width for each brain area. The two-sample test for equality of densities uses a permutation test of equality to compute the *p*-value using the same smoothing parameter to construct each density estimate (Bowman & Azzalini, 2014).

6.4 Properties of PoS and RSC HD cell tuning curves

Density estimates in the distribution of the peak firing rate showed that PoS HD cells had a mean peak firing rate of 8.49 ± 0.64 Hz, while RSC HD cells had a mean peak firing rate of 24.59 ± 2.35 Hz (Figure 6.6). A permutation test for equality of densities showed that there was a significant difference between the peak firing rate of HD cells recorded in the PoS (*n* = 93 sessions) compared to those recorded in the RSC (*n* = 115 sessions), $p < 0.001$.

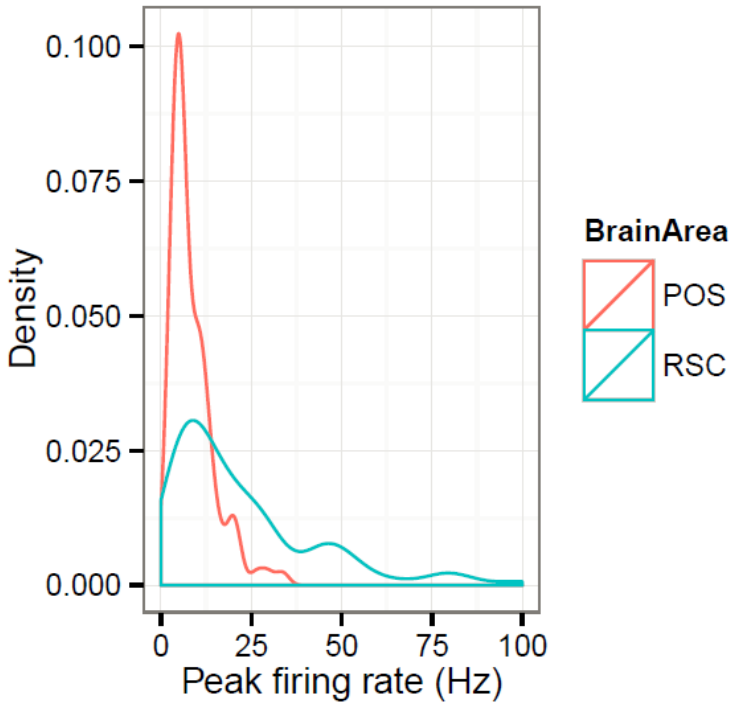

Figure 6.6 Distribution of the peak firing rate in HD cells recorded in the PoS and the RSC

In relation to the directional firing range, density estimates showed that PoS HD cells had a mean tuning width of 49.57 ± 1.42°, while RSC HD cells had a mean tuning width of 52.21 ± 1.47° (Figure 6.7). A permutation test for equality of densities showed that there was a significant difference in the tuning width of HD cells recorded in the PoS (*n* = 93 sessions), compared to those recorded in the RSC (*n* = 115 sessions), $p = 0.04$. To examine if the tuning width distribution for RSC HD cells is unimodal (Figure 6.7), Hartigan's Dip test for unimodality with simulated *p*-values (based on 5,000 replicates) was conducted. The results of

Hartigan's Dip test showed that the tuning widths of RSC HD cells correspond to a unimodal distribution, (D = 0.039, p = 0.24).

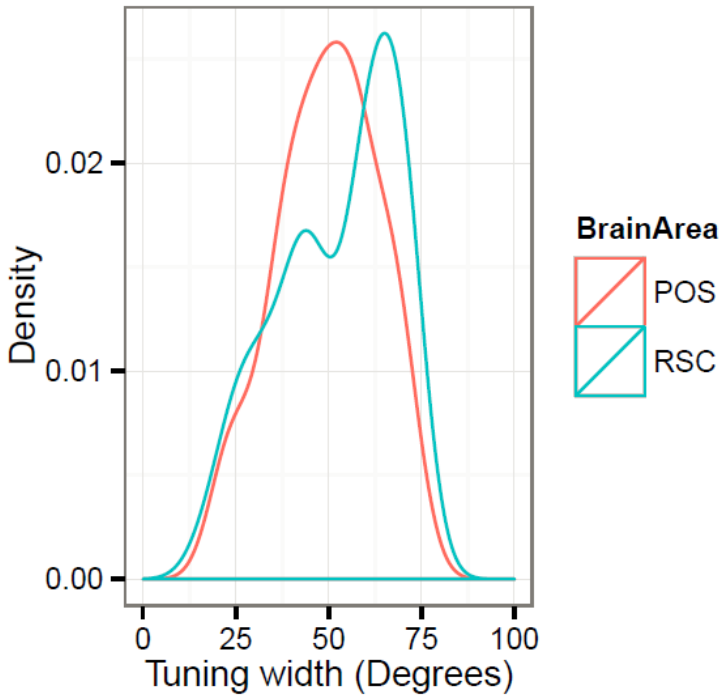

Figure 6.7 Distribution of the tuning width in HD cells recorded in the PoS (n = 94) and the RSC (n = 113).

6.5 Results of two cue card experiments

The following sections describe the results of the two cue card experiments presenting density estimates to visualise the distribution of the PFD deviations (Section 6.3.2), and summary statistics (Section 6.3.3) of these distributions that include: 1) the mean direction ($\bar{\theta}$), 2) mean vector length (R), and 3) circular variance (V). The results of the inferential circular statistics (Section 6.3.4) and Bayesian analysis (Section 6.3.5.1) are also described.

6.5.1 Subjects and cell numbers

A total of 127 HD cells were recorded in *n*=17 adult male Lister Hooded rats weighing between 317-437 g at the time of surgery. 63 HD cells were recorded in *n*=12 rats implanted in the RSC, (*n*=6 in the left hemisphere, *n*=6 in the right hemisphere), and 64 HD cells were recorded in *n*=5 rats implanted in the left hemisphere of the PoS (Table 6.1).

Brain area	Brain hemisphere	Rat number	Number of HD cells
RSC	Left	602	6
RSC	Left	599	8
RSC	Right	572	4
RSC	Left	567	2
RSC	Right	551	1
RSC	Right	537	6
RSC	Left	536	7
RSC	Right	525	10
RSC	Right	524	4
RSC	Right	519	2
RSC	Left	511	7
RSC	Left	502	6
PoS	Left	593	14
PoS	Left	592	36
PoS	Left	507	1
PoS	Left	645	5
PoS	Left	638	5

Table 6.1 Total number of HD cells recorded in each rat. The table shows the brain area and hemisphere where the drive was implanted, followed by the rat number and the total number of cells that passed the two part HD cell inclusion criteria.

The number of HD cells recorded in each rat was estimated using the assigned cell identification number which was derived based on a visual comparison of the

cluster space and the waveform peak to trough amplitude (Section 4.7.1). A record of the date when the tetrodes were lowered along with changes in the cluster space and waveform characteristics were used to track the same cells across days and assign the cell identification number. In instances when HD cells were recorded across days and the tetrodes were not lowered, the assigned cell identification number remained the same. In contrast, when a new cluster was found, a new cell identification number was assigned.

6.5.2 Are HD cells controlled by external room cues?

To examine whether RSC and PoS HD cells were stable during the baseline trials when rats were exposed to the different cue arrays and to evaluate whether they are influenced by uncontrolled external room cues during the rotation trials, independent *V*-tests were applied. The results showed that the distribution of PFD deviations were significantly clustered at a mean direction of 0° in the baseline trials, ($V_{(259)}$ = 0.63, $p < 0.0001$) and the rotation trials, ($V_{(697)}$ = 0.53, $p < 0.0001$) (Figure 6.8). These results reject the hypothesis of no landmark control and also reject the hypothesis of external room cue control, suggesting that the local cue cards had a strong influence on the PFD of RSC and PoS HD cells.

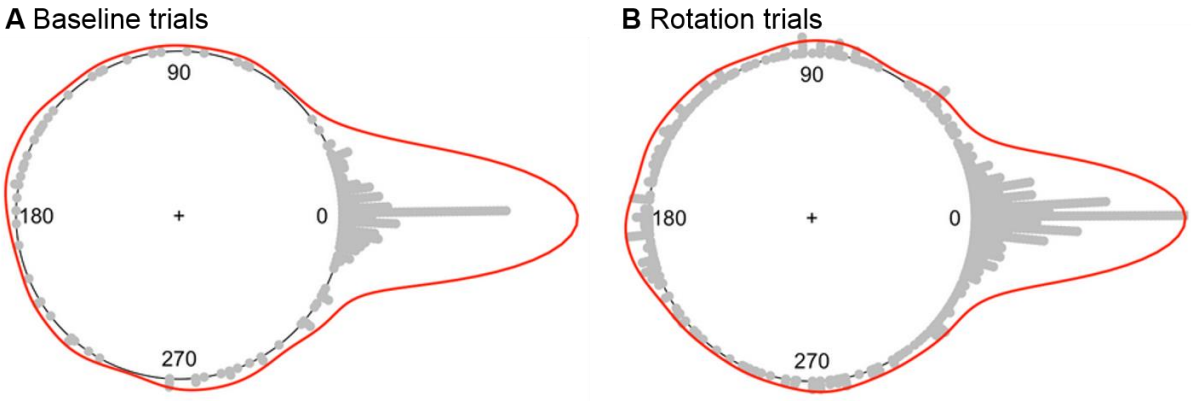

Figure 6.8 Kernel density estimates for the distribution of PFD deviations. **A.** Baseline trials, (*n*=260). **B.** Rotation trials, (*n*=698). Both KDE's had a bandwidth of 50.

To determine whether the distribution of PFD deviations from the baseline and the rotation trials could be combined, a randomised (1,000 times) Watson's two-sample U^2 test was applied. The results of this test showed that there are no significant differences between the distributions of PFD deviations of the baseline compared to the rotation trials, ($U^2_{(958)} = 0.13$, $p = 0.24$). Therefore, the baseline and the rotation trials were combined and treated as equal in the subsequent analysis. The summary statistics of the distribution of PFD deviations in the baseline trials were ($\bar{\theta} = -2.1$, $R = 0.63$, $V = 0.37$) and ($\bar{\theta} = 2.3$, $R = 0.53$, $V = 0.47$) for the rotation trials (Figure 6.8).

6.5.3 Does brain area and cue type affect landmark control?

To determine if there was an effect of brain area and cue type and decide if the distribution of PFD deviations from the RSC and the PoS could be combined, a Harrison-Kanji two-way ANOVA was conducted. The data from the control group (identical black cards) were not included in this analysis as HD cells for this condition were only recorded in the PoS since the control experiment was conducted with the rats reported in Chapter 7.

The results of the Harrison-Kanji two-way ANOVA showed that there was a significant main effect of cue type, ($F_{(4,508)} = 7.65$, $p < 0.0001$), while the main effect of brain area, ($F_{(1,508)} = 3.44$, $p = 0.064$) and the interaction between cue type and brain area was not statistically significant, ($F_{(4,508)} = 0.91$, $p = 0.087$). Based on this evidence, the data from the two brain areas was combined for each cue type.

The summary statistics for each cue type in both brain areas are displayed in Table 6.2. As can be observed from the summary statistics, the variance in the PFD deviations are similar between the RSC and the PoS within each cue card pair, suggesting that there were no major differences between brain area and cue type. Interestingly, the mean vector length R is progressively smaller in both the RSC and the PoS if one compares across the different cue types where B-W has the highest R value while T-B and R-L have the lowest value. This result suggests that the distribution of PFD deviations are strongly concentrated around the mean

direction in the B-W, V-H-p, and V-H while they are more spread out relative to the mean direction in the T-B and R-L cues.

Cue type	PoS	RSC
B-W	$\bar{\theta}$ = -2.0, R = 0.74, V = 0.26, n = 100	$\bar{\theta}$ = -6.7, R = 0.80, V = 0.20, n = 30
V-H	$\bar{\theta}$ = -2.3, R = 0.67, V = 0.33, n = 36	$\bar{\theta}$ = 2.4, R = 0.53, V = 0.47, n = 313
V-H-p	$\bar{\theta}$ = -3.6, R = 0.87, V = 0.13, n = 19	$\bar{\theta}$ = 0.1, R = 0.84, V = 0.16, n = 50
T-B	$\bar{\theta}$ = 1.6, R = 0.50, V = 0.50, n = 72	$\bar{\theta}$ = 5.5, R = 0.49, V = 0.51, n = 138
R-L	$\bar{\theta}$ = -0.9, R = 0.50, V = 0.50, n = 79	$\bar{\theta}$ = -2.9, R = 0.50, V = 0.50, n = 50
B-B	$\bar{\theta}$ = -100.3, R = 0.10, V = 0.90, n = 64	Not recorded

Table 6.2 Summary statistics for the distribution of PFD deviations in each cue card pair divided by brain area. Abbreviations denote mean direction ($\bar{\theta}$), mean vector length (R), circular variance (V) and sample size (n).

6.5.4 Does the magnitude of cue rotation affect landmark control?

To examine whether the cue rotation magnitudes (0°, 45°, 90°, 135° and 180°) had an influence on landmark control, the distributions of PFD deviations for the different cue rotations were compared with a Watson-Williams high concentration F-test conducted as a one-way ANOVA. The results showed that the distributions of PFD deviations across the different cue rotation magnitudes had a common mean direction ($F_{(4,883)}$ = 0.71, p = 0.61). These results show that cue rotation magnitude did not have a significant effect on landmark control. The summary statistics and the KDE's for the different cue rotations magnitudes are shown in Table 6.3 and Figure 6.9. As can be observed from the summary statistics and the KDE's, although the variance across the different cue rotation magnitudes differed, the distributions were primarily unimodal and concentrated at a mean direction of 0º, showing that there is strong landmark control across both the non-rotation and the different cue rotation magnitudes.

Magnitude of rotation	Summary statistics
0º	$\bar{\theta}$ = 6.8, *R* = 0.44, *V* = 0.56, *n* = 108
45º	$\bar{\theta}$ = 3.8, *R* = 0.55, *V* = 0.45, *n* = 200
90º	$\bar{\theta}$ = 1.3, *R* = 0.64, *V* = 0.36, *n* = 236
135º	$\bar{\theta}$ = -7.5, *R* = 0.54, *V* = 0.56, *n* = 224
180º	$\bar{\theta}$ = -2.6, *R* = 0.72, *V* = 0.28, *n* = 119

Table 6.3 Summary statistics for the distribution of PFD deviations for all recorded HD cells separated by the magnitude of cue rotation. Abbreviations denote mean direction ($\bar{\theta}$), mean vector length (*R*), circular variance (*V*) and sample size (*n*).

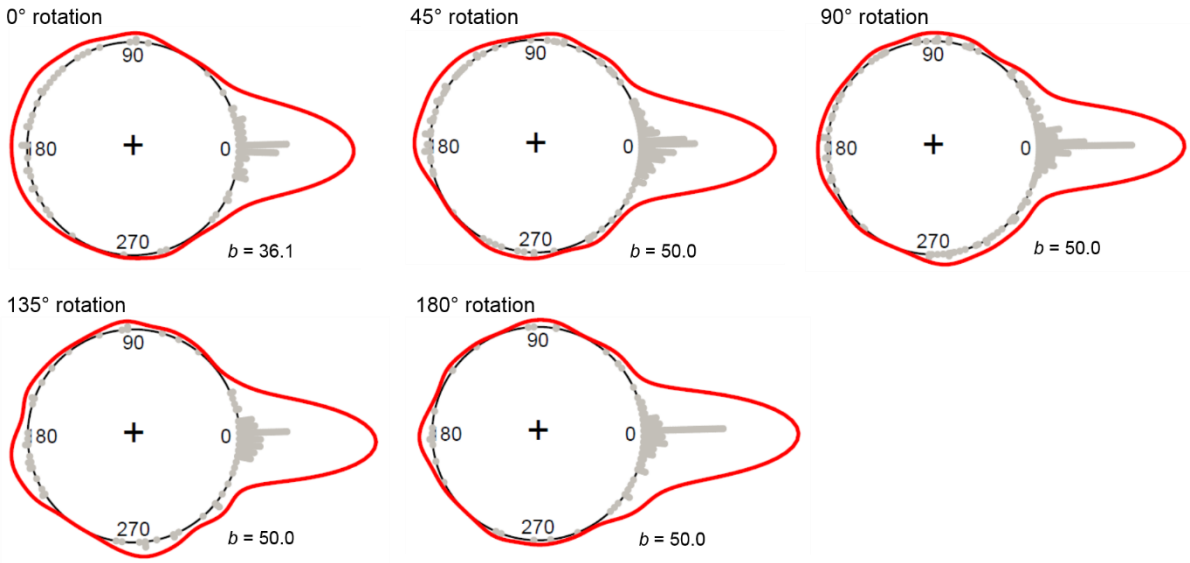

Figure 6.9 Kernel density estimates of the distribution of PFD deviations for each cue rotation magnitude. The abbreviation *b* denotes the bandwidth of each KDE.

6.5.5 Is there landmark control and discrimination for each cue type?

Since there were no differences between the baseline and the rotation trials and no main effect of brain area, the data from the PoS and the RSC were combined with the baseline and the rotations trials. Summary statistics and KDE's for the distribution of the PFD deviations in the combined data are displayed for each cue type in Table 6.4 and Figure 6.10.

Cue type	Summary statistics
B-W	$\bar{\theta}$ = -3.1, *R* = 0.76, *V* = 0.24, *n* = 130
V-H	$\bar{\theta}$ = 1.8, *R* = 0.54, *V* = 0.46, *n* = 349
V-H-p	$\bar{\theta}$ = -1.0, *R* = 0.85, *V* = 0.15, *n* = 69
T-B	$\bar{\theta}$ = 4.1, *R* = 0.49, *V* = 0.51, *n* = 210
R-L	$\bar{\theta}$ = -1.7, *R* = 0.50, *V* = 0.50, *n* = 129
B-B	$\bar{\theta}$ = -100.3, *R* = 0.10, *V* = 0.90, *n* = 64

Table 6.4 Summary statistics for the distribution of PFD deviations in each cue type. Abbreviations denote mean direction ($\bar{\theta}$), mean vector length (*R*), circular variance (*V*) and sample size (*n*).

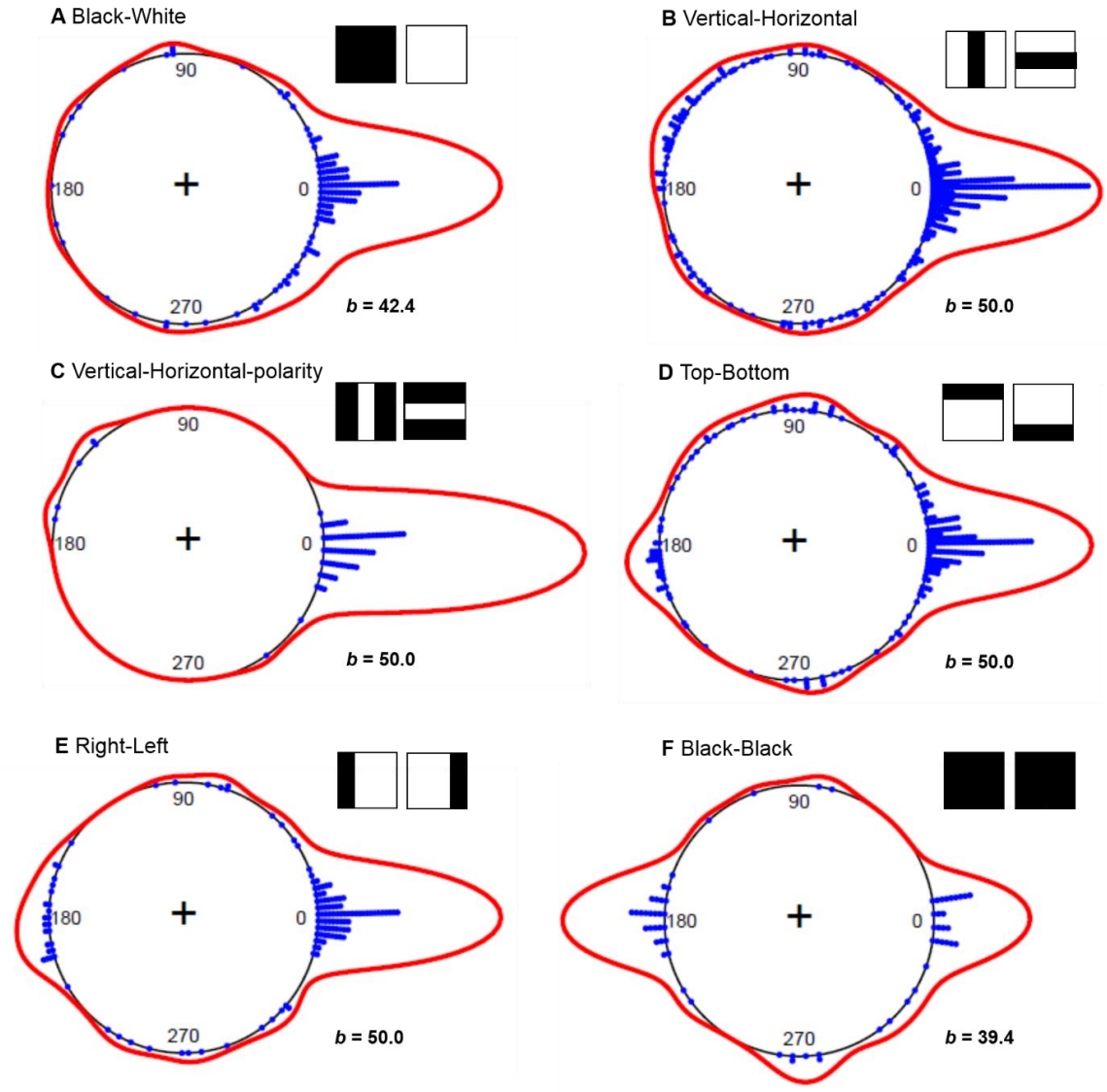

Figure 6.10 Kernel density estimates combining the distribution of PFD deviations in both brain areas for each cue type. The abbreviation *b* denotes the bandwidth of each KDE.

To examine landmark control for each cue type, a *V*-test was applied to determine if the PFD deviations were non-uniformly distributed and were instead concentrated at a mean direction of 0° as predicted if HD cells could discriminate and use the visual features of the cue cards as landmarks. Independent *V*-tests showed that the distribution of PFD deviations were significantly clustered around 0º in the B-W, ($V_{(129)}$ = 0.75, p < 0.0001), V-H, ($V_{(348)}$ = 0.54, p < 0.0001), V-H-p ($V_{(68)}$ = 0.85, p < 0.0001), T-B, ($V_{(209)}$ = 0.49, p < 0.0001), and R-L, ($V_{(128)}$ = 0.50, p < 0.0001) cue cards. These results show that PoS and RSC HD cells discriminate and use as landmarks the different visual features of the cue cards. For the control data (B-B), the distribution of PFD deviations showed a multimodal departure from uniformity as determined by a Watson's one-sample U^2 test, ($U^2_{(63)}$ = 0.58, p < 0.01). This result is consistent with HD cells not being able to discriminate the two identical cues, using either cue to reset their PFD.

Since one of the rats (r592) contributed approximately half of the HD cells recorded in the PoS, (36/64 PoS HD cells) and 28% of the total number of HD cells recorded in both the PoS and the RSC, the analysis was down-sampled, excluding all the HD cells recorded in r592 in order to determine if landmark control to the different cue types was similar. Due to the considerable reduction in the number of HD cells recorded in the V-H-p cues, the data was combined with the V-H cues. Summary statistics of the distribution of PFD deviations and KDE's per cue type are shown in Table 6.5 and Figure 6.11.

Cue type	**Summary statistics**
B-W	$\bar{\theta}$ = 5.6, R = 0.75, V = 0.25, n = 67
V-H	$\bar{\theta}$ = -1.1, R = 0.58, V = 0.42, n = 374
T-B	$\bar{\theta}$ = -4.9, R = 0.53, V = 0.47, n = 162
R-L	$\bar{\theta}$ = 3.5, R = 0.51, V = 0.49, n = 88
B-B	$\bar{\theta}$ = -100.3, R = 0.10, V = 0.90, n = 64

Table 6.5 Summary statistics for the distribution of all the PFD deviations in each cue type. Abbreviations denote mean direction ($\bar{\theta}$), mean vector length (R), circular variance (V) and sample size (n).

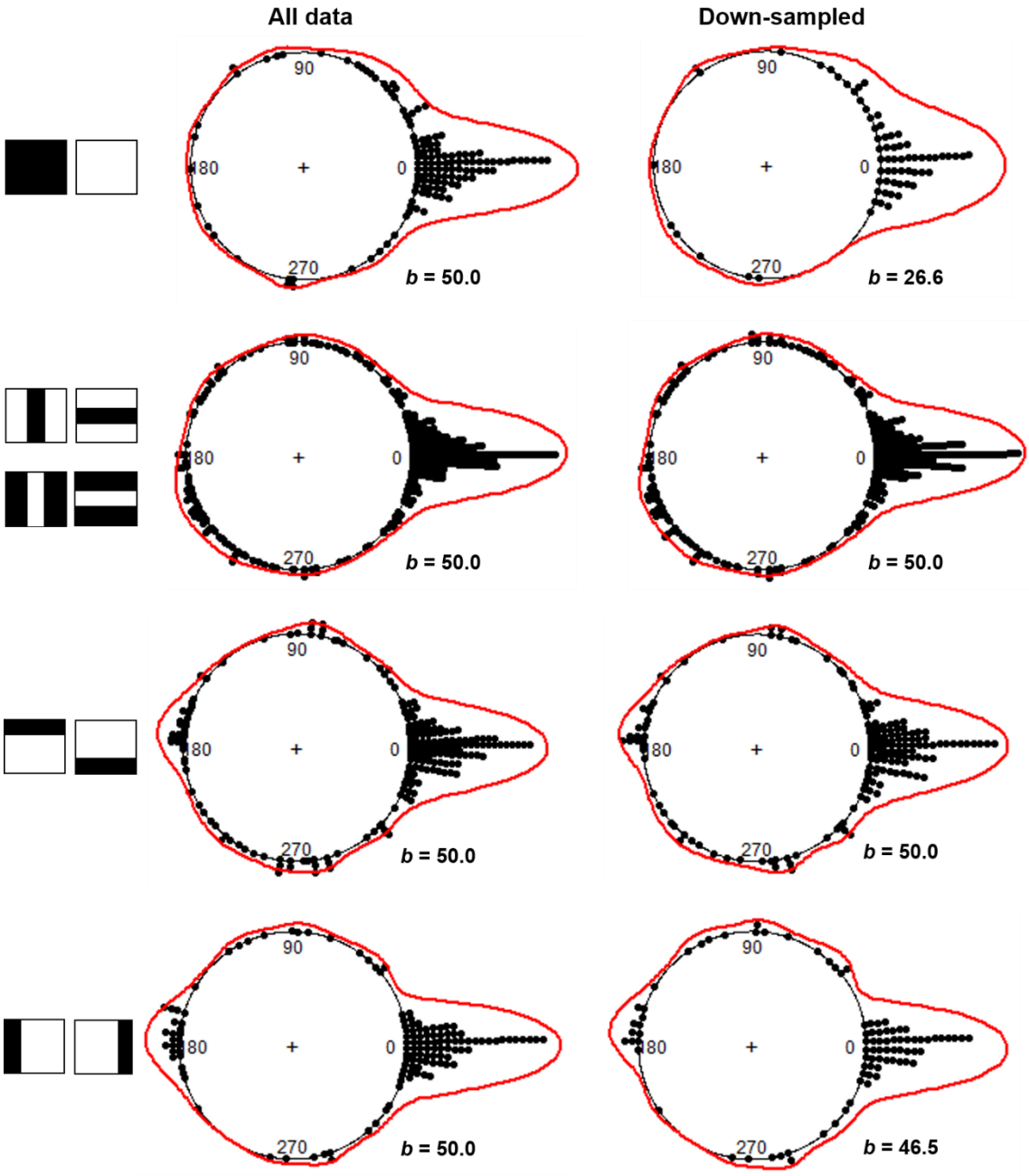

Figure 6.11 Kernel density estimates combining the distribution of PFD deviations in both brain areas for each cue type after down-sampling the data from one rat that contributed 28% of the total number of HD cells. The abbreviation *b* denotes the bandwidth of each KDE.

Independent *V*-tests showed that the down-sampled distribution of PFD deviations were significantly clustered around 0º in the B-W, ($V_{(66)}$ = 0.75, p < 0.0001),

combined V-H and V-H-p, ($V_{(373)}$ = 0.58, p < 0.0001), T-B, ($V_{(161)}$ = 0.52, p < 0.0001), and R-L, ($V_{(87)}$ = 0.50, p < 0.0001) cue cards. These results confirm that orientation, contrast and position of a bar exert landmark control in PoS and RSC HD cells after down-sampling the data from one rat that contributed a large proportion of PoS HD cells.

6.5.5.1 Bayesian estimates for cell response categories

After showing that there is landmark control in each of the cue card arrays, it is important to determine the probability that a PFD deviation will fall in a given category and evaluate which outcome is more likely. The categories separate the distribution of PFD deviations into three intervals corresponding to: Category 1, landmark control and discrimination; Category 2, landmark control and no discrimination; Category 3, no landmark control and no discrimination. To calculate the probability of obtaining a PFD deviation that would fall in one of the categories for each cue type, a Bayesian analysis is reported in the following sub-sections, while a summary of the relative frequency of the PFD deviations that fell within each category are shown Table 6.6 and Figure 6.12.

Cue type	**Category 1**	**Category 2**	**Category 3**
Black-Black (B-B)	0.39, *n* = 25	0.44, *n* = 28	0.17, *n* = 11
Black-White (B-W)	0.81, *n* = 105	0.05, *n* = 6	0.14, *n* = 19
Vertical-Horizontal (V-H & V-H-p)	0.73, *n* = 305	0.12, *n* = 51	0.15, *n* = 62
Top-Bottom (T-B)	0.66, *n* = 139	0.16, *n* = 34	0.18, *n* = 37
Right-Left (R-L)	0.68, *n* = 88	0.19, *n* = 24	0.13, *n* = 17

Table 6.6 Summary of the relative frequency and total number of observations in each category per cue type. The categories correspond to: 1. Landmark control and discrimination. 2. Landmark control and no discrimination. 3. No landmark control and no discrimination.

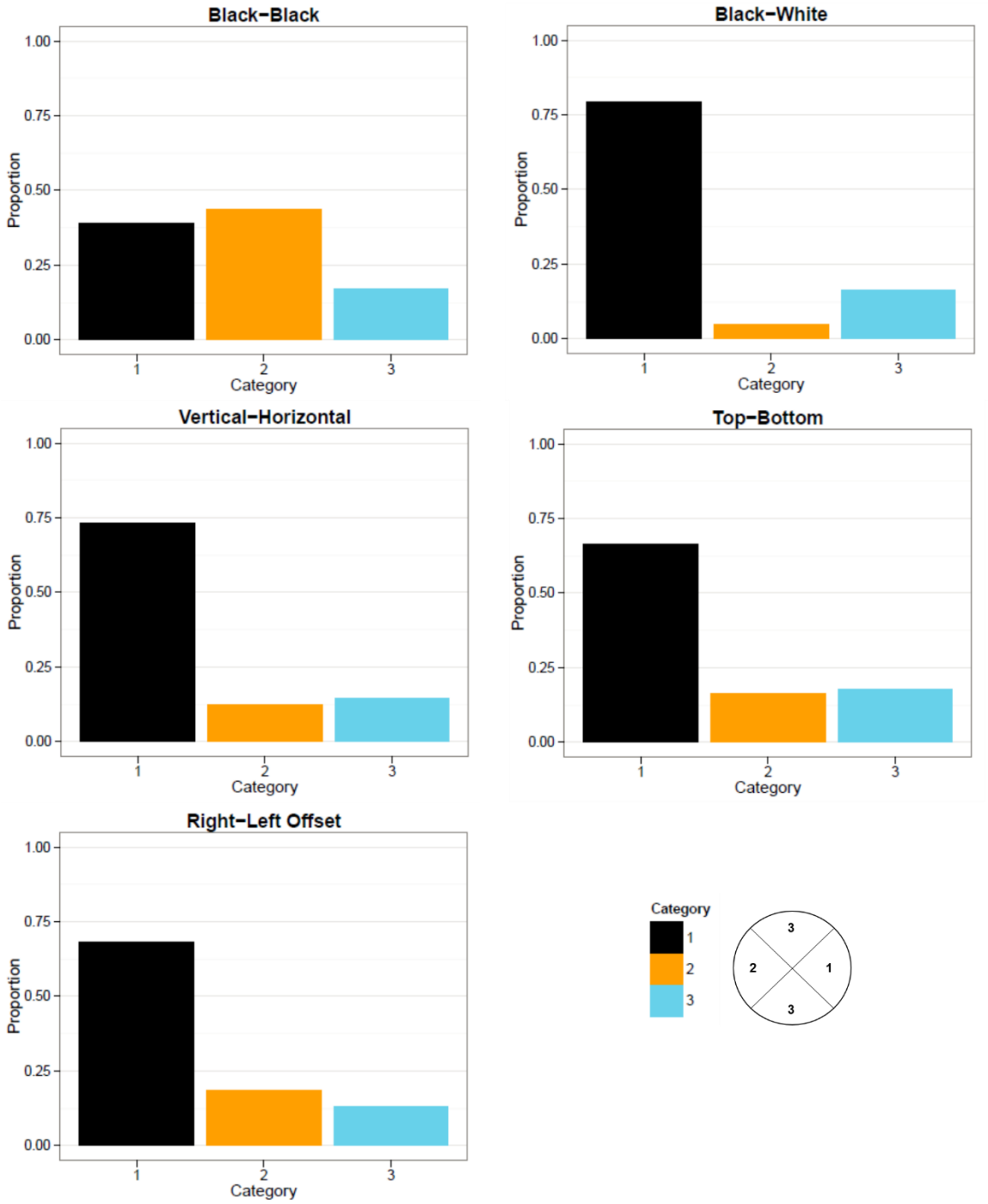

Figure 6.12 Relative frequency distribution of the PFD deviations in each category for every cue type. The categories correspond to: Category 1 Landmark control and discrimination. 2. Landmark control and no discrimination. 3. No landmark control and no discrimination.

To evaluate the evidence for the competing hypotheses given the obtained data, the median and the 95% credible interval were calculated from the posterior distribution, *p*, obtaining a parameter μ which provides an estimate of the probability that a PFD deviation would fall within a given category. If $\Delta\mu > 0$, the majority of the PFD deviations are located in category 1, indicating that HD cells showed landmark control and discrimination of a given cue card feature. In contrast, if $\Delta\mu < 0$, the majority of the PFD deviations are located in category 2, indicating that HD cells showed landmark control and no discrimination. Alternatively, if $\Delta\mu = 0$, the PFD deviations are evenly distributed between category 1 and category 2, indicating that the two cue cards exerted the same degree of landmark control, a situation that is predicted to occur if rats do not discriminate amongst the two cues, resetting their PFD relative to any of the two cue cards.

The relative frequency distribution of the PFD deviations in the different outcome categories showed that a larger proportion (above 0.5) of the observations fell in category 1 compared to category 2 or category 3 in all the cue types except for the identical cues (B-B) where the proportion of observations that fell in category 1 was similar to that of category 2 indicating that there was no discrimination of the cue cards. These results suggest that HD cells discriminate and use the different visual features that were presented as landmarks for spatial orientation. However, to provide an estimate of the probability that this would occur, Bayesian estimates were calculated and compared between category 1 and category 2.

The results of the Bayesian analysis for the B-W cues showed that the median and the 95% credible interval for each category were 0.80, [0.73, 0.86] for category 1, 0.05, [0.02, 0.09] for category 2, and 0.15, [0.09, 0.21] for category 3 (Figure 6.13). The difference between the upper and the lower 95% credible interval, [0.65, 0.83] was $\Delta\mu > 0$, providing strong evidence of landmark control and discrimination of contrast.

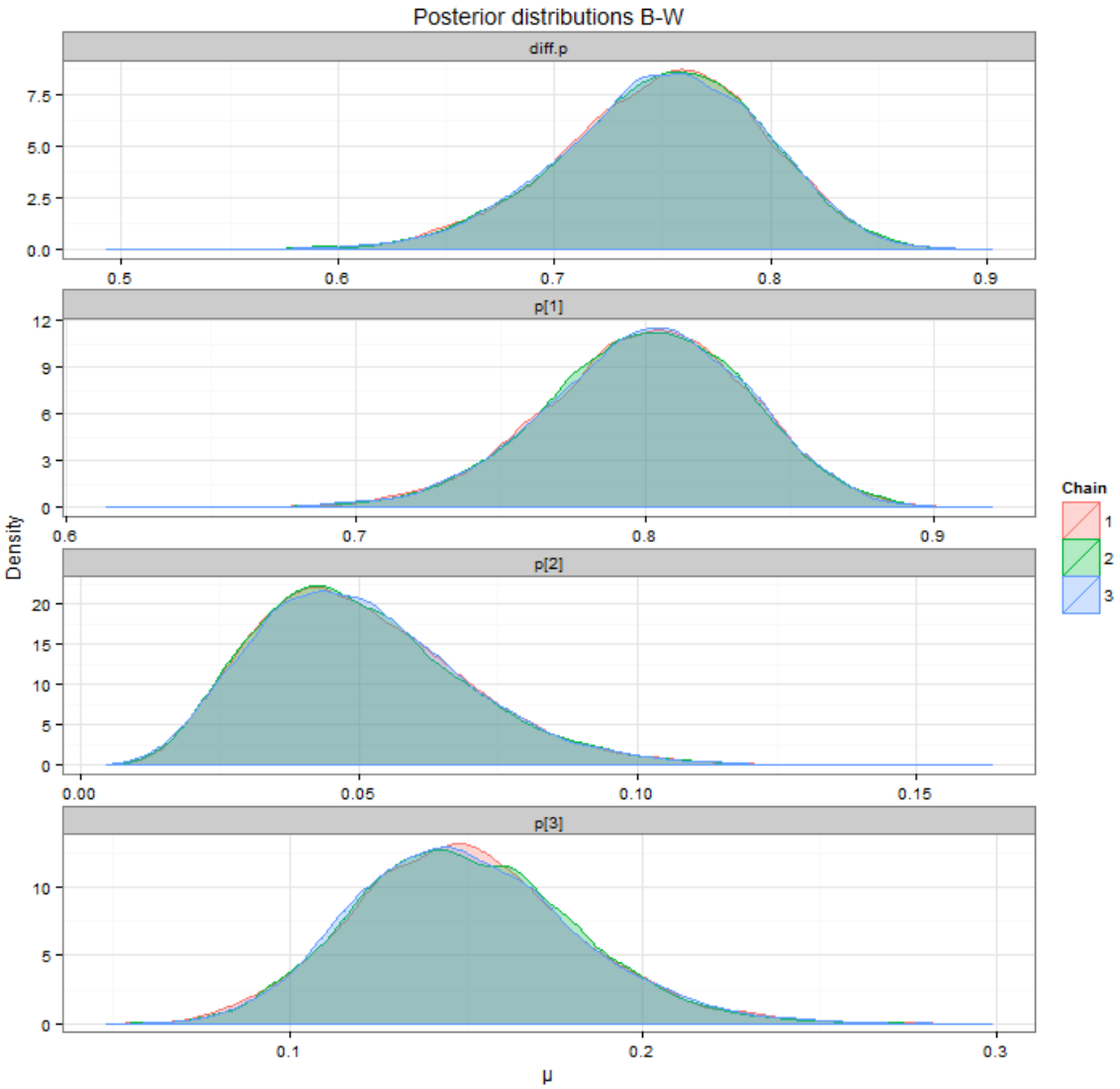

Figure 6.13 Density plots of the posterior distributions for the black-white cue cards. The letter *p* refers to the posterior distribution for each category where p[1] is category 1, p[2] is category 2 and p[3] is category 3. The difference in the posterior distributions between categories 1 and 2 is denoted as diff.p. Chain refers to parallel Markov Chain Monte Carlo simulations that were generated by randomly sampling 10,000 times the parameter values μ from the posterior distribution in each outcome category to ensure that the 95% credible interval provided an accurate estimate of the multinomial distribution given the Bayes model used.

6.5.5.2 Vertical-horizontal

For the black vertical-horizontal bars on a white cue card, the median and the 95% credible interval that the PFD deviation would fall in each category were 0.69, [0.64, 0.74] for category 1, 0.14, [0.10, 0.18] for category 2, and 0.17, [0.13, 0.21] for category 3 (Figure 6.14). The difference between the upper and the lower 95% credible interval, [0.47, 0.63] was $\Delta\mu > 0$, providing strong evidence of landmark control and discrimination of orientation of vertical and horizontal stripes.

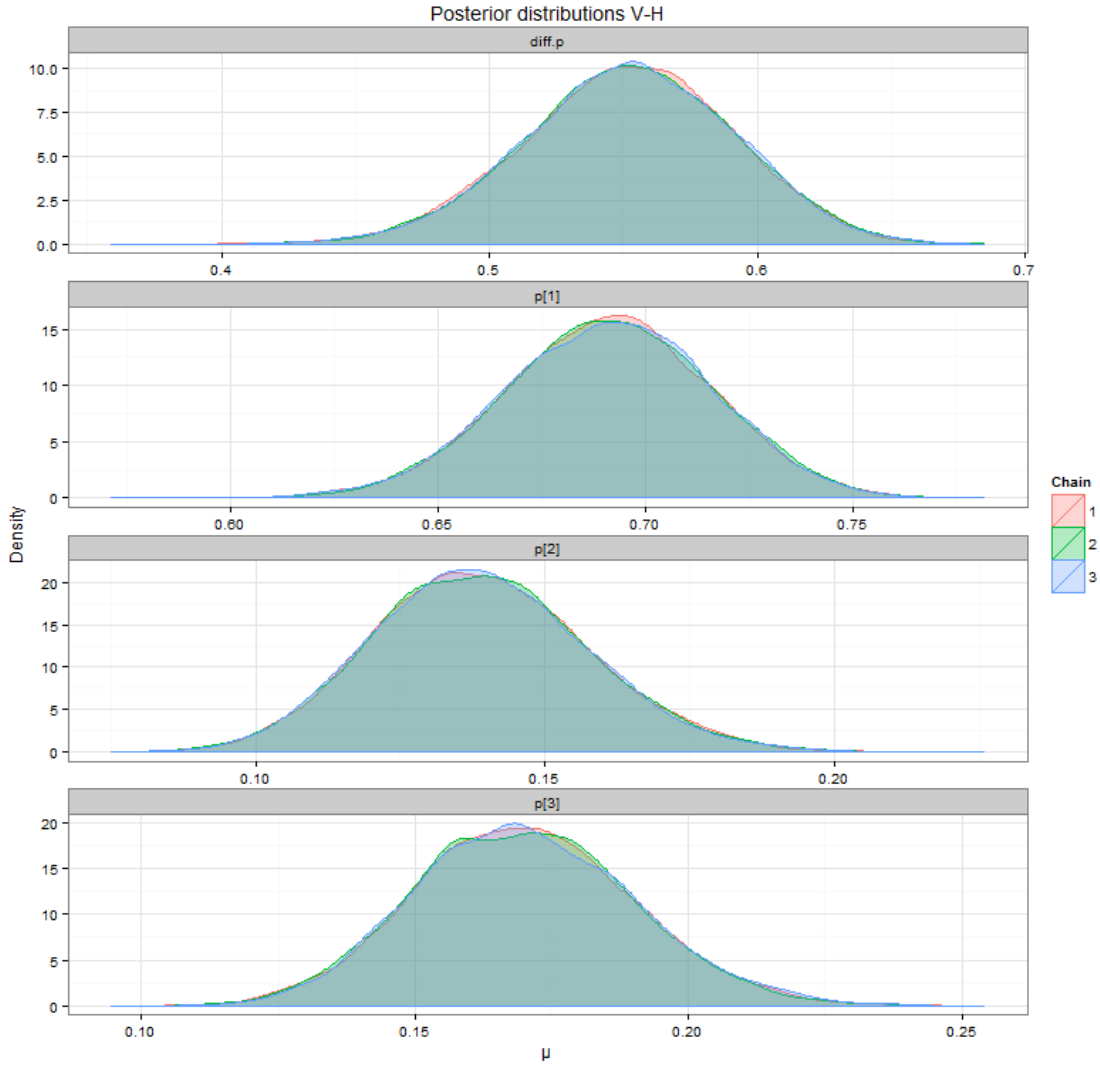

Figure 6.14 Density plots of the posterior distributions for the vertical-horizontal cue cards. The letter *p* refers to the posterior distribution for each category where p[1] is category 1, p[2] is category 2 and p[3] is category 3. The difference in the posterior distributions between categories 1 and 2 is denoted as diff.p.

6.5.5.3 Vertical-horizontal-polarity

For the white vertical-horizontal bars on a black card, the median and the 95% credible interval into which the PFD deviation would fall in each category were 0.90, [0.82, 0.96] for category 1, 0.05, [0.01, 0.11] for category 2, and 0.05, [0.01, 0.11] for category 3 (Figure 6.15). The difference between the upper and the lower 95% credible interval, [0.72, 0.94] was $\Delta\mu > 0$, providing strong evidence of landmark control and discrimination of vertical and horizontal stripes.

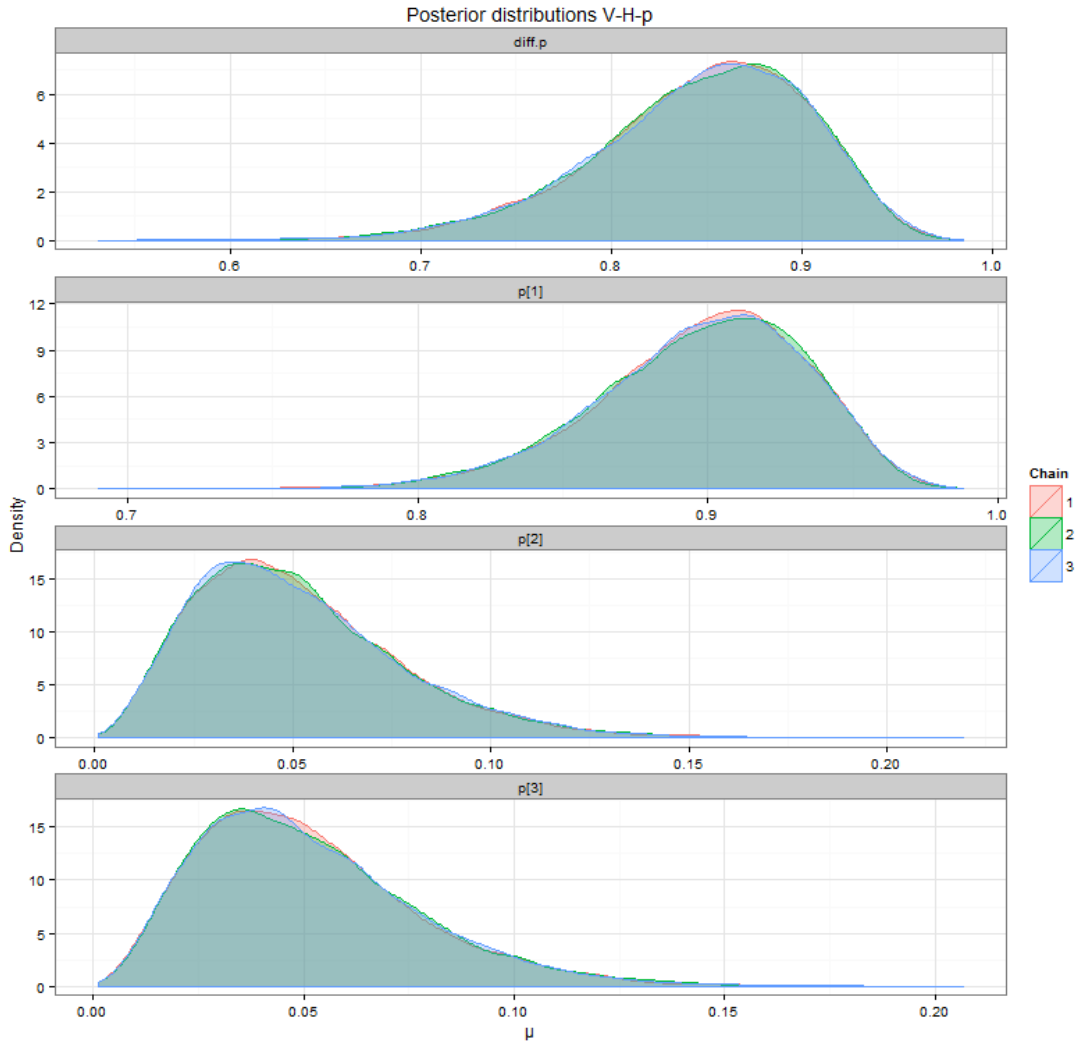

Figure 6.15 Density plots of the posterior distributions for the vertical-horizontal-polarity cue cards. The letter *p* refers to the posterior distribution for each category where p[1] is category 1, p[2] is category 2 and p[3] is category 3. The letter *p* refers to the posterior distribution for each category. The difference in the posterior distributions between categories 1 and 2 is denoted as diff.p.

6.5.5.4 Top-bottom

For the top-bottom cue cards, the median and the 95% credible interval that the PFD deviation would fall in each category were 0.66, [0.60, 0.72] for category 1, 0.16, [0.12, 0.22] for category 2, and 0.18, [0.13, 0.23] for category 3 (Figure 6.16). The difference between the upper and the lower 95% credible interval, [0.39, 0.59] was $\Delta\mu > 0$, providing strong evidence of landmark control and discrimination of the vertical position of a horizontal bar.

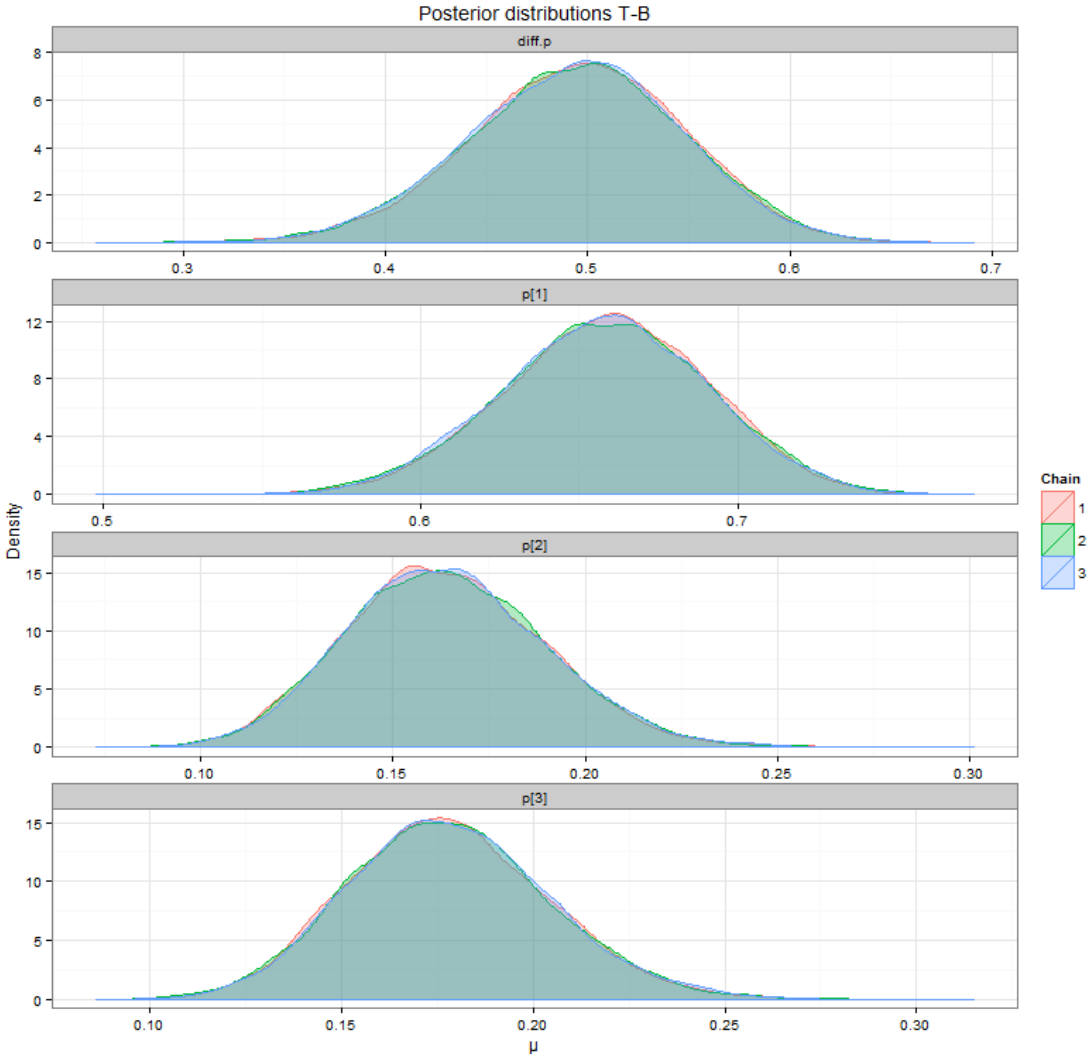

Figure 6.16 Density plots of the posterior distributions for the top-bottom cue cards. The letter *p* refers to the posterior distribution for each category where p[1] is category 1, p[2] is category 2 and p[3] is category 3. The difference in the posterior distributions between categories 1 and 2 is denoted as diff.p.

6.5.5.5 Right-left

For the right-left cue cards, the median and the 95% credible interval that the PFD deviation would fall in each category were 0.68, [0.59, 0.75] for category 1, 0.19, [0.13, 0.26] for category 2, and 0.13, [0.08, 0.20] for category 3 (Figure 6.17). The difference between the upper and the lower 95% credible interval, [0.35, 0.62] was $\Delta\mu > 0$, providing strong evidence of landmark control and discrimination of the location of a black vertical bar.

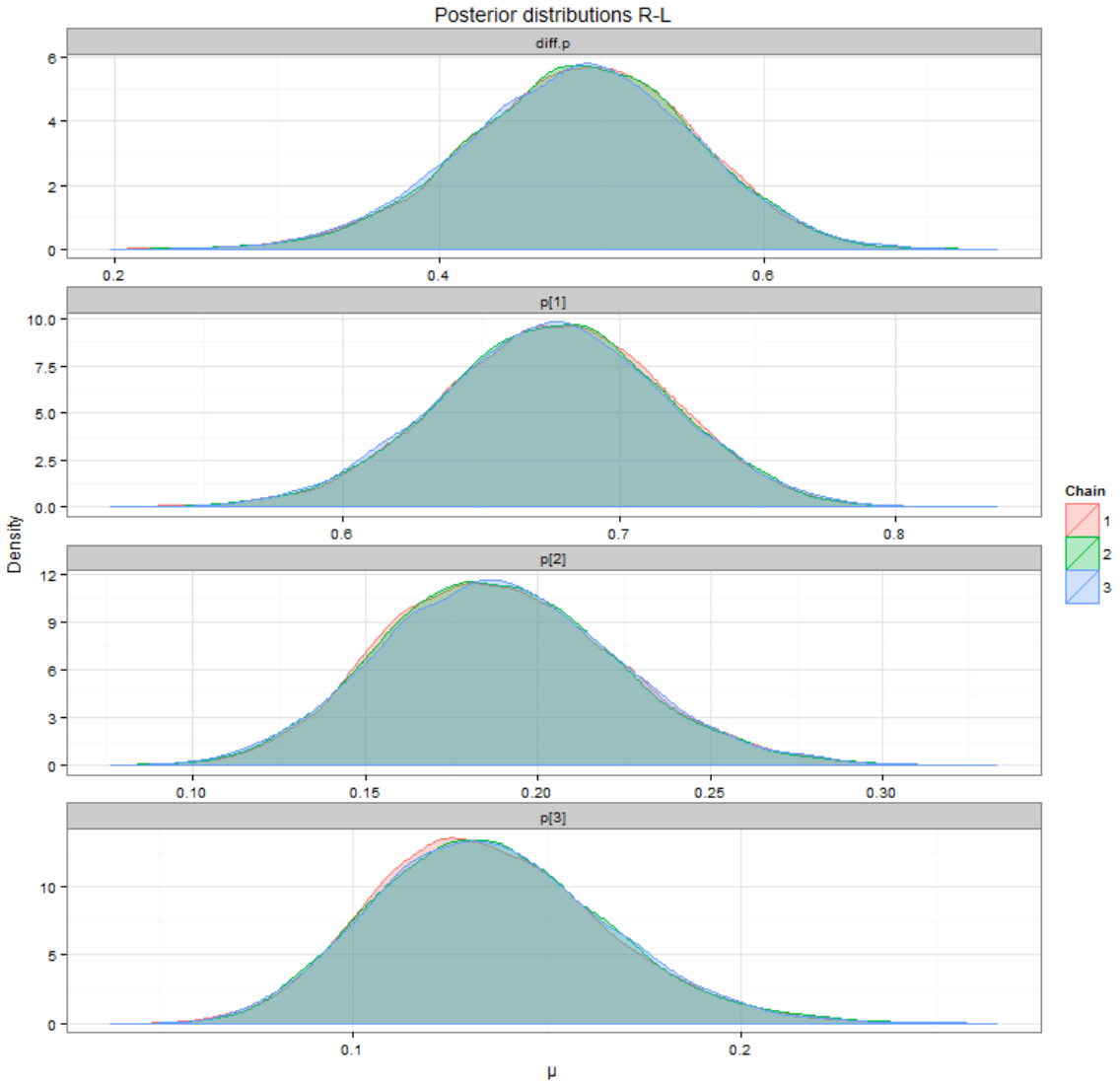

Figure 6.17 Density plots of the posterior distributions for the right-left cue cards. The letter *p* refers to the posterior distribution for each category where p[1] is category 1, p[2] is category 2 and p[3] is category 3. The difference in the posterior distributions between categories 1 and 2 is denoted as diff.p.

6.5.5.6 Black-black

For the identical black cue cards, the median and the 95% credible interval that the PFD deviation would fall in each category were 0.39, [0.28, 0.51] for category 1, 0.43, [0.32, 0.56] for category 2, and 0.17, [0.10, 0.28] for category 3 (Figure 6.18). The difference between the upper and the lower 95% credible interval between the posterior distribution of category 1 and 2 was [-0.26, 0.17], including $\Delta\mu = 0$, providing strong evidence that the two cues cannot be distinguished, indicating that the two cue cards exert a similar degree of landmark control.

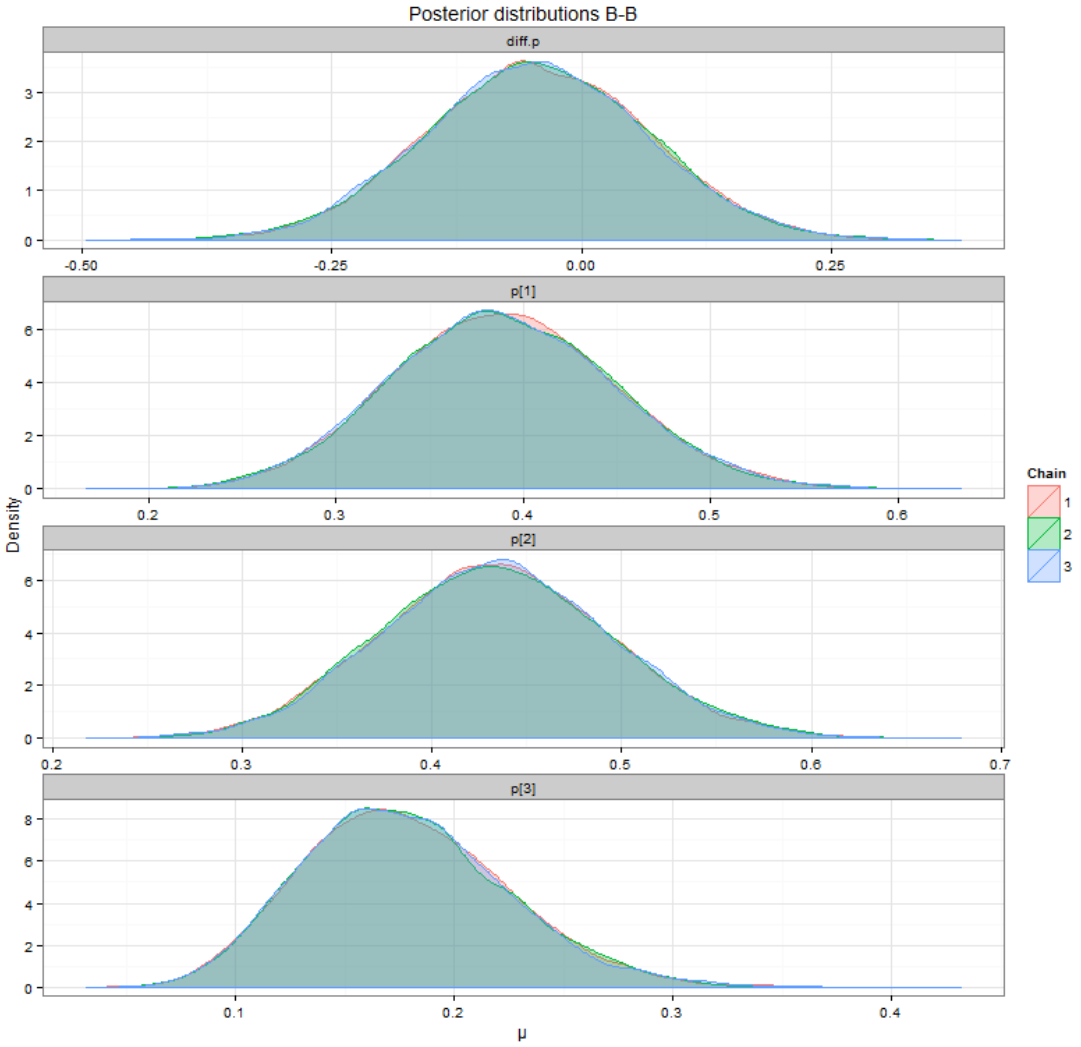

Figure 6.18 Density plots of the posterior distributions for the identical black cue cards. The letter *p* refers to the posterior distribution for each category where p[1] is category 1, p[2] is category 2 and p[3] is category 3. The difference in the posterior distributions between categories 1 and 2 is denoted as diff.p

6.5.5.7 Comparisons between cue types

While the relative frequency for each category depended on the ratio between the actual number of PFD deviations and the total number of PFD deviations recorded for a cue type, the credible interval obtained from the posterior distribution provides an estimate with a 95% likelihood that the true relative frequency for a category lies within a particular interval. As such, the credible interval can be used to make comparisons within categories in a cue type as previously described and between categories for the different cue types.

Based on the posterior distributions, comparisons between categories 1 and 2 showed that $p_1 - p_2 > 0$ for all the cue types with the exception of the control stimuli (B-B), providing support for the hypothesis that HD cells in the PoS and the RSC discriminate the visual features of the cue cards (Table 6.7). However, the range of the 95% credible interval was different amongst the cue cards, suggesting that the strength of landmark control and discrimination varied depending on the respective visual features of the cue cards (Table 6.7 and Figure 6.19). Specifically, contrast and orientation exerted strong landmark control and high discrimination, while height (top-bottom) and lateral position of a bar (right-left), exerted a somewhat weaker, albeit significant effect. Interestingly, the 95% credible interval of $p_1 - p_2$ was higher in the vertical-horizontal bars that had a negative polar display (white bars on a black foreground card) compared to the vertical-horizontal bars that had a positive polar display (black bars on white foreground card).

Cue type	Category 1	Category 2	Category 3	Category 1 – Category 2
B-W	0.73, 0.86	0.02, 0.09	0.09, 0.21	0.65, 0.83
V-H	0.64, 0.74	0.10, 0.18	0.13, 0.21	0.47, 0.63
V-H-p	0.82, 0.96	0.01, 0.11	0.01, 0.11	0.72, 0.94
T-B	0.60, 0.72	0.12, 0.22	0.13, 0.23	0.39, 0.59
R-L	0.59, 0.75	0.13, 0.26	0.08, 0.20	0.35, 0.62
B-B	0.28, 0.51	0.32, 0.56	0.10, 0.28	-0.26, 0.17

Table 6.7 Summary of the 95% credible of the parameter μ in each cell response category. The relative likelihood for each category is denoted as p_1, p_2, and p_3 while the difference between categories 1 and 2 is denoted as $p_1 - p_2$.

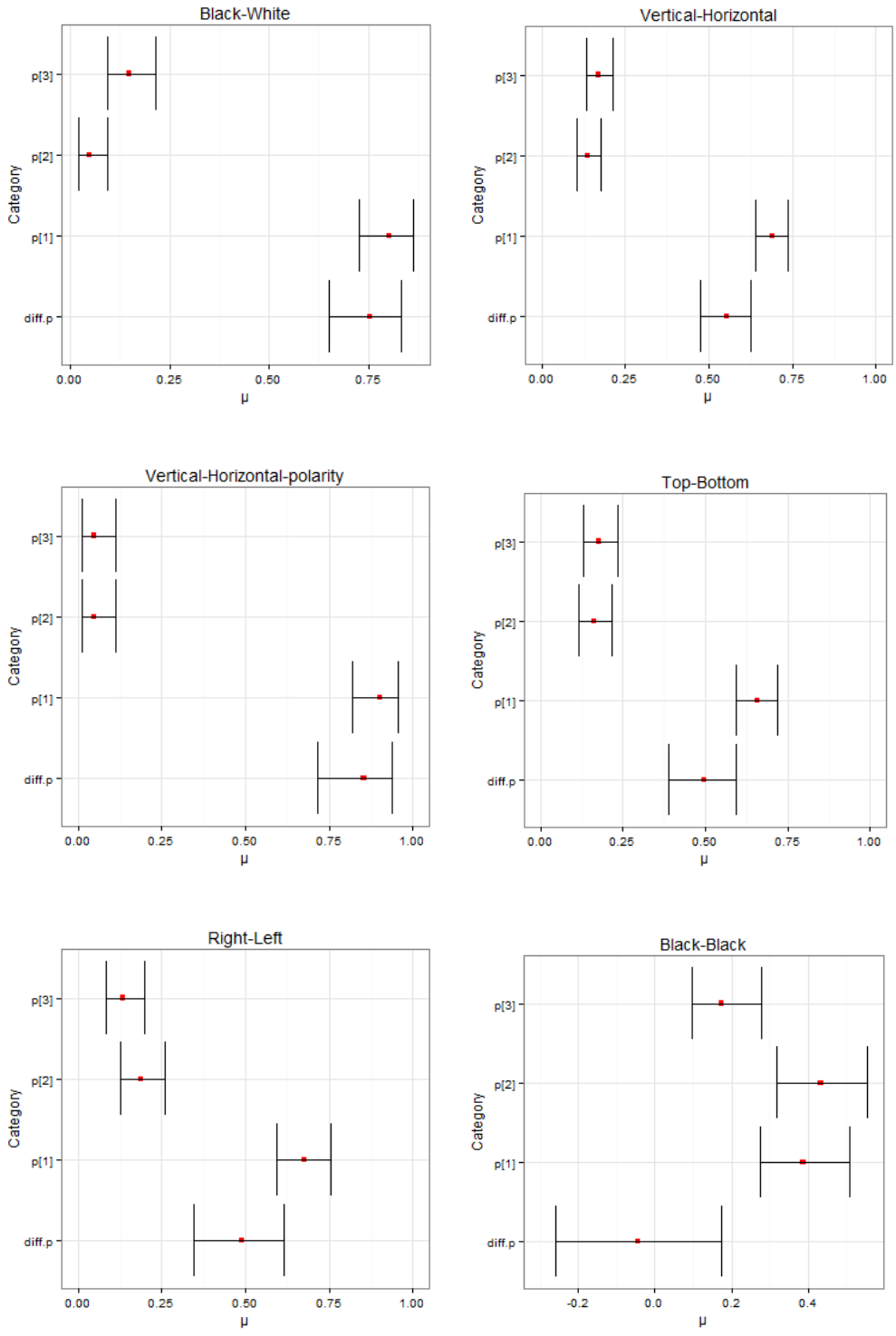

Figure 6.19 Boxplot of the median (red dot) and 95% credible interval of the posterior distribution in each outcome category for every cue type. As can be observed, with the exception of the control stimuli (B-B), all the other cue types had a difference in the 95% credible interval between category 1 and category 2 (diff.p) that included $\Delta\mu = 0$, indicating that there was landmark discrimination of the different cue card stimuli.

In addition to determining the likelihood of data falling in a given category, the credible interval can be used to predict the probability of obtaining a particular outcome based on the three categories if an HD cell is recorded in a specific cue card pair. For instance, if a cue control experiment were to be conducted using the black-white cue card pair, the likelihood of a PFD deviation falling in each category would be: 75-86% for category 1, 2-9% for category 2 and 9-21% for category 3 (Table 6.7). Therefore, if cue control experiments are conducted using the black-white cue cards it is highly likely that HD cells would discriminate and reliably use as landmarks the visual features of these cues, in this case a difference in contrast.

To examine if the strength of cue control differed between the cue types, Pearson's chi-squared test was conducted, comparing the frequencies between the three outcome categories across all the cue types (Table 6.8 and Figure 6.12). The results of the chi-squared test showed a significant difference in the likelihood of a PFD deviation falling in the three outcome categories between the cue types ($\chi^2_{(10)} = 198.62$, $p < 0.0001$). This result suggests that the strength of cue control was not the same between the cues, however, the chi-square test does not address which of the cue types differed from each other. To examine if there were differences in landmark control between the cue types, pairwise proportion tests were conducted using the frequencies of the three outcome categories. The results of the proportion tests are shown in Table 6.8.

From the *p*-values it can be observed that the strength of landmark control was different between the control stimuli (identical black cues) and the cues whose visual features correspond to contrast (B-W), orientation (V-H), vertical position (T-B) and lateral position (R-L), consistent with the observed distribution of PFD deviations (Figure 6.10 and Figure 6.11) and the results of the 95% credible obtained in category 1 (Table 6.8). This result shows that discrimination and landmark control is stronger for the distinct cue types compared to the identical control stimuli. The strength of cue control was also different between the B-W cues compared to the V-H, T-B and R-L cues, although the effect was smaller between the B-W cues and the V-H cues compared to B-W and both T-B and R-L. This result suggests that contrast exerts stronger landmark control than

orientation, vertical and lateral position. Furthermore, V-H was different from T-B and marginally different from R-L which suggest that orientation exerts stronger landmark control compared to vertical and lateral position. Finally, T-B did not differ from R-L which suggests that vertical and lateral position exert the same strength of landmark control over RSC and PoS HD cells.

	B-B	**B-W**	**V-H**	**T-B**	**R-L**
B-B	------	$p < 0.0001$	$p < 0.0001$	$p < 0.0001$	$p < 0.0001$
B-W	------	------	$p < 0.01$	$p < 0.0001$	$p < 0.0001$
V-H	------	------	------	$p < 0.01$	$p < 0.05$
T-B	------	------	------	------	$p > 0.05$
R-L	------	------	------	------	------

Table 6.8 Results of the pairwise proportion tests between the cue types. V-H and V-H-p were combined into one category.

6.6 Co-rotation activity in HD cell ensembles

To examine whether the rotation of the cue cards elicits a coherent shift in the ensemble activity of HD cells recorded in the PoS and the RSC, KDE's of the distribution of PFD angular offset shifts between pairs of simultaneously recorded HD cells were compared (Figure 6.20). The angular offset corresponds to the distance between the PFD of HD cells recorded in the same session which is compared across trials within a session and is expected to maintain a low deviation and be significantly clustered at 0° if the ensemble maintains coherency (Section 6.3.6).

In order to determine whether the activity of HD cell ensembles had a strong coupling at the population level, a *V*-test with an expected mean direction of 0° was conducted for each brain area. The *V*-test showed that the distribution of the PFD angular offset shifts was significantly clustered around 0º for both the PoS ($V_{(548)} = 0.93$, $p < 0.0001$) and the RSC, ($V_{(970)} = 0.92$, $p < 0.0001$). The summary statistics of the distribution of PFD offset shifts recorded in the RSC ($n = 971$) was ($\bar{\theta} = -0.25$, $R = 0.92$, $V = 0.08$) and ($\bar{\theta} = -0.37$, $R = 0.93$, $V = 0.07$) for HD cells

recorded in the PoS (n = 549). This result suggests that there is strong similarity in the activity of HD cells in the PoS and the RSC.

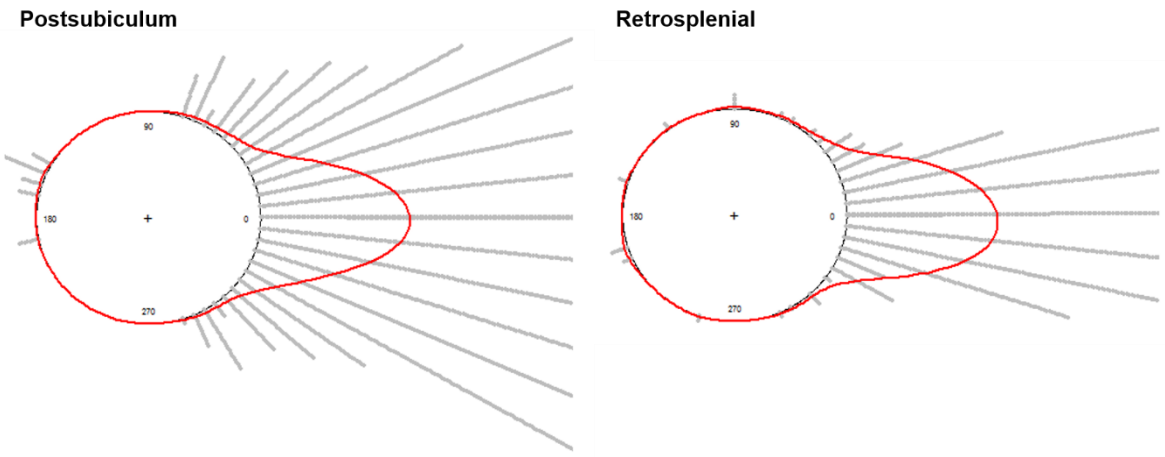

Figure 6.20 Kernel density estimates of the distribution of PFD angular offset shifts in a population of HD cells recorded in the PoS and the RSC. Both KDE's had a bandwidth of 50.

To examine whether the population activity of PFD angular offset shifts in HD cells recorded in the PoS differ from those recorded in the RSC, a Wallraff test examined if both samples have a common concentration. The Wallraff test showed that there were no statistically significant differences in the concentration values between the PoS and the RSC, ($\chi^2_{(1)} = 0.074$, $p = 0.79$). This result provides further evidence of coherent activity in HD cell ensembles and support for a strong coupling in HD cell activity between the PoS and the RSC.

6.7 Histology

The location of the recording electrodes was verified by examining 40 µm Nissl stained brain sections under a light microscope (Section 4.8). Representative examples of the histology for rats implanted in the RSC in which HD cells were recorded are shown in Figure 6.21.

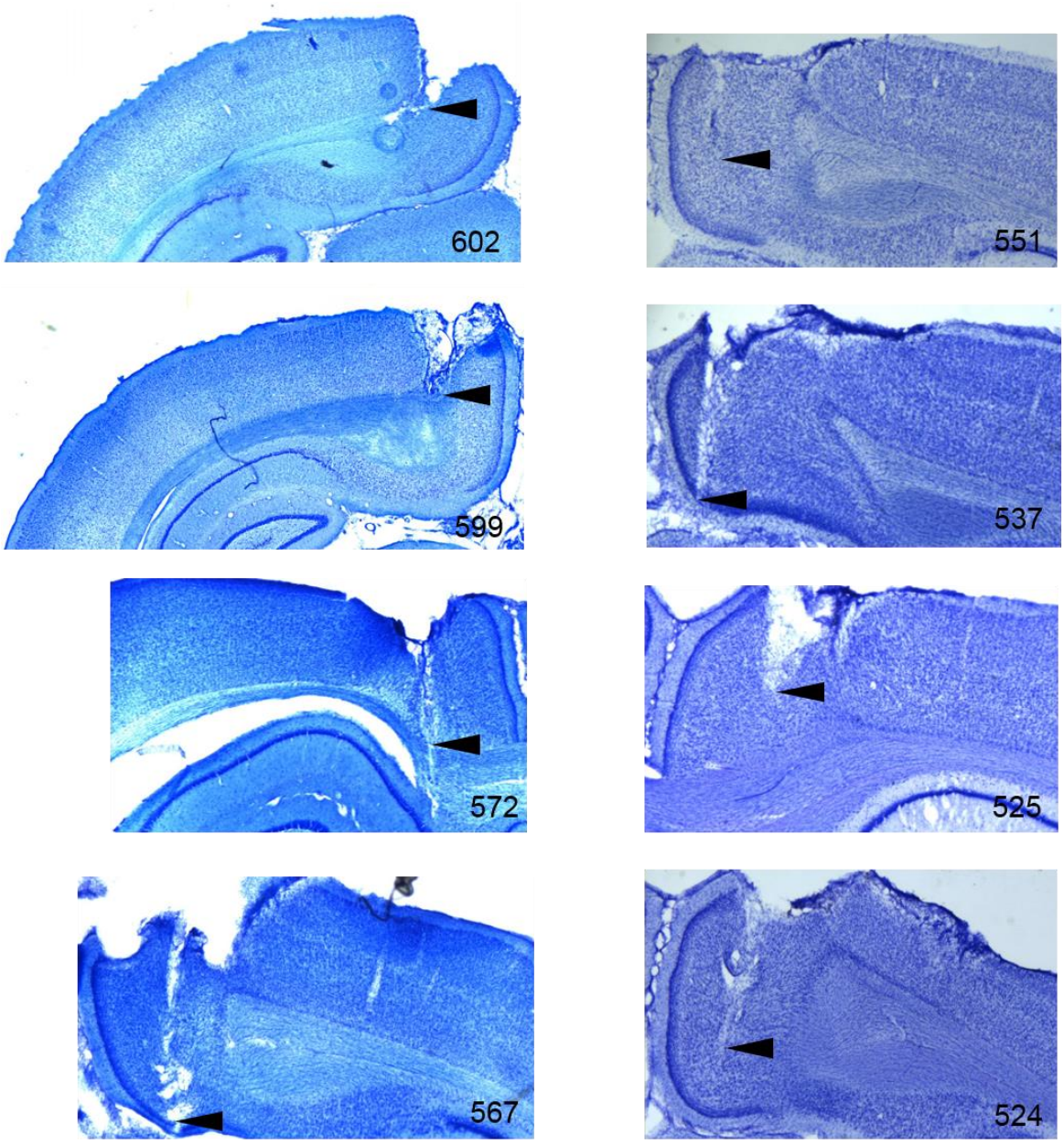

Figure 6.21 Cresyl violet-stained coronal sections showing the tetrode tracks of rats implanted in the RSC. Black triangle depicts the final electrode depth in the RSC.

6.8 Discussion

The main finding of these experiments is that HD cells in both the RSC and the PoS discriminate the visual features of the cue cards, as shown by the cells adopting a consistent firing direction within the arena relative to the cue pair. Furthermore, the strength of discrimination and landmark control varied between

the visual stimuli, where contrast (black vs white) and orientation (vertical vs horizontal) reliably reset the firing of RSC and PoS HD cells, while the vertical (top vs bottom) and lateral position of a bar (left vs right), which were also discriminated and used as landmarks for spatial orientation, showed weaker stimulus control over HD cells compared to contrast and orientation.

Although the importance of landmarks in controlling the HD signal has been well characterised and results have shown that only those visual cues that are perceived to be stable as the rat moves around a familiar environment exert control over the PFD, little is known about the landmark processing capabilities of HD cells, particularly relating to the content of the visual information that is projected from diverse visual pathways. Therefore, a good candidate structure to explore the role of landmark processing in HD cells is the PoS and the RSC as they receive abundant projections from the visual cortex and have strong reciprocal connections with each other and with the ADN.

With the aim of exploring whether the perceptual acuity of the different visual features are processed as landmarks to aid in spatial orientation, the present study focused on investigating what visual properties are integrated by HD cells. This was conducted by recording the activity of HD cells in the PoS and the RSC as rats explored a geometrically non-polarising environment (a cylindrical arena) with two opposing cue cards attached to the inner wall.

The 95% credible interval of the posterior distribution showed that with the exception of the identical cues, all the other cue types had an above chance (0.5) probability that a PFD deviation would fall in category 1, providing support that each of the visual features exerted landmark control over the activity of PoS and RSC HD cells. The results of the pair-wise proportion tests showed that contrast had the highest probability of landmark control compared to all the other cues, while orientation had a higher probability of landmark control compared to the vertical and lateral position of a bar, while vertical and lateral position had an equal probability of landmark control and identical stimuli (black cards) at chance levels. A discussion of the implications of these results are described in Chapter 8.

Furthermore, landmark control for the different cue types did not differ between the RSC and the PoS, suggesting that the activity of HD cells is similar across these two interconnected brain areas (Sugar et al., 2011). However to examine if the activity of HD cells in the RSC and the PoS is coupled as the cue cars are rotated, simultaneous recordings would need to be conducted in both brain areas examining the coherency of the changes in the tuning curves of HD cells. If such results are found, they would be consistent with attractor network models (Clark & Taube, 2012; Knierim & Zhang, 2012) and with previously reported studies where multiple HD cells have been simultaneously recorded in the ADN and PoS (Peyrache et al., 2015). Together, these results are consistent with the hypothesised role of the PoS and the RSC in landmark processing, extracting visual information and integrating this input with HD signals (Yoder, Clark, & Taube, 2011).

The results of the two cue experiments demonstrate a strong influence of the proximal cues in the directional firing of HD cells as evidenced by the distributions of PFD deviations being either unimodal or bimodal with little data falling in between. This suggests that the processing of salient visual cues likely occurs in a winner-take-all fashion as demonstrated in a study where HD cells were recorded in flies (Seelig & Jayaraman, 2015). The strong influence of the cue cards also shows that idiothetic and uncontrolled, room based cues exert little effect in controlling the PFD. If distal, room based cues had an influence on HD cell activity, the PFD would be expected to remain fixed relative to room based cues and not shift in relation to the cue cards as these are rotated. The lack of shift in the PFD during the baseline trials can also be interpreted as additional evidence of landmark control by the local cue cards, as the PFD was expected to change by 180° across trials if the rat was unable to discriminate between the two cues.

Furthermore, strong cue control was obtained despite the rats' being disoriented prior to the start of every trial. This supports the hypothesis that when continuous self-motion signals are disrupted, the visuo-spatial information extracted from the visual cues is given a greater weight compared to idiothetic cues.

In relation to the tuning curve characteristics of RSC and PoS HD cells, a strict comparisons of HD cell parameters from published papers that come from different research groups often yield somewhat variable results that may represent differences in methodology (recording equipment, spike sorting software and analysis methods), rather than actual differences between brain areas. However, it is expected that the results obtained within a lab should have internal validity and to some extent be comparable across labs if a similar methodology is used. Considering these limitations, the tuning curve characteristics of RSC and PoS HD cells recorded in the two cue experiments were compared with those of HD cells recorded in the same brain areas as rats foraged for food inside a cylindrical arena of the same dimensions as those used in the present study.

The HD cells recorded in the RSC (n = 113) had a mean peak firing rate of 24.6 ± 2.4 Hz and a mean tuning width of 52.2 ± 1.5°. These results are slightly different from the tuning curve values previously reported, in which RSC HD cells (n = 12) were reported to have a mean peak firing rate of 32.3 ± 10.7 Hz and a mean tuning width of 44.6 ± 2.7° (Cho & Sharp, 2001). For HD cells recorded in the PoS (n = 83), the mean peak firing rate was 8.5 ± 0.6 Hz which was considerably lower compared to a previous study that reported a mean peak firing rate of 24.3 ± 3.7 Hz in PoS HD cells (n = 19) (Blair & Sharp, 1995). In the same study, they reported a mean tuning width of 63.9 ± 6.3° which was slightly higher to the mean tuning width of PoS HD cells recorded in the two cue experiments, 48.3 ± 1.5°.

Although the sample size of HD cells recorded in previously published papers are much lower compared to those reported here, the tuning curve parameters are in relatively close agreement with each another providing some evidence that the true tuning curve parameters for HD cells in these areas might lie close to the observed range of values. To provide a better estimate of the tuning curve parameters, large ensembles of HD cells need to be recorded. A recent study managed to record n = 111 PoS HD cells in 7 mice using silicon probes (Peyrache et al., 2015). Although the mean firing rate was not reported, from the distribution of the peak firing rate, it can be observed that the majority of PoS HD cells had a

peak firing rate within 10-20 Hz, a value that is closer to the one obtained from PoS HD cells recorded in the two cue protocol.

Another interesting result from the present experiments was that the distribution of the peak firing rate and the tuning width were different between the RSC and the PoS. Although the functional implication of this are not known, studies that have characterised the peak firing rate and the tuning width of HD cells across different areas have reported a general trend where the peak firing rate and the tuning width becomes progressively higher in downstream areas of the HD cell circuit (PoS-RSC → ADN → LMN → DTN). The extent to which this is a strong effect or is rather due to the sample size of HD cells and differences in methodology remains to be determined, however it has been suggested although not conclusively shown that in the exploring animal, the HD tuning curves result from a different weighing and complex integration of allothetic and idiothetic information.

Furthermore in the study by Peyrache et al., 2015, 12% of ADN HD cells and 32% of PoS HD cells were not unimodal, having a second peak that was 50% or more of the maximum peak firing rate. These authors suggest that while neurons in the ADN are dedicated specifically to HD information, PoS neurons respond to a variety (multimodal) inputs which makes them appear to be 'nosier' when in fact there is likely other information (spatial or non-spatial) being conveyed by the second peak. Future studies would have to explore whether these cells are present in the RSC.

In summary, the present findings showed that HD cells in the PoS and the RSC are able to discriminate the fine details of visual landmarks. A general discussion of the pathways that might contribute to landmark processing in the PoS and the RSC, and experiments to further explore the functional role of these brain areas to spatial navigation and memory are presented in the next chapter.

Chapter 7 Configural landmark processing by head direction cells

7.1 Background and rationale

The previous chapter investigated whether different visual features are processed as landmarks by RSC and PoS HD cells, showing that contrast and orientation reliably reset the PFD. Based on these findings and the hypothesized role of the PoS in landmark processing (Yoder, Clark, & Taube, 2011), the current chapter investigates whether PoS HD cells process landmarks based on their spatial relation as an array of cues (configural processing) or based on their individual visual features (featural processing). Therefore, the aim of this chapter is to test the configural-processing hypothesis which predicts that if PoS HD cells process the multiple cues as an array, they should be sensitive to changes in the spatial relation of familiar cues such that their PFD remaps by a random amount relative to the local cues. This would indicate that introducing a change in the familiar cue configuration has triggered a reorganisation of the spatial representation and that the HD system is sensitive to this configuration.

To test this hypothesis, cue control experiments were conducted while rats explored a square environment with a black, white and stripe cue attached to the inner walls where one wall remained without a cue card. Multiple recording sessions in which the familiar cues maintained their spatial relation with one another (standard configuration) were conducted along with sessions where two of the cue cards (black and the stripe cue) swapped their positions (shuffle configuration) while the other cues remained the same (white and the wall). The experiments reported in this chapter also investigated whether landmark control with the less-familiar shuffle cue configuration was weaker compared to the more-familiar standard cue configuration.

The aim of conducting the shuffle sessions was to test the configural-processing hypothesis, examining whether changes to the position of a subset of the familiar cues trigger remapping in PoS HD cells or if instead HD cells were controlled by individual cues that did not changed their spatial position. To evaluate these

hypotheses, changes in the PFD were analysed relative to the location of the proximal cues and a fixed room reference location (Figure 7.2). The potential outcomes and the conclusions that can be derived from analysing the activity of PoS HD cells during the shuffle trials are as follows:

1) The PFD remaps by a random amount that that does not correspond to the amount by which the cards moved. This result indicates that the change in the cue configuration has triggered a reorganisation of the spatial representation and by implication that the HD system is sensitive to this configuration. This outcome predicts that the distribution of PFD deviations will be uniform (Figure 7.1A).

2) The PFD remains aligned with the cue-pair whose position did not change (the white cue and the wall) rather than being controlled by one of the shuffled cues. This result indicates that the stable cues which maintained their spatial position relative to one another exert stronger control over HD cells compared to the isolated cues that switched their spatial position. This outcome implies a lack of configural processing since the system is more likely to be controlled by a combination of non-rotated cues compared to the individual shuffled cues. This outcome predicts that the distribution of PFD deviations relative to the location of the non-shifted cues (white cue and the wall) will be unimodal with a mean direction at approximately 0° (Figure 7.1B).

3) The PFD shifts relative to either one of the two shuffled cues. This result suggests that PoS HD cells are controlled by one of the swapped cues and suggests that instead of configural processing, the HD cells may have been controlled by just one of the cue cards that changed its location. This outcome predicts that the distribution of PFD shifts relative to the location of one of the shuffled cues will be unimodal with a mean direction at approximately 0° (Figure 7.1B).

4) An alternative outcome that could occur in both the standard and the shuffle trials is that HD cells anchor to external, uncontrolled cues. If this is the case, the PFD will not shift relative to the standard or the shuffled cue array as these are rotated together. This outcome predicts that the distribution of PFD shifts relative to the room reference frame will be unimodal with a mean direction at approximately 0°. This outcome would indicate that HD cells disregard the visuo-spatial information derived from the cue cards to reset their directional firing and are instead influenced by uncontrolled extramaze cues (Figure 7.3B). If there is strong landmark control by the standard cue array, a lack of change in the PFD during the shuffle trial would imply configural processing as there is a decline in cue following when the shuffled configuration is introduced.

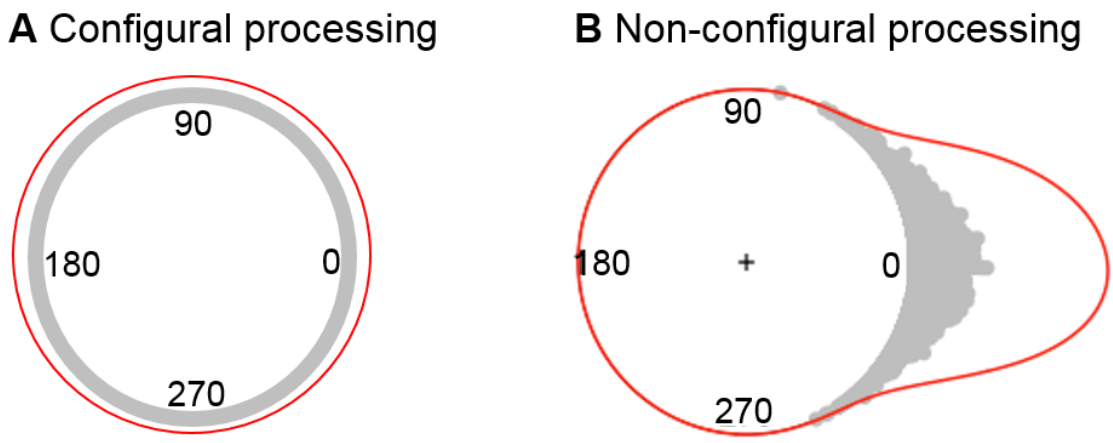

Figure 7.1 Schematic diagram that illustrates the competing hypothesis for configural cue processing. **A.** HD cells are sensitive to changes in the configuration of familiar landmarks, remapping relative to the location of each available local cue. **B.** HD cells are controlled by a subset of the cues, either those that maintained a stable spatial relation (remained unchanged) or by the cues that were shuffled. Alternatively, if HD cells are locked to external, uncontrolled room cues a unimodal distribution of PFD shifts with a mean direction at approximately 0° would be observed relative to the room reference frame.

7.2 Methods

Similar methods as those described in Chapter 4 were used to investigate if PoS HD cells are controlled by the spatial arrangement of multiple visual cues. To explore this question, three distinct cue cards 51 cm high, 50 cm wide were attached with Velcro tape to the centre of individual 100 x 100 cm wide, 60 cm high plywood walls that were painted with a light grey acrylic matt (Johnstone's Trade, UK) (Figure 7.2). One of the walls remained without a cue card throughout the experiments. The cue cards that were selected for this experiment were chosen based on the findings reported in Chapter 6, where it was found that contrast and orientation were reliably used as landmarks by both RSC and PoS HD cells.

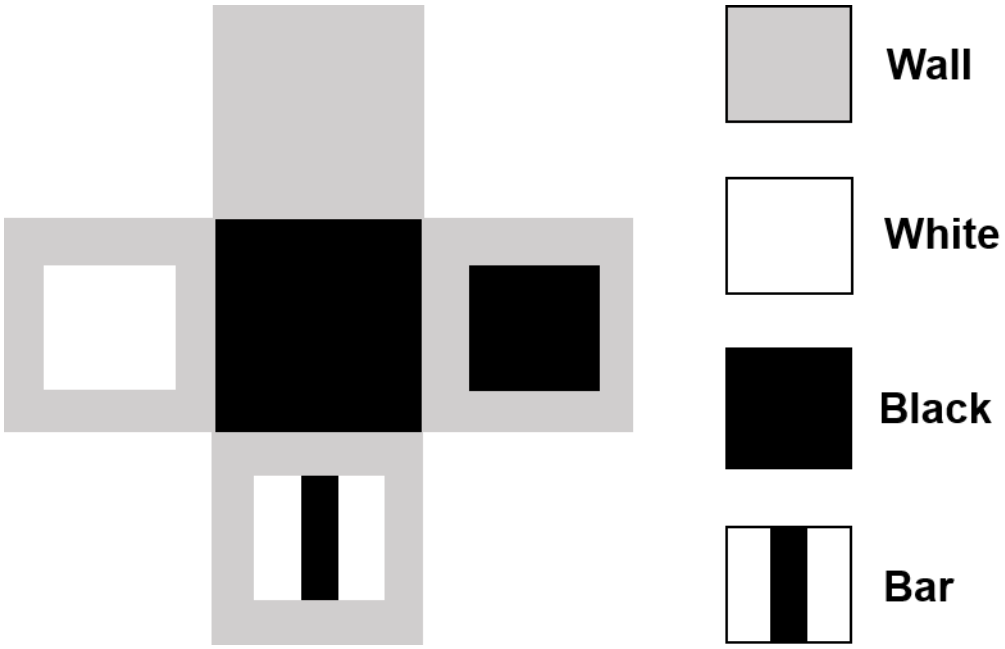

Figure 7.2 Schematic diagram of the 100 x 100 cm wide, 60 cm high recording arena showing a flattened view of the box with three distinct cue cards (51 cm high, 50 cm wide) attached to the centre of separate walls. The inner black square corresponds to the vinyl floor of the box that was used as a base and was rotated after each trial. The nomenclature for each of the cues is displayed in the right. The diagram is not drawn to scale.

The individual walls that comprised the recording arena were held together with clamps and arranged in the shape of a square. The arena was placed over a

movable black vinyl sheet (Tarkett, UK) that was used as a temporary base that was rotated across trials. An overhead radio attached to the ceiling provided a source of white noise. All screening trials carried out to identify HD cells were conducted in a room separate from where the cue control experiments took place.

7.2.1 Cue control protocol

The experiments consisted of recording PoS HD cells in rats exposed to a series of cue control sessions that are referred to as standard or shuffle. In the standard sessions, the cue cards maintained their spatial arrangement with respect to each other (Figure 7.3A), while in the shuffle sessions, trials with the standard cue configuration were followed by trials in which the position of the black and the stripe cue were swapped (Figure 7.3B). Each session consisted of 6 trials and the length of each trial was 10 minutes long.

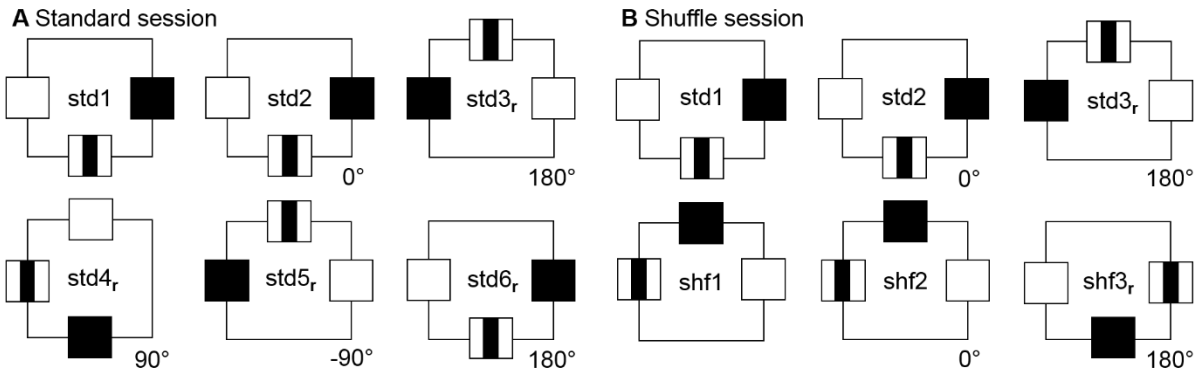

Figure 7.3 Examples of standard and shuffle cue control sessions. **A.** Cue configuration used during all the standard sessions. **B.** Shuffle session where the stripe and the black cue card changed their spatial relationship with respect to each other between trial $std3_r$ and shf1. The abbreviation std refers to standard trials were the cue cards maintained their spatial relation and shf refers to shuffle trials where a new cue configuration was introduced.

The purpose of the standard sessions was to familiarise the rats to a stable cue array and determine the reliability of landmark control, which is to say how likely

PoS HD cells are controlled by the cue array or locked to extramaze cues that remain stationary during the recordings such as the surrounding black curtains or other uncontrolled cues. In comparison, the purpose of the shuffle sessions was to test the configural processing hypothesis, which is whether PoS HD cells respond to changes in the spatial arrangement of familiar cues or if they instead reset their PFD in relation to the position of individual cues (featural processing). The standard trials with the same cue array are denoted as std, while the shuffle trials are denoted as shf where the subscript r indicates the trials that were rotated with respect to the experimental room's reference frame (the location of the room's door was used as a reference point) (Figure 7.3).

During the first two baseline trials of the standard and the shuffle sessions (std1, std2), the cue cards were not rotated with respect to the room's reference frame in order to assess the stability of PoS HD cells relative to the local cue cards prior to introducing the cue rotation trials in the standard sessions or the shuffle trials during the shuffle sessions (Figure 7.3). In the standard sessions, the two baseline trials were followed by four cue control trials ($std3_r$, $std4_r$, $std5_r$ and $std6_r$) where the cue array was pseudorandomly rotated together by ±90° or 180° to test landmark control in PoS HD cells by the standard cue configuration (Figure 7.3A).

During the shuffle sessions, the two baseline trials with the standard cue configuration (std1 and std2) were followed by one cue rotation trial ($std3_r$) of ±90° or 180° with the familiar standard cue configuration, followed by three shuffle trials (shf1, shf2 and $shf3_r$) (Figure 7.3B). The three standard configuration trials were followed by three trials with a new configuration to examine whether landmark control with a less-familiar shuffle cue configuration was weaker compared to the more-familiar configuration. If landmark control between the two cue configurations is different, this suggests that the change in the cue configuration triggered remapping, where the shuffle configuration is perceived to be less reliable and therefore landmark control would be weaker in the less-familiar configuration. In contrast, if landmark control between the two configurations does not differ, the results are consistent with either rapid learning of the new configuration, or being locked to a single, well-learned cue, as these two outcomes

cannot be distinguished because a cue removal test was not conducted in order to examine the contribution of each cue.

In the shuffle sessions after presenting the standard trials, a shuffle trial was introduced (shf1) in which the location of the black and the stripe cue were swapped, while the location of the white cue and the wall without a cue remained the same. The purpose of this manipulation was to test the configural-processing hypothesis. After introducing the shuffle trial, the same shuffled configuration was presented without being rotated in (shf2) to examine the stability of PoS HD cells to the shuffled cue configuration followed by a trial ($shf3_r$) in which the cues were rotated as an ensemble by either ±90° or 180° to examine landmark control of the shuffle cue configuration.

The same cue control protocol as the one reported in Chapter 6 was followed. Briefly, this consisted of disorienting the rat prior to the start of every trial by being passively transported inside a holding box and wiping the cue cards and the base of the arena with 75% ethanol to control for olfactory cues before placing the rat back into the recording arena facing in a pseudorandom direction. Only one recording session (either a standard or shuffle) was recorded per day in each rat.

7.3 Data analysis

Cells were classified as tuned to HD using the inclusion criterion described in Section 4.7.4. The changes in the PFD were analysed using similar methods and functions as those described in Chapter 6. To evaluate the behaviour of HD cells during the standard and the shuffle sessions (Section 7.2.1 and 7.3), the angular distance between the PFD and the position of one of the cues including the wall without a cue and a fixed room reference (the door of the experimental room) were used to quantify the change in the PFD. The circular median of these angular distances was calculated independently for each HD cell (see Section 6.3.1), providing an estimate of central tendency to which the changes in the PFD were calculated across trials within a session. When multiple HD cells were recorded in

a session, the sample median direction of the PFD deviations were calculated independently for each trial within a session, providing only one PFD shift per trial.

The distribution of PFD deviations were visualised applying a circular nonparametric KDE method described in Section 5.5.1. Density estimates of the PFD deviations were generated only when the sample size was larger than 30 observations, since a biased estimate of the underlying distribution can be obtained with a smaller sample size (Fisher, 1995). For a sample size smaller than 30 observations, circular scatter plots were used. Summary statistics, including the mean direction ($\bar{\theta}$), mean vector length (R), and sample circular variance (V) are reported to describe the main features of the distributions.

Landmark control during the standard sessions was analysed by comparing the mean direction of the distribution of PFD deviations relative to the location of one of the cue cards against a predicted mean direction of 0° using a *V*-test. Since the cue cards were rotated as an array, the location of any cue card can be chosen to calculate the PFD deviations. In contrast, to examine if HD cells are locked to external, uncontrolled room cues, the baseline trials (std1 and std2) in which the cue cards remained fixed in relation to room centred coordinates were omitted from the analysis since the lack of change in the PFD relative to room coordinates cannot be distinguished from landmark control by the cue array.

To test the competing outcomes for the cue configuration hypotheses (Section 7.1) and select the outcome that best accounted for the change in the PFD when the shuffle configuration was introduced, the minimum angular distance between the PFD and the cue location was calculated between the $std3_r$ and the shf1 trial relative to the location of individual intramaze cues and relative to the door location. The distribution which had a mean direction that was not significantly different from 0° as determined by a *V*-test (Section 6.3.3), was taken as the outcome that best accounted for the PFD shifts. For distributions whose changes in the PFD deviated from unimodality, Watson's one-sample U^2 test was applied instead of the *V*-test to examine multimodal departures from uniformity (Section 5.4).

Furthermore, since the shuffle sessions started with three standard trials (std1, std2, $std3_r$) in which the rats were presented with the familiar cue configuration, (Section 7.2.1), prior to introducing the shuffle configuration, the standard trials were analysed independently from the shuffled trials (shf1, shf2 and $shf3_r$). Subsequently, to examine whether landmark control with the less-familiar shuffle cue configuration differs from the more-familiar standard cue configuration, the distribution of PFD deviations of all the standard trials were compared with the distribution of PFD deviations of all the shuffle trials recorded during the shuffle sessions. A randomisation version of Watson's two-sample U^2 test was applied (Section 6.3.4) to determine if there were differences in landmark control between the standard and the shuffle cue configuration.

7.4 Results of the standard sessions

A total of 33 HD cells were recorded in *n*=5 adult male Lister Hooded rats weighing between 314-440 g at the time of surgery. All HD cells were recorded in rats with implanted electrodes in the PoS (bregma, -7.5 mm anterior-posterior, ±3.2 mm medial-lateral, -2.0 mm dorsal-ventral) as they foraged for rice inside a square arena with three cue cards attached to the inner walls (Figure 7.2). The implanted hemisphere and the number of HD cells and standard sessions recorded per rat are shown in Table 7.1.

Rat number	Implant brain area	Number of HD cells	Number of sessions
646	Right PoS	2	1
645	Left PoS	3	3
638	Left PoS	26	13
637	Left PoS	1	1
630	Right PoS	1	1

Table 7.1 Total number of HD cells and standard sessions recorded per rat. The table shows the rat number followed by the brain hemisphere where the tetrodes were implanted, the total number of cells that passed the HD cell inclusion criteria and the number of standard sessions conducted in each rat.

To examine whether the local cue array exerts landmark control over PoS HD cells or are instead controlled by distal, uncontrolled cues that are external to the recording environment, the PFD deviations were plotted with respect to the location of the cue array or relative to the door location which was used as reference. The trials in which the cues were not rotated were excluded from the room reference analysis as the lack of a PFD shift can be interpreted as the result of landmark control by the proximal cue card or by the uncontrolled room cues. The summary statistics of the PFD deviations are shown in Table 7.2 and the density estimates for these distributions are displayed in Figure 7.4. The distribution of the PFD deviations relative to the cue array had a mean direction that was significantly clustered at 0º, *V*-test, ($V_{(107)}$ = 0.74, p < 0.0001) (Figure 7.4A). In contrast, when the PFD deviations were plotted relative to the room reference frame, the distribution showed a multimodal departure from uniformity, Watson's one-sample U^2 test, ($U^2_{(70)}$ = 0.43, p < 0.01).

Standard sessions	**Summary statistics**
Cue array	$\bar{\theta}$ = -2.0, R = 0.74, V = 0.26, n = 108
Room reference frame	$\bar{\theta}$ = 25.3, R = 0.30, V = 0.70, n = 71

Table 7.2 Summary statistics for the distribution of PFD deviations relative to the cue array and the room reference frame during the standard sessions. Abbreviations denote mean direction ($\bar{\theta}$), mean vector length (R), circular variance (V) and sample size (n).

The clustering of the PFD deviations at 0º in relation to the cue array demonstrates strong landmark control of the standard cue configuration and provides further evidence that the visual features of the cue cards (contrast and orientation) are discriminable, reliably exerting control over the activity of PoS HD cells. Furthermore, the lack of a unimodal distribution when the PFD deviations are plotted relative to the room reference frame, provides support that the proximal cue cards and not distal, uncontrolled room cues control the firing of PoS HD cells.

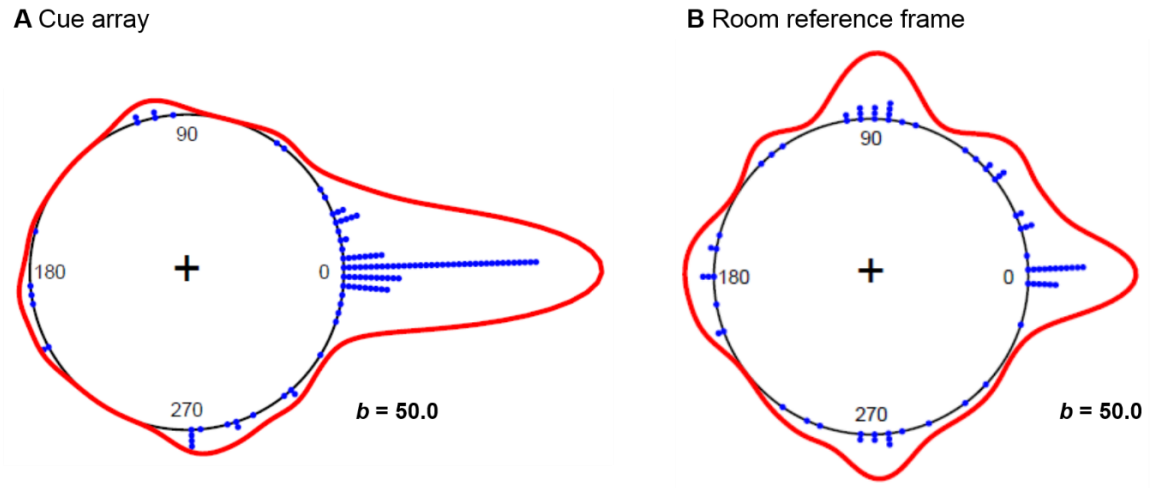

Figure 7.4 Density estimates of the PFD deviations in the standard sessions relative to **A.** the cue array and **B.** the room reference frame. The abbreviation *b* denotes the bandwidth of the KDE.

7.5 Results of the shuffle sessions

A total of 14 PoS HD cells were recorded in *n*=3 adult male Lister Hooded rats during 11 shuffle sessions. A breakdown of the number of HD cells and shuffle sessions recorded in each rat is shown in Table 7.3.

Rat number	Implant brain area	Number of HD cells	Number of sessions
645	Left PoS	8	6
638	Left PoS	4	4
630	Right PoS	2	1

Table 7.3 Total number of HD cells and shuffle sessions recorded per rat. The table shows the rat number followed by the brain hemisphere where the tetrodes were implanted, the total number of cells that passed the HD cell inclusion criteria and the shuffle sessions recorded.

7.5.1 Landmark processing of the standard cue configuration

To examine landmark control of PoS HD cells in the standard trials (std1, std2, std3$_r$) prior to introducing the shuffle trial, the PFD deviations were measured with

respect to the location of the cue array and the room reference frame (Figure 7.2B). The summary statistics for these distributions are shown in Table 7.4 and the density estimates and scatter plot are displayed in Figure 7.5.

A *V*-test showed that the distribution of the PFD deviations in relation to the standard cue configuration had a mean direction that was significantly clustered at 0º, ($V_{(32)}$ = 0.83, p < 0.0001) (Figure 7.5A). In comparison, when the PFD deviations of the rotation trials ($std3_r$) in the standard cue configuration were plotted relative to the room reference frame, there was no evidence that they were clustered at mean direction of 0º, ($V_{(10)}$ = -0.29, p = 0.91) (Figure 7.5B). These results indicate that the standard, familiar cue configuration exerts strong landmark control over PoS HD cells prior to introducing the shuffle configuration.

Standard trials in the shuffle session	**Summary statistics**
Cue array	$\bar{\theta}$ = 6.3, R = 0.84, V = 0.16, n = 33
Room reference frame	$\bar{\theta}$ = 145.5, R = 0.35, V = 0.65, n = 11

Table 7.4 Summary statistics for the distribution of PFD deviations relative to the cue array and the room reference frame in the standard cue configuration prior to introducing the shuffle trial. Abbreviations denote mean direction ($\bar{\theta}$), mean vector length (R), circular variance (V) and sample size (n).

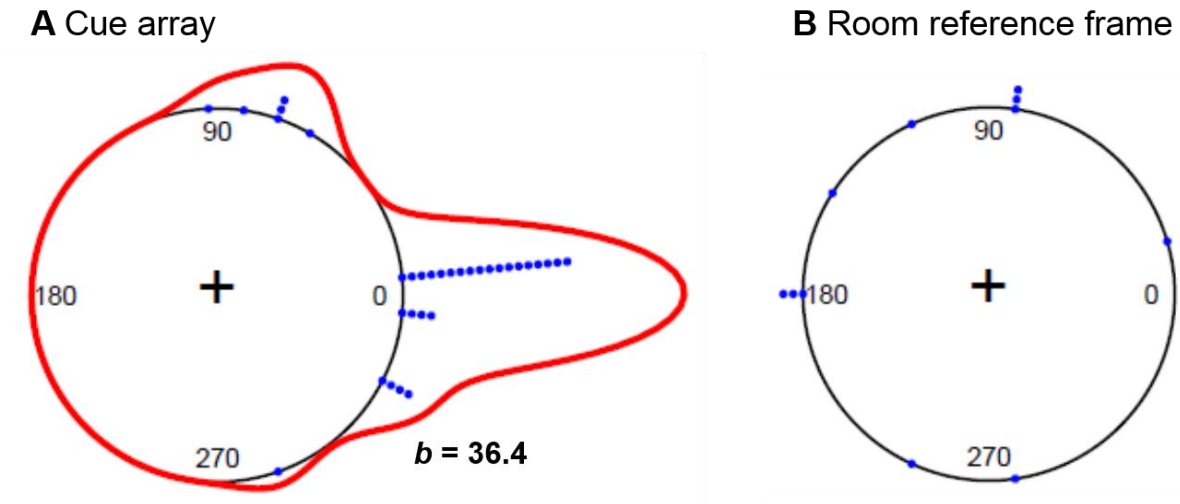

Figure 7.5 Density estimate and scatter plot of the PFD deviations relative to cue array and the room reference frame prior to introducing the shuffle trial. The abbreviation *b* denotes the bandwidth of the KDE.

Furthermore, when the rats were presented with the same cue configuration prior to and after having being exposed to the shuffle trials, there were no differences in the mean direction between the distributions of PFD deviations in the standard sessions (Figure 7.4A) compared to the shuffle sessions (Figure 7.5A), two sample Watson-Williams test, ($F_{(139)}$ = 0.28, p = 0.60). Although the number of rats and trials was smaller in the shuffle sessions compared to the standard session, these results suggest that introducing the shuffle trials does not impair landmark control of a familiar cue array. The results of the shuffle trials are described in the next section.

7.5.2 Landmark processing of the shuffled cue configuration

To examine whether PoS HD cells remap to changes in the spatial arrangement of the familiar cue array, the change in the PFD between the last trial of the standard cue configuration ($std3_r$) and the first shuffle trial (shf1) was calculated relative to the location of the cues that changed their spatial location (vertical stripe and black cue) and those that remained stable (the white, wall and the room reference frame) (Figure 7.2B). Since there was only one shuffle trial per session and a total of 11 shuffle sessions, the PFD shifts are displayed with a circular scatter plots instead of KDE due to the small sample size (Figure 7.6). The summary statistics for the PFD shifts in relation to each of the cues and the room reference frame are shown in Table 7.5.

Shuffle trial	**Summary statistics**
Vertical stripe	$\bar{\theta}$ = -167.1, R = 0.29, V = 0.71, n = 11
Black	$\bar{\theta}$ = 128.6, R = 0.29, V = 0.71, n = 11
Stable cues (white, wall, room)	$\bar{\theta}$ = -77.1, R = 0.29, V = 0.71, n = 11

Table 7.5 Summary statistics of the PFD shifts during the first shuffle trial (shf1) of all the shuffle sessions. Abbreviations denote mean direction ($\bar{\theta}$), mean vector length (R), circular variance (V) and sample size (n).

Individual V-tests showed that when the first shuffle trial was presented within a session, the PFD shifts were not significantly clustered at a mean direction of 0º

when plotted relative to the position of the stripe cue, ($V_{(10)}$ = -0.28, p = 0.91) and the black cue, ($V_{(10)}$ = 0.28, p = 0.09) (Figure 7.6). When the PFD shifts were plotted relative to the stable cues, they did not clustered at a mean direction of 0º, ($V_{(10)}$ = 0.064, p = 0.38) (Figure 7.6D).

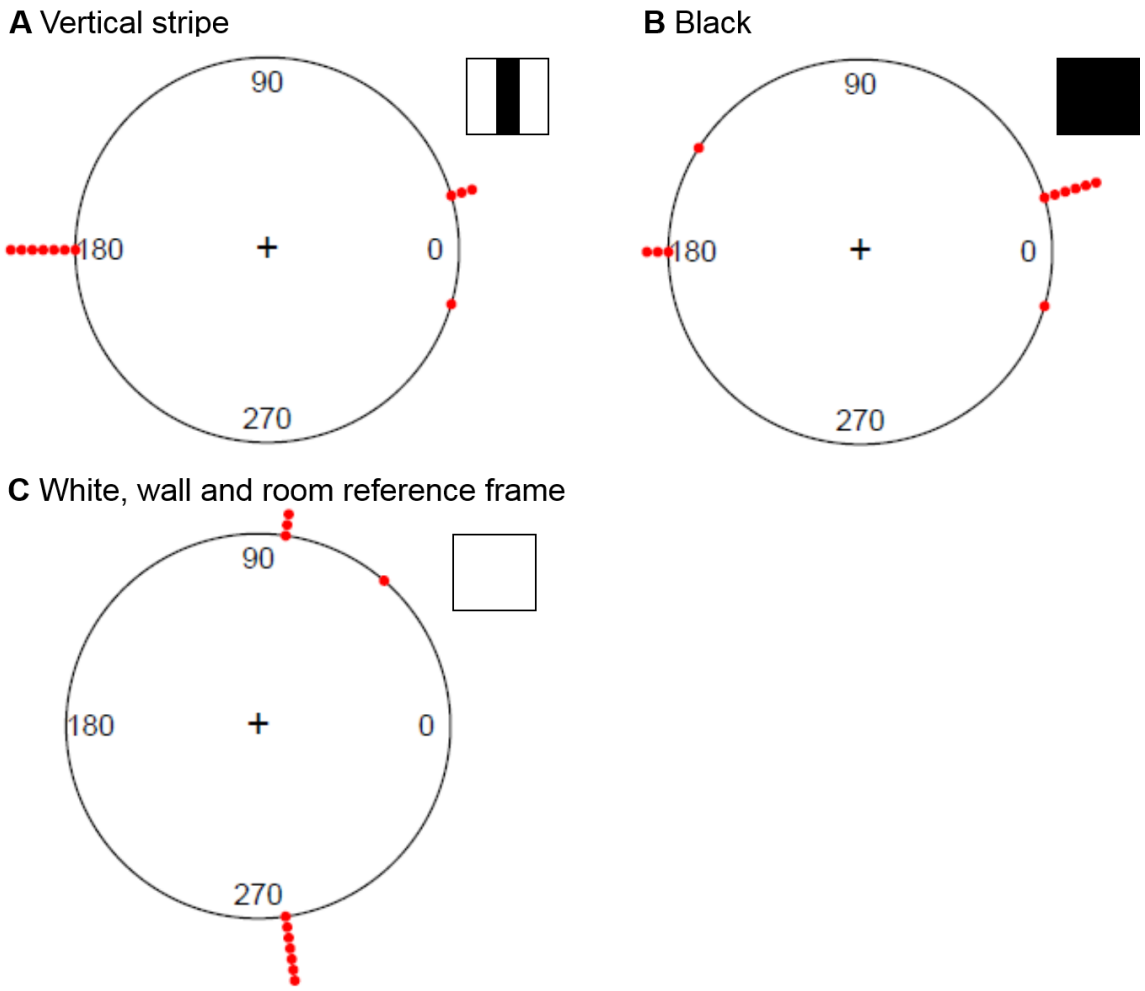

Figure 7.6. Scatter plots of the PFD shifts during the first shuffle trial (shf1) relative to the location of the stripe, black and stable cues. Each dot corresponds to a shuffle trial recorded from a total of n=11 independent shuffle sessions.

A chi square test showed that the proportion of PFD shifts that were clustered at a mean direction of 0º relative to the stripe and the black cue did not differ from what was expected by chance (0.5) if both cues had an equal likelihood of controlling the firing direction of PoS HD cells, (χ^2 = 0.82, p = 0.37). This result

does not support the configural processing hypothesis and suggests instead that PoS HD cells select either one of the cues that changed its spatial relation to reset their PFD when a familiar cue array is altered. More shuffle data would have to be collected to determine whether PoS HD cells show a preference for one of the shuffled cues or whether they are equally likely to be controlled by any local cue that changes its spatial position.

To test landmark control of the new cue configuration, the PFD deviations across the three shuffle trials (shf1, shf2 and $shf3_r$) were plotted relative to the cue array and the room reference frame. Independent *V*-tests showed that the PFD deviations were clustered around a mean direction of 0º, when plotted in relation to the cue array, ($V_{(31)}$ = 0.65, p < 0.0001) (Figure 7.7B), and were not clustered around a mean direction of 0º relative to the room reference frame, ($V_{(31)}$ = 0.63, p < 0.0001) (Figure 7.7C). The summary statistics for the PFD deviations during the cue control trials of the shuffled configuration are shown in Table 7.6.

Shuffle cue control trials	**Summary statistics**
Cue array	$\bar{\theta}$ = -1.7, R = 0.65, V = 0.35, n = 32
Room reference frame	$\bar{\theta}$ = -1.4, R = 0.10, V = 0.90, n = 10

Table 7.6 Summary statistics for the distribution of PFD deviations during the cue control experiment of the shuffled configuration. Abbreviations denote mean direction ($\bar{\theta}$), mean vector length (R), circular variance (V) and sample size (n).

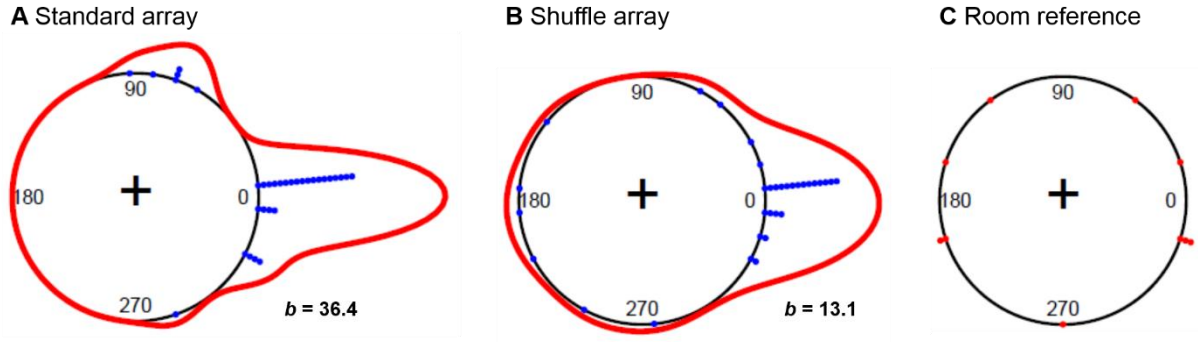

Figure 7.7 Density estimates of the PFD deviations during the cue control trials of the **A.** standard and **B.** shuffled cue configuration. **C.** PFD shifts of the shuffle trials relative to the room reference frame. The abbreviation *b* denotes the bandwidth of the KDE.

The previous result showed that there was strong landmark control by the shuffled cue configuration. Subsequently, to test if cue control with the more-familiar standard configuration (Figure 7.7A) differs from the less-familiar shuffle configuration, the distribution of PFD deviations relative to the cue array that were recorded in the shuffle sessions were compared with a randomisation version of Watson's two-sample U^2 test. The results showed that there were no significant differences between the distribution of PFD deviations in the standard compared to the shuffled cue configuration, ($U^2_{(62)}$ = 0.22, p = 0.20). These results suggest that landmark control over the activity of the less-familiar shuffled configuration is similar to that of the more-familiar shuffled cue configuration, suggesting that PoS HD cells either rapidly learned a new configuration or remained locked to one of the shuffled cues, either the black or the stripe cue card.

7.6 Histology

Verification that the recording electrodes were implanted in the PoS was conducted by examining 40 µm Nissl stained sagittal brain sections under a light microscope (Section 4.8). Representative examples for the rats in which HD cells were recorded are shown in Figure 7.8.

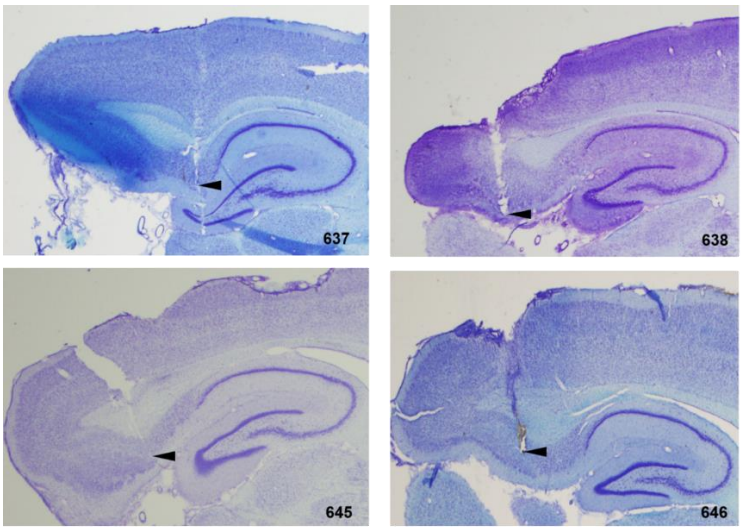

Figure 7.8 Cresyl violet-stained sagittal sections showing representative tetrode tracks of rats implanted in the PoS. Black triangle depicts the final electrode depth in the PoS.

7.7 Discussion

The present study did not find evidence in support of the configural processing hypothesis since PoS HD cells did not remap by a random amount or maintained a stable PFD in relation to the cue card array when the shuffle trial was introduced. Instead, when the spatial relation between the familiar cues was altered, PoS HD cells responded primarily by resetting their PFD relative to the cues that changed their spatial position, selecting the black and the stripe cue equally. Although only three rats were recorded in a total of 11 shuffle sessions and two rats contributed to about half of the sessions, the clustering of the changes in the PFD relative to the location of the black and the stripe cue provide consistent, although limited evidence that PoS HD cells preferentially select local cues that change their spatial location to anchor their directional firing over stationary cues.

Furthermore, since only the black and the stripe cue cards changed their location with respect to each other while the wall and the white cue card remained constant, it is not known to what extent changing the position of the wall and the white cue would yield a similar preference. A follow up experiment would have to examine if introducing a fourth cue that is known to exert strong landmark control such as a horizontal bar and presenting different cue configurations leads to remapping, as predicted from the configural processing hypothesis. Alternatively, such experiment could show that PoS HD cells select a subset of the cues from the environment for orientation as was observed in the current experiments. The results also showed that introducing the shuffled configuration of the cue cards did not impair landmark control compared to the standard sessions in which the rats were exposed to the non-changing cue array. This finding provides evidence that rats can derive reliable visuospatial information from the cue array, orienting the firing of HD cells using the features of static cue cards.

Another explanation that could account for the observed clustering of the PFD shifts at approximately 90° intervals when the shuffle trial was introduced is the use of the corners of the square arena as landmark cues by the rats. This result is consistent with both behavioural studies that have shown that the environmental geometry is important for spatial orientation in rodents (Julian, Keinath, Muzzio, &

Epstein, 2015) and single-unit recordings which have reported a strong influence of the environment's geometry on the firing of HD cells recorded in the PoS (Taube et al., 1990b) and the ADN (Golob et al., 2001). These studies have shown that when the recording arena is changed from a cylinder to a rectangle using the same set of visual cues, the PFD of PoS HD cells shifts by at least 78° without affecting the firing rate and the tuning width suggesting that the corners of the rectangular arena are used as orientation cues (Taube et al., 1990b). Another study reported that during training of a working memory task conducted in a square arena, about 23% of the trials of HD cells recorded in the ADN changed their PFD by multiples of 90° (Golob et al., 2001).

Overall, these studies provide evidence that the environment's geometry exerts some influence in the firing of HD cells over single polarising cues placed inside the recording arena. However, it is important to point out that the geometric cues in trapezoid and rectangle-shaped environments do not exert strong landmark control when multiple salient distal visual cues are placed in a curtained enclosure (Clark et al., 2010). These results suggest that there is a hierarchy in the processing of landmark cues and a complex interaction between the environment's geometry, the number, saliency and proximal-distal location of visual cues in controlling the orientation of HD cells which is not fully understood.

In contrast, when rats were exposed to the standard configuration, PoS HD cells reliably reset their directional firing with respect to the location of the local cues that maintain a constant spatial relation with respect to each other in an environment that is geometrically symmetrical. These results corroborate the findings from the previous chapter where it was shown that cue cards that differ in contrast and orientation reliably control the PFD of PoS and RSC HD cells recorded in a non-symmetrical cylindrical arena. Although most of the standard sessions (13/19) were recorded in one rat, it is unlikely that landmark control of a familiar cue configuration would have changed significantly if more sessions had been recorded with the other rats, given the high probability of landmark control in PoS and RSC HD cells when rats are presented with cue cards that vary in contrast and orientation.

The current experiments investigated whether PoS HD cells are sensitive to changes in the spatial configuration of cues that were known to reliably control the PFD. Although there was no evidence of configural processing, the strong landmark control by both the standard and the shuffle configuration suggest that knowledge about the visual features of landmarks is important for spatial orientation (Collett & Graham, 2004). In this regard, the current results do not support the view that landmarks are processed globally, as a panoramic scene, suggesting instead that they are processed locally, based on differences in their individual stimulus features.

A study that explored how changes in the position of local cues (a black and a white card) placed inside a cylindrical arena influence landmark control of place cells was conducted by Fenton, Csizmadia, & Muller, (2000). In the study the authors found that when two local cues that were separated by 135° were rotated together by ±45° or when either one of these cues was removed and the other one was rotated by the same magnitude, place cells responded primarily by changing the orientation of their firing fields relative to the available cues by an equal amount, suggesting that the cue array and the individually salient cues exerted strong landmark control.

In contrast, when the two cues were inconsistently rotated by changing their angular distance between them by ±25° bringing the two cues either together or apart, ensuring that neither card stayed at the same position relative to the laboratory frame of reference, place fields remapped, shifting their firing fields in a non-uniform manner (Fenton et al., 2000). These results showed that place cells were sensitive to changes in the angular distance between visual cues, providing evidence that the spatial relation between cues is an important factor for the processing of landmarks. A similar study has not been conducted with HD cell recordings in order to examine whether the HD system across different brain areas remaps to changes in the angular distance of local cues or if instead selects one of the cue cards to reset its PFD with all HD cells changing coherently.

Future experiments would have to explore if HD cell ensembles provide distance information to compute movement direction relative to a landmark or whether their

spatial information only encodes the instantaneous allocentric HD. A recent study found that while 3% of cells in the MEC encode the current HD, less than 1% encode both movement direction and HD, suggesting that this conjunctive signal is sparsely represented in the MEC (Raudies, Brandon, Chapman, & Hasselmo, 2015). The question arises as to whether brain regions that provide spatially modulated signals to the MEC such as the ADN, the PoS and the RSC, also provide information about egocentric movement direction or whether this constitutes and independent pathway.

In terms of the temporal dynamics for resetting the activity of HD cells relative to the local cues, that is how long it takes for an HD cell to shift its tuning curve when the shuffle trial is introduced and whether this depends on the cue card that the rat was facing at the start of the trial, was not analysed. The reason to exclude this analysis is that the current protocol does not provide the accuracy to measure changes in HD cell activity that occur faster than a few seconds due to the delay between placing the rat into the arena and the start of the trial. Also, since the rat was placed into the arena facing in a pseudorandom direction across trials, the protocol was not designed to address this question. However, based on previous studies, it is likely that the PFD transitions to a new orientation within a range of 70-90 ms (Zugaro et al., 2003) and subsequently becoming stable within 60 s, linking idiothetic information with the position of familiar landmarks to reset the PFD (Goodridge et al., 1998). Future experiments conducted in virtual-reality arenas where rats can move freely (Aronov & Tank, 2014) can better address the temporal dynamics of landmark processing.

Overall, these results provide further evidence for the role of the PoS in landmark based spatial orientation linking visual information via direct projections from the primary visual cortex with self-motion input from the ADN and learning spatial information from the environment such as the spatial relation between familiar landmarks via projections from CA1 (van Groen & Wyss, 1990). Consistent with the role of the PoS in landmark based spatial orientation, lesions to this brain area disrupt landmark control in HD cells recorded in the ADN (Goodridge & Taube, 1997), LMN (Yoder, Peck, & Taube, 2015), and CA1 place cells (Calton et al.,

2003). Furthermore, CNQX (a drug that blocks synaptic transmission and synaptic plasticity) administration into the PoS impairs landmark control of CA1 place fields when the rat is recorded in a familiar environment and does not impair landmark control when the rat is recorded in a novel environment, consistent with the role of the PoS in the retrieval of landmark based spatial representations (Bett et al., 2013).

In summary, the present findings do not provide evidence that PoS HD cells process landmarks as a configuration and instead rely on single cues as a directional reference for resetting their PFD when the spatial relation between a familiar cue array is changed. Moreover, the results suggest that local landmarks provide a reliable source of directional information, resetting the activity of PoS HD cells when: 1) they have a unique physical appearance, 2) maintain a stable distance with respect to each other, and 3) maintain a consistent configuration within an environment.

Chapter 8 General discussion and conclusion

The aim of this thesis was to explore what properties of the environment are encoded as landmarks in order to understand how visuo-spatial information is integrated with a spatial navigation signal, linking visual perception with spatial orientation. This question was examined by recording the activity of HD cells in the RSC and the PoS, two interconnected brain areas that receive direct input from the visual cortex and multisensory signals such as vestibular and optic flow from subcortical structures, thus playing an important role in integrating self-motion signals with visual landmark information.

Despite the substantial number of studies that have investigated how angular head velocity signals contribute to generating HD cell activity and the role of self-motion cues in updating the PFD, little is known about how HD cells and other spatially modulated cells select amongst different visual cues to calibrate or reset their orientation. To explain the findings of single-unit studies that have examined the role of distal and local cues in controlling the activity of spatially modulated cells, a distal sensory input model has been proposed, where visual cues set the rat's internal spatial coordinate system (encoded by the activity of HD cells), while local features of the environment such as boundaries set the scale of the spatial map (encoded by place and grid cells), providing distance estimates that the rat uses to compute self-location (Knierim & Hamilton, 2011). The distal sensory input model predicts that the visual features of landmarks are an important factor for resetting the PFD of HD cells.

In contrast, a view-based model proposes that a full retinal image resets the activity of HD cells, deriving from panoramic visual scenes global positional and directional information without the need of extracting fine visual details from the environment or features of landmarks (Zeil, 2012). Based on this model, one can predict that HD cells are insensitive to the specific visual features of landmarks and sensitive to changes in the global positional information of those landmarks.

The current results provide evidence in support of the distal sensory input model where the visual features of the cue cards (contrast, orientation, vertical and horizontal position) were used as landmarks, resetting the PFD of RSC and PoS HD cells. Furthermore, no evidence of the view-based model was found since PoS HD cells did not remap to changes in the configuration of landmarks and instead locked to individual cues that changed their spatial position. In this regard, the current results do not support the view that landmarks are processed globally, as a panoramic scene, suggesting instead that they are processed locally, based on their individual stimulus features.

Many studies have examined the role of visual cues in updating the firing of place and HD cells, however, few single-unit studies have investigated landmark processing in the RSC and the PoS and it remains relatively unexplored how signals from the visual cortex are integrated with spatially modulated cells and what properties of the panorama are used as landmarks by spatially modulated cells. Furthermore, there are a limited number of studies that have addressed whether the visual cues that are used for spatial orientation by HD cells are processed as predicted by the distal sensory input model or the view-based model. Therefore, the present experiments examined whether the visual features and spatial relation between familiar visual cues are important factors for spatial orientation, reliably resetting and stabilising the PFD in relation to landmarks.

To test these questions, changes in the PFD were analysed in response to manipulations of the features and position of visual cues as rats explored a cylindrical or a square environment. It was predicted that if HD cells distinguished the visual features of the cues and reliably use them as landmarks, the PFD's should maintain a consistent angular distance with respect to the position of the cue cards, yielding a unimodal circular distribution of PFD deviations. On the other hand, if HD cells did not distinguished the cues and were unable to reliably use the visual features as landmarks, the circular distribution of PFD deviations should cluster at two radial positions 180º apart in the case of the two cue experiments or at random directions in the multiple cues experiments. In order to analyse and draw inferences from the observed PFD deviations, a non-standard statistical

method that had not been previously applied to HD cells was developed. The non-standard statistical method consisted of applying circular KDE to visualise and obtain an estimate of the distribution of PFD deviations, while standard circular statistics were applied to examine if these distributions deviated from uniformity or unimodality. Based on the KDE's, when a large number of trials were recorded, Bayesian statistics were used to estimate the probability that a given visual feature exerted landmark control.

The main findings from the two cue experiments conducted in the cylindrical environment is that RSC and PoS HD cells discriminate and process as landmarks the visual features of the cue cards, as evidenced by the PFD deviations adopting a consistent angular distance relative to the cue card pair. However, the probability, or how reliably a given visual feature exerted landmark control over HD cells as estimated from the 95% credible interval of the posterior distribution (shown in brackets for each cue) varied between the cue cards. Specifically, contrast (black-white), [0.73-0.86] and orientation with negative polar display (white bar on a black card), [0.82-0.96] had a higher probability of landmark control followed by orientation with positive polar display (black bar on a white card), [0.64-0.74], height (top-bottom), [0.60-0.72], parity (right-left), [0.59-0.75] and identical stimuli (black-black), [0.28-0.51] which were used as a control and had a below chance level (0.5) of landmark control assuming that the two cues have complete and equal probability of resetting the PFD. Also, landmark control for the different cue types did not differ between the RSC and the PoS, providing evidence that the allocentric representation anchored to the visual cues is similar in these two brain areas under conditions where the rat is unconstrained and can move freely in any direction within the arena.

The difference in the probability of landmark control between the different stimuli are consistent with the distal sensory input model, suggesting that the visual features of the landmarks are important for resetting the PFD of HD cells. Although the present experiments did not address why landmark control varied between the cues, previous research has shown that behaving mice can detect differences in contrast assessed by psychometric curves obtained while the mice performed a

two-alternative forced-choice discrimination task (Busse et al., 2011). The strong landmark control for the vertical and horizontal bars could be the result of a strong preferred orientation tuning for cardinal compared to oblique stimuli (the oblique effect) which has been observed in a large fraction of neurons in primary (V1) (Li et al., 2003) and secondary (PMA) visual areas (Roth et al., 2012) which provide input to the PoS (Vogt & Miller, 1983) and the RSC (Makino & Komiyama, 2015; van Groen & Wyss, 2003). At the psychophysical level, the oblique effect has also been shown to bias visual perception in humans and match the local orientation distribution measured from images of natural scenes which have more cardinal compared to oblique orientations (Girshick et al., 2011).

Although little is known about the specific contribution of the PoS and the RSC to the visuospatial processing of landmarks in the rodent brain and the functional role of diverse visual projections to these areas, it is possible that the differences in cue discrimination amongst the cue types are the result of perceptual biases that arise from the processing of low-level visual features.

Furthermore, the differences in the contrast signal between the background arena and the surrounding background grey cylinder and the white stripe foreground (V-H) compared to the black stripes at the edges (V-H-p) might account for the magnitude of landmark discrimination between these two set of cues. However, since the number of trials recorded in the V-H stimuli (n=349) was five times higher than the V-H-p stimuli (n=69), the lower probability of landmark control in the V-H stimuli might be the result of a larger variance that reflects the contribution of a higher sample HD cells and rats rather than differences in discrimination and the use of these visual features for spatial orientation.

Future experiments would have to be conducted using the same stimuli and reversing the contrast between the cylinder and the cue cards (black cylinder with white foreground cue) or reversing the polarity of the T-B and R-L cue cards (black foreground cue with a white bar) to examine whether this effect persists. However, it is interesting to note that recent studies have shown that V1 neurons of the macaque brain have a preference for black over white stimuli (Xing, Yeh, & Shapley, 2010; Zurawel, Ayzenshtat, Zweig, Shapley, & Slovin, 2014). Whether

this preference is present in the rodent primary visual cortex and the extent to which it can influence the processing of landmarks by HD cells remains to be determined.

The above chance level of landmark control observed when rats were exposed to the right-left mirror-images which are symmetrical relative to the vertical axis is consistent with human fMRI studies that have shown that RSC activation does not show adaptation when mirror images of scenes are presented (Dilks, Julian, Kubilius, Spelke, & Kanwisher, 2011), a result which provides evidence that the RSC can distinguish mirror images as different given its important role in visual scene recognition, spatial navigation and landmark processing (Vann et al., 2009). Although the study did not address whether symmetry relative to the horizontal axis (a property of the top-bottom cues), leads to a strong activation of the RSC, the results of the HD cells recorded in the T-B cue cards would predict that in humans, presentation of images with horizontal symmetry would results in no adaptation of the fMRI signal in the RSC.

Furthermore, human neuroimaging studies have shown that RSC activity is strongly correlated with the processing of landmarks permanence, which is a feature of their perceived spatial stability, that is how likely they are expected to change their position across time (Auger, Mullally, & Maguire, 2012). Overall, these results are consistent with the hypothesised role of the RSC in integrating information about self-location in an allocentric reference frame (Alexander & Nitz, 2015), extracting visual and spatial information from landmarks and processing navigationally relevant information (Miller, Vedder, Law, & Smith, 2014).

Based on the results of the two cue experiments, the black, white and the stripe cue (black vertical bar on a white card) were chosen to investigate if PoS HD cells process the spatial configuration of multiple cues in a square environment. This was tested by exposing rats to a stable configuration where the cues maintained a constant position in reference to one another prior to changing the location between a subset of the cues (the black and stripe cue). The main findings from these experiments are that when the spatial arrangement of the cues is changed, HD cells respond to the new configuration by resetting relative to the cues that

changed their spatial position (the black and the stripe cue). These results are consistent with the distal sensory input model, providing evidence that the visuo-spatial relationship between the cues is an important factor used for spatial orientation by HD cells. Furthermore, the results of the multiple cues experiments showed that a stable cue configuration exerts strong control over PoS HD cells, providing further support that contrast and orientation are reliably used as landmarks to reset the PFD.

In summary, the results from these experiments provide evidence that the uniqueness in physical appearance and stable spatial position within an environment are important properties for a visual cue to be used as a landmark, reliably resetting the activity of PoS HD cells.

References

Abeles, M. (1982). Quantification, smoothing, and confidence limits for single-units' histograms. *Journal of Neuroscience Methods*, *5*, 317–325. http://doi.org/10.1016/0165-0270(82)90002-4

Alexander, A. S., & Nitz, D. a. (2015). Retrosplenial cortex maps the conjunction of internal and external spaces. *Nature Neuroscience*, *18*(8), 1143–1151. http://doi.org/10.1038/nn.4058

Arleo, A., Déjean, C., Allegraud, P., Khamassi, M., Zugaro, M. B., & Wiener, S. I. (2013). Optic flow stimuli update anterodorsal thalamus head direction neuronal activity in rats. *The Journal of Neuroscience*, *33*(42), 16790–5. http://doi.org/10.1523/JNEUROSCI.2698-13.2013

Arleo, A., & Rondi-Reig, L. (2007). Multimodal sensory integration and concurrent navigation strategies for spatial cognition in real and artificial organisms. *Journal of Integrative Neuroscience*, *6*(3), 327–366. http://doi.org/10.1142/S0219635207001593

Aronov, D., & Tank, D. W. (2014). Engagement of Neural Circuits Underlying 2D Spatial Navigation in a Rodent Virtual Reality System. *Neuron*, *84*(2), 442–456. http://doi.org/10.1016/j.neuron.2014.08.042

Artal, P., Herreros de Tejada, P., Muñoz-Tedo, C., & Green, D. G. (1998). Retinal image quality in the rodent eye. *Visual Neuroscience*, *15*(4), 597–605. http://doi.org/10.1017/S0952523898154020

Auger, S. D., Mullally, S. L., & Maguire, E. A. (2012). Retrosplenial Cortex Codes for Permanent Landmarks. *PLoS ONE*, *7*(8), e43620. http://doi.org/10.1371/journal.pone.0043620

Barry, C., Hayman, R., Burgess, N., & Jeffery, K. J. (2007). Experience-dependent rescaling of entorhinal grids. *Nature Neuroscience*, *10*(6), 682–684. http://doi.org/10.1038/nn1905

Barry, C., Lever, C., Hayman, R., Hartley, T., Burton, S., O'Keefe, J., … Burgess, N. (2006). The boundary vector cell model of place cell firing and spatial memory. *Reviews in the Neurosciences*, *17*(1-2), 71–97. http://doi.org/10.1515/REVNEURO.2006.17.1-2.71

Bassett, J. P., & Taube, J. S. (2001). Neural correlates for angular head velocity in the rat dorsal tegmental nucleus. *Journal of Neuroscience*, *21*(15), 5740–5751.

Bassett, J. P., & Taube, J. S. (2005). Head direction signal generation: Ascending and descending information streams. In S. I. Wiener & J. S. Taube (Eds.), *Head direction cells and the neural mechanisms of spatial orientation* (pp. 83–110). Cambridge: MIT Press.

Bassett, J. P., Tullman, M. L., & Taube, J. S. (2007). Lesions of the tegmentomammillary circuit in the head direction system disrupt the head direction signal in the anterior thalamus. *Journal of Neuroscience*, *27*(28), 7564–7577. http://doi.org/10.1523/JNEUROSCI.0268-07.2007

Batschelet, E. (1981). *Circular Statistics in Biology*. *Technometrics* (Vol. 24). http://doi.org/10.2307/1267831

Bennett, A. T. D. (1996). Do animals have cognitive maps? *Journal of Experimental Biology*, *199*, 219–224.

Berens, P. (2009). CircStat: A Matlab Toolbox for Circular Statistics. *Journal of Statistical Software*, *31*(10), 1–21.

Bett, D., Stevenson, C. H., Shires, K. L., Smith, M. T., Martin, S. J., Dudchenko, P. A., & Wood, E. R. (2013). The postsubiculum and spatial learning: the role of postsubicular synaptic activity and synaptic plasticity in hippocampal place cell, object, and object-location memory. *The Journal of Neuroscience*, *33*(16), 6928–43. http://doi.org/10.1523/JNEUROSCI.5476-12.2013

Bird, C. M., & Burgess, N. (2008). The hippocampus and memory: insights from spatial processing. *Nature Reviews Neuroscience*, *9*(3), 182–94. http://doi.org/10.1038/nrn2335

Bjerknes, T. L., Langston, R. F., Kruge, I. U., Moser, E. I., & Moser, M.-B. (2014). Coherence among Head Direction Cells before Eye Opening in Rat Pups. *Current Biology*, *25*(1), 103–8. http://doi.org/10.1016/j.cub.2014.11.009

Blair, H. T., Cho, J., & Sharp, P. E. (1999). The anterior thalamic head-direction signal is abolished by bilateral but not unilateral lesions of the lateral mammillary nucleus. *Journal of Neuroscience*, *19*(15), 6673–6683.

Blair, H. T., Lipscomb, B. W., & Sharp, P. E. (1997). Anticipatory time intervals of head-direction cells in the anterior thalamus of the rat: implications for path integration in the head-direction circuit. *Journal of Neurophysiology*, *78*, 145–159.

Blair, H. T., & Sharp, P. E. (1995). Anticipatory head direction signals in anterior thalamus: evidence for a thalamocortical circuit that integrates angular head motion to compute head direction. *Journal of Neuroscience*, *15*(9), 6260–6270.

Blair, H. T., & Sharp, P. E. (1996). Visual and vestibular influences on head-direction cells in the anterior thalamus of the rat. *Behavioral Neuroscience*, *110*(4), 643–660. http://doi.org/10.1037/0735-7044.110.4.643

Boccara, C. N., Sargolini, F., Thoresen, V. H., Solstad, T., Witter, M. P., Moser, E. I., & Moser, M.-B. (2010). Grid cells in pre- and parasubiculum. *Nature Neuroscience*, *13*(8), 987–994. http://doi.org/10.1038/nn.2602

Bonnevie, T., Dunn, B., Fyhn, M., Hafting, T., Derdikman, D., Kubie, J. L., … Moser, M.-B. (2013). Grid cells require excitatory drive from the hippocampus. *Nature Neuroscience*, *16*(3), 309–17. http://doi.org/10.1038/nn.3311

Bostock, E., Muller, R. U., & Kubie, J. L. (1991). Experience-dependent modifications of hippocampal place cell firing. *Hippocampus*, *1*(2), 193–205. http://doi.org/10.1002/hipo.450010207

Bowman, A., & Azzalini, A. (2014). sm: Smoothing methods for nonparametric regression and density.

Brandon, M. P., Koenig, J., & Leutgeb, S. (2014). Parallel and convergent processing in grid cell, head-direction cell, boundary cell, and place cell networks. *Wiley Interdisciplinary Reviews Cognitive Science*, *5*(2), 207–219. http://doi.org/10.1002/wcs.1272

Busse, L., Ayaz, A., Dhruv, N. T., Katzner, S., Saleem, A. B., Schölvinck, M. L., …

Carandini, M. (2011). The detection of visual contrast in the behaving mouse. *Journal of Neuroscience*, *31*(31), 11351–11361. http://doi.org/10.1523/JNEUROSCI.6689-10.2011

Buzsáki, G. (2004). Large-scale recording of neuronal ensembles. *Nature Neuroscience*, *7*(5), 446–51. http://doi.org/10.1038/nn1233

Buzsáki, G., & Moser, E. I. (2013). Memory, navigation and theta rhythm in the hippocampal-entorhinal system. *Nature Neuroscience*, *16*(2), 130–138. http://doi.org/10.1038/nn.3304

Cacucci, F., Lever, C., Wills, T. J., Burgess, N., & O'Keefe, J. (2004). Theta-modulated place-by-direction cells in the hippocampal formation in the rat. *Journal of Neuroscience*, *24*(38), 8265–8277. http://doi.org/10.1523/JNEUROSCI.2635-04.2004

Calton, J. L., Stackman, R. W., Goodridge, J. P., Archey, W. B., Dudchenko, P. A., & Taube, J. S. (2003). Hippocampal place cell instability after lesions of the head direction cell network. *The Journal of Neuroscience*, *23*(30), 9719–9731. http://doi.org/23/30/9719 [pii]

Calton, J. L., & Taube, J. S. (2009). Where am I and how will I get there from here? A role for posterior parietal cortex in the integration of spatial information and route planning. *Neurobiology of Learning and Memory*, *91*(2), 186–196. http://doi.org/10.1016/j.nlm.2008.09.015

Calton, J. L., Turner, C. S., Cyrenne, D. M., Lee, B. R., & Taube, J. S. (2008). Landmark control and updating of self-movement cues are largely maintained in head direction cells after lesions of the posterior parietal cortex. *Behavioral Neuroscience*, *122*(4), 827–840. http://doi.org/10.1037/0735-7044.122.4.827

Canto, C. B., Wouterlood, F. G., & Witter, M. P. (2008). What does the anatomical organization of the entorhinal cortex tell us? *Neural Plasticity*, 1–18. http://doi.org/10.1155/2008/381243

Cappaert, N. L. M., van Strien, N. M., & Witter, M. P. (2015). Hippocampal formation. In G. Paxinos (Ed.), *The Rat Nervous System* (Fourth, pp. 511–573). London: Academic Press. http://doi.org/10.1016/B978-0-12-374245-2.00019-X

Carandini, M., & Churchland, A. K. (2013). Probing perceptual decisions in rodents. *Nature Neuroscience*, *16*(7), 824–31. http://doi.org/10.1038/nn.3410

Cartwright, B. A., & Collett, T. S. (1983). Landmark learning in bees: Experiments and models. *Journal of Comparative Physiology*, *151*(4), 521–543. http://doi.org/10.1007/BF00605469

Cenquizca, L. a, & Swanson, L. W. (2007). Spatial organization of direct hippocampal field CA1 axonal projections to the rest of the cerebral cortex. *Brain Research Reviews*, *56*(1), 1–26. http://doi.org/10.1016/j.brainresrev.2007.05.002

Chan, E., Baumann, O., Bellgrove, M. a, & Mattingley, J. B. (2012). From objects to landmarks: The function of visual location information in spatial navigation. *Frontiers in Psychology*. http://doi.org/10.3389/fpsyg.2012.00304

Chen, L. L., Lin, L. H., Barnes, C. A., & McNaughton, B. L. (1994). Head-direction cells in the rat posterior cortex - II. Contributions of visual and ideothetic information to the directional firing. *Experimental Brain Research*, *101*, 24–34.

http://doi.org/10.1007/BF00243213

Chen, L. L., Lin, L. H., Green, E. J., Barnes, C. A., & McNaughton, B. L. (1994). Head-direction cells in the rat posterior cortex. I. Anatomical distribution and behavioral modulation. *Experimental Brain Research*, *101*, 8–23. http://doi.org/10.1007/BF00243213

Cho, J., & Sharp, P. E. (2001). Head direction, place, and movement correlates for cells in the rat retrosplenial cortex. *Behavioral Neuroscience*, *115*(1), 3–25. http://doi.org/10.1037/0735-7044.115.1.3

Clark, B. J., Bassett, J. P., Wang, S. S., & Taube, J. S. (2010). Impaired head direction cell representation in the anterodorsal thalamus after lesions of the retrosplenial cortex. *Journal of Neuroscience*, *30*(15), 5289–5302. http://doi.org/10.1523/JNEUROSCI.3380-09.2010

Clark, B. J., Harris, M. J., & Taube, J. S. (2010). Control of anterodorsal thalamic head direction cells by environmental boundaries: Comparison with conflicting distal landmarks. *Hippocampus*, *22*(2), 172–187. http://doi.org/10.1002/hipo.20880

Clark, B. J., & Taube, J. S. (2012, January). Vestibular and attractor network basis of the head direction cell signal in subcortical circuits. *Frontiers in Neural Circuits*. http://doi.org/10.3389/fncir.2012.00007

Collett, T. S., & Graham, P. (2004). Animal navigation: Path integration, visual landmarks and cognitive maps. *Current Biology*, *14*(12), R475–7. http://doi.org/10.1016/j.cub.2004.06.013

Coogan, T. A., & Burkhalter, A. (1993). Hierarchical organization of areas in rat visual cortex. *Journal of Neuroscience*, *13*(9), 3749–3772.

Cooper, B. G., & Mizumori, S. J. (2001). Temporary inactivation of the retrosplenial cortex causes a transient reorganization of spatial coding in the hippocampus. *Journal of Neuroscience*, *21*(11), 3986–4001. http://doi.org/21/11/3986 [pii]

Crowell, J. A., Banks, M. S., Shenoy, K. V, & Andersen, R. A. (1998). Visual self-motion perception during head turns. *Nature Neuroscience*, *1*(8), 732–737. http://doi.org/10.1038/3732

Cullen, K. E. (2012). The vestibular system: multimodal integration and encoding of self-motion for motor control. *Trends in Neurosciences*, *35*(3), 185–96. http://doi.org/10.1016/j.tins.2011.12.001

Czajkowski, R., Sugar, J., Zhang, S. J., Couey, J. J., Ye, J., & Witter, M. P. (2013). Superficially projecting principal neurons in layer V of medial entorhinal cortex in the rat receive excitatory retrosplenial input. *Journal of Neuroscience*, *33*(40), 15779–92. http://doi.org/10.1523/JNEUROSCI.2646-13.2013

Dilks, D. D., Julian, J. B., Kubilius, J., Spelke, E. S., & Kanwisher, N. (2011). Mirror-image sensitivity and invariance in object and scene processing pathways. *Journal of Neuroscience*, *31*(31), 11305–11312. http://doi.org/10.1523/JNEUROSCI.1935-11.2011

Dolorfo, C. L., & Amaral, D. G. (1998). Entorhinal cortex of the rat: Organization of intrinsic connections. *Journal of Comparative Neurology*, *398*(1), 49–82. http://doi.org/10.1002/(SICI)1096-9861(19980817)398:1<49::AID-CNE4>3.0.CO;2-9

Dudchenko, P. A., Goodridge, J. P., & Taube, J. S. (1997). The effects of disorientation on visual landmark control of head direction cell orientation. *Experimental Brain Research*, *115*, 375–380.

Einhäuser, W., & König, P. (2010). Getting real-sensory processing of natural stimuli. *Current Opinion in Neurobiology*, *20*(3), 389–395. http://doi.org/10.1016/j.conb.2010.03.010

Ekstrom, A. D., Kahana, M. J., Caplan, J. B., Fields, T. A., Isham, E. A., Newman, E. L., & Fried, I. (2003). Cellular networks underlying human spatial navigation. *Nature*, *425*(6954), 184–188. http://doi.org/10.1038/nature01964

Elduayen, C., & Save, E. (2014). The retrosplenial cortex is necessary for path integration in the dark. *Behavioural Brain Research*, *272*, 303–7. http://doi.org/10.1016/j.bbr.2014.07.009

Etienne, A. S., & Jeffery, K. J. (2004). Path integration in mammals. *Hippocampus*, *14*(2), 180–92. http://doi.org/10.1002/hipo.10173

Etienne, A. S., Maurer, R., Boulens, V., Levy, A., & Rowe, T. (2004). Resetting the path integrator: a basic condition for route-based navigation. *Journal of Experimental Biology*, *207*(9), 1491–1508. http://doi.org/10.1242/jeb.00906

Fenton, A. A., Csizmadia, G., & Muller, R. U. (2000). Conjoint control of hippocampal place cell firing by two visual stimuli. I. The effects of moving the stimuli on firing field positions. *Journal of General Physiology*, *116*(8), 191–209. http://doi.org/10.1085/jgp.116.2.191

Fetsch, C. R., DeAngelis, G. C., & Angelaki, D. E. (2013). Bridging the gap between theories of sensory cue integration and the physiology of multisensory neurons. *Nature Reviews Neuroscience*, *14*(6), 429–42. http://doi.org/10.1038/nrn3503

Finkelstein, A., Derdikman, D., Rubin, A., Foerster, J. N., Las, L., & Ulanovsky, N. (2015). Three-dimensional head-direction coding in the bat brain. *Nature*, *517*(7533), 159–164. http://doi.org/10.1038/nature14031

Fisher, N. I. (1995). *Statistical Analysis of Circular Data*. Cambridge: Cambridge University Press.

Furtak, S. C., Ahmed, O. J., & Burwell, R. D. (2012). Single Neuron Activity and Theta Modulation in Postrhinal Cortex during Visual Object Discrimination. *Neuron*, *76*(5), 976–988. http://doi.org/10.1016/j.neuron.2012.10.039

Gallistel, C. R. (1990). *The Organization of Learning*. Cambridge: MIT Press.

Geva-Sagiv, M., Las, L., Yovel, Y., & Ulanovsky, N. (2015). Spatial cognition in bats and rats: from sensory acquisition to multiscale maps and navigation. *Nature Reviews Neuroscience*, *16*(2), 94–108. http://doi.org/10.1038/nrn3888

Giocomo, L. M., Stensola, T., Bonnevie, T., Van Cauter, T., Moser, M. B., & Moser, E. I. (2014a). Topography of head direction cells in medial entorhinal cortex. *Current Biology*, *24*(3), 252–262. http://doi.org/10.1016/j.cub.2013.12.002

Giocomo, L. M., Stensola, T., Bonnevie, T., Van Cauter, T., Moser, M.-B., & Moser, E. I. (2014b). Topography of head direction cells in medial entorhinal cortex. *Current Biology*, *24*(3), 252–262. http://doi.org/10.1016/j.cub.2013.12.002

Girman, S. V, Sauvé, Y., & Lund, R. D. (1999). Receptive field properties of single

neurons in rat primary visual cortex. *Journal of Neurophysiology*, *82*, 301–311.

Girshick, A. R., Landy, M. S., & Simoncelli, E. P. (2011). Cardinal rules: Visual orientation perception reflects knowledge of environmental statistics. *Nature Neuroscience*, *14*(7), 926–932. http://doi.org/10.1038/nn.2831

Golob, E. J., Stackman, R. W., Wong, A. C., & Taube, J. S. (2001). On the behavioral significance of head direction cells: neural and behavioral dynamics during spatial memory tasks. *Behavioral Neuroscience*.

Golob, E. J., & Taube, J. S. (1997). Head direction cells and episodic spatial information in rats without a hippocampus. *Proceedings of the National Academy of Sciences*, *94*(7), 7645–7650. http://doi.org/10.1073/pnas.94.14.7645

Golob, E. J., Wolk, D. A., & Taube, J. S. (1998). Recordings of postsubiculum head direction cells following lesions of the laterodorsal thalamic nucleus. *Brain Research*, *780*, 9–19. http://doi.org/10.1016/S0006-8993(97)01076-7

Goodridge, J. P., Dudchenko, P. A., Worboys, K. A., Golob, E. J., & Taube, J. S. (1998). Cue control and head direction cells. *Behavioral Neuroscience*, *112*(4), 749–761.

Goodridge, J. P., & Taube, J. S. (1995). Preferential use of the landmark navigational system by head direction cells in rats. *Behavioral Neuroscience*, *109*(1), 49–61. http://doi.org/10.1037/0735-7044.109.1.49

Goodridge, J. P., & Taube, J. S. (1997). Interaction between the postsubiculum and anterior thalamus in the generation of head direction cell activity. *Journal of Neuroscience*, *17*(23), 9315–9330.

Grabska-Barwińska, A., Ng, B. S. W., & Jancke, D. (2012). Orientation selective or not? - Measuring significance of tuning to a circular parameter. *Journal of Neuroscience Methods*, *203*(1), 1–9. http://doi.org/10.1016/j.jneumeth.2011.08.026

Grieves, R. M., & Dudchenko, P. A. (2013). Cognitive maps and spatial inference in animals: Rats fail to take a novel shortcut, but can take a previously experienced one. *Learning and Motivation*, *44*(2), 81–92. http://doi.org/10.1016/j.lmot.2012.08.001

Hafting, T., Fyhn, M., Molden, S., Moser, M.-B., & Moser, E. I. (2005). Microstructure of a spatial map in the entorhinal cortex. *Nature*, *436*(7052), 801–806. http://doi.org/10.1038/nature03721

Hales, J. B., Schlesiger, M. I., Leutgeb, J. K., Squire, L. R., Leutgeb, S., & Clark, R. E. (2014). Medial Entorhinal Cortex Lesions Only Partially Disrupt Hippocampal Place Cells and Hippocampus-Dependent Place Memory. *Cell Reports*, *9*(3), 1–9. http://doi.org/10.1016/j.celrep.2014.10.009

Hall, P., Watson, G. S., & Cabrera, J. (1987). Kernel density estimation with spherical data. *Biometrika*, *74*, 751–762. http://doi.org/10.1093/biomet/74.4.751

Halsey, L. G., Curran-Everett, D., Vowler, S. L., & Drummond, G. B. (2015). The fickle P value generates irreproducible results. *Nature Methods*, *12*(3), 179–185. http://doi.org/10.1038/nmeth.3288.

Hamilton, D. A., Akers, K. G., Weisend, M. P., & Sutherland, R. J. (2007). How do room and apparatus cues control navigation in the Morris water task? Evidence for distinct contributions to a movement vector. *Journal of Experimental Psychology*

Animal Behavior Processes, *33*(2), 100–114. http://doi.org/10.1037/0097-7403.33.2.100

Hardcastle, K., Ganguli, S., & Giocomo, L. (2015). Environmental boundaries as an error correction mechanism for grid cells. *Neuron*, *86*, 1–13.

Hargreaves, E. L., Yoganarasimha, D., & Knierim, J. J. (2007). Cohesiveness of spatial and directional representations recorded from neural ensembles in the anterior thalamus, parasubiculum, medial entorhinal cortex, and hippocampus. *Hippocampus*, *17*, 826–841. http://doi.org/10.1002/hipo.20316

Hartley, T., Burgess, N., Lever, C., Cacucci, F., & O'Keefe, J. (2000). Modeling place fields in terms of the cortical inputs to the hippocampus. *Hippocampus*, *10*(4), 369–379. http://doi.org/10.1002/1098-1063(2000)10:4<369::AID-HIPO3>3.0.CO;2-0

Hayakawa, T., & Zyo, K. (1990). Fine structure of the lateral mammilary projection to the dorsal tegmental nucleus of Gudden in the rat. *Journal of Comparative Neurology*, *298*(2), 224–236. http://doi.org/10.1002/cne.902980207

Henze, D. A., Borhegyi, Z., Csicsvari, J., Mamiya, A., Harris, K. D., & Buzsáki, G. (2000). Intracellular features predicted by extracellular recordings in the hippocampus in vivo. *Journal of Neurophysiology*, *84*(1), 390–400. http://doi.org/84:390-400

Huberman, A. D., & Niell, C. M. (2011). What can mice tell us about how vision works? *Trends in Neurosciences*, *34*(9), 464–473. http://doi.org/10.1016/j.tins.2011.07.002

Jacobs, L. F., & Menzel, R. (2014). Navigation outside of the box: what the lab can learn from the field and what the field can learn from the lab. *Movement Ecology*, *2*(3), 1–22. http://doi.org/10.1186/2051-3933-2-3

Jeffery, K. J. (1998). Learning of landmark stability and instability by hippocampal place cells. *Neuropharmacology*, *37*(4-5), 677–687. http://doi.org/10.1016/S0028-3908(98)00053-7

Jeffery, K. J. (2007a). Integration of the sensory inputs to place cells: What, where, why, and how? *Hippocampus*, *17*(9), 775–785. http://doi.org/10.1002/hipo.20322

Jeffery, K. J. (2007b). Self-localization and the entorhinal-hippocampal system. *Current Opinion in Neurobiology*, *17*(6), 684–91. http://doi.org/10.1016/j.conb.2007.11.008

Jeffery, K. J., Donnett, J. G., Burgess, N., & O'Keefe, J. M. (1997). Directional control of hippocampal place fields. *Experimental Brain Research*, *117*(1), 131–142. http://doi.org/10.1007/s002210050206

Jeon, C. J., Strettoi, E., & Masland, R. H. (1998). The major cell populations of the mouse retina. *Journal of Neuroscience*, *18*(21), 8936–8946.

Johnson, A., Jackson, J. C., & Redish, A. D. (2008). Measuring distributed properties of neural representations beyond the decoding of local variables: implications for cognition. In *Mechanisms of information processing in the brain: Encoding of information in neural populations and networks* (pp. 1–31).

Johnson, A., Seeland, K., & Redish, A. D. (2005). Reconstruction of the postsubiculum head direction signal from neural ensembles. *Hippocampus*, *15*, 86–96. http://doi.org/10.1002/hipo.20033

Julian, J. B., Keinath, A. T., Muzzio, I. A., & Epstein, R. A. (2015). Place recognition and

heading retrieval are mediated by dissociable cognitive systems in mice. *Proceedings of the National Academy of Sciences*, *112*(20), 6503–6508. http://doi.org/10.1073/pnas.1424194112

Kass, R. E. (2005). Statistical Issues in the Analysis of Neuronal Data. *Journal of Neurophysiology*, *94*(1), 8–25. http://doi.org/10.1152/jn.00648.2004

Katzner, S., & Weigelt, S. (2013). Visual cortical networks: Of mice and men. *Current Opinion in Neurobiology*, *23*(2), 202–206. http://doi.org/10.1016/j.conb.2013.01.019

Klatzky, R. L. (1998). Allocentric and Egocentric Spatial Representations: Definitions, Distinctions, and Interconnections. In *Spatial cognition - An interdisciplinary approach to representation and processing of spatial knowledge* (pp. 1–17). http://doi.org/10.1007/3-540-69342-4_1

Knierim, J. J., & Hamilton, D. A. (2011). Framing Spatial Cognition: Neural Representations of Proximal and Distal Frames of Reference and Their Roles in Navigation. *Physiological Reviews*. http://doi.org/10.1152/physrev.00021.2010

Knierim, J. J., Kudrimoti, H. S., & McNaughton, B. L. (1995). Place cells, head direction cells, and the learning of landmark stability. *Journal of Neuroscience*, *15*(3), 1648–1659.

Knierim, J. J., Kudrimoti, H. S., & McNaughton, B. L. (1998). Interactions between idiothetic cues and external landmarks in the control of place cells and head direction cells. *Journal of Neurophysiology*, *80*, 425–446.

Knierim, J. J., & Zhang, K. (2012). Attractor Dynamics of Spatially Correlated Neural Activity in the Limbic System. *Annual Review of Neuroscience*, *35*(March), 267–285. http://doi.org/10.1146/annurev-neuro-062111-150351

Knight, R., Hayman, R., Ginzberg, L. L., & Jeffery, K. (2011). Geometric cues influence head direction cells only weakly in nondisoriented rats. *Journal of Neuroscience*, *31*(44), 15681–92. http://doi.org/10.1523/JNEUROSCI.2257-11.2011

Knight, R., Piette, C. E., Page, H., Walters, D., Marozzi, E., Nardini, M., … Jeffery, K. J. (2013). Weighted cue integration in the rodent head direction system. *Philosophical Transactions of the Royal Society B: Biological Sciences*, *369*(1635), 20120512–20120512. http://doi.org/10.1098/rstb.2012.0512

Kravitz, D. J., Saleem, K. S., Baker, C. I., & Mishkin, M. (2011). A new neural framework for visuospatial processing. *Nature Reviews Neuroscience*, *12*(4), 217–230. http://doi.org/10.1167/11.11.923

Kruschke, J. K. (2015). *Doing Bayesian Data Analysis: A Tutorial with R, JAGS, and Stan* (2nd ed.). London: Academic Press.

Krzywinski, M., & Altman, N. (2013). Points of significance: Significance, P values and t-tests. *Nature Methods*, *10*(11), 1041–1042. http://doi.org/10.1038/nmeth.2698

Leutgeb, S., Leutgeb, J. K., Barnes, C. A., Moser, E. I., McNaughton, B. L., & Moser, M.-B. (2005). Independent codes for spatial and episodic memory in hippocampal neuronal ensembles. *Science (New York, N.Y.)*, *309*(5734), 619–623. http://doi.org/10.1126/science.1114037

Leutgeb, S., Ragozzino, K. E., & Mizumori, S. J. Y. (2000). Convergence of head direction and place information in the CA1 region of hippocampus. *Neuroscience*,

100(1), 11–19. http://doi.org/10.1016/S0306-4522(00)00258-X

Lever, C., Burton, S., Jeewajee, A., O'Keefe, J., & Burgess, N. (2009). Boundary vector cells in the subiculum of the hippocampal formation. *The Journal of Neuroscience*, *29*(31), 9771–9777. http://doi.org/10.1523/JNEUROSCI.1319-09.2009

Lever, C., Wills, T., Cacucci, F., Burgess, N., & O'Keefe, J. (2002). Long-term plasticity in hippocampal place-cell representation of environmental geometry. *Nature*, *416*(6876), 90–94. http://doi.org/10.1038/416090a

Li, B., Peterson, M. R., & Freeman, R. D. (2003). Oblique effect: a neural basis in the visual cortex. *Journal of Neurophysiology*, *90*(1), 204–217. http://doi.org/10.1152/jn.00954.2002

Lozano, Y. R., Serafín, N., Prado-Alcalá, R. a, Roozendaal, B., & Quirarte, G. L. (2013). Glucocorticoids in the dorsomedial striatum modulate the consolidation of spatial but not procedural memory. *Neurobiology of Learning and Memory*, *101*, 55–64. http://doi.org/10.1016/j.nlm.2013.01.001

Lund, U., & Agostinelli, C. (2013). circular: Circular Statistics.

Makino, H., & Komiyama, T. (2015). Learning enhances the relative impact of top-down processing in the visual cortex. *Nature Neuroscience*, *18*(8), 1116–1122. http://doi.org/10.1038/nn.4061

Mardia, K. V, & Jupp, P. E. (2000). *Directional Statistics*. New York: John Wiley. http://doi.org/10.1002/9780470316979

McNaughton, B. L., Battaglia, F. P., Jensen, O., Moser, E. I., & Moser, M.-B. (2006). Path integration and the neural basis of the "cognitive map". *Nature Reviews Neuroscience*, *7*(8), 663–678. http://doi.org/10.1038/nrn1932

McNaughton, B. L., O'Keefe, J., & Barnes, C. A. (1983). The stereotrode: A new technique for simultaneous isolation of several single units in the central nervous system for multiple unit records. *Journal of Neuroscience Methods*, *8*, 391–397. http://doi.org/10.1016/0165-0270(83)90097-3

Miller, A. M. P., Vedder, L. C., Law, L. M., & Smith, D. M. (2014). Cues, context, and long-term memory: the role of the retrosplenial cortex in spatial cognition. *Frontiers in Human Neuroscience*, *8*(8), 586. http://doi.org/10.3389/fnhum.2014.00586

Miller, M. W., & Vogt, B. A. (1984). Direct connections of rat visual cortex with sensory, motor, and association cortices. *Journal of Comparative Neurology*, *226*, 184–202. http://doi.org/10.1002/cne.902260204

Mittelstaedt, M. L., & Mittelstaedt, H. (1980). Homing by path integration in a mammal. *Naturwissenschaften*, *67*(11), 566–567. http://doi.org/10.1007/BF00450672

Miyashita, T., & Rockland, K. S. (2007). GABAergic projections from the hippocampus to the retrosplenial cortex in the rat. *European Journal of Neuroscience*, *26*(5), 1193–1204. http://doi.org/10.1111/j.1460-9568.2007.05745.x

Mizumori, S. J., & Williams, J. D. (1993). Directionally selective mnemonic properties of neurons in the lateral dorsal nucleus of the thalamus of rats. *Journal of Neuroscience*, *13*(9), 4015–4028.

Monaco, J. D., Rao, G., Roth, E. D., & Knierim, J. J. (2014). Attentive scanning behavior drives one-trial potentiation of hippocampal place fields. *Nature Neuroscience*,

17(5), 725–31. http://doi.org/10.1038/nn.3687

Moser, E. I., Kropff, E., & Moser, M.-B. (2008). Place cells, grid cells, and the brain's spatial representation system. *Annual Review of Neuroscience*, *31*(2), 69–89. http://doi.org/10.1146/annurev.neuro.31.061307.090723

Moser, E. I., Roudi, Y., Witter, M. P., Kentros, C., Bonhoeffer, T., & Moser, M.-B. (2014). Grid cells and cortical representation. *Nature Reviews Neuroscience*, *15*(7), 466–481. http://doi.org/10.1038/nrn3766

Muir, G. M., & Taube, J. S. (2004). Head direction cell activity and behavior in a navigation task requiring a cognitive mapping strategy. *Behavioural Brain Research*, *153*(1), 249–253. http://doi.org/10.1016/j.bbr.2003.12.007

Muller, R. U., & Kubie, J. L. (1987). The effects of changes in the environment on the spatial firing of hippocampal complex-spike cells. *The Journal of Neuroscience*, *7*(7), 1951–1968.

Muller, R. U., Kubie, J. L., & Ranck, J. B. (1987). Spatial firing patterns of hippocampal complex-spike cells in a fixed environment. *Journal of Neuroscience*, *7*(7), 1935–1950. http://doi.org/10.1016/S0301-0082(96)00019-6

Muller, R. U., Ranck, J. B., & Taube, J. S. (1996). Head direction cells: properties and functional significance. *Current Opinion in Neurobiology*, *6*(2), 196–206.

Naselaris, T., Merchant, H., Amirikian, B., & Georgopoulos, A. P. (2006). Large-scale organization of preferred directions in the motor cortex. I. Motor cortical hyperacuity for forward reaching. *Journal of Neurophysiology*, *96*, 3231–3236. http://doi.org/10.1152/jn.00487.2006

Nitz, D. A. (2006). Tracking route progression in the posterior parietal cortex. *Neuron*, *49*(5), 747–756. http://doi.org/10.1016/j.neuron.2006.01.037

Nitz, D. A. (2012). Spaces within spaces: Rat parietal cortex neurons register position across three reference frames. *Nature Neuroscience*, *15*(10), 1365–1367. http://doi.org/10.1038/nn.3213

O'Keefe, J., & Burgess, N. (1996). Geometric determinants of the place fields of hippocampal neurons. *Nature*, *381*(6581), 425–428. http://doi.org/10.1038/381425a0

O'Keefe, J., & Conway, D. H. (1978). Hippocampal place units in the freely moving rat: why they fire where they fire. *Experimental Brain Research*, *31*(4), 573–90. http://doi.org/10.1007/BF00239813

O'Keefe, J., & Dostrovsky, J. (1971). The hippocampus as a spatial map. Preliminary evidence from unit activity in the freely-moving rat. *Brain Research*, *34*(1), 171–175. http://doi.org/10.1016/0006-8993(71)90358-1

O'Keefe, J., & Nadel, L. (1978). *The Hippocampus as a Cognitive Map*. United Kingdom: Oxford University Press.

Oliveira, M., Crujeiras, R. M., & Rodriguez-Casal, A. (2014). NPCirc : An R Package for Nonparametric Circular Methods. *Journal of Statistical Software*, *61*(9), 1–26.

Oliviera, M., Crujeiras, R. M., & Rodriguez-Casal, A. (2014). NPCirc: an R package for nonparametric circular methods. *Journal of Statistical Software*, *61*(9), 1–81.

Paxinos, G., & Watson, C. (2007). *The Rat Brain in Stereotaxic Coordinates*. *Academic press* (6th ed.). London: Academic Press.

Paz-Villagràn, V., Lenck-Santini, P. P., Save, E., & Poucet, B. (2002). Properties of place cell firing after damage to the visual cortex. *European Journal of Neuroscience*, *16*(4), 771–776. http://doi.org/10.1046/j.1460-9568.2002.02154.x

Penner, M. R., & Mizumori, S. J. Y. (2012). Neural systems analysis of decision making during goal-directed navigation. *Progress in Neurobiology*, *96*(1), 96–135. http://doi.org/10.1016/j.pneurobio.2011.08.010

Pewsey, A., Neuhäuser, M., & Ruxton, G. D. (2013). *Circular Statistics in R*. Oxford: Oxford University Press.

Peyrache, A., Lacroix, M. M., Petersen, P. C., & Buzsáki, G. (2015). Internally organized mechanisms of the head direction sense. *Nature Neuroscience*, *18*(4), 569–575. http://doi.org/10.1038/nn.3968

Quian-Quiroga, R., & Panzeri, S. (2009). Extracting information from neuronal populations: information theory and decoding approaches. *Nature Reviews Neuroscience*, *10*(3), 173–185. http://doi.org/10.1038/nrn2578

Quirk, G. J., Muller, R. U., & Kubie, J. L. (1990). The firing of hippocampal place cells in the dark depends on the rat's recent experience. *The Journal of Neuroscience*, *10*(6), 2008–2017.

R Core Team. (2014). *R: A Language and Environment for Statistical Computing*. Vienna, Austria: R Foundation for Statistical Computing.

Ranck, J. B. (1984). Head-direction cells in the deep layers of the dorsal presubiculum in freely-moving rats. *Society of Neuroscience Abstracts*.

Ranganath, C., & Ritchey, M. (2012). Two cortical systems for memory-guided behaviour. *Nature Reviews Neuroscience*, *13*(10), 713–726. http://doi.org/10.1038/nrn3338

Raudies, F., Brandon, M. P., Chapman, G. W., & Hasselmo, M. E. (2015). Head direction is coded more strongly than movement direction in a population of entorhinal neurons. *Brain Research*, *1621*, 355–367. http://doi.org/10.1016/j.brainres.2014.10.053

Redish, A. D. (1999). *Beyond the Cognitive Map: From Place Cells to Episodic Memory*. Cambridge: MIT Press.

Robertson, R. G., Rolls, E. T., Georges-François, P., & Panzeri, S. (1999). Head direction cells in the primate pre-subiculum. *Hippocampus*, *9*(3), 206–219. http://doi.org/10.1002/(SICI)1098-1063(1999)9:3<206::AID-HIPO2>3.0.CO;2-H

Robinson, S., Keene, C. S., Iaccarino, H. F., Duan, D., & Bucci, D. J. (2011). Involvement of retrosplenial cortex in forming associations between multiple sensory stimuli. *Behavioral Neuroscience*, *125*(4), 578–587. http://doi.org/10.1037/a0024262

Rolls, E. T. (2010). Attractor networks. *Wiley Interdisciplinary Reviews: Cognitive Science*. http://doi.org/10.1002/wcs.1

Roth, M. M., Helmchen, F., & Kampa, B. M. (2012). Distinct Functional Properties of Primary and Posteromedial Visual Area of Mouse Neocortex. *Journal of*

Neuroscience, *32*(28), 9716–9726. http://doi.org/10.1523/JNEUROSCI.0110-12.2012

Rousselet, G. a, Thorpe, S. J., & Fabre-Thorpe, M. (2004, August). How parallel is visual processing in the ventral pathway? *Trends in Cognitive Sciences*. http://doi.org/10.1016/j.tics.2004.06.003

Saleem, A. B., Ayaz, A., Jeffery, K. J., Harris, K. D., & Carandini, M. (2013). Integration of visual motion and locomotion in mouse visual cortex. *Nature Neuroscience*, *16*(12), 1864–9. http://doi.org/10.1038/nn.3567

Samsonovich, A., & McNaughton, B. L. (1997). Path integration and cognitive mapping in a continuous attractor neural network model. *The Journal of Neuroscience*, *17*(15), 5900–5920.

Sargolini, F., Fyhn, M., Hafting, T., McNaughton, B. L., Witter, M. P., Moser, M.-B., & Moser, E. I. (2006). Conjunctive representation of position, direction, and velocity in entorhinal cortex. *Science*, *312*(5774), 758–762. http://doi.org/10.1126/science.1125572

Seelig, J. D., & Jayaraman, V. (2015). Neural dynamics for landmark orientation and angular path integration. *Nature*, *521*(7551), 186–191. http://doi.org/10.1038/nature14446

Sefton, A. J., Dreher, B., Harvey, A. R., & Martin, P. R. (2015). Visual system. In G. Paxinos (Ed.), *The Rat Nervous System* (Fourth, pp. 947–983). London: Academic Press. http://doi.org/10.1016/B978-0-12-374245-2.00019-X

Sharp, P. E., Blair, H. T., & Cho, J. (2001). The anatomical and computational basis of the rat head-direction cell signal. *Trends in Neurosciences*. http://doi.org/10.1016/S0166-2236(00)01797-5

Sharp, P. E., & Koester, K. (2008). Lesions of the mammillary body region severely disrupt the cortical head direction, but not place cell signal. *Hippocampus*, *18*(8), 766–784. http://doi.org/10.1002/hipo.20436

Sharp, P. E., Tinkelman, A., & Cho, J. (2001). Angular velocity and head direction signals recorded from the dorsal tegmental nucleus of gudden in the rat: Implications for path integration in the head direction cell circuit. *Behavioral Neuroscience*, *115*(3), 571–588. http://doi.org/10.1037/0735-7044.115.3.571

Shepherd, G. M. (2004). Introduction to synaptic circuits. In G. M. Shepherd (Ed.), *The synaptic organization of the brain* (5th ed., pp. 1–38). New York: Oxford University Press. http://doi.org/10.1093/acprof:oso/9780195159561.001.

Shinder, M. E., & Taube, J. S. (2011). Active and passive movement are encoded equally by head direction cells in the anterodorsal thalamus. *Journal of Neurophysiology*, *106*(2), 788–800. http://doi.org/10.1152/jn.01098.2010

Skaggs, W. E., Knierim, J. J., Kudrimoti, H. S., & McNaughton, B. L. (1995). A model of the neural basis of the rat's sense of direction. *Advances in Neural Information Processing Systems*, *7*(1984), 173–180.

Solstad, T., Boccara, C. N., Moser, M.-B., & Moser, E. I. (2008). Representation of geometric borders in the entorhinal cortex. *Science*, *19*(322), 1865–1868. http://doi.org/10.1016/j.neuron.2014.02.014

Song, P., & Wang, X.-J. (2005). Angular path integration by moving “hill of activity”: a spiking neuron model without recurrent excitation of the head-direction system. *Journal of Neuroscience*, *25*(4), 1002–1014. http://doi.org/10.1523/JNEUROSCI.4172-04.2005

Stackman, R. W., Clark, A. S., & Taube, J. S. (2002). Hippocampal spatial representations require vestibular input. *Hippocampus*, *12*(3), 291–303. http://doi.org/10.1002/hipo.1112

Stackman, R. W., Golob, E. J., Bassett, J. P., & Taube, J. S. (2003). Passive transport disrupts directional path integration by rat head direction cells. *Journal of Neurophysiology*, *90*(5), 2862–2874. http://doi.org/10.1152/jn.00346.2003

Stackman, R. W., Lora, J. C., & Williams, S. B. (2012, July 25). Directional Responding of C57BL/6J Mice in the Morris Water Maze Is Influenced by Visual and Vestibular Cues and Is Dependent on the Anterior Thalamic Nuclei. *Journal of Neuroscience*. http://doi.org/10.1523/JNEUROSCI.4868-11.2012

Stackman, R. W., & Taube, J. S. (1997). Firing properties of head direction cells in the rat anterior thalamic nucleus: dependence on vestibular input. *Journal of Neuroscience*, *17*(11), 4349–4358.

Stackman, R. W., & Taube, J. S. (1998). Firing properties of rat lateral mammillary single units: head direction, head pitch, and angular head velocity. *Journal of Neuroscience*, *18*(21), 9020–9037.

Stein, B. E., & Stanford, T. R. (2008). Multisensory integration: current issues from the perspective of the single neuron. *Nature Reviews Neuroscience*, *9*(4), 255–266. http://doi.org/10.1038/nrn2377

Stensola, H., Stensola, T., Solstad, T., Frøland, K., Moser, M.-B., & Moser, E. I. (2012). The entorhinal grid map is discretized. *Nature*, *492*(7427), 72–8. http://doi.org/10.1038/nature11649

Stensola, T., Stensola, H., Moser, M.-B., & Moser, E. I. (2015). Shearing-induced asymmetry in entorhinal grid cells. *Nature*, *518*(7538), 207–212. http://doi.org/10.1038/nature14151

Sugar, J., Witter, M. P., van Strien, N. M., & Cappaert, N. L. M. (2011). The retrosplenial cortex: Intrinsic connectivity and connections with the (para)hippocampal region in the rat. An interactive connectome. *Frontiers in Neuroinformatics*, *5*(7), 1–13. http://doi.org/10.3389/fninf.2011.00007

Switkes, E., Mayer, M. J., & Sloan, J. A. (1978). Spatial frequency analysis of the visual environment: anisotropy and the carpentered environment hypothesis. *Vision Research*, *18*(10), 1393–1399. http://doi.org/10.1016/0042-6989(78)90232-8

Szymusiak, R., & Nitz, D. (2003). Chronic recording of extracellular neuronal activity in behaving animals. *Current Protocols in Neuroscience*, *Chapter 6*(Unit 6.16). http://doi.org/10.1002/0471142301.ns0616s21

Tafazoli, S., Di Filippo, A., & Zoccolan, D. (2012). Transformation-Tolerant Object Recognition in Rats Revealed by Visual Priming. *Journal of Neuroscience*. http://doi.org/10.1523/JNEUROSCI.3932-11.2012

Tan, H. M., Bassett, J. P., O’Keefe, J., Cacucci, F., & Wills, T. J. (2015). The Development of the Head Direction System before Eye Opening in the Rat. *Current*

Biology, *25*(4), 479–483. http://doi.org/10.1016/j.cub.2014.12.030

Tang, Q., Brecht, M., & Burgalossi, A. (2014). Juxtacellular recording and morphological identification of single neurons in freely moving rats. *Nature Protocols*, *9*(10), 2369–2381. http://doi.org/10.1038/nprot.2014.161

Taube, J. S. (1995). Head direction cells recorded in the anterior thalamic nuclei of freely moving rats. *Journal of Neuroscience*, *15*(1), 70–86.

Taube, J. S. (2007). The head direction signal: origins and sensory-motor integration. *Annual Review of Neuroscience*, *30*, 181–207. http://doi.org/10.1146/annurev.neuro.29.051605.112854

Taube, J. S., & Bassett, J. P. (2003). Persistent Neural Activity in Head Direction Cells. *Cerebral Cortex*, *13*(11), 1162–1172. http://doi.org/10.1093/cercor/bhg102

Taube, J. S., & Burton, H. L. (1995). Head direction cell activity monitored in a novel environment and during a cue conflict situation. *Journal of Neurophysiology*, *74*(5), 1953–1971.

Taube, J. S., & Muller, R. U. (1998). Comparisons of head direction cell activity in the postsubiculum and anterior thalamus of freely moving rats. *Hippocampus*, *8*(January), 87–108. http://doi.org/10.1002/(SICI)1098-1063(1998)8:2<87::AID-HIPO1>3.0.CO;2-4

Taube, J. S., Muller, R. U., & Ranck, J. B. (1990a). Head-direction cells recorded from the postsubiculum in freely moving rats. I. Description and quantitative analysis. *Journal of Neuroscience*, *10*(2), 420–435. http://doi.org/10.1212/01.wnl.0000299117.48935.2e

Taube, J. S., Muller, R. U., & Ranck, J. B. (1990b). Head-direction cells recorded from the postsubiculum in freely moving rats. II. Effects of environmental manipulations. *Journal of Neuroscience*, *10*(2), 436–447. http://doi.org/10.1212/01.wnl.0000299117.48935.2e

Taube, J. S., Wang, S. S., Kim, S. Y., & Frohardt, R. J. (2013). Updating of the spatial reference frame of head direction cells in response to locomotion in the vertical plane. *Journal of Neurophysiology*, *109*(3), 873–88. http://doi.org/10.1152/jn.00239.2012

Thompson, S. M., & Robertson, R. T. (1987). Organization of subcortical pathways for sensory projections to the limbic cortex. II. Afferent projections to the thalamic lateral dorsal nucleus in the rat. *The Journal of Comparative Neurology*, *265*(2), 189–202. http://doi.org/10.1002/cne.902650204

Tinbergen, N. (1951). *The Study of Instinct*. United Kingdom: Clarendon Press.

Tolman, E. C. (1948). Cognitive maps in rats and men. *Psychological Review*, *55*(4), 189–208. http://doi.org/10.1037/h0061626

Tsanov, M., Chah, E., Vann, S. D., Reilly, R. B., Erichsen, J. T., Aggleton, J. P., & O'Mara, S. M. (2011). Theta-modulated head direction cells in the rat anterior thalamus. *Journal of Neuroscience*, *31*(26), 9489–502. http://doi.org/10.1523/JNEUROSCI.0353-11.2011

Ungerleider, L. G., & Mishkin, M. (1982). Two cortical visual systems. *Analysis of Visual Behavior*, *549*, 549–586. http://doi.org/10.2139/ssrn.1353746

Valerio, S., & Taube, J. S. (2012a). Path integration: how the head direction signal maintains and corrects spatial orientation. *Nature Neuroscience*, *15*(10), 1445–1453. http://doi.org/10.1038/nn.3215

Valerio, S., & Taube, J. S. (2012b). Path integration: how the head direction signal maintains and corrects spatial orientation. *Nature Neuroscience*, *15*(10), 1445–53. http://doi.org/10.1038/nn.3215

van Groen, T., & Wyss, J. M. (1990a). Connections of the retrosplenial granular a cortex in the rat. *Journal of Comparative Neurology*, *300*(4), 593–606. http://doi.org/10.1002/cne.903000412

van Groen, T., & Wyss, J. M. (1990b). The postsubicular cortex in the rat: characterization of the fourth region of the subicular cortex and its connections. *Brain Research*, *529*, 165–177. http://doi.org/10.1016/0006-8993(90)90824-U

van Groen, T., & Wyss, J. M. (1992a). Connections of the retrosplenial dysgranular cortex in the rat. *Journal of Comparative Neurology*, *315*(2), 200–216. http://doi.org/10.1002/cne.903150207

van Groen, T., & Wyss, J. M. (1992b). Projections from the laterodorsal nucleus of the thalamus to the limbic and visual cortices in the rat. *Journal of Comparative Neurology*, *324*(3), 427–448. http://doi.org/10.1002/cne.903240310

van Groen, T., & Wyss, J. M. (1995). Projections from the anterodorsal and anteroventral nucleus of the thalamus to the limbic cortex in the rat. *Journal of Comparative Neurology*, *358*(4), 584–604. http://doi.org/10.1002/cne.903580411

van Groen, T., & Wyss, J. M. (2003). Connections of the retrosplenial granular b cortex in the rat. *Journal of Comparative Neurology*, *463*(3), 249–63. http://doi.org/10.1002/cne.10757

van Strien, N. M., Cappaert, N. L. M., & Witter, M. P. (2009). The anatomy of memory: an interactive overview of the parahippocampal-hippocampal network. *Nature Reviews Neuroscience*, *10*(4), 272–282. http://doi.org/10.1038/nrn2614

Vann, S. D., & Aggleton, J. P. (2004). Testing the importance of the retrosplenial guidance system: effects of different sized retrosplenial cortex lesions on heading direction and spatial working memory. *Behavioural Brain Research*, *155*(1), 97–108. http://doi.org/10.1016/j.bbr.2004.04.005

Vann, S. D., Aggleton, J. P., & Maguire, E. a. (2009). What does the retrosplenial cortex do? *Nature Reviews Neuroscience*, *10*(11), 792–802. http://doi.org/10.1038/nrn2733

Vermaercke, B., & Op De Beeck, H. P. (2012). A multivariate approach reveals the behavioral templates underlying visual discrimination in rats. *Current Biology*, *22*(1), 50–55. http://doi.org/10.1016/j.cub.2011.11.041

Vidal, P. P., Cullen, K., Curthoys, I. S., Du Lac, S., Holstein, G., Idoux, E., … Smith, P. (2015). The vestibular system. In G. Paxinos (Ed.), *The Rat Nervous System* (Fourth, pp. 805–864). London: Academic Press. http://doi.org/10.1016/B978-0-12-374245-2.00019-X

Vlasak, A. N. (2006). The relative importance of global and local landmarks in navigation by Columbian ground squirrels (Spermophilus columbianus). *Journal of Comparative Psychology*, *120*(2), 131–138. http://doi.org/10.1037/0735-

7036.120.2.131

Vogt, B. A. (2015). Cingulate cortex and pain architecture. In G. Paxinos (Ed.), *The Rat Nervous System* (Fourth, pp. 575–599). London: Academic Press. http://doi.org/10.1016/B978-0-12-374245-2.00019-X

Vogt, B. A., & Miller, M. W. (1983). Cortical connections between rat cingulate cortex and visual, motor, and postsubicular cortices. *Journal of Comparative Neurology*, *216*(2), 192–210. http://doi.org/10.1002/cne.902160207

von Frisch, K. V. (1974). *Animal Architecture*. United Kingdom: Harcourt.

Wallace, D. J., Greenberg, D. S., Sawinski, J., Rulla, S., Notaro, G., & Kerr, J. N. D. (2013). Rats maintain an overhead binocular field at the expense of constant fusion. *Nature*, *498*(7452), 65–9. http://doi.org/10.1038/nature12153

Whitlock, J. R., Sutherland, R. J., Witter, M. P., Moser, M.-B., & Moser, E. I. (2008). Navigating from hippocampus to parietal cortex. *Proceedings of the National Academy of Sciences*, *105*(39), 14755–14762. http://doi.org/10.1073/pnas.0804216105

Wiener, S. I., Berthoz, A., & Zugaro, M. B. (2002). Multisensory processing in the elaboration of place and head direction responses by limbic system neurons. *Cognitive Brain Research*, *14*, 75–90. http://doi.org/10.1016/S0926-6410(02)00062-9

Wilber, A. A., Clark, B. J., Demecha, A. J., Mesina, L., Vos, J. M., & McNaughton, B. L. (2015). Cortical connectivity maps reveal anatomically distinct areas in the parietal cortex of the rat. *Frontiers in Neural Circuits*, *8*(146), 1–14. http://doi.org/10.3389/fncir.2014.00146

Wilber, A. A., Clark, B. J., Forster, T. C., Tatsuno, M., & McNaughton, B. L. (2014). Interaction of egocentric and world-centered reference frames in the rat posterior parietal cortex. *Journal of Neuroscience*, *34*(16), 5431–46. http://doi.org/10.1523/JNEUROSCI.0511-14.2014

Winter, S. S., Clark, B. J., & Taube, J. S. (2015). Disruption of the head direction cell network impairs the parahippocampal grid cell signal. *Science*, *347*(6224), 870–4. http://doi.org/10.1126/science.1259591

Wolbers, T., & Wiener, J. M. (2014). Challenges for identifying the neural mechanisms that support spatial navigation: The impact of spatial scale. *Frontiers in Human Neuroscience*, *8*(8), 1–12. http://doi.org/10.3389/fnhum.2014.00571

Wyss, J. M., & Van Groen, T. (1992). Connections between the retrosplenial cortex and the hippocampal formation in the rat: a review. *Hippocampus*, *2*(1), 1–11. http://doi.org/10.1002/hipo.450020102

Xing, D., Yeh, C.-I., & Shapley, R. M. (2010). Generation of black-dominant responses in V1 cortex. *The Journal of Neuroscience*, *30*(40), 13504–13512. http://doi.org/10.1523/JNEUROSCI.2473-10.2010

Yoder, R. M., Clark, B. J., Brown, J. E., Lamia, M. V, Valerio, S., Shinder, M. E., & Taube, J. S. (2011). Both visual and idiothetic cues contribute to head direction cell stability during navigation along complex routes. *Journal of Neurophysiology*, *105*(6), 2989–3001. http://doi.org/10.1152/jn.01041.2010

Yoder, R. M., Clark, B. J., & Taube, J. S. (2011). Origins of landmark encoding in the brain. *Trends in Neurosciences*, *34*(11), 561–571. http://doi.org/10.1016/j.tins.2011.08.004

Yoder, R. M., Peck, J. R., & Taube, J. S. (2015). Visual landmark information gains control of the head direction signal at the lateral mammillary nuclei. *Journal of Neuroscience*, *35*(4), 1354–67. http://doi.org/10.1523/JNEUROSCI.1418-14.2015

Yoder, R. M., & Taube, J. S. (2009). Head direction cell activity in mice: Robust directional signal depends on intact otolith organs. *Journal of Neuroscience*, *29*(4), 1061–1076. http://doi.org/10.1523/JNEUROSCI.1679-08.2009

Yoganarasimha, D., & Knierim, J. J. (2005). Coupling between place cells and head direction cells during relative translations and rotations of distal landmarks. *Experimental Brain Research*, *160*(3), 344–359. http://doi.org/10.1007/s00221-004-2016-9

Yoganarasimha, D., Yu, X., & Knierim, J. J. (2006). Head direction cell representations maintain internal coherence during conflicting proximal and distal cue rotations: comparison with hippocampal place cells. *Journal of Neuroscience*, *26*(2), 622–631. http://doi.org/10.1523/JNEUROSCI.3885-05.2006

Zar, J. H. (2010). *Biostatistical Analysis* (5th ed.). London: Prentice Hall.

Zeil, J. (2012). Visual homing: An insect perspective. *Current Opinion in Neurobiology*. http://doi.org/10.1016/j.conb.2011.12.008

Zugaro, M. B., Arleo, A., Berthoz, A., & Wiener, S. I. (2003). Rapid spatial reorientation and head direction cells. *Journal of Neuroscience*, *23*(8), 3478–3482. http://doi.org/23/8/3478 [pii]

Zugaro, M. B., Arleo, A., Déjean, C., Burguière, E., Khamassi, M., & Wiener, S. I. (2004). Rat anterodorsal thalamic head direction neurons depend upon dynamic visual signals to select anchoring landmark cues. *European Journal of Neuroscience*, *20*(2), 530–536. http://doi.org/10.1111/j.1460-9568.2004.03512.x

Zugaro, M. B., Berthoz, A., & Wiener, S. I. (2001). Background, but not foreground, spatial cues are taken as references for head direction responses by rat anterodorsal thalamus neurons. *Journal of Neuroscience*, *21*, RC154. http://doi.org/20015390 [pii]

Zugaro, M. B., Tabuchi, E., Fouquier, C., Berthoz, A., & Wiener, S. I. (2001). Active locomotion increases peak firing rates of anterodorsal thalamic head direction cells. *Journal of Neurophysiology*, *86*, 692–702.

Zugaro, M. B., Tabuchi, E., & Wiener, S. I. (2000). Influence of conflicting visual, inertial and substratal cues on head direction cell activity. *Experimental Brain Research*, *133*, 198–208. http://doi.org/10.1007/s002210000365

Zurawel, G., Ayzenshtat, I., Zweig, S., Shapley, R., & Slovin, H. (2014). A contrast and surface code explains complex responses to black and white stimuli in v1. *The Journal of Neuroscience*, *34*(43), 14388–402. http://doi.org/10.1523/JNEUROSCI.0848-14.2014